VNIVERSITAT DE VALÈNCIA
Escola Tècnica Superior d'Enginyeria

Departament d'Enginyeria Química

Control of volatile organic compounds from air emissions by anaerobic bioscrubber: process performance and process simulation

Programa de doctorado: Ingeniería Química, Ambiental y de Procesos

Departamento de Ingeniería Química

Memoria que, para optar al Título de Doctor por la Universitat de València, presenta **Daniel Bravo Martínez**

Directores de tesis,
Dra. Carmen Gabaldón García
Dr. F. Javier Álvarez Hornos

Valencia, octubre de 2017

Dña. CARMEN GABALDÓN GARCÍA, Profesora Titular del Departament d'Enginyeria Química de la Universitat de València, y **D. F. JAVIER ÁLVAREZ HORNOS,** Profesor Contratado Doctor Interino del Departament d'Enginyeria Química de la Universitat de València.

CERTIFICAN: Que **D. Daniel Bravo Martínez**, con Título de Ingeniería Química y Máster Universitario en Gestión Sostenible y Tecnologías del Agua, ha realizado bajo su dirección el trabajo que bajo el título de: **"CONTROL OF VOLATILE ORGANIC COMPOUNDS FROM AIR EMISSIONS BY ANAEROBIC BIOSCRUBBER: PROCESS PERFORMANCE AND PROCESS SIMULATION"** presenta en esta Memoria y que constituye su Tesis para optar al Título de Doctor por la Universitat de València.

Y para que conste a los efectos oportunos firman el presente certificado en Valencia a …….. de 2017.

Fdo.: Dra. Carmen Gabaldón García Fdo.: Dr. F. Javier Álvarez Hornos

Agradecimientos

En primer lugar, me gustaría a gradecer a mis directores de tesis Carmen Gabaldón y Javier Álvarez su gran esfuerzo, implicación y dedicación para la elaboración de esta tesis, su realización no hubiera sido posible sin su apoyo durante la parte experimental y en la redacción de la misma. Por supuesto, quiero extender este agradecimiento al resto de miembros de GI^{2}AM (Marta, Paula, y Vicente) por acogerme como un miembro más del grupo desde el principio.

Me gustaría agradecer a Josep Peñarrocha su ayuda durante la puesta en marcha del sistema y durante el desarrollo de la tesis. Tu dedicación y enseñanzas de dos semanas permitió mantener el prototipo industrial funcionando durante un año y medio.

Gracias a Pablo, mi compañero de artículo, y a Nadine, mi compañera de proyecto, por vuestro apoyo y por los buenos momentos vividos en el laboratorio y en el prototipo industrial. Gracias a Pau, María Keysi, Lidia y Carlos por compartir con una sonrisa el tiempo convivido en el despacho y en el laboratorio.

A mis compañeros de Pure Air Solutions, Salva, David y Dani Vílchez por acompañarme en mi estancia en Holanda desde el principio. A Feliu, por las charlas interminables a través de Skype para resolverme todos los problemas que pasaban durante la operación del prototipo industrial.

A mis amigos de Holanda, Bea, Javi y Pau, pues con vosotros viví grandes momentos en tierras holandesas durante mi época en Pure Air Solutions.

Así mismo, no puedo dejar de mencionar aquellos amigos que han estado siempre conmigo y me han apoyado allá donde he estado. A David, Ana Mari, María, Nieves, Juanan, Antonio, Paco, Gabi, Mar, Manolo, Elena, Jose y Sara por ser mi mejor momento de desconexión cuando más lo necesitaba.

También agradecer a mi familia por estar siempre que les he necesitado. En especial a mi madre, mi hermana y mi padre por ser mi pilar fundamental desde los comienzos. No quiero dejar de mencionar a personas importantes, que me han dado muy buenos consejos durante toda la tesis como son Jose, Tito, Paqui, Rita y Rafa.

A Mariola, porque esta tesis es tanto mía como tuya. Tu apoyo y confianza en mí durante todo este tiempo han sido clave. Porque siempre has estado ahí, sin importar la distancia que nos ha separado.

I would also like to thank the Company Pure Air Solutions BV, for providing the experimental setup of this thesis and giving me the opportunity to join the team, and of course to thank Astrid, Albert, André and Bart for their help during the whole project and after it.

The research leading to these results has received funding from the People Programme (Marie Curie Actions-ITN) of the European Union's Seventh Framework Programme FP7/2007-2013/ under REA grant agreement n_606942 (TrainonSEC).

Resumen

La contaminación atmosférica es un problema para la salud humana y para el medio ambiente. Dentro de los posibles contaminantes atmosféricos, los compuestos orgánicos volátiles son una de las causas asociadas al empeoramiento de la calidad ambiental. Una gran parte de estos compuestos son emitidos a la atmosfera por industrias que utilizan disolventes en su proceso productivo, estando reguladas estas emisiones industriales por la Directiva Europea de Emisiones Industriales (2010/75/EU). La industria flexográfica es uno de los sectores industriales afectados por esta normativa y, por tanto, deben de reducir sus emisiones. Estas industrias pueden enfocar la reducción de los compuestos orgánicos volátiles de dos maneras: mediante la reducción del consumo de disolventes o mediante la eliminación de las emisiones gaseosas de compuestos orgánicos volátiles empleando técnicas de tratamiento. En lo que respecta al tratamiento de estas emisiones, las tecnologías basadas en los procesos biológicos aerobios (biofiltros, biofiltros percoladores y biolavadores) han demostrado su eficacia en el control de las emisiones atmosféricas de este sector industrial. Se pueden destacar los estudios realizados por el grupo de investigación en ingeniería ambiental GI^{2}AM de la Universitat de València en la aplicación de biofiltros percoladores tanto a escala de laboratorio como a escala industrial gracias a la colaboración con la empresa Pure Air Solutions BV (Paises Bajos). Sin embargo, el uso de estas tecnologías se ha visto limitada para industrias con un elevado consumo de disolventes debido a los elevados costes de operación y a la elevada superficie requerida para su instalación. Es por ello, que el desarrollo de una tecnología basada en la degradación anaerobia es una alternativa atractiva para este tipo de actividades.

En este contexto, el grupo de investigación en ingeniería ambiental GI^{2}AM de la Universitat de València, en colaboración con la compañía Pure Air Solutions BV han desarrollado una nueva tecnología de biolavador anaerobio en el marco del proyecto europeo TrainonSEC, en el cual se enmarca la presente tesis doctoral. Esta tecnología (patentada ES2542257) se basa en la transferencia de los disolventes de la fase gaseosa a la fase líquida en un absorbedor y la posterior degradación de los disolventes contenidos en la corriente líquida en un reactor anaerobio granular de lecho expandido, con la producción de una corriente gaseosa rica en metano y una corriente líquida que se emplea en el absorbedor para la transferencia de los contaminantes del aire. De esta manera, el sistema de biolavador anaerobio se opera en ciclo cerrado para la corriente de agua principal entre el absorbedor y el reactor anaerobio. Esta nueva tecnología de tratamiento de emisiones atmosféricas de compuestos orgánicos volátiles permitiría el tratamiento de mayores cargas

orgánicas, por tanto de emisiones atmosféricas provenientes de empresas con un mayor consumo de disolventes, con un requerimiento de superficie menor y, además, generaría una corriente de biogás que podría ser utilizada por la propia industria como fuente de energía en su proceso productivo.

Alcance y objetivos

Este trabajo de tesis doctoral ha sido realizado con el objetivo de estudiar el funcionamiento de un prototipo industrial de biolavador anaerobio para la depuración de emisiones de compuestos orgánicos volátiles en aire procedentes del uso industrial de disolventes a fin de demostrar la estabilidad del proceso y optimizar el funcionamiento. Este objetivo general se ha dividido en dos líneas de trabajo, las cuales se describen a continuación:

1. En primer lugar, un estudio experimental de la tecnología de biolavador anaerobio mediante el uso de un prototipo industrial instalado en una industria flexográfica durante un periodo de aproximadamente un año y medio. La finalidad de esta primera fase es evaluar el rendimiento de esta tecnología en función de los principales parámetros de operación del absorbedor y del reactor anaerobio, así como la obtención de los criterios de diseño para el escalado del biolavador anaerobio. En el absorbedor se evaluaron las condiciones de operación que permitían cumplir con los requerimientos legales fijados en la normativa asociados a las emisiones de compuestos orgánicos volátiles a la atmosfera, así como el desarrollo de un protocolo para el control de la perdida de presión. En el reactor anaerobio se determinó la carga orgánica máxima que puede degradar esta unidad sin poner en riesgo la estabilidad del proceso y se evaluaron las reglas de control diseñadas para mantener el pH y la concentración de nutrientes en el rango óptimo para la degradación de la materia orgánica.
2. En segundo lugar, el desarrollo de una herramienta de simulación implementada en el software comercial Aspen Plus® que incluye los principales mecanismos involucrados en la transferencia de los compuestos orgánicos volátiles de la fase gas a la fase líquida en el absorbedor, y la posterior degradación de éstos en el reactor anaerobio. La herramienta de simulación desarrollada en esta tesis doctoral tiene como finalidad simular y predecir la respuesta del biolavador anaerobio frente a una emisión de compuestos orgánicos volátiles determinada. Además, se pretende que dicha

herramienta pueda ser de utilidad para los investigadores y las empresas en la fase de diseño del biolavador anaerobio, así como en la optimización del funcionamiento de esta tecnología.

Materiales y métodos

El prototipo industrial empleado durante la fase del estudio experimental estaba compuesto por un absorbedor de 3.06 m de altura y de 0.5 m de diámetro, donde se podían instalar hasta 2 m de material de relleno. La fase liquida con los disolventes disueltos obtenida en esta unidad se trataba en un reactor de 5.08 metros de altura y 1.59 m de diámetro, lo que supone un volumen efectivo de agua de 8.7 m^3. El biolavador anaerobio se completaba con varios tanques intermedios, sumando un volumen total de agua de 16 m^3. Este biolavador anaerobio trataba parte de las emisiones de una industria flexográfica, siendo los disolventes presentes en mayor proporción: etanol, acetato de etilo y 1-etoxi-2-propanol. Estas emisiones se caracterizaban por patrones de concentración y de composición variable y por la presencia de periodos de tiempo en que no se producía la emisión de compuestos orgánicos volátiles a causa de las paradas programadas en el proceso productivo de la industria flexográfica.

El estudio experimental se puede dividir en dos partes: una primera parte donde se establece y se evalúa los protocolos para la comprobación del sistema de control, de puesta en marcha y de operación de la instalación y, en segundo lugar, la evaluación del rendimiento de la instalación durante un periodo de aproximadamente un año y medio. Esta segunda parte del estudio se divide a su vez en 5 fases caracterizadas por el tipo de configuración evaluada en el absorbedor. Durante la primera y la segunda fase se estudió la configuración de torre de relleno, usando para ello dos materiales de relleno estructurado en cada una de estas fases: relleno de flujo cruzado (material de relleno A) y relleno de flujo vertical (material de relleno B). Posteriormente, en la tercera fase se evaluó la configuración de pulverización. Por último, el absorbedor se volvió a operar como torre de relleno instalando el material B y el material A en las dos últimas fases, e implementando el protocolo de control de perdida de presión desarrollado en esta tesis. Durante estas cinco fases, el líquido lavador con los disolventes disueltos obtenido en el absorbedor fue depurado en el reactor anaerobio con el objetivo de estudiar la estabilidad de esta unidad al tratar una carga orgánica variable e intermitente.

Una vez finalizado el estudio experimental, se procedió al desarrolló del modelo en estado estacionario en el simulador Aspen Plus®, realizando su calibración y validación con los resultados obtenidos en el estudio experimental. Este simulador comercial se seleccionó de entre los disponibles en el mercado ya

que permite utilizar el modelo termodinámico ELECNRTL. Este modelo termodinámico es una extensión del modelo termodinámico NRTL, y se muestra apropiado para sistemas con equilibrios ácido/base, lo que permite estimar el valor de pH y el contenido de metano y dióxido de carbono de la corriente de biogás. A continuación, se crearon dos modelos para las dos unidades principales del biolavador anaerobio. El absorbedor se simuló empleando el módulo RadFrac de Aspen Plus®, el cual es un modelo riguroso para la simulación de operaciones de destilación y de absorción. Los parámetros de calibración del modelo del absorbedor fueron el número de etapas teóricas de equilibrio para cada uno de los disolventes, ajustadas mediante las desviaciones entre los valores experimentales y predichos de las concentraciones de compuestos orgánicos volátiles en la corriente gaseosa de salida del absorbedor. Una vez calibrado y validado el absorbedor, se procedió a la creación del modelo del reactor anaerobio. El desarrollo de este modelo se abordó mediante la simulación de las distintas etapas de la degradación anaerobia de la materia orgánica en diferentes módulos de Aspen. De esta manera, fueron necesarios 4 módulos de Aspen conectados en serie: uno para la hidrólisis, uno para la acidogénesis, uno para metanogénesis acetoclástica y uno para la metanogénesis hidrogenotrófica. El modelo implementado en estos módulos fue una simplificación del modelo ADM1. A continuación, se definieron las rutas de degradación de cada uno de los disolventes. Estas rutas se basaron en datos bibliográficos y en los análisis de la composición del agua realizados durante la etapa experimental. El objetivo fue reducir la ruta de degradación a los pasos limitantes. Finalmente, se procedió a definir la cinética de estos pasos limitantes, que tras la simplificación del modelo ADM1 y los resultados experimentales obtenidos pasarían a seguir una cinética de Monod o ser simuladas mediante reacciones de conversión

La calibración y validación del modelo se realizó mediante la conexión de Aspen plus® con el programa matemático Matlab®, con el objetivo de utilizar las herramientas de optimización de este programa y poder realizar un gran número de simulaciones en un corto periodo de tiempo.

Resultados y discusión

Los resultados obtenidos en la primera parte del estudio experimental son presentados en el capítulo 5 de esta tesis doctoral. Los protocolos propuestos tanto para la comprobación del sistema de control, la puesta en marcha y la operación del prototipo industrial se mostraron adecuados para tal fin, pues permitieron mantener las condiciones físicas y químicas de las dos unidades en el rango deseado durante aproximadamente un año y medio. Especial atención se ha de prestar a los protocolos seguidos en la puesta en marcha del reactor anaerobio. Éste se inoculó

con biomasa de un reactor anaerobio que trataba las aguas residuales de una fábrica de cerveza. Esta biomasa se eligió debido a los resultados publicados por Lafita et al. (2015), quienes demostraron la capacidad de esta biomasa de degradar un agua residual compuesta por los principales disolventes usados en el sector flexográfico. La carga orgánica media utilizada durante el periodo de puesta en marcha fue de 3.2 kg Demanda Química de Oxígeno (DQO) m^{-3} d^{-1}, que se encuentra comprendida en el intervalo propuesto por Colussi et al. (2009). Esta carga orgánica permitió poner en marcha el reactor en un periodo inferior a 15 días, manteniendo una concentración de ácidos grasos volátiles en la corriente de salida del reactor inferior a 200 mg ácido acético L^{-1} y manteniendo el pH de esta corriente por encima de 7.0. Es de destacar que la puesta en marcha realizada en este estudio es el primer ejemplo de puesta en marcha de un reactor anaerobio con cargas variables en composición y en concentración encontrado en la bibliografía.

Por último, cabe mencionar que durante la etapa inicial de puesta en marcha del biolavador anaerobio se rediseñó el reactor con el objetivo de reducir el metano disuelto en su efluente líquido y mejorar, de esta manera, la eficacia de recuperación de metano en la corriente de biogás. Los cambios propuestos permitieron reducir la sobresaturación en metano del efluente líquido del reactor de 360% a 120%, siendo este valor inferior a los encontrados en la bibliografía (Hartley y Lant, 2006).

Una vez puesto en marcha el prototipo industrial se procedió a evaluar su rendimiento. Los resultados de este estudio son presentados en el capítulo 6 de esta tesis doctoral. El uso del material de relleno A demostró ser la mejor configuración en el absorbedor para su aplicación industrial. La eliminación de los compuestos orgánicos volátiles con esta configuración varió entre 83% y 93% para una relación volumétrica de los caudales de agua y aire entre $3.5 \cdot 10^{-3}$ y $9.1 \cdot 10^{-3}$, mientras que la eliminación con el material B varió entre 75% y 85% para relaciones volumétricas entre $3.9 \cdot 10^{-3}$ y $10.1 \cdot 10^{-3}$. La evolución de la perdida de presión en el absorbedor en la primera y segunda fase indicó la necesidad de utilizar un protocolo de control de presión para evitar la acumulación de biomasa en el material de relleno, que provocaba que se alcanzaran valores superiores al valor recomendado de 200 Pa m^{-1} (Janssen et al. 2013). El protocolo que se implementó y evaluó en esta tesis doctoral demostró su eficacia, pues la perdida de presión se mantuvo por debajo del valor recomendado de funcionamiento con los dos materiales de relleno en las dos fases finales del estudio. Con respecto a la configuración de torre de pulverización, la eliminación media fue del 55%, siendo inviable su uso a escala industrial ya que sería necesario un elevado caudal de agua para obtener eficacias de eliminación comparables a las obtenidas con las configuraciones de torre de

relleno. El reactor anaerobio registró un rendimiento estable durante toda la fase del estudio experimental pese a los patrones de carga comentados anteriormente, siendo la eliminación media de materia orgánica soluble del 93 $\pm$ 5% en unidades de DQO. La carga máxima que se pudo aplicar al reactor sin desestabilizar el sistema fue de 24 kg DQO m^{-3} lecho d^{-1}, produciéndose una acumulación de ácidos grasos volátiles en la salida del reactor a partir de dicha carga. La acumulación de ácidos grasos en el efluente líquido del reactor pone de manifiesto que las bacterias acidogénicas son capaces de degradar los picos de carga orgánica asociados a los picos de emisiones de compuestos orgánicos volátiles por parte de la industria flexográfica, pero las bacterias metanogénicas no son capaces de consumir el ácido acético producido, causando de esta manera una acumulación del mismo en el efluente líquido del reactor. Por último, las reglas de dosificación, tanto de la disolución alcalina como de la disolución de nutrientes, fueron capaces de mantener unas condiciones óptimas para la biomasa a lo largo de los 484 días. El pH se mantuvo por encima de 6.83, y las reglas relacionadas con los nutrientes aseguraron su disponibilidad a lo largo del todo el periodo experimental, evitando que se alcanzasen concentraciones inhibitorias para la biomasa. Es más, las condiciones mantenidas en el sistema permitieron obtener un biogás con una concentración media de metano del 88 $\pm$ 6% vol., con una concentración máxima de ácido sulfhídrico de 12 ppm, es por ello que es recomendable su uso en futuras plantas industriales.

Parte del estudio experimental del biolavador anaerobio ha sido publicado en:

Bravo, D., Ferrero, P., Penya-roja, J.M., Álvarez-Hornos, F.J. and Gabaldón, C. (2017). Control of VOCs from printing press air emissions by anaerobic bioscrubber: Performance and microbial community of an on-site pilot unit. Journal of Environmental Management 197: 287-295.

Los datos obtenidos gracias a la operación del prototipo industrial fueron utilizados para el desarrollo del modelo del biolavador anaerobio en Aspen Plus®, el cual es presentado en el capítulo 7 de la presente tesis doctoral. El desarrollo del modelo supone las etapas de calibración y validación de las dos unidades principales que conforman esta tecnología, dichas etapas son explicadas y comentadas a continuación.

La calibración del absorbedor consistió en determinar el número de etapas teóricas de equilibrio para cada uno de los tres disolventes principales presentes en la emisión gaseosa de la industria flexográfica y para los dos materiales de relleno utilizados en el estudio experimental del absorbedor. El número de etapas teóricas

se determinó comparando la capacidad de eliminación experimental y predicha para cada disolvente y para los dos materiales de relleno. Los datos utilizados para la calibración corresponden a varios experimentos realizados en el absorbedor durante la fase experimental. En dichos experimentos se midió: el caudal de la corriente líquida y gaseosa, la temperatura de entrada y salida de ambas fases y la concentración de compuestos orgánicos volátiles y composición de la corriente gaseosa a la entrada y salida del absorbedor. La relación de los caudales de agua y aire de estos experimentos cubrían todo el rango de relaciones estudiado en la parte experimental. El número de etapas teóricas obtenido en la calibración para el material de relleno A fueron 0.99 ± 0.07, 0.95 ± 0.1 y 0.94 ± 0.04 m^{-1} para el etanol, acetato de etilo y 1-etoxi-2-propanol, respectivamente. Los resultados obtenidos con el material de relleno B fueron 0.7 ± 0.06, 0.73 ± 0.06 y 0.78 ± 0.03 m^{-1} para etanol, acetato de etilo y 1-etoxi-2-propanol, respectivamente. Los resultados obtenidos en la calibración mostraron que el número de etapas teóricas para cada material de relleno variaba muy poco para las condiciones probadas y para los disolventes de interés de esta tesis. Es por ello, y con la intención de simplificar el modelo, que se decidió hacer uso del valor medio para la modelación del absorbedor, siendo la altura equivalente de plato teórico 1.05 $\pm$ 0.08 y 1.37 $\pm$ 0.11 m para el material de relleno A y B, respectivamente. La torre de pulverización no se calibró, al ser descartada para su aplicación industrial. Una vez realizada la calibración del modelo se procedió a su validación, esta se realizó haciendo uso de los datos obtenidos durante las fases de estudio experimental en las cuales se empleaba una configuración de torre de relleno. Los resultados de la validación mostraron que el modelo es capaz de predecir la concentración de compuestos orgánicos volátiles de la fase gaseosa a la salida del absorbedor, siendo el error relativo medio inferior al 10%. Este error relativo se tradujo en un error relativo medio inferior al 5% en la predicción de la carga orgánica alimentada al reactor anaerobio.

Con respecto al reactor anaerobio, el primer paso fue decidir aquellos procesos del modelo ADM1 que no se iban a tener en cuenta en la modelación del reactor anaerobio. Las hipótesis del modelo estuvieron relacionas con las condiciones experimentales mantenidas en la operación del prototipo industrial. Los procesos eliminados de este modelo fueron: (i) reducción del nitrato y sulfato debido a su baja concentración en el líquido de entrada al reactor; (ii) limitación debido a la escasez de nutrientes, pues su dosificación fue controlada y en función de la carga orgánica; (iii) inhibición debido a desviación del pH de los valores óptimos, pues su valor fue controlado mediante la dosificación de una disolución alcalina; y (iv) crecimiento y muerte de biomasa, pues el volumen de lecho se

mantuvo constante en 3 m^3 durante todo el estudio experimental. Tras esto se definió la ruta de degradación de los principales disolventes encontrados en la emisión de la industria flexográfica de acuerdo a datos bibliográficos y a los resultados obtenidos en la fase experimental. El etanol se degradaría a ácido acético e hidrogeno, el acetato de etilo a etanol y ácido acético, y el 1-etoxi-2-porpanol a etanol y acetona, que posteriormente se degradaría a ácido acético. El acetato de etilo no fue detectado en los análisis de composición del efluente líquido del reactor anaerobio, por lo que se decidió tomar una conversión del 100% para la reacción de hidrolización de este disolvente. En lo que respecta a la degradación de acetona, no fue incluida en el modelo, pues la acetona tampoco fue detectada en los análisis de composición del efluente líquido del reactor realizados durante el estudio experimental, por lo que la degradación 1-etoxi-2-propanol fue simulada en un solo paso a etanol y ácido acético. En base a esto, los parámetros iniciales necesarios para la calibración del modelo fueron los correspondientes a la cinética de Monod de la acidogénesis del etanol y del 1-etoxi-2-propanol y la metanogéneis acetogénica. Dichos parámetros fueron las velocidades especificas máximas y las constantes de semi-saturación de degradación del etanol, del 1-etoxi-2-propanol y del ácido acético ($\nu_{max,\ EtOH}$, $\nu_{max,\ Et2Pr}$, $\nu_{max,\ ácido\ acético}$, $K_{s,\ EtOH}$, $K_{s,\ Et2Pr}$ and $K_{s,\ ácido\ acético}$). Con el objetivo de simplificar el modelo, se realizó un estudio de sensibilidad para detectar los parámetros de mayor influencia en su respuesta, de tal manera que serían los parámetros a calibrar, estimando el resto de parámetros en base a la bibliografía. El resultado del estudio de sensibilidad indicó que los parámetros a calibrar debían ser la velocidad volumétrica específica de degradación de etanol a ácido acético y la velocidad volumétrica específica de conversión del ácido acético a metano. A continuación, se procedió a realizar la calibración con los datos obtenidos en la primera fase del estudio experimental del absorbedor, correspondiente al uso del material de relleno A. La validación se realizó haciendo uso del resto de fases en las que el absorbedor se operó con la configuración de torre de relleno. Tras la calibración y posterior validación, el modelo demostró que es capaz de simular la producción de metano con un error relativo medio del 23%. En lo referente a las concentraciones de ácidos grasos volátiles, el modelo mostró la capacidad de simular dichas concentraciones para aquellas cargas orgánicas inferiores a 24 kg DQO m^{-3} lecho d^{-1}. Sin embargo, el modelo fue incapaz de predecir la concentraciones de ácidos grasos volátiles para cargas orgánicas superiores a dicho valor, debido a que el modelo fue construido en estado estacionario y, por lo tanto, no puede simular la acumulación de ácidos volátiles grasos que se produce a lo largo de los días. Por último, el modelo termodinámico fue capaz de simular el equilibrio alcanzado entre efluente líquido del reactor y el biogás, siendo el error

relativo medio en la predicción de la composición de metano en la corriente de biogás del 5%. En lo que respecta al pH en el reactor anaerobio, el valor simulado es ligeramente inferior al experimental, debido a que no se tuvo en cuenta la presencia de otros iones en el sistema, más allá del ácido acético y de las especies carbonatadas.

Tras comprobar la validez del modelo creado se procedió a desarrollar una herramienta de diseño del biolavador anaerobio. Esta herramienta se construyó gracias a la conexión entre los programas Aspen Plus® y Matlab®. La herramienta desarrollada permite obtener unas gráficas en 3D con toda la información necesaria para diseñar el biolavador anaerobio. Con respecto al diseño de la torre de absorción, es posible obtener gráficas que relacionan la capacidad de eliminación de esta unidad con la velocidad del líquido lavador, el caudal de aire y la altura del material de relleno para una determinada emisión de compuestos orgánicos volátiles. En lo que respecta al reactor anaerobio, las gráficas que se pueden obtener para facilitar su diseño relacionan la concentración de ácidos volátiles en el efluente del reactor con el tiempo de residencia hidráulico y la carga orgánica alimentada a esta unidad. Además, esta herramienta permite crear gráficas con datos importantes sobre la operación de la futura planta, como por ejemplo la variación de la eliminación del absorbedor en función de los cambios de composición de la emisión de compuestos orgánicos volátiles de la industria flexográfica, o el biogás producido y concentración de ácidos grasos volátiles a la salida del reactor en función de la carga orgánica alimentada al reactor.

Parte de los resultados obtenidos en la creación del modelo del biolavador anaerobio han sido mandados para su posible publicación a Journal of Environmental Management como:

Bravo, D., Álvarez-Hornos, F. J., Penya-roja, J.M., San-Valero, P. and Gabaldón, C. Aspen Plus process-simulation model: Producing biogas from VOC emissions in an anaerobic bioscrubber.

Conclusiones y perspectivas

El objetivo general de esta tesis doctoral es estudiar el funcionamiento de un prototipo industrial de biolavador anaerobio para la depuración de emisiones de compuestos orgánicos volátiles en aire procedentes del uso industrial de disolventes a fin de demostrar la estabilidad del proceso y optimizar el funcionamiento.

A partir del estudio experimental, se demostró la viabilidad y robustez del biolavador anaerobio para el tratamiento de las emisiones gaseosas del sector flexográfico. Fruto del estudio experimental, se estableció los protocolos de puesta

en marcha y operación de futuras plantas industriales. La operación de la torre de absorción permitió definir la configuración de absorbedor que obtiene una mayor eficacia de eliminación de compuestos orgánicos volátiles con una menor relación de caudales agua y aire. Conjuntamente, se implementó y evaluó un protocolo de control de perdida de presión que permitió mantener la pérdida de presión en el absorbedor por debajo del valor recomendado en la bibliografía. Con respecto al reactor anaerobio, el estudio experimental indicó la carga orgánica máxima que puede ser tratada sin poner en riesgo la estabilidad del sistema, además de comprobar las reglas de control para la dosificación de la disolución que aporta alcalinidad y la disolución de nutrientes para su uso en futuras plantas industriales

A partir de los datos obtenidos en el estudio experimental, se desarrolló un modelo en Aspen Plus® para las dos unidades principales del biolavador anaerobio. El modelo del absorbedor consistió en el módulo Radfrac de Aspen y fue capaz de predecir satisfactoriamente la concentración de compuestos orgánicos volátiles en el efluente gaseoso de dicha unidad. El número de etapas teóricas obtenidas en la calibración de esta unidad fueron prácticamente constantes para los dos materiales de relleno usados en el estudio experimental, por lo que se tomó el valor medio para cada material con el fin de simplificar el modelo. El desarrollo del modelo del reactor anaerobio se abordó mediante la conexión en serie de varios módulos de reactor de Aspen. Este enfoque propuesto para implementar el reactor anaerobio en el simulador permite ampliarlo a otros bioprocesos con el fin de integrar los sistemas anaerobios con otras operaciones unitarias o a otros disolventes de interés industrial como por ejemplo el isopropanol. El modelo del reactor anaerobio fue capaz de predecir la producción de metano, mientras que la concentración de ácidos grasos volátiles fue predicha para cargas orgánicas inferiores a 24 kg DQO m^{-3} lecho d^{-1}. Sin embargo, el modelo del reactor anaerobio fue incapaz de simular la acumulación de ácidos grasos para cargas superiores a 24 kg DQO m^{-3} lecho d^{-1} debido a su naturaleza de estado estacionario. Por otra parte, la elección del modelo termodinámico ELECNRTL permitió simular el contenido de metano del biogás. Por último, el modelo creado en Aspen se conectó a Matlab®, lo que permitió una alta velocidad de transferencia de datos entre ambos programas. Dicha velocidad, se utilizó para crear una herramienta que puede ser utilizada para diseño u optimización del funcionamiento del biolavador anaerobio.

Los trabajos futuros derivados de esta tesis doctoral podrían dirigirse a la creación del modelo del reactor anaerobio en estado dinámico y a la inclusión de otros iones presentes en el sistema, con el objetivo de simular la acumulación de ácidos grasos volátiles que se produce a lo largo de los días y corregir el pequeño error en la predicción del pH.

Summary

Air pollution is human health and environmental concern. Within possible atmospheric pollutants, the Volatile Organic Compounds (VOCs) are one of the most important causes associated with deterioration of the air quality. A large amount of these compounds is emitted by industries which use solvents in their production processes, being these industrial emissions regulated by the European Directive on industrial emssions 2010/75/EU. The flexographic facilities are one of the affected industrial sectors by this directive, and therefore, they must reduce their emissions. These industries can approach the reduction by two forms: reducing the consumption of solvents or the abatement of the volatile organic compound gas emissions by treatment techniques. Among the treatment of waste gas, the technologies based on aerobic processes (biofilters, biotrickling filters and bioscrubbers) have widely demonstrated their efficiency for the waste gas emission control for this industrial sector. Within the available studies, it should be pointed out that the studies performed by the research group GI^{2}AM of the University of Valencia in the use of biotrickling filters at laboratory scale and at industrial scale have been performed thanks to the collaboration with the private company Pure Air Solutions BV (The Netherlands). However, widespread use of biotechniques has been limited to companies with a high use of solvents due to the high cost of operation and high foot print required for its installation. Therefore, the development of a technology based on anaerobe degradation of the solvents is an attractive alternative for this kind of activities.

Within this context, the research group GI^{2}AM of the University of Valencia, in collaboration with the company Pure Air Solutions, has developed the anaerobic bioscrubber as a new abatement technology in the framework of the European Project TrainonSEC to which this thesis project belongs. This technology (patent ES2542257) is based on the transfer of the solvents from the gas phase to the liquid phase in the scrubber, and the subsequent degradation of the solvents contained in the liquid stream in an expanded granular sludge bed reactor, with the production of a gas stream with a high content of methane and a liquid stream that is used in the scrubber for the transfer of the pollutants from the air. Thus, the anaerobic bioscrubber works in water-closed recirculation between the scrubber and the anaerobic reactor. This new technology for the treatment of volatile organic compound emissions will allow the treatment of higher organic loads; and therefore, the gas emissions coming from facilities with a great consumption of solvents, in a lesser footprint and, in addition, the production of a biogas stream that can be used as a source of energy in the production process.

Objectives

This doctoral thesis has been performed with the aim of study the performance of an industrial prototype of anaerobic bioscrubber for the abatement of volatile organic compound air emissions from the industrial use of solvents, in order to demonstrate its stability and to optimize its performance. This general objective has been divided in two work lines, which are described hereafter:

- Firstly, an on-site experimental study of the anaerobic bioscrubber by using an industrial prototype installed in a flexographic facility during a period of approximately one year and a half. The objective of this first phase is to evaluate the efficiency of this technology based on the main operational parameters of the scrubber and the anaerobic reactor, as well as to obtain the design criteria for the scale-up of the anaerobic bioscrubber. The operational conditions of the scrubber were evaluated in order to meet the legal threshold associated to the volatile organic compound gas emission established in the directive, as well as the development of a protocol to control the pressure drop through the scrubber. In the anaerobic reactor, the maximum organic loading rate that this unit can treat without compromising the stability of the process was determined. The control rules designed to maintain the pH and the nutrient concentration in an optimum range for the organic substrate degradation were evaluated.

- Secondly, the development of simulation tool in the commercial software Aspen Plus®, which includes the principal mechanisms involved in the transfer of volatile organic compounds from the gas phase to the liquid phase in the scrubber, and the subsequent degradation of the solvents in the anaerobic reactor. The objective of the simulation tool developed in the framework of this thesis is to simulate and to predict the response to a determined volatile organic compound emission. Moreover, this simulation tool should assist to the researchers and the private companies in the design phase of the anaerobic bioscrubber, as well as the performance optimization of this technology.

Material and methods

The industrial prototype, which was operated to perform the on-site experimental study, comprised by a scrubber unit that had a total height of 3.06 m

and a diameter of 0.5 m and an available height for the packing material of 2.00 m. The liquid stream with the dissolved solvents obtained in this unit was treated in an anaerobic reactor that had a total height of 5.08 m and diameter of 1.59 m, with an effective water volume of 8.7 m^3. Two intermediate tanks completed the setup; resulting in a total 16 m^3 effective water volume. The anaerobic bioscrubber treated a fraction of the total air emission of a flexographic facility, which was mainly composed by: ethanol, ethyl acetate and 1-ethoxy-2-propanol. The pattern emission was variable in concentration and composition and intermittent due to the closure periods of the flexographic facility.

The experimental study can be divided in two phases: firstly, the protocols to check the control software, the commissioning, the start-up and operational protocols were established and evaluated; and secondly, the performance of the industrial prototype was assessed during a period of approximately one year and a half. This second phase can be divided in 5 stages, which were characterized by the configuration tested in the scrubber. The packed bed configuration was tested in the first and second stage by installing two different structured packing materials in each stage: cross-flow fill (packing material A) and vertical flow fill (packing material B). Afterwards, the scrubber was tested as a spray column in the third stage. Finally, the scrubber was operated again as packed bed in the last two stages by installing the packing material B and the packing material A, and implementing the pressure drop control protocol developed in this thesis. During these five stages, the anaerobic reactor degraded the liquid stream with the dissolved solvents obtained in the scrubber unit, with the aim to evaluate the stability of the anaerobic reactor treating a variable and intermittent organic load.

After finishing the experimental study, the simulation model in steady-state in the software Aspen Plus® was developed by calibrating and validating the model with the results obtained in the experimental study. This commercial simulator was selected within the available ones in the market because it permits to use the thermodynamical model ELCNRTL. This thermodynamical model is an extension of the NRTL model, and it is appropriate for systems with acid/base equilibriums, which allows to estimate the pH and the methane and carbon dioxide content of the biogas stream. Then, two models for the two main units of the anaerobic bioscrubber were developed. The scrubber unit was modelled using Radfrac Aspen Plus® Module. This module is the rigorous one for simulating distillation and absorption operations. The calibration parameters of the scrubber model were the number of theoretical stages for each solvent, they were fitted by the deviations between experimental data and the model predictions of volatile organic compound concentration in the effluent gas stream of the scrubber. Once the scrubber model

was calibrated and validated, the anaerobic reactor model was developed. The approach to implement the anaerobic reactor consisted in simulate each stage of the anaerobic degradation of the organic substrate in a different Aspen Plus® module. In this way, four modules of Aspen connected in series were needed: one for the hydrolysis, one for the acidogenesis, one for the acetoclastic methanogenesis and one for the hydrogenotrophic methanogenesis. The model implemented in these modules was a simplification of the ADM1 model. Afterwards, degradation routes for each solvent were defined. These routes were based on bibliography data and the composition analyses of the water effluent of the anaerobic reactor carried out in the experimental stage. The objective was to reduce the degradation route to the limiting steps. Finally, the kinetic of the defined routes were established, which were defined as Monod-type or conversion reactions based on the performed simplification of ADM1 and the obtained experimental results.

The calibration and the validation of the model were conducted by connecting Aspen Plus® with Matlab®, with the aim of using the optimization algorithms of this last software and making a lot of simulations in a short period of time.

Results and discussion

The results obtained in the first phase of the experimental study are presented in chapter 5 of this doctoral thesis. All proposed protocols in order to check the control software, the commissioning, the start-up and operational were appropriated, since they maintained the physical and chemical conditions within the desired range for about one year and a half. Special attention should be paid to the protocols implemented in the start-up of the anaerobic reactor. Granular sludge from an anaerobic reactor installed in a brewery was selected as the source of biomass. This source of sludge was selected based on the research carried out by Lafita et al. (2015). These researchers demonstrated that this biomass is able to degrade wastewater composed by the main solvents used in the flexographic sector. The organic loading rate applied in the start-up period was 3.2 kg COD m^{-3} d^{-1}, which is in the range proposed by Colussi et al. (2009). The use of this organic loading rate allowed to start-up the anaerobic reactor in less than 15 days, maintaining the volatile fatty acid (VFA) concentration of the liquid effluent of the anaerobic reactor below 200 mg acetic acid L^{-1} and keeping the pH of this stream over 7.0. This thesis is the first attempt of anaerobic reactor start-up under intermittent and variable load found in the literature.

Finally, it is important to mention that the anaerobic reactor was retrofitted in order to reduce the dissolved methane in the liquid effluent and to improve, in

this way, the recovery of methane in the biogas stream. The proposed changes reduced the methane oversaturation of the liquid effluent of the anaerobic reactor from 360% to 120%, being this value lower to those ones found in the literature (Hartley and Lant, 2006).

Once the commissioning and the start-up of the industrial prototype were performed, its performance was evaluated. Results obtained in this study are presented in chapter 6 of this doctoral thesis. Packing A resulted to be the best scrubber configuration for industrial application. The removal efficiency of volatile organic compounds obtained with this configuration ranged between 83% and 93% with a liquid to air volumetric ratio between $3.5 \cdot 10^{-3}$ and $9.1 \cdot 10^{-3}$, while the removal efficiency with packing B was between 75% and 85% with a liquid to air volumetric ratio ranged between $3.9 \cdot 10^{-3}$ and $10.1 \cdot 10^{-3}$. Pressure drop evolution through the scrubber in the first and second stage stated the need of implementing a pressure drop control protocol to avoid the accumulation of biomass onto the packing material, since pressure drop higher than the recommended value of 200 Pa m^{-1} was reached (Janssen et al. 2013). Pressure drop control protocol implemented and evaluated in this thesis demonstrated its efficiency, since the pressure drop through the scrubber with the two tested packing materials in the last two phases of the experimental study was below the recommended limit. Average removal efficiency with the spray tower configuration was 55%; pointing that this configuration is unfeasible at industrial scale due to high-water flow rate needed to achieve packed bed configuration removal efficiency. The anaerobic reactor registered a stable performance during the whole experimental study, despite of the load pattern mentioned previously, being the removal efficiency of organic substrate 93 ± 5% in COD units. The maximum organic load that can be applied ensuring the system stability was 24 Kg COD m^{-3} bed d^{-1}, obtaining a VFA accumulation at the effluent of the anaerobic reactor if higher loads are applied. The accumulation of volatile fatty acids at the liquid effluent of the anaerobic reactor indicated that the acidogenic bacteria could degrade the peak of organic load associated to the peaks of volatile organic compound emissions from the flexographic facility; however, the methanogens could not metabolize the produced acetic acid, resulting in an accumulation of volatile fatty acids at the liquid effluent of the anaerobic reactor. Finally, the alkali solution and nutrient solution dosage control rules were able to maintain optimum conditions for the biomass during the 484 days. The pH was over 6.83, and the control rules related to nutrients dosage avoided to reach inhibition concentration for the biomass. Moreover, the conditions established in the system allowed to obtain a biogas stream whose methane content was 88 ± 6% Vol., with a

maximum hydrogen sulphide concentration of 12ppm, thus these rules have been adopted to be used in the future industrial installations.

Part of the experimental study of the anaerobic bioscrubber has been published in:

Bravo, D., Ferrero, P., Penya-roja, J.M., Álvarez-Hornos, F.J. and Gabaldón, C. (2017). Control of VOCs from printing press air emissions by anaerobic bioscrubber: Performance and microbial community of an on-site pilot unit. Journal of Environmental Management 197: 287-295.

Data obtained from the experimental study of the industrial prototype was used for developing the anaerobic bioscrubber model in Aspen Plus®, which is presented in the chapter 7 of this doctoral thesis. The development of the model enclosed the calibration and validation stages of the two main units of the anaerobic bioscrubber, these stages are explained and commented hereafter.

The calibration of the scrubber resulted in values of the number of equilibrium stages for the three main solvents of the volatile organic compound emission of the flexographic facility and for the two structured packing materials tested in the experimental study of the scrubber. The number of equilibrium stages were fitted by comparing the experimental and predicted removal efficiency for each solvent and for each packing material. Data used for the calibration corresponded to a set of experiments performed in the experimental study. Data measured on these experiments were: liquid and gas flow rate, inlet and outlet temperature of both phases and inlet and outlet composition of gas phase and inlet and outlet volatile organic compound concentration of the gas phase. The liquid to air volumetric ratio of these experiments covers the ratio tested in the experimental study. The number of equilibrium stages obtained in the calibration of packing A were 0.99 ± 0.07, 0.95 ± 0.1 y 0.94 ± 0.04 m^{-1} for ethanol, ethyl acetate and 1-ethoxy-2-propanol, respectively. The number of equilibrium stages resulted in the calibration of packing B were 0.7 ± 0.06, 0.73 ± 0.06 y 0.78 ± 0.03 m^{-1} for ethanol, ethyl acetate and 1-ethoxy-2-propanol, respectively. The results obtained in the calibration stated that the number of equilibrium stages for each packing material were very similar at the tested conditions and for the solvents of interest in this thesis. Thus, and with the aim of simplified the model, it was decided to use the average value of the number of equilibrium stages as a calibrated parameter, being the height equivalent to theoretical plate 1.05 $\pm$ 0.08 y 1.37 $\pm$ 0.11 m for packing material A and B, respectively. The spray tower configuration was not calibrated, since its industrial application was discarded. Once the scrubber model was calibrated, the validation of the scrubber model was performed by using the data

obtained during the experimental stages where the packed bed configuration was tested. Obtained results exposed that the model predicts the volatile organic compound concentration of the effluent gas phase of the scrubber, being the average relative error below 10%. The relative error in the prediction of the organic load fed to the anaerobic reactor was below 5%.

Regarding the anaerobic reactor, the first step was to decide which process from ADM1 model should be omitted for the model of the anaerobic reactor. Main hypotheses of the model were related to the conditions maintained in the experimental study of the industrial prototype. The processes omitted were: (i) nitrate and sulphate reduction due to the low concentration in the liquid influent of the anaerobic reactor; (ii) nutrient limitation because the dosage was controlled and depended on the organic load; (iii) inhibition due to deviation form optimum pH, since its value was controlled by alkali solution dosage control rules; and (iv) biomass growth and decay because of stable volume of the granular sludge (3 m^3) in the reactor. Then, degradation routes of the main solvents of gas emission of the flexographic facility were defined according to bibliographic data and results obtained at the experimental phase. Ethanol is decomposed into acetic acid and hydrogen, ethyl acetate would be transformed into ethanol and acetic acid, and 1-ethoxy-2-propanol results in ethanol and acetone, which is further degraded into acetic acid. The analyses of the solvent composition of the liquid effluent of the anaerobic reactor did not detect ethyl acetate, hence it was decided to establish full conversion of this solvent to ethanol. Regarding acetone, it was not included in the model, since acetone was not detected in the composition analyses of the liquid effluent of the anaerobic reactor, thus the degradation of 1-ethoxy-2-porpanol was simulated in one step to ethanol and acetic acid. On basis of the above, initial parameters needed for the calibration of the model were those ones related with the Monod-kinetic of ethanol and 1-etoxy-2-propanol acidogenesis and the acetoclastic methanogenesis, which means the volumetric growth rates and the half saturation constants of the ethanol, 1-etoxi-2-propanol and acetic acid ($\nu_{max,\ EtOH}$, $\nu_{max,\ Et2Pr}$, $\nu_{max,\ acetic\ acid}$ $K_{s,EtOH}$, $K_{s,Et2Pr}$ and $K_{s,acetic\ acid}$). With the objective of simplifying the model, a sensitivity analysis was carried out to determine the dominant parameters of the model, which will be selected as the parameters to be calibrated, estimating the rest of parameters based on the literature. The results of the sensitivity analysis determined that the parameters with higher influence were the volumetric maximum growth rate of ethanol and acetic acid. Afterwards, the model was calibrated by using the data obtained in the first stage of the experimental study of the scrubber, which corresponds to the use of packing material A. The validation of the model was performed by using the data of the other

stages where the scrubber was operated as a packed bed. After the calibration and the subsequent validation, the model demonstrated that is able to predict the methane production with an average relative error of 23%. Regarding the volatile fatty acids, the model was able to simulate the volatile fatty acid concentration of the liquid effluent of the anaerobic reactor for those organic loads lower than 24 Kg COD m^{-3} bed d^{-1}, on the other hand, the model was not able to simulate the volatile fatty acid concentration for organic loads higher than the mentioned one, due to the steady-state nature of the model, since it cannot simulate the intraday accumulation of volatile fatty acids. Finally, the thermodynamic model was able to simulate the equilibrium reached between the liquid effluent of the anaerobic reactor and the biogas, being the average relative error in the prediction of the methane content of the biogas stream 5%. Regarding the pH in the anaerobic reactor, the simulated value was slightly lower than the experimental one, since no other ions were taken into account in the system, further on the acetic acid and the carbonates species.

After corroborating the validation of the created model, a design tool for the anaerobic bioscrubber was developed. This tool was created thanks to the connection between Aspen Plus® and Matlab® software. The developed tool permitted to obtain 3D diagrams with all the necessary information to design the anaerobic bioscrubber. Regarding the scrubber design, it is possible to obtain diagrams that relate the removal efficiency of this unit with the liquid velocity, the air flowrate and the height of the packing material for a determinate volatile organic compound emission. Regarding the anaerobic reactor design, the graphs that could be obtained relate the volatile fatty acid concentration of the liquid effluent of the anaerobic reactor with the hydraulic residence time and the organic loading rate fed to this unit. In addition, this tool allows the creation of diagrams with important information regarding the operation of future installations, such as the change of the removal efficiency of the scrubber based on the change in the volatile organic compound emission of the flexographic facility, or the produced biogas and the volatile fatty acid concentration based on the organic loading rate fed to the anaerobic reactor.

Part of the results obtained in the development of the anaerobic bioscrubber model have been recently submitted to Journal of Environmental Management as:

Bravo, D., Álvarez-Hornos, F. J., Penya-roja, J.M., San-Valero, P. and Gabaldón, C. Aspen Plus process-simulation model: Producing biogas from VOC emissions in an anaerobic bioscrubber.

Conclusions and perspectives

The general objective of this doctoral thesis is the study of the performance of an industrial prototype of anaerobic bioscrubber for the abatement of volatile organic compound air emissions from the industrial use of solvents, in order to demonstrate its stability and to optimize its performance.

From the experimental study, the viability and robustness of the anaerobic bioscrubber technology for the abatement of the gas emissions of the flexographic facilities were demonstrated. As a result of the experimental study, the protocols for the commissioning, start-up and operate future installations were established. The study of the scrubber permitted to define the scrubber configuration that obtains a higher removal efficiency of volatile organic compounds with a lower liquid to air volumetric ratio. Moreover, a pressure drop control protocol was implemented and evaluated. This protocol allowed to keep the pressure drop through the scrubber lower than the recommended value in the bibliography. Regarding the anaerobic reactor, the experimental study indicated that the maximum organic load that can be degraded ensuring the stability of the system; in addition, the control rules for the alkali solution and nutrient solution were checked for their future application in industrial facilities.

By using the data obtained at the experimental study, a process simulation model in Aspen Plus® for the two main units of the anaerobic bioscrubber were developed. The scrubber model consisted in a Radfrac module of Aspen Plus® and it was able to satisfactorily predict the concentration of the volatile organic compounds of the gas effluent of the mentioned unit. The number of equilibrium stages obtained in the calibration step were quite constant for the two packing materials tested in the experimental study, thus it was assumed the average value as a calibrated parameter for each packing with the aim of simplifying the model. The approach to model the anaerobic reactor consisted in using several Aspen Plus® reactor modules connected in series. This approach to implement the anaerobic reactor in Aspen Plus® can be expanded to other bioprocess in order to integrate anaerobic systems with other unit operations and also to other solvents of industrial interest such as isopropanol. The anaerobic reactor model was able to predict the production of methane, while the volatile fatty acid concentration was accurately predicted for organic loads lower than 24 Kg COD m^{-3} bed d^{-1}. However, the anaerobic reactor model was not able to simulate the accumulation of the volatile fatty acids for organic loads higher than 24 Kg COD m^{-3} bed d^{-1}, due to the steady-state nature of the model. Furthermore, the election of the ELECNRTL thermodynamic model permitted to simulate the methane content in the biogas.

Finally, the model created in Aspen Plus® was connected to Matlab®, this connection allowed a high transfer of data between both software. This high transfer was used to create a tool that can be used for design and operational optimization purpose of the anaerobic bioscrubber technology.

Future works derived from this doctoral thesis could continue in the line of creating the dynamic anaerobic reactor model and to include other ions in the chemistry of the system, with the aim of simulating the intraday accumulation of volatile fatty acids and correct the slight error in the prediction of the pH value.

TABLE OF CONTENTS

1 INTRODUCTION

1.1 Air pollution

Air pollution is a worldwide public health concern. It ranks eighth among the main risk factors, with a 2.5% of total death in developed countries (Genc et al., 2012), moreover it is responsible for 3 million premature deaths each year (Mills et al., 2009). The European Environmental Agency (EEA) indicated that air pollution has substantial economic impacts, increasing medical costs and reducing productivity through lost working days (EEA, 2013). In particular, according to the World Health Organization (WHO), air pollution contributes to lung cancer, cardiovascular and respiratory disease (WHO, 2008). Furthermore, Genc et al. (2012) have documented how air pollution may act on the nervous system, and van Kempen et al. (2010) reported by a few epidemiological studies some association between impaired cognitive function and exposure to air pollution.

Regarding ecosystems, air pollution also damages the environment. EEA (2013) estimated that two-thirds of the protected sites in the European Union (EU) Natura 2000 network are currently severely threatened with air pollution. Besides, climate change and air pollution are linked in several important ways, since ground-level ozone has a contribution to global warming, absorbing part of the infrared energy emitted by the earth and creating warming effects in its surroundings.

In this sense, the reduction of the air pollution is a key factor in the protection of the human health and ecosystem, defining the air pollution as "*the presence of a diverse and complex mixture of chemicals, particulate matter, or of biological material in the ambient air which causes harm or discomfort to humans or other living organism*" (Genc et al., 2012). In accordance with this definition, there are a lot of pollutants and they can be physic (acoustic pollution, electromagnetic o radioactive radiation) or chemical. Regarding chemical pollution, it can be classified as primaries, emits directly to the atmosphere, and secondary pollutants, which are not emitted directly to the atmosphere and they are produced as a result of the interactions of other species. A list of pollutants emitted to the air are itemized in annex 2 of Directive 2010/75/EU of the European Parliament and of the council of 24 November 2010 on industrial emissions (integrated pollution prevention and control), this list is detailed below:

1. Sulphur oxides and other sulphur compounds.
2. Oxides of nitrogen and other nitrogen compounds.
3. Carbon monoxide.

4. Volatile organic compounds (VOCs).
5. Metals and their compounds.
6. Dust including fine particular matter.
7. Asbestos (suspended particulates, fibers).
8. Chlorine and its compounds.
9. Fluorine and its compounds.
10. Arsenic and its compounds.
11. Cyanides.
12. Substances and mixtures which have been proven to possess carcinogenic or mutagenic properties or properties which may affect reproduction via the air.
13. Polychlorinated dibenzodioxins and polychlorinated dibenzofurans.

1.2 Importance of VOC control

The volatile organic compounds are defined in the current law as any organic compound as well as the fraction of creosote, having at 293.15 K a vapor pressure of 0.01 kPa or more, or having a corresponding volatility under the particular conditions of use (Directive 2010/75/EU).

However, all compounds do not have the same reactivity, in this sense the EEA makes a difference between non-methane volatile organic compounds (NMVOC) and methane (CH_4). This distinction is made because each group has different impacts in the environment. Absorption capability of infrared radiation that is emitted by the earth is the main concern about methane emissions, as it increases greenhouse effect with a global warming potential 28 times higher than CO_2 (Intergovernmental panel on climate change (IPCC), 2014). On the other hand, main impacts associated to NMVOC emissions are:

- Potential harm to human health and environment due to their toxicities, carcinogenic and others physiologic effects.
- Odors
- Tropospheric ozone precursors

About this last impact, some perspectives have defined ozone as the main cause of premature death in 2050 (Organization for Economic Co-Operation and Development (OECD), 2012). Ozone is not emitted directly; it is formed by chemical reactions involving primarily NO, NO_2 (emitted during fuel combustion) and VOC in the atmosphere. The chemistry of O_3 formation can be summarized as follows: NO_2 dissociates in atomic oxygen (O) and NO when sunlight is absorbed. Atomic oxygen will form ozone reacting rapidly with molecular oxygen (O_2) to form O_3. On the other hand, NO reacts with O_3 to form NO_2 and O_2 in the air (titration reaction) and therefore contributing to the decay of O_3 concentrations. These reactions keep the atmosphere in an equilibrium state where the amount of ozone is controlled by the relative amounts of NO_2 and NO as well as the intensity of sunlight without the presence of other gaseous substances. However, this state is being perturbed by other pollutants, increasing the level of ozone. For example, VOCs are degraded to produce substances that react with NO to produce NO_2 without consuming O_3, thus perturbing the equilibrium of the titration reaction.

This increase of ground-level ozone can damage the environment by impairing reproduction and growth of the plants, reducing biodiversity and decreasing photosynthesis, thereby reducing plant uptake of carbon dioxide (EEA, 2010). Ozone can also have effect on human health, estimating that some 21 000 premature deaths and 14 000 respiratory hospital admissions per year are linked with ozone within 25 European Countries (WHO, 2008). Excessive exposure to O_3 can cause respiratory health problems, such as breathing problems, asthma, reduced lung function, and other lung diseases. There is also new evidence linking long‐term exposure to ozone with deterioration in productive health (WHO, 2013).

In addition to these previous effects, ozone is the third-most important greenhouse gas, after CO_2 and CH_4; but O_3 is a short-lived greenhouse hence a decrease in the ground level production will reduce atmospheric ozone concentrations within a short period of time (EEA, 2013). In order to face all these problems, Directive 2008/50/EC of the Parliament and of the Council of 21 May 2008 on ambient air quality and cleaner air for Europe establishes the threshold for ozone (Table 1.1).

Table 1.1. Air quality standards for ozone as defined in the Air Quality Directive (Directive 2008/50/EC).

Objective	Period	Target or threshold value	Number of allowed exceedances
Human health	Maximum daily 8-hour mean	120 μg m^{-3} (c)	25 days per year averaged over three years
Vegetation	*AOT40 accumulated over May-July	18 00 (μg m^{-3}) h averaged over five years	
LTO (a) health	Maximum daily 8-hour mean	120 μg m^{-3}	
LTO vegetation	AOT40 accumulated over May-July	6 000 (μg m^{-3}) h	
Information	One hour	180 μg m^{-3}	
Alert (b)	One hour	240 μg m^{-3}	

(a) Long Term Objective
(b) To be measured over three consecutive hours
(c) Target value to be met by 1 January 2010.
* index of accumulated exposure index above a threshold concentration of 40 ppb

Target value threshold for O_3 of 120 μg/m^3 was exceeded on more than 25 days per year at a large number of stations across Europe in 2014, as it can be observed in Figure 1.1 where the 26th-highest recorded daily maximum 8-hour average O_3 concentration is plotted. Higher concentrations in some Mediterranean countries could be explained due to the need of sunlight in the formation of O_3. It is important to note that WHO establishes the 8-hour mean ozone concentration in 100 μg m^{-3}, reducing the previous limit from 120 μg m^{-3} 8-hour mean based on the conclusive links between daily mortality and O_3 concentrations below 120 μg m^{-3} (WHO, 2006).

The amount of the primarily emissions responsible for the formation of harmful ground level O_3 since 2000 to 2014 have decreased in the EU-28, carbon monoxide emissions were cut by 35 %, NMVOC by 40 %, NO_X by 40 %, and CH_4 by 25 %, approximately (EEA, 2016). Anyway, the NMVOC reduction should continue

to achieve the goal of 57% reduction of emissions in 2030 established by the European Commission (EC) (EC, 2013). The main contributor to NMVOC emissions in 2014 is the industrial source (EEA, 2016), whose contribution has reduced around 20% compared to 2000, but efforts on VOC control are still required.

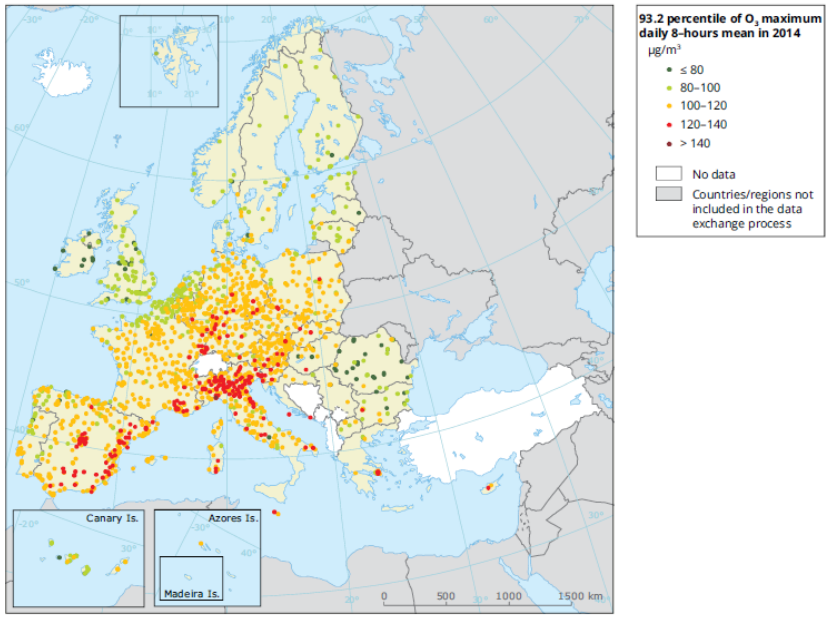

Notes: Observed concentrations of O_3 in 2014. The map shows the 93.2 percentile of the O_3 maximum daily 8-hour mean, representing the 26th highest value in a complete series. It is related to the O_3 target value, allowing 25 exceedances over the 120-µg/m³ threshold. At sites marked with red and dark red dots, the 26th highest daily O_3 concentration were above the 120-µg/m³ threshold, implying an exceedance of the target value threshold. Only stations with more than 75 % of valid data have been included in the map.

Figure 1.1. 26th-highest recorded maximum daily 8-hour average O_3 concentration at each monitoring station in 2014 (EEA, 2016).

It is noted that in the specific literature the term VOC refers to non-methane volatile organic compounds. Therefore, the term VOC refers to non-methane VOC hereafter in this document.

1.3 Industrial sources of VOCs

Emission of VOCs can come from human activities or from natural sources. The main natural source is the vegetation; whose emission depends on the temperature. The main anthropogenic sources are activities that involve the use of solvents, road transport and refineries. Figure 1.2 shows the main human sources

contributing to VOC emissions in EU in 2014. The most important VOC source was industrial processes and product use, whose contribution was 49%.

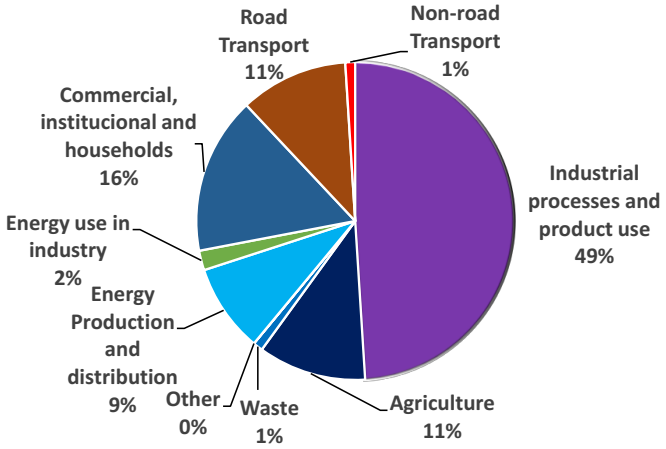

Figure 1.2. Contribution to EU VOC from main source sectors (EEA, 2016).

Regarding the distribution of emissions within EU-28, Table 1.2 summarizes the five countries that emitted more VOC and their contribution to the total emission in Europe. As it can be seen, the contribution of these countries, including Spain, is close to 60% of the total emission.

Table 1.2. Countries within EU-28 whit more percentage of emission in the year 2014 (EEA, 2016).

Country	Emissions, Gg	%
Germany	1041	15.5
Italy	849	12.6
United Kingdom	819	12.2
France	639	9.5
Spain	614	9.1

Within industrial processes and product use, the use of solvents plays a significant role, EEA (2014) estimated that its share in 2012 was 44% of the VOC total emission in EU-28. The industry of solvent contributes substantially to the economic and social welfare in Europe: it directly employs more than 10 000 people in Europe, but indirectly accounts for more than 10 million jobs. More than 80% of the companies are Small and Medium Sized Enterprises (SME). Manufacturers of solvents across Europe have an estimated combined turnover of about €2.5-3.5

billion. Companies using solvents have an estimated combined turnover of more than €200 billion (European Solvents Industry Group, 2015).

This thesis dissertation focuses in the flexographic industry which is included in the surface treatment and ink sectors. A brief overview of the flexographic industry is provided in the next section.

1.3.1 Flexographic industry

The graphic sector, to which the flexographic industry belongs, represents 17% of the European printing technologies, contributed around 1.7% of the total turnover in 2003 (Ernst and Young, 2007). Regarding European printing industry, it is highly fragmented and more than 85% of the industrial structure is composed by SME employing less than 20 workers in 2004. There were around 125 000 printing firms, employing 970 000 people in the 25 European countries. UK, Germany, France, Italy, Belgium, The Netherlands and Spain account for more than 80% of the overall EU turnover, representing more than 72% of the overall number of companies in EU-25 (EC, 2007).

Flexography is the printing method with rotary press raised image, which uses plates or stencils of highly-resilient flexible material and quick-drying fluid inks, with evaporation by means of hot air, or, as in the offset system, by using infrared or ultraviolet radiation. Flexographic technology is mainly used to print plastic containers, corrugated paper, cardboard, paper bags, labels, paper for wrapping food products and industrial uses and shower curtains. In general, the ink is transferred by an inking cylinder to the transfer cylinder, located above the plate cylinder, which inks the surface of the stencil or flexography plate. The ink is transferred by contact onto the support to be printed, which in turn is pressed by the impression cylinder.

The inks used in the flexographic industry can be classified in UV-inks, solvent-based or water-based inks. UV inks, which are increasingly applied in flexo printing, consist of binders, additives, photo-initiators and the dyestuff. All these components are solid material and they do not contain solvent. In water-based inks, the water concentration in the purchased printing inks is normally in the range of 50- 60%. Aqueous dispersions, such as styrene-acrylate copolymer are mainly used as binding agents. As drying additives, ethanol and isopropanol are added in low concentration, mostly below 5%. In solvent-based inks, the concentration of the organic solvent in the ink ranges between 60 – 80%. The most common solvents are ethanol and ethyl acetate. Isopropanol, n-propanol, methoxy propanol and ethoxy

propanol are other solvents that can be found in less quantity. In general, the solvent choice will depend on many aspects, such as the need to avoid solvent attack on a film or solvent coating, and to ensure that as little solvent as possible remains in the product, especially with food packaging. Only very rarely it is necessary to deviate from ethanol, ethyl acetate and mixture of the two. Occasionally MEK, acetone, toluene (packaging for medical purposes) or isopropanol (non-food paper product) may be found. The solvent-based inks are more used, since UV- and water-based inks need more energy to dry. UV inks need UV light to cure it and special equipment on the press. As the high-energy supply to the lamp is turned into heat, large installations for cooling are also needed. For water-based inks, an increase in the energy consumption of the driers of some 10% is often found (EC, 2007).

Regarding flexographic air emissions, they are characterized by high air flow rates and low VOC concentration (Sempere et al., 2012), temperatures ranging in 40 and 70°C and relative humidity varied from 5 and 15% (Rothenbuhler et al., 1995). The compounds in the air emission will depend on the organic solvents employed in the package printing process. Table 1.3 shows a choice of typical organic solvents together with their field of application. The Henry constant of the solvents at 25°C have been included in Table 1.3, since the selection of the technology for the abatement of VOC emissions is sometimes driven by Henry constant value. Their values are collected in Sander (2015). This compilation contains 17 350 values of Henry constant for 4 632 species from 689 references.

Table 1.3. Typical solvents used in solvent-based packaging printing processes (EC, 2007; Sander,2015).

Solvent	Vapor pressure, kPa at 25°C	Henry constant, H_{cp} M atm^{-1} at 25°C	Field of application
Ethyl acetate	9.2	6.5	Thinner, cleaning agent
Ethanol	5.9	$2.0 \cdot 10^2$	Solvent in ink, cleaning agent
Isopropanol	4.3	$1.3 \cdot 10^2$	Solvent in ink, cleaning agent
Isopropyl acetate	6.1	2.9	Viscosity adjuster
Methyl ethyl ketone	10.5	$2.0 \cdot 10^1$	Solvent in adhesives and some varnishes
n-Butanol	1.2	$1.3 \cdot 10^2$	Retarder
Methoxy propanol	1.1	---	Retarder
n-Propanol	2.5	$1.3 \cdot 10^2$	Retarder
Ethoxy propanol	0.65	---	Retarder

Directive 2010/75/EU of the European Parliament and of the council of 24 November 2010 on industrial emissions (integrated pollution prevention and control) specifies that these emissions should be treated. Annex VII of this law established the technical provisions relating to installation and activities consuming organic solvents. Available technologies to treat these emissions were summarized by EC in the Best Available Techniques (BAT) Reference Document for Common Waste Water and Waste Gas Treatment/Manage Systems in the chemical sector (EC, 2016). The techniques are classified in recovery techniques, such as membrane separation, condensation, adsorption and wet scrubbing and abatement techniques such as bioprocesses (biofiltration, bioscrubbing, biotrickling) and thermal oxidation. These techniques and their principles are described hereafter.

1.4 Techniques to control air emissions of VOCs

Air emissions can be controlled by two strategies: source control or waste gas treatment. Source control involves the reduction of emissions through raw product substitution, reduction or recycling. These mechanisms could reduce the quality of the product or may increase costs. Among waste gas treatment, the selection of the technology is often dictated by economic and ecological constraints and sometimes combinations of various technologies may be required to meet regulatory standards (Devinny et al., 1999). However, it is recommended to take into account the flow rate and the pollutant concentration to select the proper method. Figure 1.3 gives the applicability range of various air pollution control technologies based on the air flow rate and the pollutant concentration (Singh et al., 2005). It is important to note that this Figure does not consider the nature of the pollutant, hence it can be used as a screening of the possible solutions for a specific emission. Next sections provide a brief summary of available waste gas treatments and their applicability.

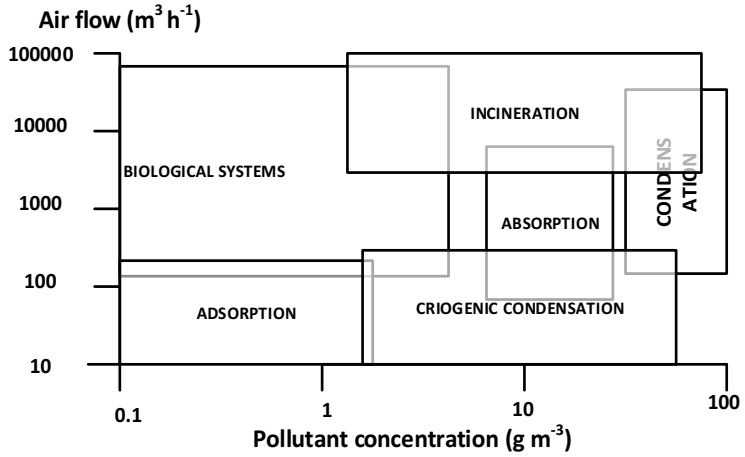

Figure 1.3. Recommendations for the selection of the technology to treat VOC emissions based on the air flow rate and VOC concentration. Adapted from Singh et al. (2005).

1.4.1 Thermal oxidation

Thermal oxidation is the most widely used control technique, but costs are high for low concentration pollutant vapors because of the need for large amounts of fuel (Devinny et al., 1999). Regenerative or recuperative heat systems are often used as an attempt to reduce these fuel-operating costs. Thermal incineration involves the combustion of pollutants at temperatures of 700 to 1 400^{o}C, while the use of catalysts allows process temperatures between 300 and 700^{o}C. Due to energy costs, incinerators are better applied to air with high concentrations of organics. The removal efficiency of this technology ranges from 95% to 99% destruction of VOCs, but dioxin production is possible. As advantages, incineration is insensitive to fluctuations, downtime, and the type of pollutant treated (Delhoménie and Heitz, 2005). The drawback of this technology is that it produces NOx, which contributes to other environmental problems (such as smog and acid rain) and even with recuperative heat systems, it still consumes a considerable amount of energy if the inlet VOC concentration is below the autothermal limit, which is about 2-3 g m^{-3}. The burner always needs a pilot flame which consumes energy (EC, 2007).

1.4.2 Adsorption

The adsorption is a physical process where the gas molecule is adhered to the solid surface (adsorbent), which has more affinity to certain compound, hence

they are eliminated from the waste gas. Each adsorbent has a maximum capacity of adsorption, once this limit is reached the efficiency decreases. At this point, the adsorbent needs to be reactivated and the solvents may be recovered or destroyed. Desorption is often performed by sweeping with a hot gas stream, but can also be carried out by vacuum or by heat treatment. Adsorbents more widely used are activated carbon and zeolite. This technique could reach removal efficiencies ranged between 90-99% and should be applied for waste gases with solvent concentration up to 0.8 g m^{-3} (Delhoménie and Heitz, 2005; EC, 2007). As a drawback, the humidity should be less than 50% because water vapor will also be adsorbed, thus reducing the adsorption capacity of the adsorbent. As it has been mentioned, the absorbent should be regenerated, and after a longer period the adsorbent cannot be fully reactivated and should be disposed of.

1.4.3 Absorption

The most common absorption technologies are spray chambers, sieve trays, plate columns or packed columns. These units try to enhance the mass transfer process between the gas phase and liquid phase. Absorption units are designed to achieve removal efficiencies ranged between 90-98% but this technology could be only applied to VOC with high solubility in the liquid phase. The main drawback of this technology is that the liquid stream with the solvents should be treated (Delhoménie and Heitz, 2005). Since mass transfer underlies in all design equations, a brief overview of this process is provided hereafter.

Basically, mass transfer into each fluid stream is accomplished by two mechanism. The pollutant species move from the bulk of the gas stream to the gas-liquid interface by turbulent eddy motions. Very close to the interface, the pollutant must pass the remaining distance by molecular diffusion. On the liquid side of the interface the process is reversed. The mass transfer rate, N_A, for each phase could be expressed in terms of the mass transfer coefficient, *k,* and a driving forced based on the bulk and interfacial concentrations for that phase. For the liquid phase:

$$N_A = k_L (C_{Ai}-C_{AL}) = k_x(x_{Ai}-x_{AL}) \quad (1.1)$$

Where k_L is the individual liquid mass transfer coefficient based on concentration, in m s^{-1}; C_{Ai} is the concentration of solute A in the liquid phase at the interface, mol m^{-3}; C_{AL} is the concentration of A in the bulk of the liquid, mol m^{-3}; k_x is the individual liquid mass transfer coefficient based on mole fractions, mol s^{-1} m^{-2}; x_{Ai} and x_{AL} are the mole fraction of A in the liquid phase at the interface and in the bulk of the liquid phase, respectively.

For the gas phase:

$$N_A = k_G (P_{AG}-P_{Ai}) = k_y (y_{AG}-y_{Ai}) \quad (1.2)$$

Where k_G is the gas phase mass transfer coefficient based on partial pressure, in moles m^{-2} s^{-1} Pa^{-1}; P_{AG} and P_{Ai} are the partial pressure of A in the bulk of gas phase and at the interface the gas phase in Pa, respectively. k_y is the gas mass transfer coefficient based on mole fractions, mol s^{-1} m^{-2}; y_{AG} and y_{Ai} are the mole fraction of A in the bulk of gas phase and at the interface the gas phase, respectively.

In general, this approach to determine N_A is not practical, since values of k_X and k_y are difficult to obtain, and the values of concentration in the interface are also difficult to measure. When mass transfer rates are reasonably low, so the major resistances to mass transfer still lie in the liquid and gas phases, and not at the interface, it is convenient to express the rate N_A by the equation (1.3).

$$N_A = K_G (P_{AG}-p_A^*) = K_y (y_{AG}-y_A^*) \quad (1.3)$$

Where K_G and K_y are defined by these equations as local overall mass transfer coefficients. The interpretation of P_A^* is the equilibrium partial pressure of solute A in a gas phase which is in contact with a liquid having the concentration C_{AL} in the bulk of the absorption liquid. The quantity y_A^* is defined similarly in terms of a liquid with a mole fraction X_{AL} of the bulk liquid. The usefulness of equation (1.3) is usually restricted to the situation where the resistance to mass transfer is primarily in the gas phase, which characterizes most of absorption problems in air pollution work (Wark et al., 1998).

1.4.4 Condensation

The VOC concentration should be above 5 000 ppm (Khan and Ghosal, 2000) and the contaminants should have a high boiling point (above 40°C) to apply this technology. The waste gas contaminants will be partially recovered by simultaneous cooling and compressing of the gaseous vapors. This technique must often be followed by additional removal technologies for compliance with regulatory standards (Delhoménie and Heitz, 2005). Condensation by applying temperatures above 0°C is only applicable to low volatile solvents. If temperatures below 0°C are used, the humidity in the waste gas will cause icing, requiring de-icing at regular intervals. Usually condensation step at temperatures above 0°C is used upstream to reduce water content.

1.4.5 Membrane systems

Membrane systems can be used to transfer VOCs from an air stream to a water phase. The separation is driven by a pressure differential between both sides of the membrane, a higher vapor pressure can be maintained on the air-feed side than on the permeate side of membrane (approximately 310 to 1 400 kPa). The compressed mixture can be processed through a condenser where portions of the organic vapors are recovered. The remaining air stream is then passed across the surface of a microporous hydrophobic membrane constructed of materials such as polyethylene and polypropylene. The resulting products are permeated stream containing most of the organic compounds and air stream containing residual organic compounds. The performance of VOC recovery is 50-98%, the VOCs are concentrated 5-100 times, hence it is possible to valorize them. Membrane separation processes are capable of handling large amount of VOC but the major drawback is the electricity required to maintain differential pressure across the membrane (Delhoménie and Heitz, 2005).

1.4.6 Biological treatment

Biotechnologies use microbial metabolic reactions to treat contaminated air. Contaminants are transferred from a gas to an aqueous phase were biological reactions occur, converting mainly the contaminants to carbon dioxide, water vapor and organic biomass. These air pollutants are used as energy and, sometimes, as a carbon source for the maintenance and growth of microorganism populations. Biological treatment can treat effectively and economically air flows ranged between 60 and 150 000 m^3 h^{-1} with lower VOC concentrations than other technologies (Berenjian et al., 2012). The particular contaminants must be biodegradable and non-toxic for biological air treatment. The most successful removal in gas-phase bioreactors occurs for low molecular weight and highly soluble organic compounds with simple bond structures. Compounds with complex bond structures generally require more energy to be degraded, which is not always available to the microbes. Organic compounds such as alcohols, aldehydes, ketones, and some simple aromatics demonstrate excellent biodegradability (Delhoménie and Heitz, 2005). Some compounds that show moderate to slow degradation include phenols, chlorinated hydrocarbons, polyaromatic hydrocarbons, and highly halogenated hydrocarbons. The aerobic degradation of the solvents from the flexographic have been widely tested in biotrickling systems with pure compounds such as isopropanol (San-Valero et al., 2013), or a mixture of ethanol, ethyl acetate and methyl- ethyl ketone (Sempere et al., 2008) and at industrial scale (Sempere et

al., 2012). The advantage of these systems lies in the fact that they do not produce NO_x, besides they are an adaption of the process by which atmosphere is self-cleaned (Rothenbuhler et al., 1995). Biological treatments are economical and environmentally sustainable technologies that are considered to be alternative to physicochemical treatments for treating pollutants of low concentration, soluble and biodegradable in nature (Cox and Deshusses, 1998; Le Cloriec et al., 2001).

In the 1980s, biofiltration market grew rapidly, and 1990s were the golden era of R&D on biological waste gas technology in Europe. The 3 major constructions are biofilter, biotrickling and bioscrubbers, with a total of 7 500 biological waste gas systems in Europe in 2005 in the odour control field (van Groenestijn and Kraakmaan, 2005). The differences between these technologies are in the phase of microbes (may be suspended or fixed) and the state of the liquid that may be flowing or stationary; their principles are explained hereafter.

1.4.6.1 *Biofilters*

Microorganisms grow on a biofilm in the surface of a medium or are suspended in the water phase surrounding the medium particles. The filter-bed medium consists of relatively inert substances (compost, peat, etc.), which ensures large surface attachment areas and additional nutrient supply. As the air passes through the bed, the contaminants in the air phase are transferred to the biofilm and onto the filter medium, where they are biodegraded. Biofilters use a combination of basic processes: adsorption, degradation and desorption of gas-phase contaminants. The moisture and the nutrients are controlled by adding water. In general, the gas stream is humidified before entering the biofilter reactor. However, if humidification proves inadequate, direct irrigation of the bed may be needed (van Groenestijn and Hesselink, 1993).

The removal capacity of a biofilter is governed by the properties and characteristics of the support medium, which include porosity, degree compaction, water retention capabilities, and the ability to host microbial populations. Biofilters are typically used for the treatment of large volumes of air streams containing low VOCs or odorants concentration. The advantages are the cost-effective treatment of large volume of low VOC concentration, combining with the fact that secondary wastes are not produced (Rene et al., 2013). The disadvantages are the clogging of the medium due to particulate matter, the progressive deterioration of the medium and its low efficiency at moderately high concentrations of pollutants.

1.4.6.2 *Biotrickling filters*

The biotrickling filters (BTFs) are similar to the biofilters. The footprint required is less than for biofilters, but their height is usually larger. In BTF, the pollutant gas is fed either up-flow or down-flow to the bioreactor. The main difference between the BTF and biofilter is that a liquid phase is continuously fed or recirculated over the packed bed in the BTF. This allows better control of parameters such as medium acidification or filter bed drying out (Kennes and Veiga, 2013). These kinds of processes are more adapted for the elimination of water soluble VOCs, being the solubility specifications less stringent than for bioscrubber (Henry coefficient <0.1 gas concentration/liquid concentration, dimensionless), since the contact between microorganisms and the pollutants occur simultaneously (Cox and Deshusses, 1999). The advantages of this technology are low operating capital cost, low pressure drop and capability to treat acid degradation products of VOCs. Limitations are accumulation of excess of biomass in the filter bed and production of secondary waste streams.

This technology is currently applied in the flexographic sector. It should be pointed out that the protocols developed in the laboratory and at pilot scale by the research group GI^2AM of the University of Valencia have been a reference in the application of this technology for the treatment of high soluble VOCs in the flexographic sector. Sempere et al. (2012) published the first example in Europe of a BTF as a final solution for the flexographic sector. This paper compiled the performance of the BTF during 12 months for the treatment of emissions mainly composed by ethanol, n-propanol, n-propyl acetate and 1-methoxy-2-propanol. The reported elimination capacity was 50 ± 11 g-C m^{-3} h^{-1} for 56 ± 15 g-C m^{-3} h^{-1} of inlet loads at an empty bed residence time of 32 ± 7 s. The maximum elimination capacity obtained in this study was 122 g-C m^{-3} h^{-1} for an inlet load of 138 g-C m^{-3} h^{-1}. A second example was published by San Valero et al. (2015). These researchers studied an industrial BTF located in a flexographic facility whose emission was composed by a mixture of VOCs (63% ethanol, 22% ethyl acetate and 13% 1-ethoxy-2-propanol). The BTF was operated for more than one year and elimination capacity values of 17.9 and 29.1 g-C m^{-3} h^{-1} were obtained for inlet loads of 27.5 and 46.5 g-C m^{-3} h^{-1}, respectively.

1.4.6.3 *Bioscrubber*

The absorption occurs in a scrubber unit in bioscrubber technology and afterwards the contaminants degradation is performed by a suspended growth biological process in a separated reactor (Figure 1.4). Absorption may be achieved

in packed column, spray tower or bubble column. The water is transferred to the bioreactor, where optimal environmental conditions for degradation are maintained. This step regenerates the scrubbing liquid. Nutrients may be added to the scrubbing liquid if necessary to stablish optimal conditions for the growth of microorganisms.

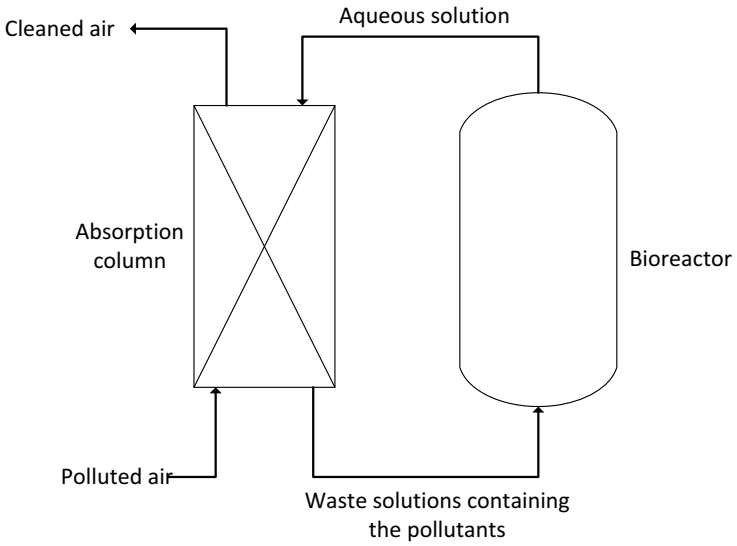

Figure 1.4. Schematics of a bioscrubber unit.

Van Groenestijn and Hesselink (1993) classified the feasibility of biotrickling and bioscrubber to treat VOC emissions depending on the Henry constant. According to these authors, biotrickling filter is recommended for pollutants with Henry coefficient lower than 0.1 (H_{cc}, gas concentration/liquid concentration, dimensionless), and in case bioscrubber technology, if Henry coefficient is lower than 0.01 (H_{cc}, gas concentration/liquid concentration, dimensionless). Bioscrubbers provide substantial advantages for waste gas treatment because of less space requirements, reliable operation, process control, low risk of clogging, low operating cost and capacity to handle higher gas loads (up to 3 000 - 4 000 m^3 m^{-2} h^{-1}) than biotrickling filters and biofilters. In this system, volumetric air to liquid ratio usually varies from 300 to 500, which corresponds to volumetric liquid to air ratio ranging between $2 \cdot 10^{-3}$ and $3.33 \cdot 10^{-3}$ (Kennes et al., 2009). Bioscrubbers offer more advantages than conventional biofilters and biotricklings and chemical scrubbers when high amount of contaminants should be treated. However, bioscrubbers are less popular treatments for VOCs since most of VOCs are volatile and low water soluble, but recent advances on process designs indicate a growing

interest in its applications (Le Cloriec et al., 2001). Kellner and Flauger (1998) suggested that soluble VOCs such as alcohols and ketones at concentrations of less than 5 g m^{-3} were efficiently treated in bioscrubber.

Some specific examples can be found in the literature for pure solvents. Hammervold et al. (2000) investigated the elimination of acetone from an air stream using a slurry bioscrubber. They reported 81.5% acetone removal with an air flow rate of 0.75 m^3 min^{-1} and liquid flow rate of 2 L min^{-1}, the acetone concentration in the air flow ranged between 10 and 100 ppm_v. DeHollander et al. (1998) reported the control of methanol emissions using a single-stage, laboratory-scale, suspended-growth bioscrubber with efficiencies varied from 69% to over 80%. The experiments on the absorption efficiency were conducted using once-through flow of tap water with a temperature of 12-13°C and water flow rates ranged from 0.5 to 1.0 L min^{-1}. Regarding the gas phase, air flow rates was 500 L min^{-1} and methanol concentrations was either 50 or 100 ppm_v. Le Cloriec et al. (2001) studied the ethanol removal using a bioscrubber, they obtained removal efficiencies higher than 90% with an air load of 0.819 kg $m^{-2}s^{-1}$ and liquid load of 0.560 kg m^{-2} s^{-1} for an inlet concentration of 559 mg m^{-3}.

Some attempts to treat waste gas emissions from printing sectors have been also reported. Le Cloriec and Humeau (2013) reported a bioscrubber treating a gaseous emission from a paint workshop. The air flow was 31 000 m^3 h^{-1} and the emission was mainly composed by ethanol, ethyl acetate, acetone, methyl ethyl ketone, isopropanol and ethoxypropanol at concentrations between 0 and 10 g-C m^{-3}. The achieved removal efficiency was 80% with an inlet concentration of 900 mg m^{-3}. The energy balance of the system gave a consumption of about 1 170 MWh per year. The investment was 230 000€, and the operating cost was 68 000€ for 5 280 h per year. Other example was the research carried out by Dobslaw et al. (2007), the bioscrubber treated a waste air of a printing company, the main compounds treated were ethanol, butanol and the ethers 1-methoxy-2-propanol and 1-ethoxy-2-propanol. Waste gas concentrations were up to 1 200 mg-C m^{-3} and concentration in the treated air did not reach 150 mg-C m^{-3}. Granström et al. (2002) ran an experiment to treat an air stream from a printing process, the average exhaust gas flow rate channeled to the bioreactor unit ranged between 1.68 and 3.72 m^3 h^{-1}. The composition of the gas stream from the printing press was per m^3 of VOCs: 4.7 g ethanol, 0.7 g 3-ethoxy-1-propanol, 0.5 g ethyl acetate, 0.3 g isopropanol, 0.1 g n-propanol, 0.04 g 1-methoxy-2-propanol, giving a total concentration of 3.4 g-C m^{-3}. After the bioscrubber column the VOC concentration dropped down to a level of 20 mg-C m^{-3} being only 0.6% of the original carbon amount.

In spite of these attempts, aerobic bioscrubber is not still well-utilized within the biotreatment market due to the high-energy consumption of the aerobic bioreactor. In contrast, anaerobic degradation of solvents could be an alternative to recycle waste gases into bioenergy with a positive net energy balance. To the best of our knowledge, there are not previous literature about coupling a scrubber and an anaerobic reactor for treating VOC waste gases, although the anaerobic degradation of solvents such alcohols (Eichler and Schink, 1985; Widdel, 1986; Zellner and Winter, 1987) or esters (Oktem et al., 2007; Yanti et al., 2014) is well documented.

1.5 Anaerobic degradation of solvents

As it has been reported, the scrubber technology is suitable for the treatment of VOC emissions, but the scrubbing liquid should be treated to reuse it. According to Ince et al. (2011) anaerobic processes, compared to aerobic treatment, have several advantages such as low volume requirements, low sludge production, low energy consumption and generation of biogas, mainly composed of methane, that can be used to obtain energy in the facilities where the anaerobic reactor is installed. In addition, this technology is gaining popularity for a wide range of industrial effluents that contain organic solvents.

1.5.1 Process fundamentals

The anaerobic degradation process can be divided in three steps (Tchobanoglous et al., 2003) and it is summarized in Figure 1.5:

- Hydrolysis: this stage is carried out by the action of extracellular enzymes excreted by the fermentative bacteria, and it consists in the transformation of complex organic matter such as proteins, carbohydrates and lipids into simple soluble products like sugars, long-chain fatty acids, amino acids and glycerin.
- Acidogenesis: the compounds from hydrolysis step are broken down to more simple compounds with lower molecular weight such as acetic acid, propionic and butyric, mainly, other minor products can be obtained such as alcohols, ammonium, carbon dioxide and hydrogen, depending on the conditions. The intermediate compounds obtained in the previous step are broken down to acetic acid, hydrogen and carbon dioxide, which are the appropriate substrates to methanogenic step.

- Methanogenesis: Finally, both acetic acid and hydrogen are raw material for the growth of methanogenic bacteria, converting acetic acid and hydrogen to biogas that is composed mainly by methane, carbon dioxide, with some hydrogen sulfide. Approximately, 70% of the methane is formed from acetic acid by acidotrophic methane bacteria. The remaining 30% are obtained by the utilization of hydrogen and carbon dioxide by hydrogenotrophic bacteria (Grady, 1997; Schink, 1997). If hydrogen concentration increases above a minimal level (10^{-4} atm), the conversion to acetate by the acetogens will be reduced.

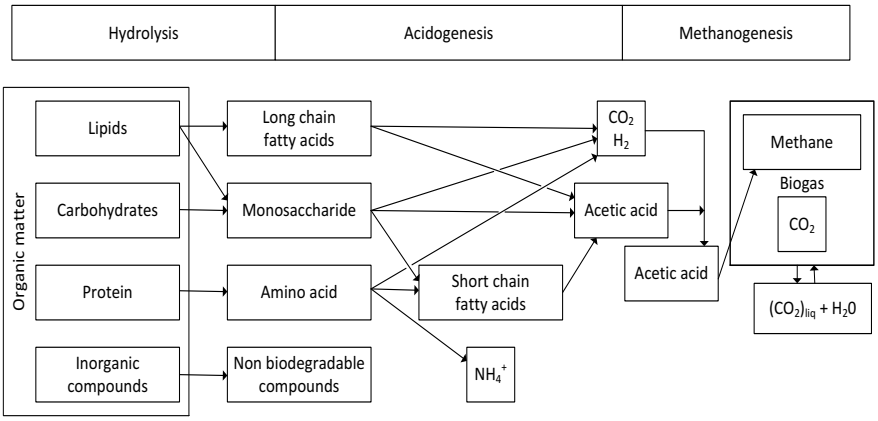

Figure 1.5. Schematic of the process responsible for the degradation of complex organic substances to CH_4 and CO_2.

Almost all of the removed energy from the liquid being treated is recovered in methane with the exception of the electrons incorporated into the formed cell material. Chemical oxygen demand (COD) is a measure of the oxygen required to accept the electron available in an organic compound when the compound is completely oxidized to carbon dioxide and water. One mole of methane requires two moles of oxygen. Consequently, each 16 grams of methane correspond to the removal of 64 grams of COD from the liquid. At temperature of 0°C and pressure of 1 atm, this corresponds to 0.35 Nm^3 of methane for each kg of removed COD (Grady et al., 2011).

Hereafter is presented the anaerobic degradation mechanism of the solvents of interest of this thesis (ethanol, ethyl acetate and glycol ethers), which are typically found in the flexographic sector emissions.

1.5.1.1 *Anaerobic degradation of ethanol*

The anaerobic degradation of ethanol can occur by different ways, depending on the sulfate concentration in the wastewater. The several acetogenesis, sulfate-reducing and methanogenesis reactions involve in the degradation of ethanol are summarized in Table 1.4. In absence of sulfate, most of the anaerobic degradation of ethanol is performed by a syntrophic relation between acetogenic bacteria and methanogenic archaea. If there is sulfate in the wastewater, ethanol is used as a substrate for sulfate-reducing bacteria, obtaining hydrogen sulfide as a final product.

Table 1.4. Acetogenic, sulfate reducing and methanogenic reactions involve in anaerobic degradation of ethanol. Adapted from Kalyuzhnyi et al. (1997) and Thauer et al. (1977).

Acetogenic reactions		
$C_2H_5OH + H_2O \rightarrow CH_3COO^- + H^+ + 2H_2$	$\Delta G^0 = +9.6$ kJ mol^{-1}	(1.4)
Sulfate reducing reactions		
$2C_2H_5OH + SO_4^{2-} \rightarrow 2CH_3COO^- + H^+ + HS^- + 2H_2$	$\Delta G^0 = -66.4$ kJ mol^{-1}	(1.5)
$CH_3COO^- + SO_4^{2-} \rightarrow 2HCO_3^- + HS^-$	$\Delta G^0 = -47.6$ kJ mol^{-1}	(1.6)
$4H_2 + H^+SO_4^{2-} \rightarrow HS^- + 4H_2O$	$\Delta G^0 = -38.1$ kJ mol^{-1}	(1.7)
Methanogenic reactions		
$CH_3COO^- + H_2O \rightarrow CH_4 + HCO^-$	$\Delta G^0 = -31$ kJ mol^{-1}	(1.8)
$4H_2 + HCO_3^- + H^+ \rightarrow CH_4 + 3H_2O$	$\Delta G^0 = -33.9$ kJ mol^{-1}	(1.9)

1.5.1.2 *Anaerobic degradation of ethyl acetate*

The information about the mechanism used by the anaerobic microorganism for the degradation of ethyl acetate is scarce, only some approximations from previous studies about other esters have been found. The anaerobic degradation of this compound is performed by acetogenic bacteria, obtaining acetic acid as a product. Yanti et al. (2014) proposed that ethyl butanoate and ethyl hexanoate is degraded by hydrolytic bacteria into ethanol and butanoic and hexanoic acid, respectively. The carboxylic acid and alcohol will be further degraded through acetogenesis stage into acetic acid and hydrogen, which will be converted into methane. According to this mechanism, ethyl acetate would be degraded into ethanol and acetic acid.

1.5.1.3 *Anaerobic degradation of glycol ethers*

The anaerobic mechanism for glycol ether cleavage, which is generally accepted in the literature, is based on the dioldehydratase-catalyzed reactions.

Kawai (2002) hypothesized the following mechanism for the anaerobic degradation of polyethylene glycol. Gem-diol is produced by a double H/OH interchange (transhydroxylation) (Speranza et al., 2002), then this product collapses to the carbonyl or keto group C=O. Same mechanism could be followed by the 1-methoxy-2-propanol resulting in acetone and methanol (Lafita et al., 2015). So, in the case of 1-ethoxy-2-propanol, it was hypothesized that the final products would be acetone and ethanol.

1.5.1.4 *Anaerobic degradation of acetone*

Acetone is an expected intermediate product in the anaerobic degradation of glycol ethers. Symons and Buswell (1933) proposed that the anaerobic degradation of acetone followed the next general reaction:

$$CH_3COCH_3+H_2O\rightarrow 2CH_4+CO_2 \quad (1.10)$$

Platen and Schink (1987) further observed in an enrichment methanogenic culture that anaerobic degradation of acetone is produced by two cultures that form a syntrophic relation. A fermenting bacterium produces acetate that is further degraded by a co-culture acetate-utilizing methanogens.

$$CH_3COCH_3 + H_2O + CO_2 \rightarrow 2CH_3COO^- + 2H^+ \quad (1.11)$$

1.5.2 Operational process parameters

Due to the complexity of the anaerobic biological process, it is mandatory to control the different factors that can influence on the optimization of the anaerobic process. These factors can be environmental or operational, impacting both to the development and maintenance of a proper microbial population. Hereafter, the main factors that influence on the anaerobic reactor operation are explained. Special reference to granular biomass systems is done, since it was selected to develop the experimental work of this thesis.

1.5.2.1 *Temperature*

The performance of the anaerobic processes is impacted by operating temperature, which influenced in the maximum substrate utilization rates of microorganism. In general, lowering the operational temperature produces a decrease in the maximum specific growth and substrate utilization rates (Lettinga et al., 2001). The operating temperature can be classified depending on the working range in: psychrophilic (below 20 °C), mesophilic (20-45 °C) and thermophilic (over

45 °C) (Wiegel, 1990). Best performance is typically obtained in the optimal region of one of the two higher temperatures ranges, i.e. 30 to 40 degrees for mesophilic or 50 to 60°C for thermophilic. Most anaerobic processes are designed to do so (Grady et al., 2011). The effect of the temperature on the acidogenesis is not very significant because a mixed population of bacteria perform this step and there are always some bacteria that can work at running temperature. On the other hand, methanogenesis is only carried out by a specialized microorganism and they are more sensitive to temperature changes. Nevertheless, anaerobic bacteria have a big capacity to adapt to temperature changes, if the temperature limits of these ranges are not exceeded (Rajeshwari et al., 2000).

In spite of the best performance of the anaerobic processes is in mesophilic and thermophilic ranges, psychrophilic applications are considered appropriate for a big range of wastewater, especially in warm climate areas (Enrigh et al., 2005). There are some successful examples found in the literature, such as the studies of Rebac et al. (1995), who studied an Expanded Granular Sludge Bed (EGSB) reactor fed with a mixture of Volatile Fatty Acids (VFA). They reported 90% of COD removal with Organic Loading Rate (OLR) up to 12 g COD L^{-1} d^{-1} at 10-12°C. Scully et al. (2006) reached 99% of phenol removal at 9.5-15°C with at phenol loading rate of 2 kg m^3 d^{-1}. Furthermore, several authors (Kettunen and Rintala, 1997; Lettinga et al., 1999) observed that anaerobic degradation in psychrophilic conditions is carried out by mesophilic microorganisms that tolerate low temperatures, hence if an acclimation to the low temperatures is performed, high removal efficiencies could be reached.

Despite of the adverse impact of low temperature in the anaerobic process, the rate of growth of methanogenic and acetogenic microorganisms increase when the temperature decreases, since the decay rate is very low at temperatures below 15°C. Thus, it is possible to preserve the anaerobic sludge for long periods without losing much of its activity for seasonal treatment (Lettinga et al., 2001).

1.5.2.2 *pH and alkalinity*

pH has a significant impact on the performance of anaerobic processes, there is a greater decrease in methanogenic activity as the pH deviates from its optimum value. A pH range of 6.8 to 7.4 provides optimum conditions for the methanogens, whereas a pH between 6.4 and 7.8 is considered necessary to maintain adequate activity (Grady et al., 2011). The influence of pH on the acidogenesis ranges from 4.0 to 7.9. A decrease in pH increases the production of VFAs, particularly propionic and butyric acid, at expense of acetic acid. The pH is typically maintained at conditions more optimal for methanogens to prevent the

predominance of acid-forming bacteria, which may cause the accumulation of VFAs (Colussi et al., 2009).

An important parameter in anaerobic digestion is alkalinity, which is a measure of the chemical buffering capacity of the aqueous solution. It is essential that the reactor contents provide enough buffering capacity to neutralize any possible VFA accumulation in the reactor and to maintain pH in the range of 6.8 to 7.4 for stable operation (Tchobanoglous et al., 2003). Among the chemical to fix the alkalinity, sodium bicarbonate is used for supplementing the alkalinity, since it shifts the equilibrium to the desired value without disturbing the physical and chemical balance of the fragile microbial population. Moreover, it is noted that alkalinity is not only important for pH regulation, but also as pool for CO_2. The concentration of bicarbonate alkalinity in solution is related to the carbon dioxide content of the gas and the bioreactor pH:

$$S_{BALK} = 6.3 \cdot 10^{-4} \left(\frac{P_{CO_2}}{10^{-pH}} \right) \quad (1.12)$$

Where S_{BALK} is bicarbonate alkalinity (mg $CaCO_3$ L^{-1}) and P_{CO_2} is partial pressure of carbon dioxide in the gas space (atm). Bicarbonate alkalinity can be obtained from the total alkalinity (S_{TALK}, mg $CaCO_3$ L^{-1}) and VFA concentration (S_{VFA}, mg CH_3COOH L^{-1}) by using the equation (1.13).

$$S_{BALK} = S_{TALK} - 0.71 \cdot S_{VFA} \quad (1.13)$$

The factor 0.71 converts the VFA concentration expressed as acetic acid to $CaCO_3$ and corrects the fact that approximately 85% of VFA anions are titrated to the acid form at a pH of 4 (Grady et al., 2011).

1.5.2.3 *Nutrients*

The presence of ions in the feed is an important parameter because they are required for the production of biomass. The bacteria in the anaerobic digestion process require macronutrients and trace elements for the growth of biomass. The required optimum C:N:P ratio for enhanced yield of methane has been reported to be 100:2.5:0.5 (Rajeshwari et al., 2000). Table 1.5 shows the elemental composition of the methane forming bacteria in the bacterial consortium. In general, nutrient concentration in the influent should be adjusted to a value equal to twice the minimal required nutrient concentration in order to ensure that there is a small excess of nutrients.

For granular systems, the presence of divalent anions in water enhances the formation of primary granules and it has a positive effect of the flocculation ability. Singh et al. (1999) recommended for flocculation of the anaerobic sludge a calcium concentration between 80-150 mg L^{-1}. Same researchers reported that the growth of several methanogens is stimulated by Mg^{2+}, shortening the generation time and they recommended a concentration of 35 mg L^{-1}.

Table 1.5. Elemental composition of methane bacteria. Adapted from Rajeshwari et al. (2000).

Macronutrients		**Micronutrient**	
Element	Concentration, mg kg^{-1}	Element	Concentration, mg kg^{-1}
N	65	Fe	1800
P	15	Ni	100
K	10	Co	75
S	10	Mo	60
Ca	4000	Zn	60
Mg	3000	Mn	20
		Cu	10

1.5.2.4 *Organic loading rate*

Organic load rate plays an important role in anaerobic wastewater treatment. If anaerobic reactor is overloaded high production of biogas will be reached and biomass will wash out and foam will form at the Gas Liquid Solid separator (GLS). Specifically for granular sludge, granulation process is adversely impacted by a high biogas production because it causes shear-off of bacteria cells from granule surface, hence eroding the granule (Syutsubo et al., 1997). On the other hand, Alphenaar et al. (1993) indicated a relationship between substrate concentration in the reactor and granule size. The diameter is probably controlled by substrate diffusion in the biomass. Substrate limitation in the granule center will reduce bacterial growth there, or even cause lysis, which will weaken the granule, resulting in breaking up of the structures.

Other important factor is the variation of OLR, since there is a delicate balance between primary processes (hydrolysis and acidogenesis) and the conversion of the acid products by methanogenic bacteria to methane and carbon dioxide. Strong variation on flow and concentration may adversely influence on the efficiency of the anaerobic process, which can result in accumulation of VFA during overloading. Borja and Banks (1995) tested the effect of shock loads on the

performance of a fluidized bed reactor fed with synthetic ice-cream wastewater. They increased the flow rate by 100 and 150% for 6 and 12 h periods, using the same influent concentration. The response of the reactor was a drop in the pH (from 7.1 to 6.6) with an increase of VFA in the effluent. These authors also tested an increase of the influent COD by 100 and 150% for 6 and 12 h. The effect was essentially the same, but less pronounced. Bhatia et al (1985) investigated the response of a step change in concentration and flow rate in a 9.8 L Upflow Anaerobic Sludge Blanket (UASB) reactor that treated wastewater composed of acetic, propionic and butyric acids. The changes were carried out by varying the concentrations of each acid separately from 600 to 900 mg L^{-1} for 12 h. They concluded that the reactor took approximately one residence time to recover from the shock. Leitão (2004) studied the robustness and stability of UASB treating sewage under tropical conditions. The research was performed by using a set of seven pilot-scale UASB; four reactors were fed with constant flow of 20 L h^{-1} and COD between 200 and 800 mg L^{-1}, the other three reactors were fed with similar COD (800 mg L^{-1}), but different Hydraulic Residence Time (HRT) varying from 2 to 6 h. Under shock load conditions, the reactor resulted in COD removal efficiencies in the same range as during steady state conditions. The effluent COD fluctuated in the same range of the inlet COD variation, demonstrating that the reactors are unable to attenuate strong variations in the OLR.

1.5.2.5 *Hydraulic retention time*

The HRT is related to the up-flow velocity, hence to the contact between the sludge and the wastewater. This parameter is important in granular sludge systems. An acceptable HRT reduces the formation of gas pockets and helps in degasification of the granules (Rizvi et al., 2015). In addition, several studies have demonstrated that the granulation process is carried out at relative high superficial velocities, pointing out that it is not possible the development of the granules if physic stress conditions are not present in the reactor (Alves et al., 2000; O´Flaherty et al., 1997). So, the granulation process is assisted by short HRT and high superficial velocities, because the bacteria that are not able to form granules are washed out from the reactor.

1.5.3 High-rate anaerobic reactors

One of the major successes in the development of anaerobic wastewater treatment was the introduction of high-rate reactors in which biomass retention and liquid retention are not the same. The Anaerobic Filter (AF), developed by James

C. Young in 1968, was one of the first reactors where the Sludge Retention Time (STR) and HRT were not the same. In AF, biomass remain in the reactor by attachment to inert porous support material. During initial experiments with AF, Dr. Lettinga observed that a large proportion of the present sludge aggregated to form granules within the interstitial voids of support media. This finding plus the observation of a completely granular sludge in a full scale clarigester in South Africa, led Dr. Lettinga to conclude that inert support media for biomass attachment was not essential for retention of high levels of active sludge in the reactor (McHugh. et al., 2003). The retention of a high biomass concentration within the system allows the application of high OLR. The maximum permissible load is governed by the amount of the anaerobic bacteria which are in full contact with the wastewater constituents. In anaerobic high rate systems, high sludge concentrations are obtained by physical retention and/or immobilization of anaerobic sludge. This retention can be achieved by all the technologies mentioned in the next subsections.

1.5.3.1 *Anaerobic filter*

AF system uses upflow bioreactors that are filled with media. The presence of the packing allows for the growth of some attached biomass, but the primary role of the media is to retain suspended growth. The OLR for this kind of reactor varied between 5-15 kg COD m^{-3} d^{-1} (Grady et al., 2011).

1.5.3.2 *Upflow anaerobic sludge blanket*

UASB process (Figure 1.6) uses granular sludge biomass, environmental conditions created in the bioreactor lead on the development of a large and dense particles named granules, which allow very high concentrations of suspended solids. The biogas obtained in the reactor is separated by the GLS system that is integral with the bioreactor. The reported value for upflow velocity in UASB ranges between 0.5 and 1 m h^{-1} (van Lier et al., 2008). The ratio between the height and the width of reactor varies between 0.2 and 0.5. This reactor is usually able to treat OLR of 10-15 kg COD m^{-3} d^{-1} (Lim and Kim, 2014).

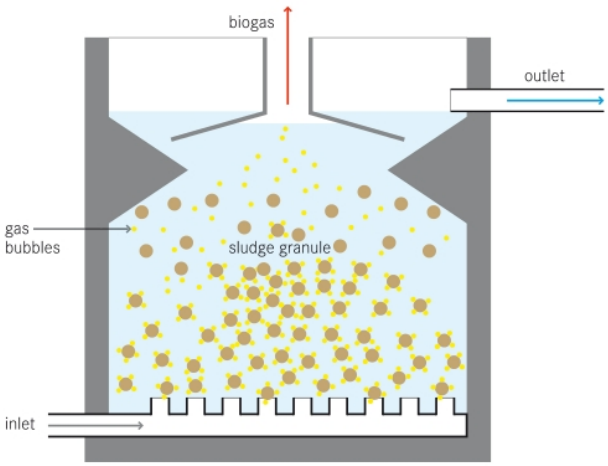

Figure 1.6. UASB reactor.

The EGSB and the Fluidized Bed (FB) systems are regarded as the second generation of sludge bed reactor, achieving higher OLR than UASB.

1.5.3.3 *Anaerobic expanded granular sludge bed*

The EGSB is a modified reactor from UASB in which higher superficial liquid velocities of 5-10 m h^{-1} are applied by recirculating part of the effluent. These high liquid velocities, together with the lifting action of gas evolved in the bed, lead to an expansion of the sludge bed. As a result, an excellent contact between sludge and wastewater prevails in the reactor, hence higher OLR can be applied compared to conventional UASB. The OLR treated by EGSB reactors could be higher than 30 kg COD m^{-3} d^{-1} according to Lim and Kim (2014). Average OLR of 20 kg COD m^{-3} d^{-1} was recorded from 198 full scale EGSB installations (McHugh et al., 2003). Rebac et al. (1995) studied these systems under psychrophilic conditions, treating wastewater with high soluble content with OLR up to 12 kg COD m^{-3} d^{-1} at 10-12°C. The dilution of the inlet thanks to the recirculation allows this system to treat biodegradable compounds that are toxic at high concentration, hence it is suitable to treat industrial and urban wastewater (Zoutberg and Frankin, 1996).

The Internal Circulation (IC) reactor is a modification of EGSB reactor. The IC reactor consists of two inter-connected UASB compartments on top of each other. First one is the expanded sludge bed where most of the organic pollution is converted to biogas and second one is the polishing section where the rest of the

organic pollution is converted. The biogas produced in the first part is collected in a lowest gas hood module, the biogas flows up through the riser to the GLS on the top of the reactor. When the biogas flows up it caused a gas lift and drags on water to the GLS. The water and the biogas is separated in the GLS and the water comes back to the bottom and it is mixed with the influent. The water from the first UASB flows to the second one, where the rest of biodegradable material is converted to biogas that is collected in the second gas hoods module and flows up to the GLS dragging on water with it. The up-flow velocities achieved in this reactor range from 25-30 m h^{-1}, causing an almost complete mixing of the reactor medium with the available biomass (van Lier et al., 2015).

By comparing UASB and EGSB technologies, the UASB reactor is the most widespread system. The success of the UASB concept relies on the establishment of a dense self-granulated sludge in the bottom of the reactor (Seghezzo et al., 1998), but nowadays the major constructors sells more EGSB than UASB due to the growing experience and the higher availability of the seed material (van Lier, 2008). Moreover, the use of UASB leads to a shortage of substrate and a deterioration in the physical and biological characteristics of the granules in the case of low to medium organic strength at moderate temperature. To overcome this problem, the EGSB was developed to improve wastewater-granule contact by expanding the sludge bed and increasing hydraulic mixing by effluent recirculation (Yoochatchaval et al., 2008).

1.5.3.4 *Fluidized bed*

The FB reactor is based on the bacterial attachment to mobile carrier particles (such as fine sand, basalt, plastic, etc.). The FB could reach OLR of 50-60 kg COD m^{-3} d^{-1} due to the good mass transfer, however long-term stable operation appears to be problematic (van Lier et al., 2015).

1.5.4 Treatment of wastewater containing solvents

The use of anaerobic reactor in the treatment of solvent wastewater is reported in the literature, this section introduces examples of anaerobic reactors treating wastewater that contained solvents typically use in the flexographic facilities. Table 1.6 compiles anaerobic reactors found in the literature treating wastewater of several industrial sectors. Key component in the table refers to the solvent of interest in this thesis.

Table 1.6 . Examples of anaerobic reactor treating solvents used in the flexographic sector.

Sector wastewater	Reactor	Key component	OLR, kg COD m^{-3} d^{-1}	pH	Temperature, °C	Removal efficiency, %	Reference
Synthetic water[a]	EGSB-Anaerobic	Acetate, ethanol	5-10	7.5	15	70-98	Scully et al. (2006)
Brewery	EGSB, 15L	Ethanol	9.7 5.5	---	20 15	85 85	Xing et al. (2009)
Synthetic ethanol	UASB, 0.6L	Ethanol	36.5	6.5-7	37	88	Fukuzaki et al. (1995)
Distillery	UASB, 476 m^3	Ethanol	2.5-12	6.4-7.5	35-37	60-80	Kolukirik et al.
Brewery	UASB, 500 m^3	Ethanol	2.6	6.8-7	28-31	81-92	Díaz et al. (2010)
Distillery	UASB, 11.9 L	Ethanol	30	7.0-7.5	55	85	Syutsubo et al.
Distillery	UASB, 5.75 L	Ethanol	86.4	---	Thermophilic	60	Wiegant et al. (1985)
Distillery	UASB, 1.05 L	Ethanol	15	> 7	35	90	Goodwin and Stuart (1994)
Distillery	UASB, 100L	Ethanol	24	> 7.4	20-24	75	Sánchez et al. (1985)

[a] Water consisting of acetate, butyrate, propionate and ethanol, in the COD ratio of 1:1:1:1

(Continued)

Table 1.6 cont. Examples of anaerobic reactor treating solvents used in the flexographic sector.

Sector wastewater	Reactor	Key component	OLR, kg COD m^{-3} d^{-1}	pH	Temperature, °C	Removal efficiency, %	Reference
Pharmaceutical[b]	FB + support matrix at upper part, 20L	Ethyl acetate	4	~8	---	86	Henry et al. (1996)
Pharmaceutical[c]	UASB, 14 L	Ethyl acetate	6	7-8	----	75	Oktem et al. (2007)

[b] Total influent 8 100 mg O_2 L^{-1}, where 500 mg O_2 L^{-1} was ethyl acetate, the rest of COD was acetate, ethanol, propionate, butyrate and methanol in a ratio 2: 2: 1: 1: 1 based on COD

[c] Main organic compounds were n-butyl acetate, dimethyl formamide, isopropyl alcohol, ethyl acetate and methylene chloride

More recently, Lafita et al. (2015) demonstrated the feasibility of EGSB technology for the treatment of packaging wastewater at mesophilic and psychrophilic conditions. The solvent wastewater consisted in ethanol and a glycol ether (1-methoxy-2-propanol) in a mass ratio of 4:1, with a HRT of 1.85 h. The biomass needed an adaptation period to start to degrade the glycol ether due to the lack of enzymes for ether cleavage. The adaptation period lasted for 45 days at 25°C and more than two months for 18°C. The achieved removal efficiency was higher than 95% after the adaptation period, working at loads of 29 and 43 kg COD m^{-3} d^{-1} at 18 and 25°C, respectively. The same study demonstrated that the reactor needed 40 days to degrade the glycol ether again after a period of 28 days without supplying any fed. Finally, it was pointed out that discontinuous supply of substrate caused a decline in the maximum rate of 1- methoxy-2-propanol, from 9 kg COD m^{-3} d^{-1} to 7.2 kg COD m^{-3} d^{-1} at 25°C.

Literature data demonstrates that solvents used in the flexographic sector can be degraded in anaerobic conditions. Specially, previous work of the GI^2AM research group (Lafita et al., 2015) shows that 1-methoxy-2-propanol can be anaerobically degraded under discontinuous loading, which are typical from industrial facilities. Hence, the combination of scrubber and anaerobic reactor (hereafter anaerobic bioscrubber) is a potential technology for the abatement of VOCs from flexographic sector.

2 ANAEROBIC BIOSCRUBBER

The proposed system in this thesis for the treatment of VOCs emissions from the flexographic sector is the anaerobic bioscrubber, a technology that combines scrubbing and anaerobic degradation. VOCs will be transferred from the gas stream to liquid phase in the scrubber, emitting clean gases to the atmosphere. The scrubbing liquid containing the dissolved solvents will be fed to the anaerobic reactor, where solvents will be degraded by anaerobic microorganisms, allowing to reuse scrubbing liquid in the scrubber unit. This chapter is divided in two parts, the first one describes the theory that underlines in the design process of these both units. These fundamentals are implemented in process simulators, which will be described in the second part of this chapter. The process simulators are software well appreciated by industries and researches, as they can accurately estimate the real scenario and they can be used to predict process behaviour by using material and energy balance equations, equilibrium relationships and reaction kinetics.

2.1 Fundamentals in process design

2.1.1 Scrubber

The primary function of an absorber unit is to provide a gas liquid contactor under conditions that favor VOCs mass transfer from gas phase to aqueous medium. Absorber units are designed to provide large liquid surface area with a minimum gas pressure drop, since mass transfer rate is proportional to interface surface area between both phases. Different configurations of absorber units are used to enhance the mass transfer, such as spray towers, venturi absorbers and packed beds. Spray towers consist of empty vessel with nozzles that spray liquid. Normally, the gas stream enters at the bottom and moves upward, while liquid is sprayed downward, often at different levels. This technology is based on the contact of the exhaust gas with large amount of fine droplets, providing a large surface area for pollutant absorption. Venturi absorber is based on the Venturi effect. The dispersion of the liquid is accomplished by the high velocity gas stream and it is characterized by high energy consumption. Packed bed is the most usual configuration, in which packing material enhances the gas-liquid mass transfer (Cooper and Alley, 2011). Packed towers are generally recommended to absorb compounds with relatively poor solubility in water, i.e. compounds with Henry's

coefficient below 0.01 (H_{cc}, gas concentration/liquid concentration, dimensionless) (Nielsen and Richard, 1997); which is equivalent to Henry's coefficient H_{cp} higher than 4.1 M atm^{-1} at 25°C.

The Figure 2.1 shows a schematic diagram of a packed absorption column. Counter-current configuration is considered better for scrubber configuration, since the absorption efficiency is higher, and with lower pressure drop and with lower associated energy costs than co-current configuration. The only drawback of counter-current operation is the larger volume compared to the co-current tower (Singh et al., 2005). In countercurrent configuration, the liquid flows continuously down the column over the packing surface, and the gas flows counter-currently up the column.

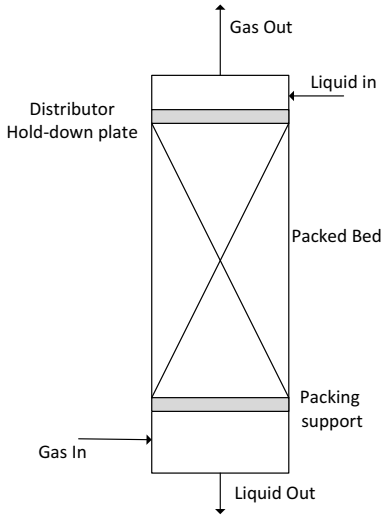

Figure 2.1. Schematic diagram of packed scrubber tower.

There are several options for packing material, with a wide variety in size, contact surface area, pressure and material of construction. They can be classified in two big categories: structured packings with a regular geometry and property shape, and random packings that are dumped into the column and take up a random arrangement. Once the packing material has been chosen, the next steps in the process design are the packed bed height calculation, which provides the desired separation, and the determination of the diameter to handle the liquid and gas flow rates.

The determination of the column height can be obtained by two methods: the theoretical stages method and the transfer unit method. The first one is based on the concept of Height Equivalent to Theoretical Plate (HETP), being the height of the packed bed (H) obtained by the equation (2.1) (Towler and Sinnot, 2012).

$$H = HETP \cdot N \qquad (2.1)$$

Where HETP is the height of packing that will give the same separation as an equilibrium stage. For an equilibrium stage, compositions of the liquid and vapor streams leaving the stage are given by the equilibrium relationship. N is the number of theoretical stages, which can be obtained by several methods such as Lewis-Sore method, McCabe-Thile method, Hengstebeck method or Aiche method, among others. The suppliers of the packing material normally provide graphs in their catalogs that relate the operational conditions and the number of stages. As an example, the data specified by Sulzer Chemtech for its structured packing Mellapak™ is provided in Figure 2.2. This figure shows the number of stages against the F factor, which depends on the velocity of the gas and its density.

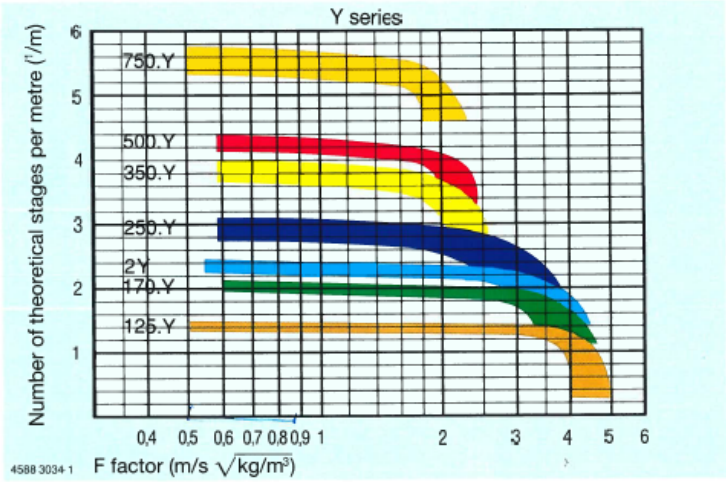

Figure 2.2. Number of theoretical stages for Mellapak™ structured packing material from Sulzer Chemtech.

The graph also shows that the F factor that is recommended by the suppliers ranged between 0.5 to 5 m s^{-1} $kg^{0.5}$ $m^{-1.5}$, which corresponds to velocities between 0.55 and 5.5 m s^{-1} for air.

The other method to obtain the packed height is the transfer unit method. The transfer unit is a part of column height where the change in vapor concentration equals to average driving force. The driving force is the difference between the equilibrium (y_e) and the actual vapor concentration (y). The column height can be calculated by (2.2) (Towler and Sinnot, 2012).

$$H = NTU \cdot HTU \tag{2.2}$$

Where NTU is the number of transfer unit and HTU is the height of transfer unit. There is not any entirely satisfactory method to calculate the HTU. This value will depend on the physical properties and flow rates of the gas and liquid, but also on the uniformity of the liquid distribution throughout the column, which is dependent on the column height and diameter. Whenever possible, estimates should be based on actual values obtained from operating columns of similar size to that being designed. The NTU is given by the equation (2.3) (Towler and Sinnot, 2012):

$$NTU = \int_{y_2}^{y_1} \frac{dy}{y - y_e} \tag{2.3}$$

Where y_1 and y_2 are the mol fractions of the solute in the gas at the bottom and top of the column, respectively and y_e is the concentration in the gas that would be in equilibrium with the liquid concentration at any point.

After calculating the height, the diameter of the scrubber is determined by selecting a cross sectional area that will provide gas and liquid mass velocities enough for a good interfacial contact. At a constant liquid flow, interfacial contact between both phases will increase as gas flow increases until a limit. This limit is the flooding point, when the gas interferes with the downward flow liquid, producing a water accumulation until is forced out the top of the tower. Cooper and Alley (2011) suggested to operate the tower at 40-70% of the flooding gas velocity, which is estimated by using Figure 2.3 (a logarithmic plot of K_4 vs F_{LV}).

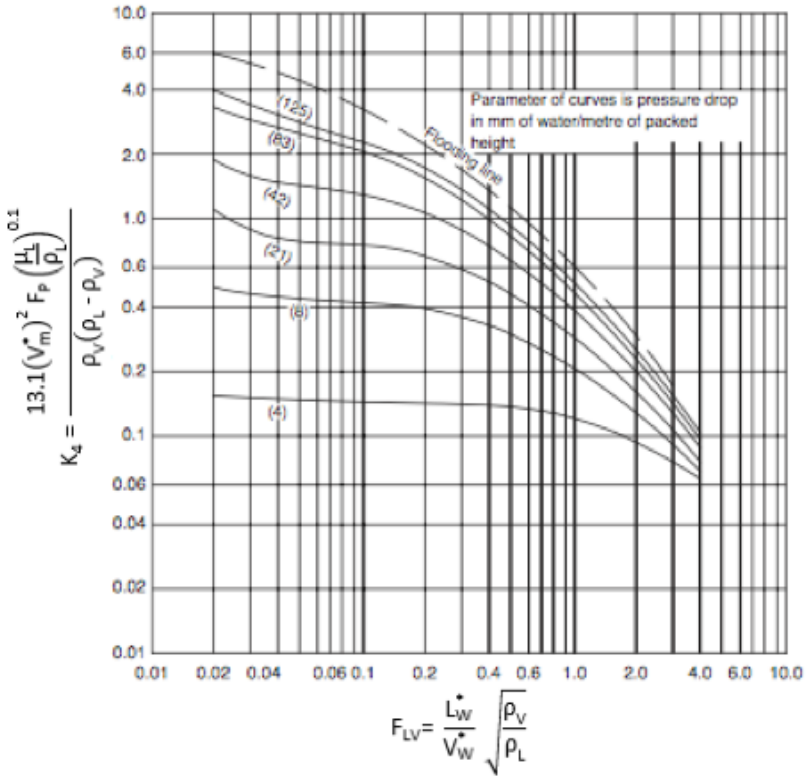

Figure 2.3. Generalized correlation for flooding and pressure drop. Adapted from McCabe et al. (1985).

Where V_m^* (kg m^{-2} s^{-1}) is gas mass flow rate per unit column cross- sectional area, μ_L (Ns·m^{-2}) is the liquid viscosity, ρ_V and ρ_L (kg m^{-3}) are liquid and vapor densities respectively, L_W^* and V_W^* (kg m^{-2} s^{-1}) are the liquid and the gas mass flow rate per unit area column cross-sectional area respectively, and F_P (m^{-1}) is the packing factor, a characteristic of the size and type of the packing. Some values for packing factor for various packings are provided in Table 2.1.

Table 2.1. Design data for various packings. Adapted from Towler and Sinnot (2012).

	Size, mm	Bulk density, kg m^{-3}	Surface area, m^2 m^{-3}	Packing factor Fp, m^{-1}
Rasching rings ceramic	13	881	368	2100
	25	673	190	525
	38	689	128	310
	51	651	95	210
Metal, density for carbon steel	13	1201	417	980
	25	625	207	375
	38	785	141	270
	51	593	102	190
	76	400	72	105
Pall rings metal, density for carbon steel	16	593	341	230
	25	481	210	160
	32	385	128	92
	51	353	102	66
	76	273	66	52
Plastics, density for polypropylene	16	112	341	320
	25	88	207	170
	38	76	128	130
	51	68	102	82
	89	64	85	52
Intalox saddles ceramic	13	737	480	660
	25	673	253	300
	38	625	194	170
	51	609	108	130

One of the main objectives of this thesis is to determine the best hydraulic conditions in the scrubber, which permit to obtain the maximum removal efficiency of VOCs with the minimum flow of liquid. This is crucial since the flow of the scrubbing liquid will determine the size of the EGSB reactor. The design of the reactor is explained in the next section.

2.1.2 Anaerobic reactor

The design of the anaerobic reactor is based on empirical data and a comprehensive review of design consideration has been provided by Lettinga and Hulshoff Pol (1991). The organic loading rate, superficial velocity, and effective volume must all be considered to determine required reactor volume and dimensions. The effective treatment volume comprises the volume occupied by the sludge blanket and active biomass. There is an additional volume between the effective volume and the gas collection unit, where some additional solids separation occurs and the biomass is diluted. The effective liquid volume of the reactor (V_N) is obtained by equation (2.4).

$$V_N = \frac{Q\,S_0}{OLR} \qquad (2.4)$$

Where Q ($m^3\ h^{-1}$) is the influent flow rate, S_O (kg COD m^{-3}) is the inlet concentration and OLR (kg COD $m^{-3}\ d^{-1}$) is the organic loading rate. An effective factor is used in order to determine the total liquid volume below the GLS. This factor may vary from 0.8 to 0.9, so the required total liquid volume of the reactor (V_L) is given by equation (2.5).

$$V_L = \frac{V_N}{E} \qquad (2.5)$$

The area will be given by the up-flow velocity (v, m h^{-1}) and the influent flowrate by the equation (2.6)

$$A = \frac{Q}{v} \qquad (2.6)$$

The liquid height of the reactor is determined by using the following relationship:

$$H_L = \frac{V_L}{A} \qquad (2.7)$$

The GLS adds an additional height of 2.5 to 3 m.

Other important factor that needs to be taken into account is the control of the anaerobic process. Although in terms of reactor concept anaerobic treatment is a fairly simple technology, the microbiology and the process are very complex. It is in this aspect when a model becomes handy. With respect to anaerobic digestion, the Anaerobic

Digestion Model 1 (ADM1) is widespread and generally accepted as the reference model. The ADM1 was first presented at the 9th IWA Conference on anaerobic digestion in 2001 in Antwerp (Batstone and Keller, 2003) and the related scientific and technical report was published by IWA in early 2002. The novel aspect, in comparison with other previously models, was the implementation of the disintegration step (Batstone et al., 2002). Cellular solubilisation steps were divided into disintegration and hydrolysis. The next phases were included according to the generally accepted theory: hydrolysis of particulates and the stepwise degradation of the hydrolyzed substrates. Hence, it is assumed that organic particulate polymers disintegrate into inert materials, carbohydrates, proteins and fats, which are then hydrolyzed to sugars, amino acids, and long chain fatty acids. Afterwards, sugars and amino acids are fermented to generate propionate, butyrate, valerate, acetate and hydrogen. Propionate, butyrate and valerate are further degraded to acetate and hydrogen. Finally, methane is produced by the degradation of acetate and the reduction of carbon dioxide by hydrogen. The model considers seven microbial trophic groups. Kinetic equations take into account the microbial growth process and biomass decay, which are described producing inert and degradable particulate organic matter that again undergoes to the degradation step. Biomass growth rate is proportional to degradation rates of organic matter and are described by Monod-like dependencies, for which the general expression is:

$$\mu = \mu_{max} \frac{S}{K_S + S} \qquad (2.8)$$

Where μ is the specific growth rate of the microorganism, μ_{max} is the maximum specific growth rate of the microorganism, S is the concentration of the limiting substrate for growth and K_S is the half-velocity constant, value of S when μ is half of μ_{max}. The kinetic equations are completed with the inhibitive effects of pH, hydrogen, ammonium, and long chain fatty acids (Batstone et al., 2002).

The physicochemical process of stripping the gaseous compounds (hydrogen, methane and carbon dioxide) was included to represent the production of biogas. The pH calculation was based upon six additional physic chemical processes, describing the acid/base equilibria of CO_2/HCO_3^- , NH_4^+/NH_3 , acetic acid/acetate, propionic acid/propionate, butyric acid/butyrate and valeric acid/valerate (Batstone et al., 2002).

The model was designed to be readily extendible. The most common extensions were sulfate reduction, mineral production and other minor extensions such as the introduction of diversity between organisms with the same function.

The extension of sulfate introduced in the model the fact that sulfate acts as electron acceptor for oxidation of VFAs but reacts preferably with hydrogen. In addition, the sulfide is inhibitory, affects the pH and it is gaseous. Fedorovich et al. (2003) published a sulfate reduction extension. This extension involves four additional groups of microbes that can oxidize butyrate/valerate, propionate, acetate and hydrogen respectively, using sulfate as electron acceptor to produce hydrogen sulfide. Inhibition, acid-base chemistry, and gas stripping were also taken into account. The new microbes compete with those ones presented in the original ADM1 for these substrates. The model was effective in predicting the behavior of a UASB fed with up to 6 g-S L^{-1}.

The precipitation of soluble components is a relatively simple extension, the fully dissociated anion, cation and precipitate should be modelled as a separate state by using algebraic or differential equations (Batstone and Keller, 2003).

Ramirez et al. (2009) extended the standard ADM1 for modeling microbial diversity. ADM1 does not distinguish between microorganisms performing the same reaction, which implies that all of them are assumed to have the same properties. Seven functional groups are defined in ADM1, corresponding to the degradation of sugar, amino acids, long chain fatty acids, valerate and butyrate, propionate, acetate and hydrogen and one microbial population was associated to each reaction. These authors arbitrarily set 10 species per reaction, keeping the inhibition by extreme pH values, accumulation of H_2 inhibits the anaerobic oxidation, the inhibition of methanogens by high free ammonia, which were originally implemented in ADM1. The model represented the macroscopic experimental data, but was moreover able to get insight in underlying microbiology.

The main drawback pointed out for ADM1 is the calibration of the large number of model parameters and the requirement of full substrate characterization (Astals et al., 2013). Evaluation of all model parameters and fraction of all individual components in substrate are not practical in many cases (Kleerebezem and van Loosdrecht, 2006). To overcome this issue, some studies have used default values of the kinetic and stoichiometric parameters, which were determined for the digestion of municipal wastewater sludge. Although the use of the default parameters may not be suitable for

other applications. Blumensaat and Keller (2005) overcame the problem eliminating some phenomena from ADM1 model. These researchers simulated the dynamic behavior of a pilot-scale process for anaerobic two-stage digestion of sewage sludge. The omitted phenomena form ADM1 model were:

- Production of lactate from glucose fermentation.
- Sulphate reduction and sulphide inhibition.
- Nitrate reduction.
- Long chain fatty acid (LCFA) inhibition.
- Competitive uptake of H_2 and CO_2 between hydrogenotrophic methanogenic archaea and homoacetogenic bacteria.
- Solids precipitation due to high alkalinity or other chemical precipitation reactions.

The model predicted adequately the process at operational conditions, where it was presumed that none of the above processes significantly influence the modelled system.

2.2 Process simulation

The physico chemical processes, which commonly occur in the scrubber and anaerobic reactor, such as gas liquid transport, liquid- liquid reaction (ion association or dissociation), liquid solid transformation (precipitation and solubilization of ions) are implemented in the core of the process simulators. By developing a model for the anaerobic bioscrubber process and implementing it in a process simulator, it may be manageable to solve the process with a small number of inputs in a faster and more reliable manner.

2.2.1 Classification of process simulators

The process simulators could be classified in three main groups, depending on the type of variable (discrete or continuous), evolution of time (dynamics or static) and degree of uncertainty (deterministic or stochastic).

The state variables in the discrete models instantly change in different points of the time; every time that a variable changes is defined as an event. The cause and when it changed should be known to follow the state variables, hence the discrete simulation consists in tracking the changes of the system when the events happen. On the other hand, the implicated variables in the continuous models take a value within a range, changing continuously along the time.

Regarding the type of models depending on the time, they will be classified as dynamic if there are some variables that are time dependent and the model will be classified as static if the variables do not depend on the time and their values remain constant. Although, there is not static model in the real life, since a lot of processes are designed to keep constant along the time, using a control system to achieve this goal.

Finally, simulators could be deterministic and stochastic, a deterministic model assumes that its outcome is certain if the input to the model is fixed. On the other hand, one or more outcomes are random within a stochastic model. Stochastic modeling is for the purpose of estimating the probability of outcomes within a forecast to predict what conditions might be like under different situations. The random variables are usually constrained by historical data.

The majority of the commercial simulators are deterministic, continuous and depending on the time, they can work in static or dynamic.

Other classification is based on the configuration and how it solves the equations. Within the classification based on the configuration, it can be differed two kind of simulators, modular and non-modular. Based on the mode that the equations are solved, they can be classified in sequential or simultaneous. Hence, the simulators can be classified in sequential modular, non-modular simultaneous and modular simultaneous.

A sequential modular simulator considers every equipment as an independent calculation unit. The equations associated to an equipment (mass and energy balance, equilibrium equations, etc.) are grouped together in a module. In that way, every module obtains the outlet streams taking only into account the inputs, but no the information source or how these outputs will be used in the model afterwards. This strategy is followed by the main commercial simulation software such as Aspen Plus® (Aspen Technologies, USA), Chemcad® (Chemistations, USA), Aspen-HYSYS® (Aspen

Technologies, USA), Prosim (Prosim, France), Design II (WinSiM, USA) or SuperPro Designer (Intelligen, USA).

Sequential modular approach has some clear advantages for process flow sheeting, the main advantages of these simulators are the strength and reliability, since the specific solution methods, including the initialization, are well developed for each process unit, allowing an easy control of convergence. Another advantage is the friendly user form, which makes easy to understand the process because it is similar to the flow diagram. In addition, the unit blocks can be easily added to or removed from the flowsheet and they can be prepared and tested separately (as a computer program subroutine).

In the non-modular simultaneous simulators, the process is defined as a whole set of equations for every unit and streams. This set of equations is solved simultaneously obtaining the value of variables that are non-known. Some commercial simulation software that follow this strategy are Ascend (Carnegie Mellon University USA), Abacus (Dassault systemes, USA) or gProms (Process systems enterprise, United Kingdom).

The simultaneous modular approach combines the modularizing of the equations related to specific equipment with efficient algorithms for solving simultaneous equation. For each unit, an additional module is written, which approximately relates each output value by a linear combination of all input values. Accordingly, rigorous models are used at unit level, which are solved sequentially, while linear models are used at flowsheet level, solved globally.

Within these options, the type of simulator more extended is the sequential modular, the next section will explain the architecture of this kind of software.

2.2.1.1 *Sequential modular simulators*

The structure of a sequential modular simulator can be divided into several components:

1. Component data bank: A database with the required parameters to calculate the physical properties.
2. Thermodynamic property prediction methods: A set of thermodynamic methods to estimate the physical and thermodynamic property data.

3. Flowsheet builder (graphical user interface): Provides to the user an interface to generate the flowsheet of the process under a graphical environment.
4. Unit module library: Subroutines to perform energy and material balances and design calculations for the typical process engineering units.
5. Numerical routines: A collection of mathematical methods for solving systems of linear, nonlinear, and differential equations.
6. Data output generator: Reports the results of the simulation by tables and graphical displays.
7. Executive program (flowsheet solver): The heart of any process simulator, which controls the sequence of the calculations and the overall convergence of the simulation.

These components can be grouped in three sections, central or general logic, section to estimate the physicochemical properties and unit module library. The first section is responsible for the administration of the different processes to carry out the simulation. This part of the simulator should process the flow diagram and decides if the problem can be solved in a linear sequence or if there is any cycle. In this last case, it should be decided the variables that will be iterated and it should determine the order, depending on the cutting flows, in which the operational units will be solved. There are several methods to carry out these actions (Ledet and Himmelblau, 1970; Sargent and Westerberg, 1964; Tarjan, 1971). Once the different partitions are determined, the next step is to decide the minimum number of cutting streams to solve the problem. The main algorithms detailed in the literature are the proposed by Christensen and Rudd (1969), Barkley and Motard (1972), Pho and Lapidus (1973) and Upadhye and Grens II (1975). After the decisions for solving the problem are established, the iterative process to find the exact solution should be carried out by applying methods of convergence to limit the number of iterations. Some of these methods are direct substitution, Wegstein, Broyden and Newton-Raphson method.

The second section is the one responsible for obtaining the physicochemical properties. An essential part of a simulation package is the component data bank, which commonly contains more than a thousand chemical compounds. For chemicals that are

not available in the data bank, process simulators provide a user-added component facility to include the required compounds in the simulation. A short overview of the data needed in the simulation and design of processes are:

- Phase equilibrium: Boiling and melting points, vapor pressure, fugacity activity coefficients and solubility.
- PVT behavior: Density, molar volume, compressibility, critical properties, acentric factor.
- Transport properties: Heat capacity, latent heat, ionic conductivity, enthalpy, entropy.
- Chemical reaction equilibrium: Equilibrium constants, association/dissociation constants, enthalpy of formation, enthalpy of combustion, heat of reaction, Gibbs free energy of formation, reaction rates.
- Boundary property: Surface tension.
- Molecular properties: Virial coefficients, ion radius and volume, molecular weight, and dipole moment.
- Safety Characteristics: Flash point, explosion limits, toxicity, maximum working place concentration, lower and upper flammability limits.

The properties required for the design of a chemical process depend upon the temperature, pressure, and concentration. To predict phase equilibrium, a thermodynamic model should be chosen, which often turns into a crucial decision in the simulation. Current process simulators offer a model selection wizard to guide the user to the proper method. The decision becomes complex since different thermodynamic packages can be used for different parts of the flowsheet.

Finally, as it was mentioned, the last section is the Unit module library that is composed by subroutines to perform energy and material balances and calculations to design the typical process engineering units.

There are a great variety of commercial sequential modular simulators, such as:

- Aspen Plus® is a market leading process modeling tool for the design, operation and optimization for the chemical, polymer, specialty chemical, metals and minerals and coal power industries.
- Aspen-HYSYS® is a market-leading process modeling tool used by the oil and gas producers, refineries and engineering companies for process simulation and process optimization in design and operations.
- SuperPro Designer is a process simulator that facilitates modeling, evaluation and optimization of integrated processes in a wide range of industries. The combination of manufacturing and environmental operation models in the same package enables the user to concurrently design and evaluate manufacturing and end-of-pipe treatment processes and practices waste minimization via pollution prevention as well as pollution control.
- Chemcad hemstations is one of the world's leading providers of process simulation in the chemical engineering industry. Chemcad software allows users to interactively generate flow charts, simulate all major processes including control procedures and create diagrams of results.
- Prosim is a steady-state simulator that enables improved process design and operational analysis. It is designed to perform rigorous heat and material balance calculations for a wide range of chemical processes such as, petroleum, natural gas, solids processing and polymer.

2.2.2 Selection of process simulator for anaerobic bioscrubber

The software selection should be made to achieve high accuracy degree of both units: the scrubber and the anaerobic reactor. Within the possible process simulators, Aspen simulation package has a large experimental databank for thermodynamic and physical parameters, even for electrolytes. This is the most important advantage of Aspen for its potential application, since the chemical equilibrium plays an important role in the anaerobic bioscrubber. Aspen has been widely used in the scrubber simulation as it is shown in the Table 2.2. This Table shows the source of the waste gas, the main pollutant in the gas phase and the scrubbing liquid in the different studies.

Table 2.2. Examples of scrubbers modelled with Aspen Plus.

Source of waste gas	**Pollutant in gas phase**	**Scrubbing liquid**	**References**
Biomass gasification	n-hexadecane, trans-decalin, 2,2,4,4,6,8,8-heptamethylnonane	Canola oil, biodiesel conventional diesel	Srinivas et al. (2013)
Solid waste treatment	Sulfur dioxide	Calcium hydroxide solution	Cimini et al. (2005)
Power generation from municipal solids waste	Nitrogen oxides	Lime	Jannelli and Minutillo (2007)
Natural gas sweetening	Carbon dioxide	Monoethanolamine or diethanolamine solution	Bae et al. (2011)
Post combustion CO2 capture plant	Ammonia	Acid solution	Khakharia et al. (2014)
coal fired power plant	Carbon dioxide	Monoethanolamine solution	Atuman et al. (2015)
Gasification of biomass	Benzene, toluene and ethylbenzene	Vegetable oil	Bhoi et al. (2015)
Waste to energy plant	Hydrochloric acid	Sodium hydroxide solution or lime	Grieco and Poggio (2009)
Gold refinery	Nitrogen oxides	Sodium hydroxide solution	Aidan et al. (2011)

Regarding the application of simulators to bioprocesses, the rich theory available for synthesizing standard chemical process flowsheets has not been applied to the same extent to their biochemical counterpart (Brunet et al., 2012a, 2012b). Development of simulators specific for biochemical processes began in the mid-eighties. Bioprocess simulators (from Aspen Technology, Inc) was the first tool of this type; but it has had limited commercial success because it was designed as an extension of Aspen Plus® and it cannot satisfactorily represent batch biochemical processes.

SuperPro Designer is an extension of BioPro Designer (Inc. Intelligen, USA), which was the second product in this category. This extension was created to address industries as water purification and end-of-pipe treatment process. It can handle material and energy balances, equipment sizing and costing economic evaluation, environmental impact assessment, process scheduling, and debottlenecking of batch and continuous processes. SuperPro Designer has been recently applied to biological process. For example, Mel et al. (2015) analyzed the cost of biogas production from agricultural biomass, and Forgács et al. (2014) analyzed economically the methane production from feather waste. This software has also been linked with MATLAB® for process optimization. Brunet et al. (2012a, 2012b) optimized single product biotechnological facilities. The connection between both software allows to avoid multiobjective optimization approaches used in process design, which rely on monolithic algebraic formulation that embed "shortcut" models. By connecting both software, the detailed equations of the process that are embedded in the simulator are used by optimization software, hence they do not use approximated shortcut models.

Aspen Plus® has also been linked with multi-objective tools for optimization of processes, taking into account economic and environmental considerations (García et al. 2014; Quirante et al., 2015). Moreover, Aspen has been used for the simulation of anaerobic degradation, finding in the literature two different approaches. Barta et al. (2010) investigated the techno-economic aspects of spruce-to-ethanol, including wastewater anaerobic treatment. They assumed degradation factors: 90% for soluble sugars, organic acids, ethanol, glycerol, enzyme, and yeast; 50% for polysaccharides, extractives, degradation products and waste-soluble lignin; and 0% for water-insoluble lignin. The methane and anaerobic digestion sludge yields were assumed to be 0.35 Nm^3 kg^{-1} COD removed and 0.03 kg DM (dry matter) kg^{-1}COD fed, respectively. On the other hand, Rajendran et al. (2014) implemented ADM1 in Aspen by FORTRAN code. The hydrolysis reactions are based on fractional conversion of reactants to products

(reaction set a) and acidogenic, acetogenic and methanogenic reactions functioned on a kinetic basis (reaction set b). The hydrolysis equations were included as carbohydrates, proteins and fats. Carbohydrates were incorporated as cellulose, starch and hemicelluloses. Proteins were defined based on their solubility. Fats comprised of tripalmate, triolein, palmito-olein, and palmito-linolein. In the reaction set b, different FORTRAN programs were implemented to determine the rate of reactions in acidogenic, acetogenic and methanogenic phases. In total, ten different subsets were used for glycerol, valeric acid, butyric acid, propionic acid, linoleic acid, amino acids, sugars, palmitic acid, oleic acid, methanogenesis and hydrogen utilizing reactions. In each calculator block, the inhibitions in the form of pH, temperature, and ammonia were embedded as logic loops. The model was able to simulate laboratory and industrial studies. The average difference in biogas production between simulation results and real scenario was up to ±20%.

For the simulation of a combined scrubber and biological reactor, Aspen Plus® has the advantage of a richer thermodynamic library than SuperPro designer, so Aspen has been selected as the process simulator software for the creation of the model to simulate the anaerobic bioscrubber

3 OBJECTIVES

The general aim of this thesis is to optimize the performance of an anaerobic bioscrubber industrial prototype and to demonstrate its stability to show it as a potential new technology for the abatement of VOC air emissions from the flexographic sector. This general objective can be divided in two following objectives:

- On-site field experimental study of an anaerobic bioscrubber as a VOC emission control technology in a flexographic facility by using an industrial prototype. The goal of this part is to establish the operating conditions to meet the legal threshold and to provide a set of empirical parameters for the scale-up of the process.
- Integration of the anaerobic bioscrubber process in the commercial simulator Aspen Plus® to predict the scrubber and anaerobic performance and to provide a design tool.

The partial objectives can be itemized in the specific objectives detailed below:

The **on-site field experimental study** of the anaerobic bioscrubber covers:

- To implement the protocols to start-up the industrial prototype.
- To evaluate the best scrubber configuration (packed bed and spray tower) and the hydraulic conditions that achieves high VOC removal efficiencies; while at the same time keeps under control the pressure drop and minimizes the liquid flow fed to the anaerobic reactor.
- To determine the maximum organic loading rate that the anaerobic reactor can treat under intermittent and variable waste gas emissions.
- To study the performance of the anaerobic bioscrubber during long term operation.

The **development of the simulation model** using the experimental data from the operation of the industrial prototype encloses:

- To calibrate and validate the scrubber model that correlates the outlet VOC emissions from the scrubber with the operating conditions for two tested packing materials.

- To develop a mathematical model of the anaerobic process degradation of solvents based on a simplification of the ADM1 model and its calibration and validation in Aspen Plus®.
- To integrate the anaerobic reactor and the scrubber model simulators to validate the experimental performance of the industrial prototype.
- To apply the integrated simulator in order to show its capability as a design tool.

4 MATERIAL AND METHODS

This chapter describes the experimental set-up of the industrial prototype, the analytical procedures and the description of the process simulation model.

4.1 Industrial prototype

The industrial prototype was provided by Pure Air Solutions BV (Heerenveen, The Netherlands). This prototype was installed in Altacel Transparant Verpakkingsind (Weesp, The Netherlands), a flexographic facility. This location was selected because it is a good example of practice in this sector. The main used solvents are ethanol, ethyl acetate and 1-ethoxy-2-propanol. The pattern emission depends on the printed orders, it is variable along the day and the facility works in two shifts with closure periods on Saturday evening and Sunday. Detailed information about the facility emission is provided in future chapters.

The prototype, whose scheme is shown in Figure 4.1, comprises the two main units: scrubber and anaerobic reactor. The scrubber unit, which is shown in Figure 4.2, had a total height of 3.06 m and a diameter of 0.5 m. The available height for the packing material was 2.00 m. The scrubber unit was assembled onto a bottom tank of 2 m^3 of volume. The anaerobic reactor, which is shown in Figure 4.3a on the installation day and in Figure 4.3b assembled, had a total height of 5.08 m and diameter of 1.59 m, with an effective water volume of 8.7 m^3. The anaerobic reactor was operated as EGSB configuration. Two intermediate tanks completed the setup; resulting in 16 m^3 of total effective water volume.

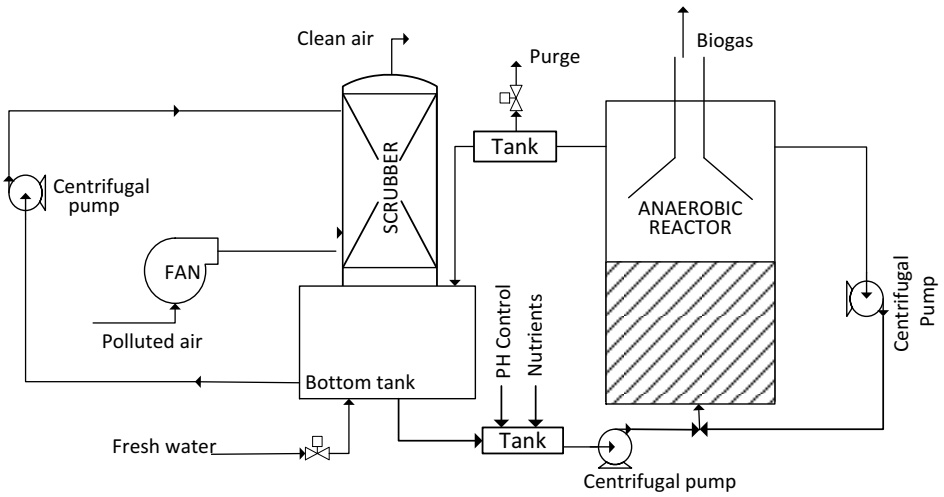

Figure 4.1. Scheme of the industrial prototype.

Figure 4.2. Scrubber of the industrial prototype.

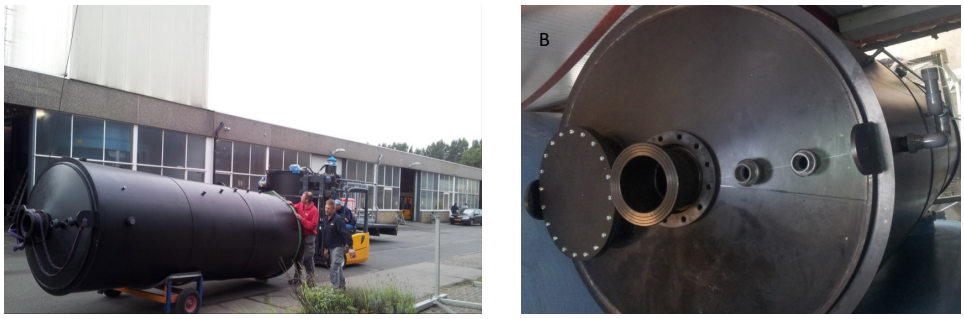

Figure 4.3. Anaerobic reactor of industrial prototype. A) reactor in installation day and B) assembled.

The main equipments that completed the prototype were a variable-speed fan with 1 500 m^3 h^{-1} of maximum flow (Slingerland Techniek Ventilatoren, The Netherlands), and three centrifugal pumps with a head of 20 meters of water column at 6 m^3 h^{-1} (model CEA80/5, Lowara, EEUU).

The scrubber was operated in the counter-current mode; VOC-polluted air coming from the factory was introduced to the bottom by the blower, and the water was sprayed from the top and collected in the bottom tank. Several configurations were tested, volumetric liquid to gas ratio (L/G, m^3 water m^{-3} air) and contact time varied between $1.9 \cdot 10^{-3}$-$9.1 \cdot 10^{-3}$ m^3 water m^{-3} air and 1.3-4.1 s, respectively. The outlet water stream flowed to an intermediate tank for supplementation with macronutrients (N, P, S, K) and sodium carbonate for pH control prior to pump it to the EGSB for solvent degradation. The nutrient and alkali solution were stored in different intermediate bulk container (IBC). The macronutrients were added by a dosing pump (Series P+7, LMI Roytronic, EEUU) and the sodium carbonate solution was supplemented by a dosing pump (model series GTM A, LMI Roytronic, EEUU). Details of dosing pumps are shown in Figure 4.4. Calcium, Magnesium and trace elements (B, Co, Cu, Fe, Mn, Mo, Ni, Se, Zn) and yeast extract were discontinuously supplemented. The EGSB was operated at a constant up-flow velocity (3 m h^{-1}) in the whole study, by combining the feeding and recirculation water streams with a total flow rate of 6 m^3 h^{-1}. After degrading the solvents and before recirculating the water to the scrubber, the dissolved methane was removed by a degasser. The hydraulic residence time of the reactor was controlled by the feeding pump. The hydraulic residence time of the overall process was controlled by the daily purge from the effluent of the reactor. The daily purge was done overnight when biogas production did not usually occur.

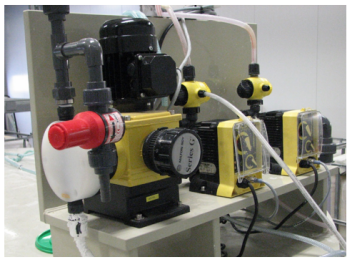

Figure 4.4. Dosing pumps.

The industrial prototype was provided with a programmable logic controller (PLC) with Twinsoft® software (Servelec technologies, United Kingdom) to monitor and control the parameters of the system. The monitored parameters were the biogas (gas counter, model BG4, Ritter, Germany), the temperature of the air (model Voeler PT100, 0-140 ºC, Be De Lier BV, The Netherlands). The controlled parameters were the air and the liquid flowrates (airflow meter, model SMV 25, Stienen B.E.,

The Netherlands; water flow meter, model 10D25-5CGA1aa05AA+M1, Endress + Hauser BV, Switzerland), the water temperature (model Voeler PT100, 0-140ºC, Be De Lier BV, The Netherlands), the pH (pH sensor, Be De Lier BV, The Netherlands), the conductivity (conductivity sensor, Be De Lier BV, The Netherlands) and the water level of the tanks (Liquidphant FTL50, Endress + Hauser BV, Switzerland). A detailed description of the PLC program and the on-line monitoring is provided in chapter 5.

4.2 Materials

4.2.1 Packing material

The scrubber column held up to two meter of packing material. Two types of packing material were tested. Packing A (Cross-fluted flow fills FKP 319, GEA, Germany) and Packing B (vertical flow fills KVP323, GEA, Germany). The technical data of both packing materials are detailed in Table 4.1. The path followed by the water in Packing A is shown in Figure 4.5c, and a picture of packing A and B is presented in Figure 4.5a and Figure 4.5b, respectively. The main differences between both packing materials were the specific surface area and the path-water. Packing A was more efficient in the abatement of VOCs, but it could clog more easily due to biomass accumulation. Packing B was less efficient, but the path-water makes clogging more difficult.

The scrubber unit was also tested as a spray column, removing the packing material and installing 3 nozzles (MP156N 60°, BETE, USA) spaced 55 cm. This configuration was tested, since it does not have clogging problems. This configuration was tested at L/G of $1.9 \cdot 10^{-3}$ and $3.7 \cdot 10^{-3}$ m^3 water m^{-3} air.

Table 4.1. Technical data of the tested packing materials in the scrubber unit.

	Packing A	**Packing B**
Material	Polypropylene	Polypropylene
Specific surface (m^2 m^{-3})	150	125
Corrugation height (mm)	19	23
Max Length (mm)	2400	2400
Max width (mm)	600	600
Height (mm)	300/600	300/600
Max. Application temp (°C)	80	80
Void ratio (%)	>97	>97
$L/G \cdot 10^3$ (m^3 water m^{-3} air)	3.5-9.1	3.8-10.1
Contact time (s)	1.7-4.1	1.4-3.6

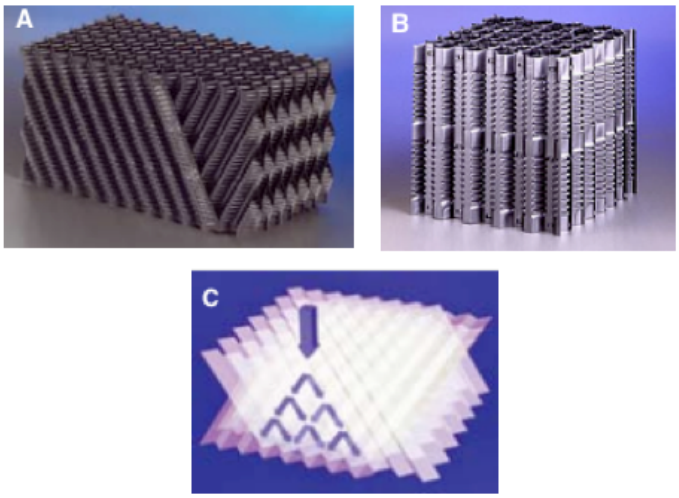

Figure 4.5. Packing materials. A) Packing A, B) Packing B and C) Cross flow in Packing A.

4.2.2 Sludge source

The industrial prototype was filled with 3.5 m^3 of granular sludge from an IC, which treated brewery wastewater (Heineken, The Netherlands), without further acclimation, in order to simulate the operational protocols at industrial scale. A detail of the granular sludge is shown in Figure 4.6, where it can be seen that it was tightly packed spherical granules with a uniform brown color.

The source of the sludge was chosen based on the research carried out by Lafita et al. (2015), who demonstrated that water brewery sludge coming from IC reactor is able to degrade water-solvents of the printing sector, when the main compound is ethanol.

Figure 4.6. Detail of the sludge source.

4.2.3 Nutrient supply

4.2.3.1 *Composition*

Two compositions of macronutrients were used during the experimental period. Initially, NH_4Cl was used to ensure the availability of $N\text{-}NH_4^+$ (nutrient solution I). Afterwards, this compound was changed to Urea (nutrient solution II), a cheaper compound, so more affordable for industrial use. The composition of both solutions are shown in Table 4.2 and Table 4.3, respectively. The grade of purity of the compounds was technical grade (Boom Laboratoriumleverancier, The Netherlands).

Table 4.2. Macronutrient solution I.

Compound	**Composition, kg m^{-3}**
NH_4Cl	50
$(NH_4)_3PO_4$	10
$KHSO_4$	4

Table 4.3. Macronutrient solution II.

Compound	Composition, kg m^{-3}
$CO(NH_2)_2$	28
$(NH_4)_3PO_4$	10
$KHSO_4$	4

Both nutrient solutions contained $KHSO_4$, which acts as a source of potassium and sulphur. Potassium is required for microorganism growth. Sulphur is required for the maintenance growth of methanogenic bacteria. It was dosed since the fresh water did not contain enough sulphate for microbiological requirements. The dose of sulphur was minimized to avoid the emission of H_2S in the biogas.

The composition of the micronutrient solution is shown in Table 4.4. It was prepared separately from macronutrient solution to avoid precipitation of phosphate and trace elements.

Table 4.4. Composition of the micronutrient solution.

Compound	Composition, g L^{-1}	Compound	Composition, g L^{-1}
$FeCl_3 \cdot 6H_2O$	30	$ZnSO_4 \cdot 7H_2O$	1.04
$NiSO_4 \cdot 6H_2O$	1.6	$MnSO_4 \cdot H_2O$	0.36
$CoCl_2 \cdot 6H_2O$	1.2	$CuSO_4 \cdot 5H_2O$	0.36
$Na_2MoO_4 \cdot 2H_2O$	0.6	Al_2Cl_3	0.8

Calcium chloride and yeast extract were manually added to the system periodically. These compounds were not dosed with the macronutrient solutions in order to avoid the precipitation of salts. Calcium has a positive effect on the flocculation ability of the anaerobic sludge, but authors do not agree on the optimal amount of calcium to be added. It is reported to be around 200 mg Ca^{2+} L^{-1}, between 100 and 200 mg L^{-1} or under 120 mg L^{-1} (Chen et al., 2008). Excessive amounts will cause carbonate or phosphate precipitation and the accumulation of minerals in the water content leads to inhibit some cellular metabolisms. This phenomenon is reported to start at concentrations above 120 or 300 mg L^{-1} (Chen et al., 2008). In this thesis, it was decided that the maximum concentration would be 100 mg L^{-1}. The yeast extract was added as a source of vitamins, which functions as coenzymes or as building blocks for coenzymes. The dosage was 0.5 kg $week^{-1}$.

4.2.3.2 *Dosage*

The dosage of nutrients was calculated by taking into account the consumption of methanogenic bacteria needed to growth. Afterwards, the results from the periodical chemical water analyses allowed its precise regulation. If an anaerobic bioscrubber system of constant volume is considered, the streams that should be taken into account for a mass balance of the nutrients are shown in Figure 4.7.

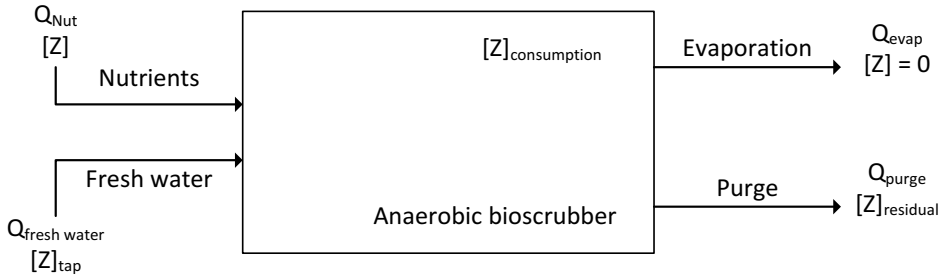

Figure 4.7. Streams required for the mass balance of nutrients.

The consumption term is based on the requirement for methanogenic bacteria growth and it is calculated by equation (4.1).

$$\text{Consumption} = Y \cdot OL \cdot [Z]_{\text{methanogenic bacteria}} \quad (4.1)$$

Where Y is the bacterial growth and it was assumed to be 0.035 g Volatile Suspended Solids (VSS) g^{-1}-$COD_{removed}$ (Colussi et al., 2012), OL is the organic loading, kg COD d^{-1} and $[Z]_{methanogenic\ bacteria}$ is the elemental composition of methane forming bacteria in g L^{-1}, as it was defined in Table 1.5.

The mass balance of nutrients is introduced in the equation (4.2):

$$Q_{purge} \cdot [Z]_{residual} - Q_{Nut} \cdot [Z] - Q_{fresh\ water.} \cdot [Z]_{tap} = - Y \cdot OL \cdot [Z]_{methanogenic\ bacteria} \quad (4.2)$$

Where [Z], g L^{-1}, is the concentration of the element Z in the nutrient solution. The composition of the nutrient solutions were shown in Table 4.2 and Table 4.3 for macronutrients and Table 4.4 for micronutrients. Q_{Nut}, L day^{-1}, is the flow rate of the nutrient solution, $[Z]_{residual}$ is the residual concentration of element Z and $[Z]_{tap}$ is the concentration of element Z in the tap water.

The chemical composition of the tap water was determined by ionic chromatography analysis (Table 4.5).

Table 4.5. Chemical composition of tap water in the selected flexographic facility.

Cations	Concentration, mg L^{-1}	Anions	Concentration, mg L^{-1}
Ca^{2+}	45	Cl^{-}	66
Mg^{2+}	6.4	$N\text{-}NO^{3-}$	1
Na^{+}	50	$S\text{-}SO_4^{2-}$	1.7
K^{+}	3		

The recommended residual concentration, $[Z]_{residual}$ in equation (4.2), for macronutrients are 5 and 1 mg L^{-1} for nitrogen and phosphorus, respectively (Chong et al., 2012). The residual concentrations for the micronutrients were selected as 0.03 mg L^{-1} for all of them, except for Fe that was 0.45 mg L^{-1}.

The mass balance, equation (4.2), is based on a system whose volume is constant. In that case and considering negligible the flow rate of nutrients, the water flow rate of fresh water can be obtained by equation (4.3).

$$Q_{fresh\ water} = Q_{purge} + Q_{evaporation} \quad (4.3)$$

Where, Q_{purge}, $m^3\ d^{-1}$, is the daily water volume purged and Q_{evap}, $m^3\ d^{-1}$, is the daily water volume lost as evaporation.

Taking into account the equations (4.2) and (4.3), the dosage of nutrients can be calculated by (4.4):

$$Q\cdot[Z] = Q_{purge}\cdot\left([Z]_{residual} - [Z]_{tap}\right) - Q_{evap.}\cdot[Z]_{tap} + Y\cdot OL\cdot[Z]_{methanogenic\ bacteria} \quad (4.4)$$

4.2.4 Alkali solution

The alkali solution had a concentration of 100 kg Na_2CO_3 m^{-3} and it was prepared on-site in an IBC of 1 m^3. The alkalinity and the pH are key parameters in the performance of the anaerobic reactor, hence the dosage of the alkali solution followed special control rules that were implemented in the PLC program. These rules and the dosage of the alkali solution will be explained in chapter 5.

4.3 Analytical procedures

4.3.1 VOC concentration and composition

The VOC concentration was determined by two total hydrocarbon analyzers in three points of the industrial prototype. These points were located at the inlet and outlet air of the scrubber and at the outlet air of the water degasser. The composition of the VOC emissions at the inlet and outlet air of the scrubber were also determined.

4.3.1.1 *Total hydrocarbon analyzer*

Initially, a total hydrocarbon analyzer (Nira Mercury model 901, Spirax Sarco, Spain), which distinguishes between methane and non-methane volatile organic compounds was used. This equipment was used to determine the methane and NMVOC at the outlet air stream of the water degasser and the scrubber. Both measurements were used to determine the methane removal efficiency of the water degasser. So, it was corroborated that a total hydrocarbon analyzer that did not distinguish between methane and VOC was appropriated for monitoring the efficiency of the scrubber in terms of abatement of VOCs and the methane removal efficiency of the water degasser. The frequency of the analysis was 6 seconds and the duration of the measurements was 15 min.

For the continuous on-line monitoring of the VOC concentration, a second total hydrocarbon analyzer (model RS 53-T, Ratfisch Analysensysteme, Germany) measured VOC concentration at the air inlet and outlet of the scrubber and at the outlet air stream of the degasser. The analyzer was calibrated once per month with a bottle containing propane with a concentration of 48.6 ppm_v (Praxair, EEUU). The total hydrocarbon analyzer was connected to a set of electro valves with a control system that allowed to measure in a cycle, sampling the inlet air of the scrubber during 20 minutes, 5 minutes the outlet air of the scrubber and 5 minutes the outlet air stream of the water degasser. The control system of the analyzer recorded data every 6 seconds.

4.3.1.2 *Gas chromatography*

The composition of the inlet and the outlet gas of the scrubber were measured by carbon sorbent tubes and post GC analysis, following the norm NEN-EN 13649, December 2001 (Stationary source emissions- Determination of mass

concentration of individual gaseous compounds- Activation carbon and solvent desorption method). These analyses were performed every time the configuration of the scrubber was changed. The data from these analyses were determined to calculate the removal efficiency per compound of each scrubber configuration and to obtain data for each solvent to calibrate the simulation model of the scrubber unit.

The composition of the inlet air was mainly composed by ethanol (EtOH), ethyl acetate (EA) and ethoxy propanol (Et2Pr), reaching the three together the 96% of weight of the total VOC emission of the facility.

4.3.2 Biogas composition

The biogas composition was measured with an optical infrared analyzer dual wavelength (Combimass GA-m, Binder, Germany). The sampling point was located before the gas counter. A total of 9 measurements were performed during the study. These measurements were done at the beginning, in the middle and at the end of the study. The sampling time was 5 minutes while checking that H_2S concentration kept constant.

4.3.3 Water quality

Main parameters of the liquid phase were monitored in situ with photometric commercial kits twice a week during the first 4 months, then the analyses were spaced once per week. The parameters measured were: chemical oxygen demand (COD), volatile fatty acids (VFA), and nutrients (N-NH_4^+ and P-PO_4^{3-}) concentration with LCK 014, LCK 365, LCK 303 and LCK 348 kits from HACH Lange GmbH (Germany), respectively. Alkalinity was determined with titrimetric kit (Method titrimetric with titration pipette MColortestTM, Merk Millipore, Germany).

One sample per week was analyzed in the first three months of operation in the University of Valencia. The analyzing time was spaced after three months to one sample per month. The parameters analyzed in the University of Valencia were the cation and the anion concentrations, due to their importance for biomass growth, and the solvent composition of the water samples to corroborate the degradation pattern for each solvent.

The ion concentration was measured following the norm 5310 A standard method in an ionic chromatograph (Ionic Chromatograph 88, Basic IC Plus,

Metrohm, Sweden). The determined cation concentrations were Ca^{2+}, Mg^{2+}, N-NH_4^+, Na^+ and K^+. The measured anion concentrations were S-SO_4^{2-}, N-NO_3^-, P-PO_4^{3-} and Cl^{-1}.

A gas chromatograph (model 789A, Agilent Technologies, EEUU) equipped with a flame ionization detector, a Restek Rtx-VMS column (length 30 m and 0,25 inner diameter x 1,4 μm phase) and helium as carrier gas was selected to determine the solvent composition of the liquid phase. The samples were injected to the chromatograph using split injection at 190°C. A ramp temperature (35°C during 21 minutes and increase of 10°C min^{-1} till reach 110°C) was applied. The temperature of the detector was 240°C.

4.4 Process simulation model

A model of the anaerobic bioscrubber was built in Aspen Plus® V 8.0. The physico chemical processes that control the scrubber and the anaerobic reactor are implemented in the core of this simulator. The selection of this commercial simulator was due to the availability of use the thermodynamic model Electrolyte NRTL (ELECNRTL). This thermodynamic model is an extension of the NRTL model for its application in aqueous solutions with electrolyte. The NRTL model is an extension of Wilson model and it is able to represent vapor-liquid, liquid-liquid and vapor-liquid-liquid equilibrium. Wilson model was the first model that applied activity coefficients and it is recommended to non-ideal systems. The ELECNRTL thermodynamic package calculates the liquid properties from its activity coefficient model, the vapor phase properties from the Redlich-Kwong equation of state and the aqueous and aqueous/organic electrolyte systems are represented with a single set of binary interaction parameters (Aspen Technology, 2013).

In the next sections, it is described the equations implemented in the selected modules for scrubber and the anaerobic reactor within the available ones in Aspen Plus®. A detailed explanation of the model definition along with its calibration and validation is included in chapter 7.

4.4.1 Scrubber unit

The scrubber unit was modelled using Radfrac Aspen Plus® Module, which is a rigorous module for all types of multistage vapor-liquid operations simulations, including absorption. The traditional way to model such scrubber in simulator programs, including Aspen Plus®, is by using the theoretical stages method

-equation (2.1)-, where a certain height of packing can be modelled as one equilibrium stage. The most rigorous analysis of absorption can be made based on a stage-by-stage analysis. This is done by performing component and energy balances on each stage assuming that equilibrium is achieved between both phases. A conceptual representation of the stage is shown in Figure 4.8.

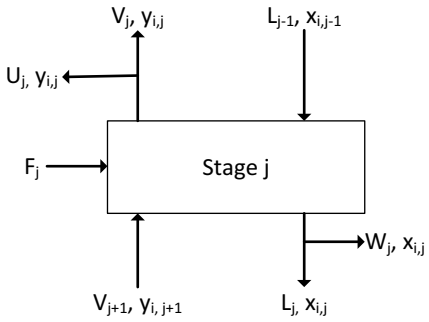

Figure 4.8. Equilibrium stage in the scrubber unit.

In this stage, the liquid enters the stage j with a flow rate of L_{j-1} and composition $x_{i,j-1}$, and leaves with a flow rate and composition of L_j and $x_{j,i}$. A similar convention is used for the vapor with V and y notation. A fresh feed can be added to the stage with flow rate of F_j and composition $z_{j,i}$. Side streams (W_j and U_j) can be drawn from the vapor and/or liquid streams. The total material balances in this stage is given by equation (4.5):

$$V_{j+1}+L_{j-1}+F_j-\left(1+r_j^V\right)V_j-\left(1+r_j^L\right)L_j=0 \tag{4.5}$$

Where $r_j^V = U_j/V_j$ and $r_j^L = W_j/L_j$ are the draw ratios. Similarly, a component balance can be written

$$V_{j+1}\cdot y_{i,j+1}+L_{j-1}\cdot x_{i,j-1}+F_j\cdot z_i-\left(1+r_j^V\right)V_j\cdot y_{i,j}-\left(1+r_j^L\right)L_j\cdot x_{i,j}=0 \tag{4.6}$$

In addition, the heat balance of the stage is given by the equation (4.7)

$$V_{j+1}\cdot H_{j+1}^V+L_{j-1}\cdot H_{j-1}^L+F_j\cdot H_j^F-\left(1+r_j^V\right)V_j\cdot H_j^V-\left(1+r_j^L\right)L_j\cdot H_j^L=0 \tag{4.7}$$

Where H denotes the enthalpy.

The above model is completed by adding the equilibrium constraint on the products leaving the stage. This is usually express as:

$$y_{i,j}=k_{i,j}x_{i,j} \tag{4.8}$$

Regarding the number of equilibrium stages, Aspen Plus® only allows integer number of transfer units; hence Murphree efficiency per compound should be defined. The Murphree efficiency is the most widely used efficiency in separation process calculations and it is obtained by the equation (4.9):

$$E_{i,j}^{MV} = \frac{y_{i,j} - y_{i,j+1}}{y_{i,j}^{*} - y_{i,j+1}} \qquad (4.9)$$

Where $E_{i,j}^{MV}$ is the Murphree vapor efficiency for the component i on stage j, $y_{i,j}^{*}$ is the composition of vapor in equilibrium with the liquid leaving the tray, and $y_{i,j}$ and $y_{i,j+1}$ are the actual composition in vapor in stage j and j+1, respectively.

4.4.2 Anaerobic reactor unit

A simplified ADM1 model has been developed in this thesis. The model of the anaerobic reactor aims to simulate the degradation of solvents at typical operational conditions, hence a number of processes of anaerobic degradation of wastewaters stablished in ADM1 have been excluded in order to further reduce the complexity of the model. Processes being omitted from the model concept developed herein were:

- Sulphate reduction and sulphide inhibition.
- Nitrate reduction.
- Long chain fatty acid inhibition.
- Competitive uptake of H_2 and CO_2 between hydrogenotrophic methanogenic archaea and homoacetogenic bacteria.
- Free ammonia inhibition and ammonia limitation.
- pH inhibition.
- Decay processes.
- Nutrient uptake.

The proposed reduction model will decrease running time, number of parameters to be estimated and implementation workload. The steps followed to implement the simplified ADM1 model in Aspen Plus® were: the definition of the reactions, the kinetic of the reaction that governed the degradation of the solvents and the selection of the Aspen Plus® Blocks. These steps are explained hereafter.

4.4.2.1 *Definition of the solvent degradation reactions*

The reactions defined in the model were based on the anaerobic degradation mechanism of the main solvents found at the emissions of the facility (ethanol, ethyl acetate and 1-ethoxy-2-propanol), which were described in chapter 1.

Although the ethanol degradation depends on the sulphate concentration, in this case the role of sulfate-reducing bacteria has been considered negligible, since the dose of sulfate was limited to the minimum requirements for biomass growth. The degradation of 1-ethoxy-2-propanol was assumed to result in acetone and ethanol, while acetone is fully degraded to acetic acid. This assumption was supported by the fact that acetone was not detected in the water effluent of the reactor. For this reason, the acidogenesis of 1-ethoxy-2-propanol has been modelled by one step. According to these, the acidogenesis reactions defined in the model were:

Ethanol	$C_2H_5OH + H_2O \rightarrow CH_3COOH + 2H_2$	(4.10)
Ethyl acetate	$C_4H_8O_2 + H_2O \rightarrow CH_3COOH + C_2H_5OH$	(4.11)
1-ethoxy-2-propanol	$C_5H_{12}O_2 + H_2O + CO_2 \rightarrow 2\ CH_3COOH + C_2H_5OH$	(4.12)

The acetic acid and hydrogen produced in the reaction (4.10) to (4.12) were further degraded in the methanogenesis step, which were defined by the next equations.

Acetic acid	$CH_3COOH \rightarrow CO_2 + CH_4$	(4.13)
Hydrogen	$4H_2 + CO_2 \rightarrow 2H_2O + CH_4$	(4.14)

4.4.2.2 *Definition of kinetics*

The substrate uptake kinetics were defined in the model by two kind of reactions: full conversion and Monod kinetic. The hydrolysis of ethyl acetate reaction (4.11) and the hydrogenotrophic methanogenesis reaction (4.14) were modelled by a full conversion reaction. The hydrolysis of ethyl acetate was defined as full conversion because ethyl acetate was not detected in the water effluent of the anaerobic reactor. For the rest of reactions (4.10), (4.12) and (4.13), Monod type -equation (2.8)- was chosen, since subprocesses of anaerobic treatment have been successfully modelled by following Monod kinetics (Pavlostathis and Giraldo-Gomez, 1991).

4.4.2.3 *Selection of Aspen Plus® Blocks*

The model has been built in Aspen by using five different Aspen modules. The selected Aspen modules were: two RStoic, two RCSTR and a Flash2 module. The first four modules were used to simulate the degradation of the solvents to biogas. The selection of these modules was driven by the kind of reaction run in them, being RSToic module selected for conversion reactions and RCSTR modules for rate-controlled reactions. Finally, Flash2 module was used to simulate the separation of the gas (biogas) and the liquid (water effluent) phases. The equations implemented in these modules are explained hereafter.

The water with the dissolved solvents entered firstly in an RStoic module. This module is the simplest reactor block of Aspen Plus®. It permits the use of several reactions with the molar extent of conversion or fractional conversion of a component, specified for each reaction. This module was used to simulate the degradation of ethyl acetate, which follows the equation (4.11), assuming full conversion.

Afterwards, the water entered in the acidogenesis reactor, where ethanol -reaction (4.10)- and 1-ethoxy-2-propanol -reaction (4.12)- were degraded. These reactions were kinetically limited by Monod and modelled in an RCSTR Aspen Plus® module. The effluent stream of the acidogenesis reactor entered in another RCSTR module, where the methanogenesis step was modelled -reaction (4.13)-. The anaerobic reactor was simulated as a continuous stirred tank reactor because EGSB reactors are characterized by an improved hydraulic mixing, independent from the biogas production, in which all the retained sludge is optimally mixed with the incoming wastewater (Fuentes et al., 2011; van Lier at al., 2015). The implemented mass balance for each of the three components in the two modules was the equation (4.15), considering the RCSTR shown in Figure 4.9 and assuming that kinetic rates follow Monod equation.

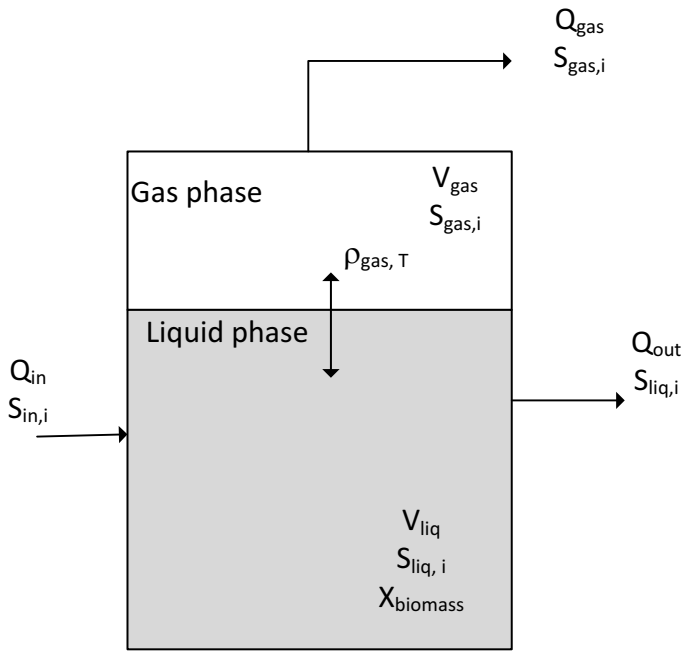

Figure 4.9. Schematic of a typical RCSTR reactor.

$$\frac{Q_{in}S_{in,i}}{1000V_{liq}} - \frac{Q_{out}S_{liq,i}}{1000V_{liq}} - \nu_{max,i}\frac{S_{liq,i}}{K_{s,i}+S_{liq,i}} = 0 \qquad (4.15)$$

When this equation is applied to the acidogenesis reactor block, $S_{in,i}$ is the inlet concentration (mg COD L^{-1}) of ethanol and 1-ethoxy-2-propanol. $S_{liq,i}$ (mg COD L^{-1}) is the concentration of these compounds in the reactor. For both compounds, $\nu_{max,i}$ is the volumetric maximum growth rate, expressed as kg COD m^{-3} h^{-1} and $K_{S,i}$ is the half-saturation constant in mg COD L^{-1}, where i denotes ethanol or 1-ethoxy-2-propanol. When the equation (4.15) is applied to the methanogenesis reactor, $S_{in,i}$ is the inlet concentration of acetic acid, expressed as mg COD L^{-1}. $S_{liq,i}$ (mg COD L^{-1}) denotes the concentration of acetic acid in the reactor. ν_{max} (kg COD m^{-3} h^{-1}) is the volumetric maximum growth rate for acetic acid uptake and K_S (mg COD L^{-1}) is the half-saturation constant of acetic acid. For both reactors, Q_{in} and Q_{out} (m^3 h^{-1}) are the influent and effluent volumetric flow rate, respectively, and V_{Liq} (m^3) denotes the water volume of the reactor. Monod-type kinetic was implemented in Aspen Plus® using the Langmuir-Hinshelwood Hougen-Watson reaction type, which after algebraic operation mimics Monod-type expression (it will be further explained in chapter 7).

The outlet stream of the second RCSTR module entered into an RStoic module, where hydrogen is fully converted to methane by following the hydrogenotrophic methanogenesis -reaction (4.14)-. The outlet stream of this last reactor was composed by two phases (biogas and liquid effluent). The separation of these phases was carried out in the Flash2 module. The outlet streams of this module were the biogas stream and the liquid effluent of the anaerobic reactor, being these two phases in equilibrium. The equations implemented in this module were the equilibrium relations, which are defined in the core of the software and are the same ones defined in a stage of the scrubber unit.

5 INDUSTRIAL PROTOTYPE: OPERATIONAL PROTOCOLS

The experimental of this thesis was carried out at industrial scale by using a prototype installed in a flexographic facility located in the Netherlands. This set-up was chosen in order to ensure the applicability of the anaerobic bioscrubber as an abatement VOC technology for this sector. The performance of the system was evaluated during more than a year (484 days), since it was necessary to check the stability of the anaerobic reactor working under fluctuated and intermittent loads. The system was operated virtually as a closed-system, with a small daily purge, in order to minimize the consumption of fresh water. So, it was necessary to check the potential adverse influence of accumulation of electrolytes and non-biodegradable compounds in anaerobic granular biomass performance. It was also necessary to ensure that the pressure drop in the scrubber kept below an established limit, in order to guarantee a reasonable electricity consumption in the scale-up.

This chapter explains the control plan implemented in the PLC program that was evaluated in this thesis in order to check its functionality for industrial scale. Other aspects that were evaluated in the framework of this thesis were the commissioning and the start-up of the industrial prototype. The protocols to check the software control are really important, since their objective is to be sure that the control rules have been properly programmed, hence they should be checked at every condition. The protocols applied during the start-up and the commissioning of the prototype are important for their application in the scale-up.

Finally, the performance of the installation in a normal working week is exposed as an example, in order to show the data generated in the operation of the industrial prototype. The section will illustrate the operation, monitoring and data collection of a typical period, which has been selected as representative.

5.1 Description of the air emission of the facility

The industrial prototype treated the air emissions ---------- of Altacel Transparant Verpakkingsind (Weesp, The Netherlands). The industrial prototype was designed to treat 10 tones of solvent per year, a fraction of the total air emission of the facility, ----------. The flexographic site operates on a two-shift (16 h) basis from Monday to Friday and on an one-shift (8 h) basis on Saturday. High variable emissions associated to the number of printing press in operation occurred, as it can be seen in Figure 5.1 where the air inlet VOC concentration at the scrubber in a normal working week (from day 30 to day 37) is shown. Moreover, the VOC air emission was linked to facility production, stopping every night and from Saturday midday till Monday morning.

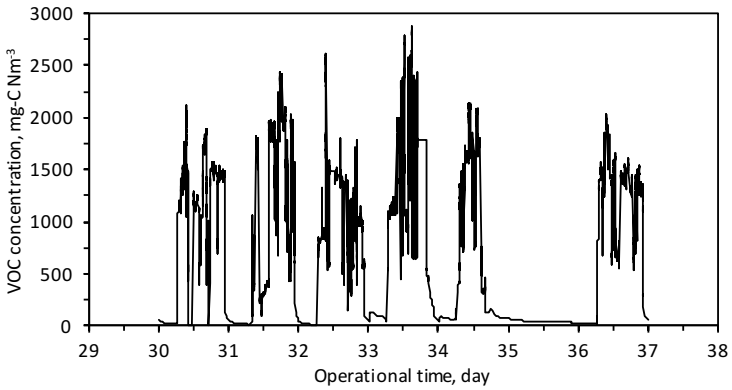

Figure 5.1. Inlet VOC concentration since day 30 to day 37 of the operation of the industrial prototype.

The air emission of the facility was mainly composed by EtOH, EA and Et2Pr, reaching the three together the 96% of weight of the total VOC concentration, as it is shown in Table 5.1. This table summarizes the average composition of the air emissions with the standard deviation of 14 measurements done along the 484 days. The composition is characteristic of the flexographic sector, according to EC (2007) the solvents used in the flexographic sector very rarely deviate from ethanol, ethyl acetate and mixtures of the two. Moreover, the investigations found in the literature about the VOC treatment from printing sector reported emissions where the major compounds detected at the air emissions were ethanol, ethyl acetate and a glycol ether that could be 1-methyl-propanol or 1-ethoxy-2-propanol (Granström et al., 2002; Le Cloriec and Humeau, 2013; Sempere et al., 2012).

It is noted that the VOC emission is mainly composed by EtOH, EA and Et2Pr, therefore an average VOC inlet composition is assumed to study the performance and to develop the process simulation model of the anaerobic bioscrubber. This average composition is based on the measurements shown in Table 5.1 and it was 65.5% of EtOH, 25.4% of EA and 9.1% of Et2Pr.

Table 5.1. Average composition of the solvent emission of the chosen flexographic facility (n=14).

	Composition, $\%_{weight}$
ethanol	63.0 ± 3.3
isopropanol	0.6 ± 0.4
Ethyl acetate	24.4 ± 4.5
isopropyl acetate	0.1 ± 0.1
1-methoxy-2-propanol	1.2 ± 3.5
n-propylacetate	0.6 ± 0.7
1-ethoxy-2-propanol	8.8 ± 5.3
1-methoxy-2-propanolacetate	0.7 ± 0.4
n-propanol	0.3 ± 0.6
butanol	0.1 ± 0.1

The average temperature during the 484 days at the inlet gas phase of the prototype was 40 ± 6°C, being the average exhaust gas temperature at the outlet of the press printers 53 ± 3°C. The moisture of the inlet air was 0.0133 kg H_2O kg^{-1} dry air ----------.

5.2 Control protocol of the industrial prototype

5.2.1 Description of the complete diagram of the industrial prototype

The scheme of the industrial prototype was provided in chapter 4, where the main units of the industrial prototype (scrubber and anaerobic reactor) were explained. The complete diagram of the system (Spanish patent ES254257R1) along with the installed instruments is presented in Figure 5.2..

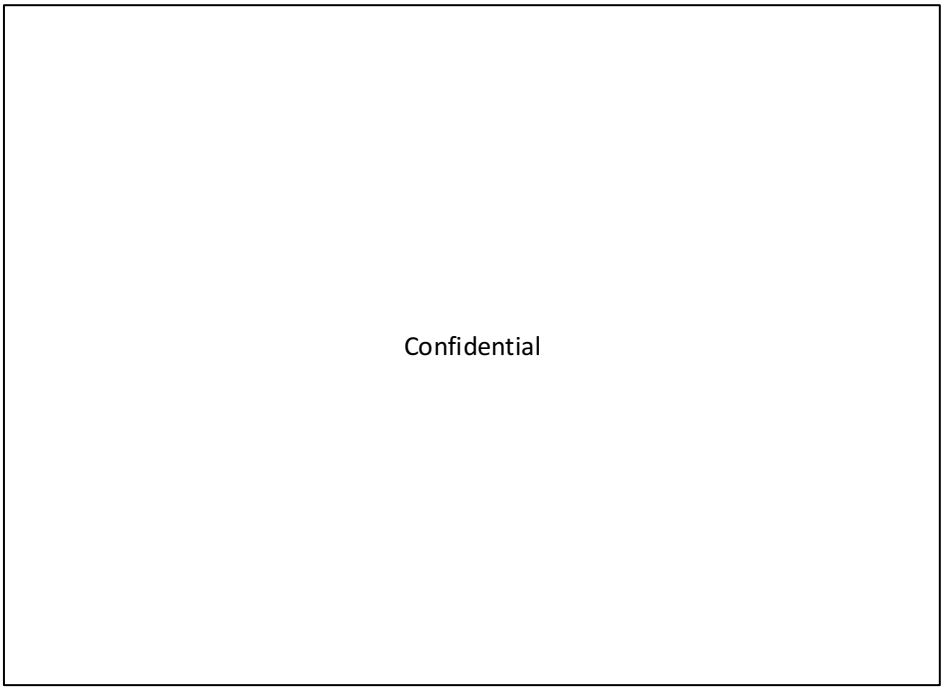

Figure 5.2. Complete diagram of the industrial anaerobic bioscrubber prototype.

As it was mentioned in chapter 4, the VOC-polluted air coming from the factory was introduced to the bottom of the scrubber by the blower, and the water was sprayed from the top and collected in the scrubber tank.----------
---

---------- The water with the dissolved solvents was collected in the scrubber tank and flowed to the buffer tank. The macro- and micro-nutrients, sodium carbonate, and yeast extract were supplemented to the water in this tank prior to pumping it to the EGSB for solvent degradation. The dissolved solvents were degraded in the anaerobic reactor obtaining a water effluent and a biogas stream.

---------- The water after removing the dissolved methane was ----------
---------- pumping again through the scrubber.

5.2.2 Description of the PLC program

The industrial prototype was controlled by the installed instruments and the PLC program. The sophisticated PLC program allowed to operate the unit remotely. The PLC program was implemented in TBOX MS[15] Remote Terminal Unit (RTU), which apart from controlling the process, came with web server and datalogging capabilities already built in. In particular, the web server allowed the control software programmer to implement a web-based SCADA, making remote monitoring and control possible in real time. As an example, the initial pop-up window of the PLC program is shown in Figure 5.3. This window allowed to access to 2 pop-up windows. The first one (Figure 5.4) shows the buffer tank, the scrubber and the scrubber tank along with the nutrients and base tanks. The second pop-up window (Figure 5.5) shows the anaerobic reactor and ----------
---------- the drainage tank. The initial pop-up window also gave the possibility to access to time settings, cycle settings ----------, which will be explained after.

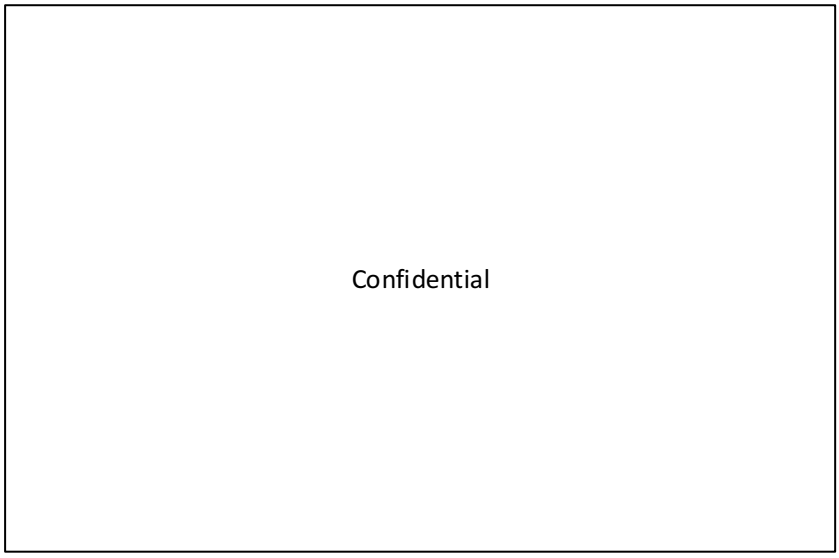

Figure 5.3. Start screen of the PLC program of the anaerobic bioscrubber.

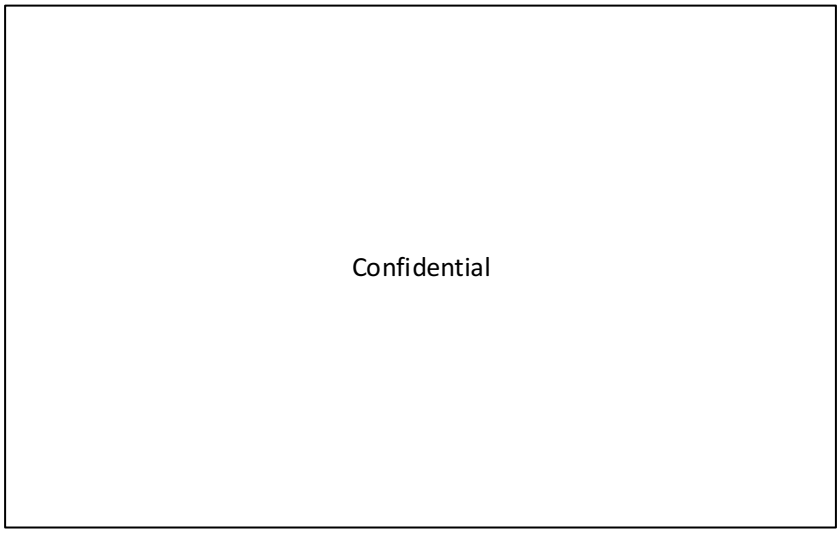

Figure 5.4. Scrubber and buffer tank pop-up window in the PLC program.

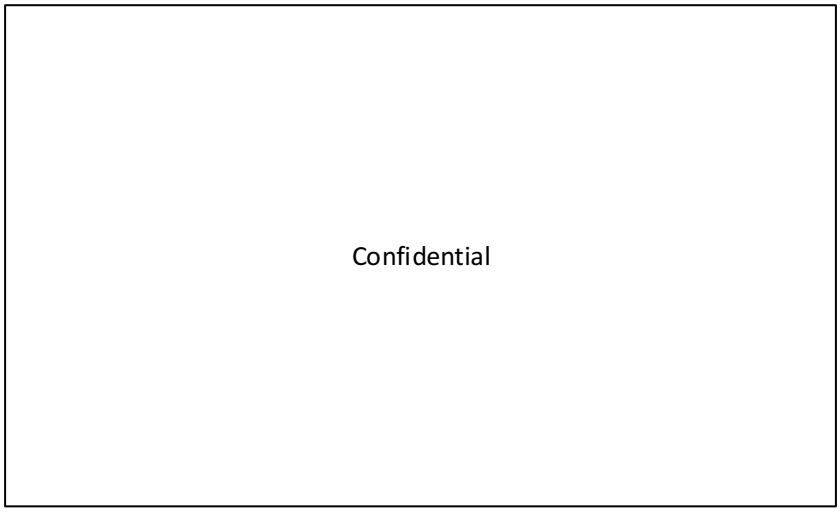

Figure 5.5. Anaerobic reactor ---------- pop-up window in the PLC program.

Both pop-up windows, Figure 5.4 and Figure 5.5, show the different instruments installed at the industrial prototype. Table 5.2 shows a brief description of the instruments function along with their tag for their identification in the PLC program.

Table 5.2. Instruments installed for on-line operation and monitoring.

Type	**----------**	**Description**
----------	----------	----------
Water flow	----------	Flow indicator to scrubber.
	----------	----------
	----------	----------
Air Flow	----------	Air flow transmitter at the inlet of the scrubber.
----------	----------	----------
	----------	----------
	----------	----------
	----------	----------

Table 5.2 cont. Instruments installed for on-line operation and monitoring.

Type	----------	**Description**
----------	----------	----------
Biogas Flow	----------	Biogas flow meter.
Dosing pump	----------	To dose macronutrients.
	----------	To dose sodium carbonate.
	----------	----------
Blower	----------	Air flow regulator of polluted air through the scrubber.
	----------	----------
pH sensor	----------	At water outlet of the reactor.
	----------	At water the inlet of the reactor.
----------	----------	----------
	----------	----------
----------	----------	----------
	----------	----------
	----------	----------
----------	----------	----------
----------	----------	----------
	----------	----------
	----------	----------
	----------	----------
	----------	----------
	----------	----------
	----------	----------
	----------	----------
Air pressure transmitter	----------	At the air inlet of the scrubber.
	----------	At the air outlet of the scrubber.

Table 5.2 cont. Instruments installed for on-line operation and monitoring.

Type	----------	Description
----------	----------	----------
	----------	----------
	----------	----------
Temperature transmitter	----------	----------
	----------	----------
	----------	----------
	----------	To monitor air temperature at the outlet of the scrubber.
	----------	----------
	----------	----------
	----------	----------
	----------	To monitor water temperature at the anaerobic reactor.
	----------	----------
	----------	----------

A maintenance plan to corroborate the calibration of the instruments was set-up. Main actions consisted of a monthly checking of:

- The pH ----------.

- The pressure transmitters ----------.
- The airflow regulator of the main air blower ----------.
- The biogas flowmeter ----------.

The instruments installed shown a robustness performance along the 484 days, being only necessary to recalibrate the pH sensors every two months.

The PLC program allowed to access to these instruments by clicking on it. The pop-up windows of the instruments gave the possibility to establish warning and/or alarm values. The PLC program showed an alarm if any of these values were reached. As an example, the corresponding pop-up window of ----------, temperature----------, pH ---------- and water flow transmitter ---------- are illustrated in Figure 5.6, Figure 5.7,Figure 5.8,Figure 5.9 and Figure 5.10, respectively.

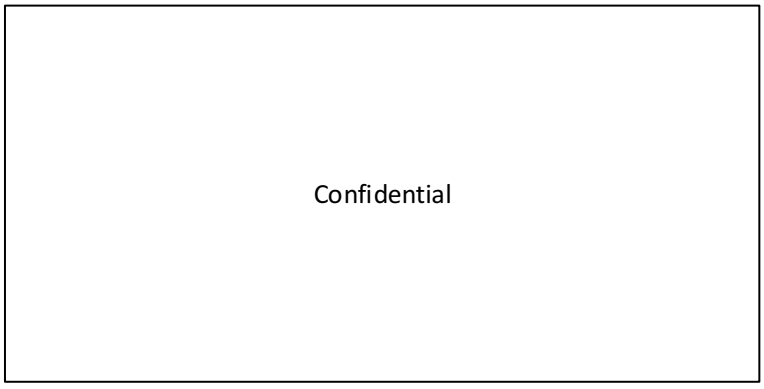

Figure 5.6. Pop-up window ----------.

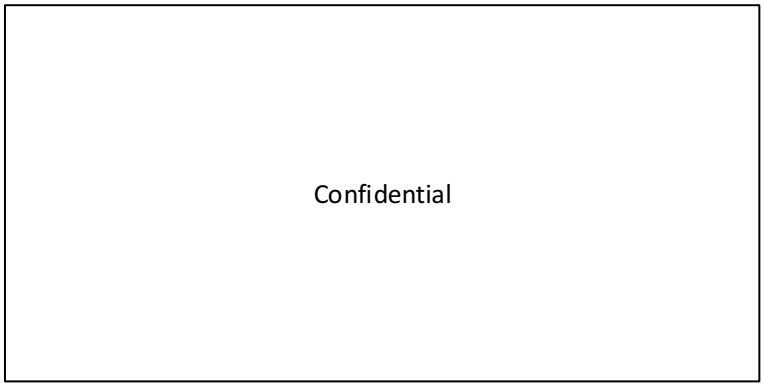

Figure 5.7. Pop-up window of the temperature transmitter installed to measured water temperature at the anaerobic reactor ----------.

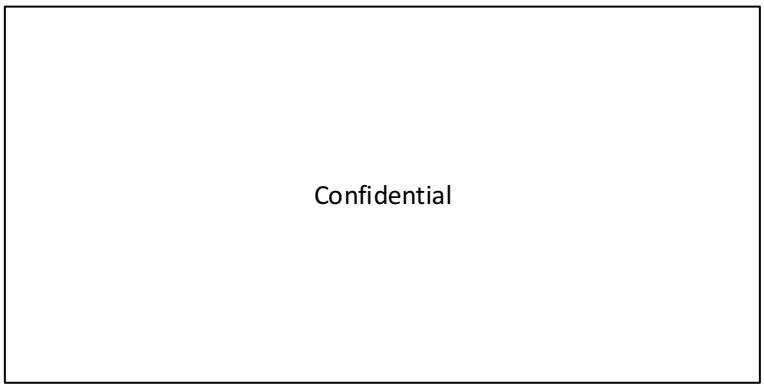

Figure 5.8. Pop-up window of the pH transmitter at the water effluent of the anaerobic reactor ----------.

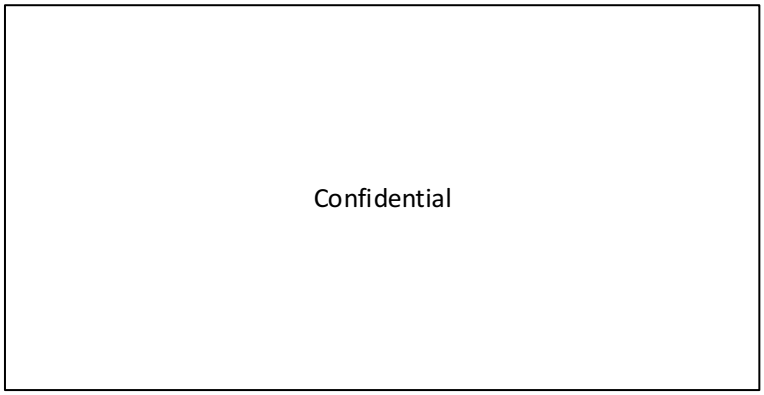

Figure 5.9. Pop-up window ----------.

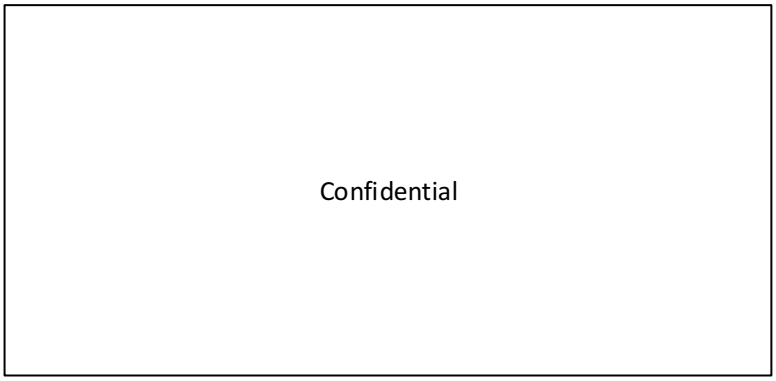

Figure 5.10. Pop-up window of the flow transmitter that measures the water flow through the scrubber ----------.

The blowers, centrifugal pumps and dosing pumps had their own pop-up window. The pop-up windows of the blowers and pumps allowed to set the proportional-integral-derivate controller (PID controller) parameters. The pop-up window of the dosing pumps allowed to introduce the calibration parameters ----------, which correlated the frequency of the pump and the dose to the system. As an example, the Figure 5.11,Figure 5.12 and Figure 5.13 show the pop-up window of the blower that blows air through the scrubber ----------, the centrifugal pump that drives water to the anaerobic reactor ---------- and the dosing pump that dose alkali solution to the system ----------, respectively.

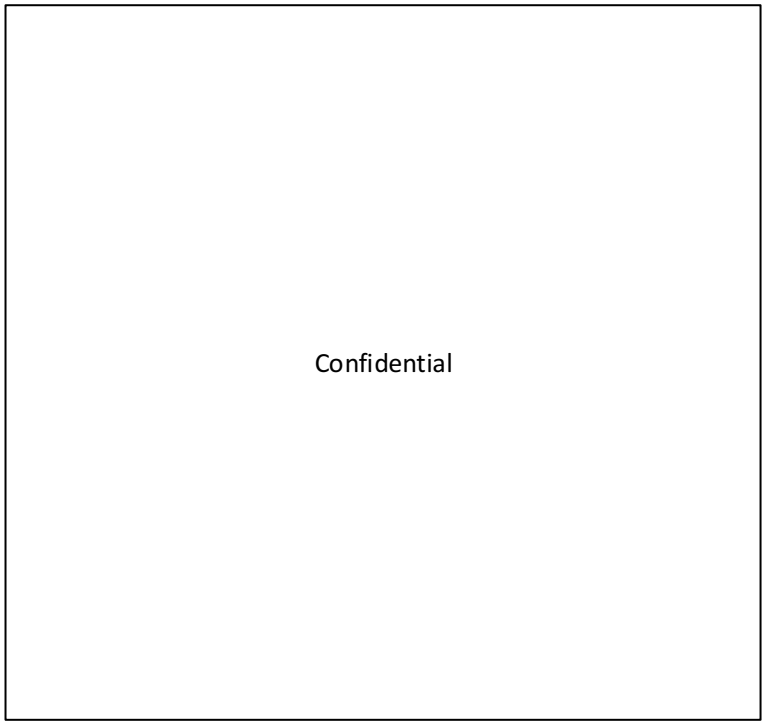

Figure 5.11. Pop-up window of the air blower to scrubber ----------.

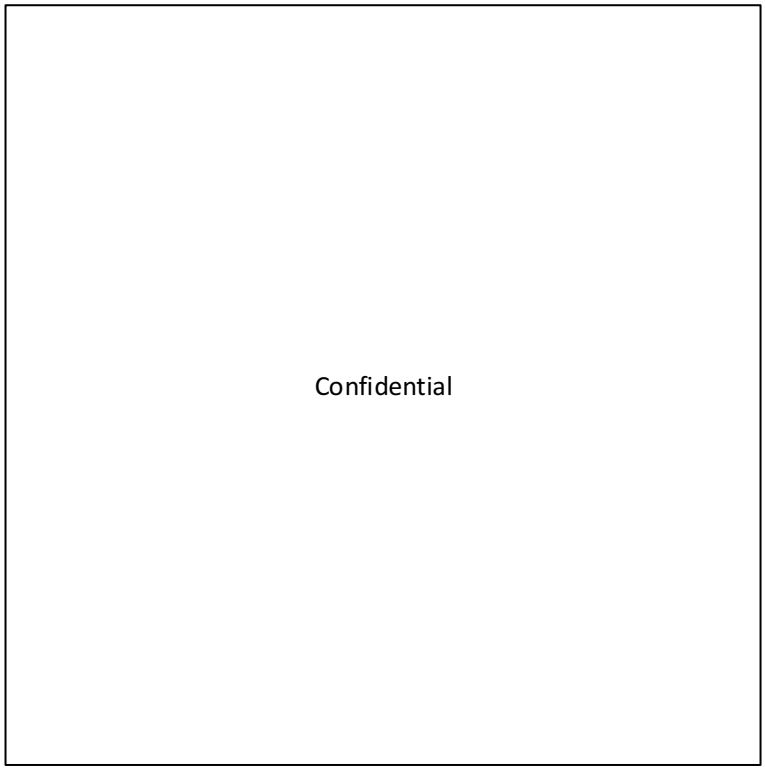

Figure 5.12. Pop-up window of the centrifugal pump to anaerobic reactor ----.

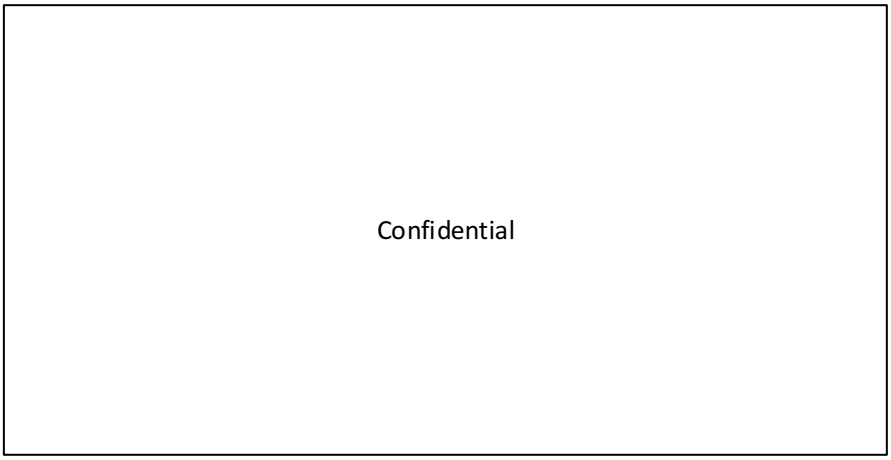

Figure 5.13. Pop-up window of the sodium carbonate dosing pump ----------.

5.2.3 Operational modes

The rules for operating and control the industrial prototype were developed for facilities that work under shifts, hence it was possible to define two kind of operational modes: production and non-production mode. Production mode matched with the production hours of the facility. The plant operated in non-production mode the rest of the time. The main difference between both modes lied on the circulation of the water. ----------
---

---------- The circulation of the water ---------- is clarified in Figure 5.14----------
---

---.

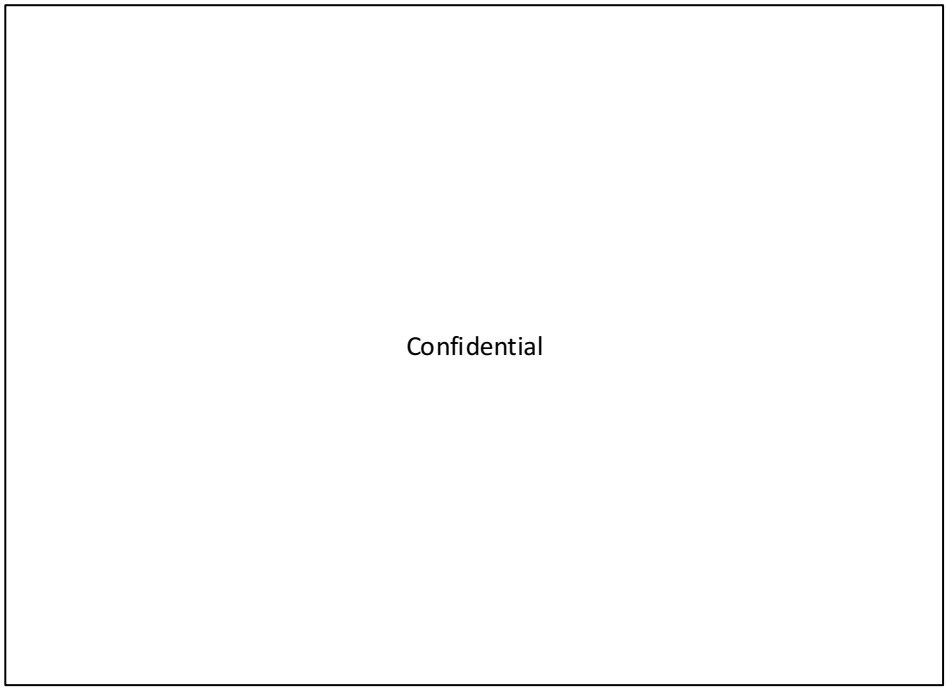

Figure 5.14. Complete diagram of the industrial anaerobic bioscrubber prototype indicating with blue arrow the circulation of water in non-production mode.

The two operational modes were defined in the Time settings pop-up window, which is shown in Figure 5.15, and it appeared by clicking on the Time Settings button in the initial pop-up window (Figure 5.3). The Figure 5.15 shows that, in this example, production mode was selected from Monday to Friday starting at 6:30 and finishing at 22:30 and on Saturday starting at 6:00 and finishing at 16:30. Sunday was not selected as production mode, i.e. non-production mode was assigned.

An additional rule linked with the water effluent pH of the reactor to avoid acidification of the anaerobic reactor was set-up: ----------
---

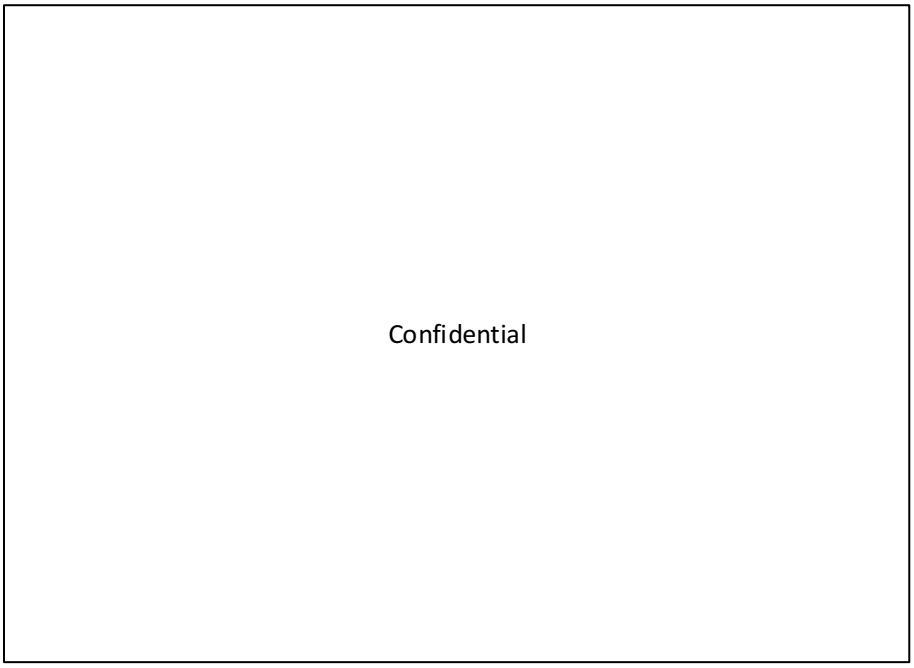

Figure 5.15. Time settings pop-up window in the PLC program.

The two operational modes shared the rules that control the level of water in the tanks. ---------- ---------- ---------- ---------- ---------- ---------- ---------- As an example, ---------- ---------- is shown in Figure 5.16.

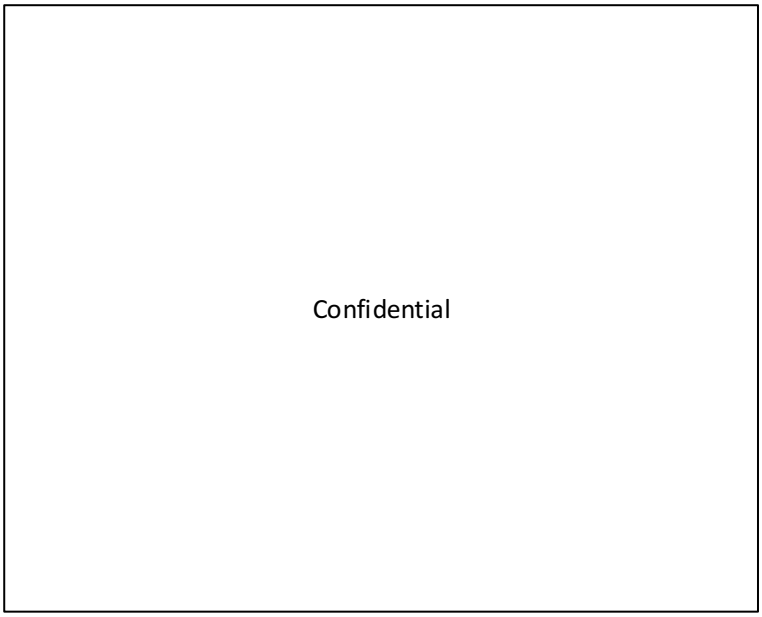

Figure 5.16. Pop-up window ----------

5.2.3.1 *Production mode*

The whole system ----------
---------- was hydraulically connected ----------. The main settings (air flow, water flow and rate of sodium carbonate and nutrient dosing) were defined in the cycle settings pop-up window that is shown in Figure 5.17 and it appeared by clicking on cycle setting button in the initial pop-up window (Figure 5.3).

---------- The flow of the recirculation pump was set to keep constant the up-flow velocity in 3 m h^{-1} for the whole experimental period.

Nutrients and alkali solution were added ----------

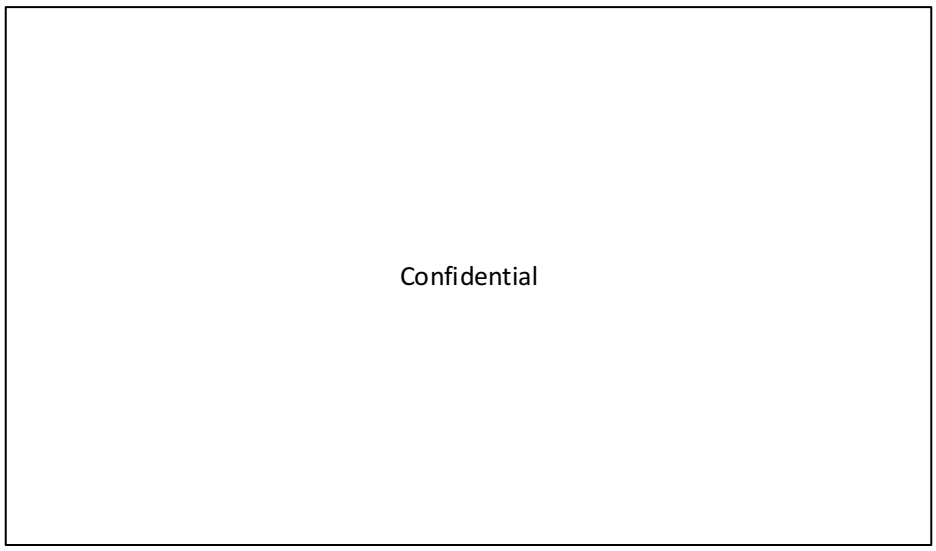

Figure 5.17. Cycle setting pop-up window in the PLC program.

For macronutrients dosing, the parameters were fixed to provide the quantities estimated according to the section 4.2.3.2.

The dose of the alkali solution was selected to keep the pH of the water effluent of the anaerobic reactor in the range of 7 and 7.5----------. These parameters of the liquid

phase are related with the methane content of the biogas, Table 5.3 provides a relation between pH in the reactor, alkalinity in water and CO_2 content of biogas. ----------

Table 5.3. Theoretical Na_2CO_3 concentration depended on CO_2 biogas content and pH reactor. Adapted from Tchobanoglous et al. (2003).

pH	**Gas phase CO_2, %**			
	30	20	15	10
6.8	1281	854	641	427
7	2030	1354	1015	677
7.2	3218	2145	1609	1073
7.3	4051	2701	2026	1350
7.4	5100	3400	2550	1700
7.5	6421	4281	3210	2140
7.7	10176	6784	5088	3392
8	20305	13536	10152	6768

5.2.3.2 *Non-production mode*

The Non-production mode ran when the facility was closed, as there were no VOC air emissions----------

The specific control rules implemented in the PLC program for the non-production mode were related with ----------. These rules were

implemented to ----------

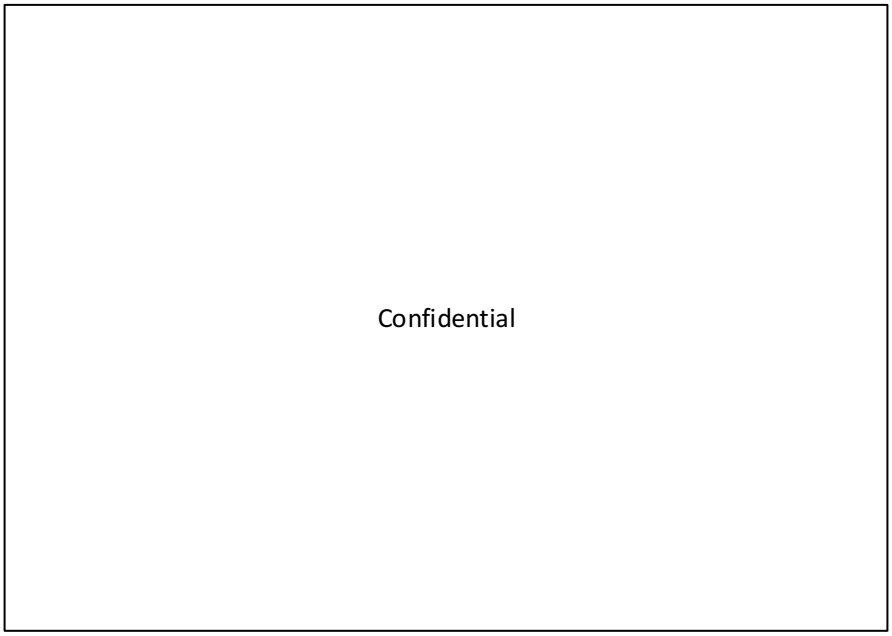

Figure 5.18. ----------

5.2.3.3 *Pressure drop control of the scrubber*

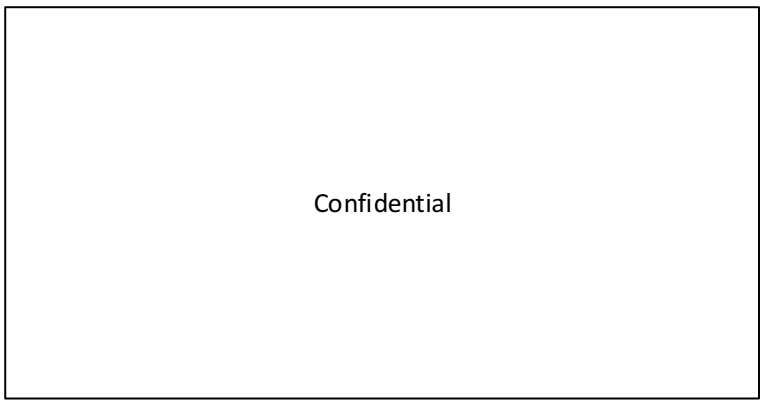

Figure 5.19. ---

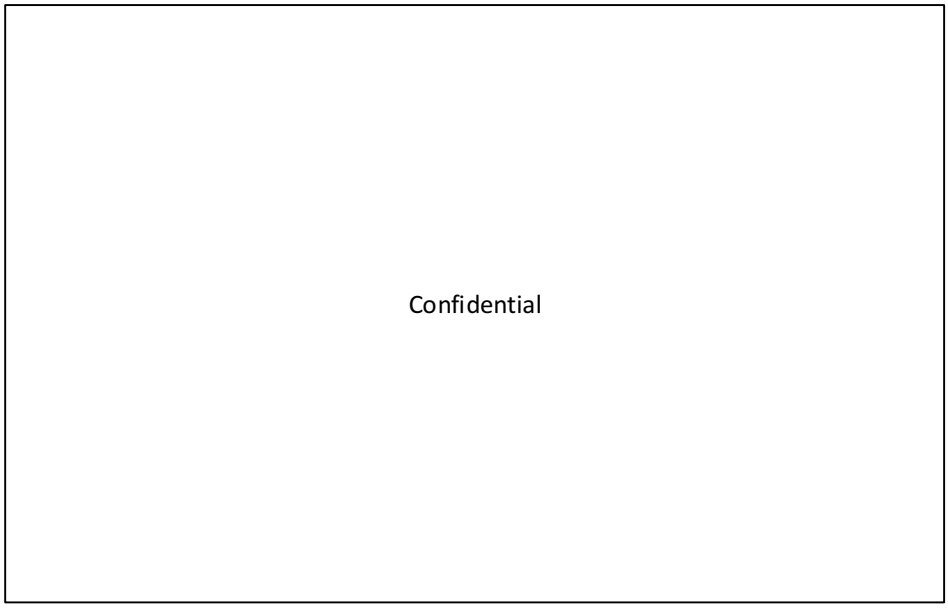

Figure 5.20. ----------

5.3 Monitoring of the industrial prototype

Due to the complexity of the system, it was necessary to monitor and store the historical data in order to evaluate if the protocols applied on the industrial prototype could be applied in the scale-up of the technology. The control, the operational and on-line monitor protocols allowed running the installation during 484 days without stopping it, unless to change the scrubber configuration. On-line monitoring was temporarily saved on TBOX RTU, but the internal memory of this unit was only enough for storing few days, so a software application named Remus®, which was developed by Pure Air Solutions BV (The Netherlands), was used to collect, store, export and visualize the historical data. In general, Remus® simplified the processing of the data and allowed to visualize the time evolution of the on-line parameters monitored in the prototype. As an example, the pressure drop in the scrubber for three months is presented in Figure 5.21.

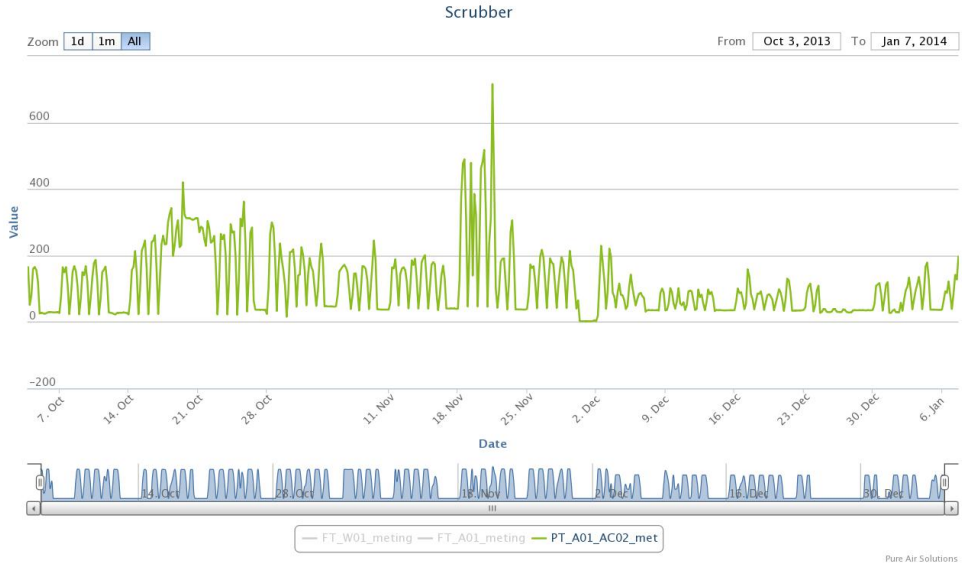

Figure 5.21. Evolution of the pressure drop in the scrubber from day 180 to 265. Y axis represent the pressure drop in Pa units.

The Remus® software also permitted to retrieve data for a specific period of time and it also automatically calculated the daily averages. This functionality has been used in this work to determine the performance of the system that will be discussed in chapter 6. The main parameters studied from the on-line monitoring are introduced herein.

5.3.1 Scrubber unit

The parameters selected to determine the performance of the scrubber during production mode in a day were the pressure drop (on-line monitored parameter) and the VOC removal efficiency (RE_{VOC}), which was calculated by the equation (5.1).

$$RE_{VOC} = \frac{Cg_{VOC,in} - Cg_{VOC,out}}{Cg_{VOC,in}} \cdot 100 \qquad (5.1)$$

Where $Cg_{VOC,in}$ and $Cg_{VOC,out}$ are average VOC concentration (mg-C Nm^{-3}) in the inlet and outlet air of the scrubber during production mode in a day. These concentrations were on-line monitored. ----------
---

The average values during production mode in a day of gas phase temperature at the inlet and outlet of the scrubber and the spraying water temperature were also monitored and stored, since they could influence on the performance of the scrubber. Figure 5.22 shows the monitored data in production and non-production mode in the scrubber operation. The lower part shows the inlet and out VOC concentration and the upper part shows the temperature of the of both phases at the inlet and outlet streams.

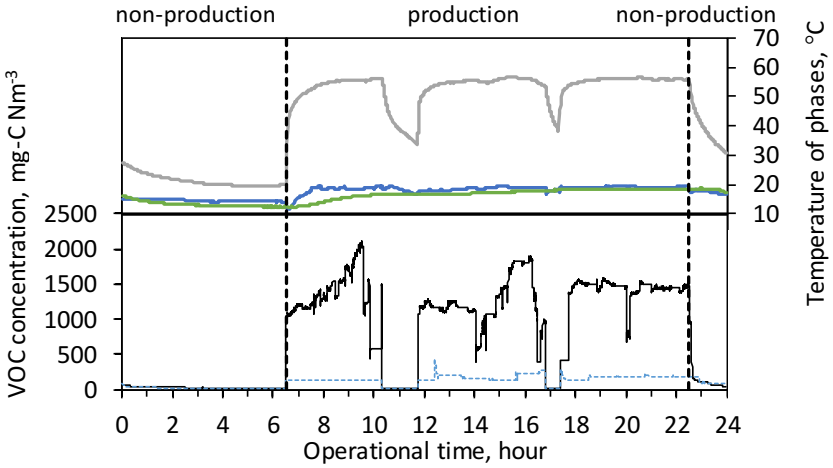

Figure 5.22. Continuous monitoring of the scrubber performance. (–) Inlet VOC concentration, (--) Outlet VOC concentration, (–) inlet air temperature, (–) outlet air temperature and (–) inlet air temperature.

5.3.2 Anaerobic reactor

The selected parameters to determine the daily performance of the anaerobic reactor were the OL (kg COD h^{-1}) in ---------- and the biogas rate (m^3 h^{-1}). The fed OL was calculated by the equation (5.2).

$$OL_{in} = \frac{Q_{air,SC} \cdot (Cg_{VOC,in} - Cg_{VOC,out})}{10^6} \cdot F_{COD} \qquad (5.2)$$

Where $Q_{air,SC}$ (m^3 h^{-1}) is the average airflow to the scrubber ---------- and F_{COD} is the conversion factor from mg-C to COD. This factor depends on the composition of the air emission, since each solvent has a different ratio COD to C. In this work, this factor was fixed in 3.8 g-COD $g\text{-}C^{-1}$,

assuming as representative the average composition of 65.5% of EtOH, 25.4% of EA and 9.1% of Et2Pr for the VOC emissions of the facility.

The biogas rate ($m^3\ h^{-1}$) was on-line monitored and stored to determine the performance of the anaerobic reactor. Three different average biogas rate were defined to study the performance of the anaerobic reactor: in production mode, in non-production mode and the daily production. The average biogas rate in the non-production periods indicated if the anaerobic reactor was overloaded, since non-degraded solvents were accumulated in the system and degraded during this period.

The temperature of the water in the anaerobic reactor, the ---------- ---------- of the influent and effluent water of the anaerobic reactor were also on-line monitored and stored, since a deviation from the recommended values can adversely impact on the performance of the reactor.

The monitoring of the mentioned on-line parameters was accompanied by the on-site chemical analyses of the water effluent of the anaerobic reactor described in chapter 4.

5.3.3 Methane production

Since COD stabilization in anaerobic processes is directly related to methane production, this parameter should be followed to evaluate the performance of the anaerobic reactor in terms of COD removal efficiency (RE_{COD}). Along with measuring the biogas production, it is necessary to determine the methane concentration in the liquid effluent of the anaerobic reactor in order to perform the mass balance related to the solvent degradation, and taking into account that the proposed technology works in water closed-recirculation mode. ---------- ---------- ---------- This section explains how the methane production has been measured in this thesis.

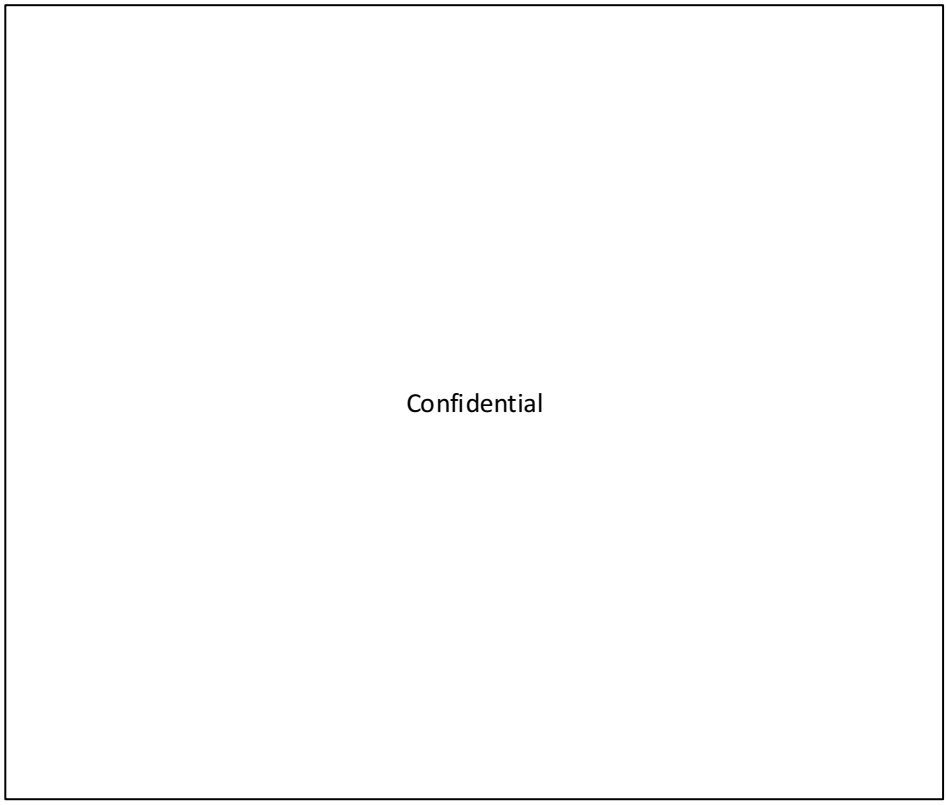

Figure 5.23. Gas monitoring points of methane in the anaerobic bioscrubber.

The main monitoring point of methane in the prototype was the biogas production. As it has been mentioned, the methane content of the biogas is linked with the bicarbonate concentration and pH in the reactor by equation (1.12). This equation can be used if there is not any anion that interferes with the alkalinity measurement**.** The methane content calculated with this equation was compared with the experimental methane content periodically measured. The results of this comparison are shown in Table 5.4 along with sulfhydric acid content. The alkalinity concentrations shown in Table 5.4 corresponds to the alkalinity due to carbonate species and volatile fatty acids concentrations. The table shows that the methane content of biogas produced in the anaerobic bioscrubber prototype was higher than 90%, indicating that the implemented pH control rules kept the methane content at high values. The maximum error predicted by the equation (1.12) was 3.9% on day 20, so henceforth the equation (1.12) can be used to estimate the methane content in the biogas. In addition, the average H_2S concentration was 5.1 ± 4.5 ppm, with a

maximum value of 12 ppm, indicating that the dose of the nutrients, hence the sulfur added to the system, was well controlled and nutrient dosage control rules kept H_2S concentration at low values.

Table 5.4. Measured biogas composition and comparison with calculated one by the equation (1.12).

Day of operation	**CH_4, $\%_{VOL}$**	**CO_2, $\%_{VOL}$**	**H_2S, ppm**	**pH**	**----------**	**VFA, mg acetic acid L^{-1}**	**CH_4 calculated eq. (1.12), $\%_{VOL}$**	**Error, %**
20	94.3	5.7	2.0	7.5	----------	89.4	90.7	3.9
24	95.5	4.5	10.0	7.53	----------	112	93.3	2.3
96	94.1	5.9	11.0	7.49	----------	122	91.7	2.5
233	90.1	9.9	2.0	7.47	----------	180	89.8	0.3
245	91.1	8.9	0.0	7.40	----------	87.5	87.8	3.5
267	96.8	3.2	3.0	7.76	----------	46.5	94.4	2.5
285	94.6	5.4	12.0	7.49	----------	74.6	92.7	2.1
331	98.4	1.6	3.0	8.12	----------	48.4	97.0	1.4
338	95.5	4.5	3.0	7.87	----------	92.1	95.0	0.6

The total methane production accounts for the methane collected in the biogas stream and the methane dissolved in the water effluent collected through the degasser.----------
---

---------- (5.3)

5.4 Commissioning, start-up and retrofitting of the industrial prototype

This section describes the protocols followed during the commissioning, the start-up and the retrofitting of the industrial prototype.

5.4.1 Commissioning

The commissioning of the industrial prototype included the hydraulic test and the validation of the control rules implemented in the PLC program. Same protocols would be applied in future industrial installations.

The objective of the hydraulic test was to ensure that pipes were completely sealed and to check the calibration of the instruments. These tasks were done by running the unit with water during a whole week before inoculating the anaerobic reactor.

The calibration of each instrument was carried out by checking the on-line measured parameter against a calibrated instrument. The pH sensors were calibrated using two buffers with pH 7 and 4.02. ----------
---

---------- The pressure drop through the scrubber was also checked by measuring it manually. The flows of the dosing pumps and the flowmeter of the blower that drives polluted air to the scrubber were also checked. The dosing pumps were checked by measuring the volume dosed. The air flowmeter was calibrated by determining the correction factor that related the percentage in the frequency controller of the blower and the airflow. In Figure 5.24 is shown the calibration parameter of the blower of the scrubber (----------, Figure 5.4). The instruments were monthly checked.

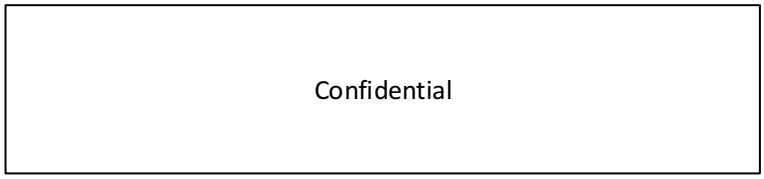

Figure 5.24. Detail of flowmeter ---------- pop-up window in the PLC Program.

Once the hydraulic test was completed, the control rules implemented in the PLC program were validated against the following actions:

1. The industrial prototype changed according to production/non-production mode based on the set-points defined by the user in the PLC program.
2. The control rules associated to the water levels in the tanks worked properly.
3. The drain cycle worked as expected.
4. The dosage of nutrients and alkali solution followed the rules implemented in the PLC program.

5.4.2 Start-up

After checking the hydraulic and control protocols, the 16 m^3 of water of the prototype (anaerobic reactor + intermediate tanks) was filled with fresh clean water. This was done in January, resulting in a water temperature lower than 10°C. So, the unit ran during a weekend on production mode to heat the water by the influent dry air to scrubber, which transfers the heat to water by humidification of the existing air. After that, the unit was connected to the emissions of the facility to accumulate some organic substrate (at least 2 000 mg L^{-1} COD) before seeding. Once the system was ready in terms of temperature and soluble organic matter, the intermediate vessels, with 7.3 m^3 of total volume of water, were kept without emptied while the anaerobic reactor was emptied till 1 m^3 of water. This volume of water in the anaerobic reactor served as a water bed to avoid damage of biomass granules during filling from the top with the granular sludge.

Granular sludge from an IC reactor installed in a brewery (Heineken, The Netherlands) was selected as source of biomass. This source of sludge was selected based on the research carried out by Lafita et al. (2015). These researchers demonstrated that water brewery sludge coming from IC reactor is able to degrade

water-solvents of the printing sector when the main compound is ethanol. The physico-chemical properties of the sludge from the brewery were determined to corroborate its quality. The settle velocity of the granules was between 50.4 and 75.6 m h^{-1}, which is consider a good settling velocity since it is over 50 m h^{-1} (Schmidt and Ahring, 1996). The settle velocity was closed to the common value of 60 m h^{-1} for UASB reactor according to Hulshoff-Pol et al. (2004). Similar settle velocities were reported by Fukuzaki et al. (1995) in a reactor treating a synthetic wastewater where the carbon source was ethanol with a COD of 6.5 g COD L^{-1} and HRT of 4.3 h. The particle size was quite homogeneous, with an average De Brouckere diameter of 775 μm and a maximum concentration of granules at the diameter of 1000 μm (Figure 5.25). This corresponds with the expected sizes for granules growing with ethanol or volatile fatty acid substrates versus other substrates as starch, which originates bigger and less dense granule (Fukuzaki et al., 1995). The ash content in the seed sludge was 7.9%, closed to the range of 11-21% reported by Bhatti et al. (1995) in a study analyzing the characteristics of methanogenic granular sludge treating industrial waste under different conditions. After corroborating the adequate physical properties of the granular sludge, a total volume 5.7 m^3 was added to the anaerobic reactor. After running the system for 3 days, the volume of the sludge was reduced to 3.5 m^3.

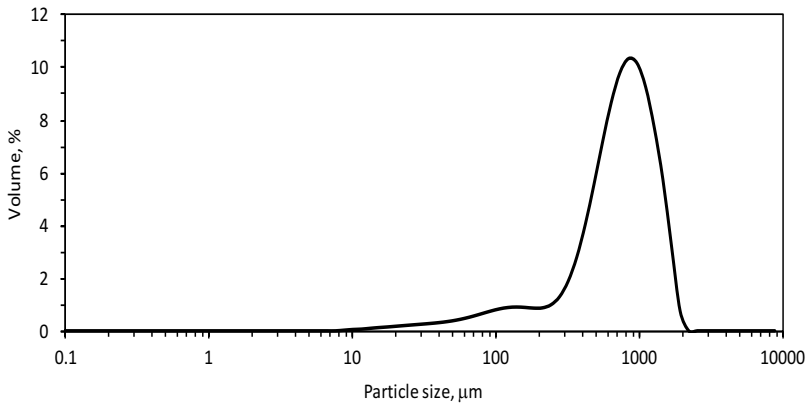

Figure 5.25. Particle size distribution of the granular sludge used for the start-up of the industrial prototype.

After filling the anaerobic reactor with the biomass, the plant was changed to production mode and it started to treat the air emission of the facility. A low

organic load was fixed to promote the acclimation of the biomass to the new organic substrate by fixing the airflow set point of the blower to the scrubber at 400 m^3 h^{-1}. The water flow rate to the scrubber was fixed at 3 m^3 h^{-1}. The scrubber at these conditions had an average RE_{VOC} of 89 ± 2%, being the daily average VOC concentration at the outlet gas phase of the scrubber 153 ± 31 mg-C Nm^{-3} with inlet daily average VOC concentration of 1 414 ± 650 mg-C Nm^{-3}. The average organic load at these conditions was 1.86 ± 0.44 kg COD h^{-1}, ranging between 0.86 (on day 2) and 2.34 (on day 8). The average organic load corresponded to an organic loading rate of 3.2 kg COD m^{-3} d^{-1} (on basis of the 16 hours of production and the total volume of the reactor). This value is in the range proposed in the literature for the anaerobic reactor start-up (2.0-4.5 kg COD m^{-3} d^{-1}) (Colussi et al., 2009). The pH in the water effluent of the reactor was kept over 7.0 and VFA concentration was below 200 mg acetic acid L^{-1}, maximum recommended value selected for the start-up periods according to Ghangrekar et al. (2005). The average biogas flowrate was 0.52 ± 0.14 m^3 h^{-1} with an average composition of 90 ± 1% of methane. The methane yield was 0.32 Nm^3CH_4 kg^{-1} COD removed, close to the stoichiometric value (0.35 m^3 CH_4 kg^{-1} COD removed), verifying that the degradation of the solvents was biologically produced.

The biogas rate in non-production periods was selected to indicate if the system was overloaded due to production peaks in the facility. Biogas will be produced significantly during non-production periods in case of overloading, which causes an accumulation of solvents in water. Overloading occurred eventually during the start-up. Figure 5.26 shows the daily average organic load and the daily average biogas rate in production and in non-production periods during start-up. It can be seen that the system was overloaded on day 5 (2.32 kg COD h^{-1}), causing that the biogas rate production was almost the same in production and non-production periods. After that, overloading was not observed, even at similar loads such in day 8. This graph shows that the start-up using granular sludge from water-brewery reactors, where ethanol is the main component in the wastewater, required very few days despite of the intermittent and fluctuating loads. Any start-up under intermittent and fluctuating loads have not been found in the literature but similar results have been reported with continuous loads. Enright et al. (2005) studied two EGSB-AF reactors inoculated with granular sludge from IC bioreactor treating citric acid production wastewater. They fed the reactors with synthetic wastewater consisting of ethanol, acetic acid and methanol in COD ratio of 1:1:1, with a total of 5 g COD L^{-1}. Both reactors showed a rapid start-up, achieving RE_{COD} over 80% after the first 20 days of operation with OLR of 2.5 kg COD m^{-3} d^{-1}. Enright et al. (2009) studied two EGSB-AF reactors seeded with different source of biomass. One

granular sludge was obtained from a full-scale IC used to treat industrial alcohol production wastewater and the other was obtained from a full-scale granular biomass nursery plant. The reactors were fed with synthetic wastewater consisting of ethanol, acetone, propanol and methanol in COD ratio of 1:1:1:1 in a total of 3 g COD L^{-1}, the researchers reported RE_{COD} over 80% after 20 days of operation at an OLR of 2.4 kg COD m^{-3} d^{-1}.

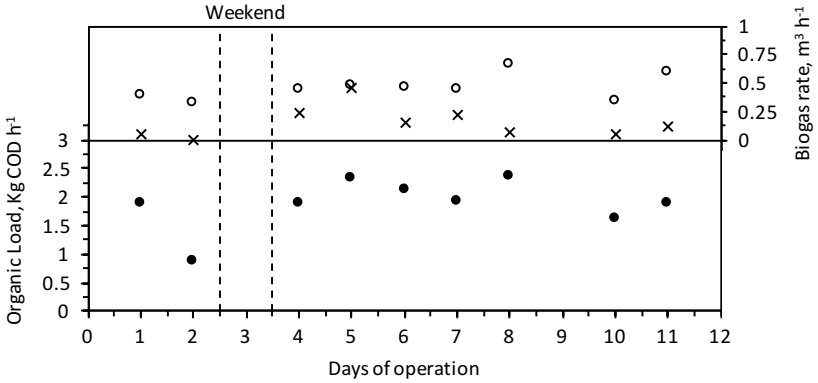

Figure 5.26. (●) Daily average organic load applied to the reactor and daily average biogas rates: in (○) production and (x) non-production periods during start-up.

5.4.3 Retrofitting

The dissolved methane in the water effluent of the anaerobic was calculated by equation (5.3). The concentration in the water was 84 ± 47 mg L^{-1}, which is 3.6 times higher than the saturation value (23 mg CH_4 L^{-1} at 20°C). This oversaturation value matched with the value reported by Noyola et al. (1998) which was 3.8. These researchers studied a rotating-stationary fixed-film reactor treating domestic sewage with an OLR of 1.7 kg COD m^{-3} day^{-1} at 29°C.

The oversaturation of dissolved methane in the water effluent of the anaerobic reactor indicated that the hydraulic conditions in the anaerobic reactor interfered in the performance of the GLS and the collection of methane in the gas phase. To avoid this interference, the anaerobic reactor was retrofitted to enhance the recovery of methane in the biogas. ----------
---

These changes were evaluated in terms of methane recovery efficiency in biogas, as this is a factor of special relevance (economic and environmental) for future industrial installations.

(5.4)

The distribution pipe of influent water to the anaerobic reactor was also changed. The initial and retrofitted design are shown in Figure 5.27. ----------
---
---------- The objective was to minimize internal mass transfer limitations. This change also avoided the formation of big bubbles of biogas that could be easily escaped via the water effluent.

Confidential

Figure 5.27. Distribution pipe of influent water to the anaerobic reactor. A) Initial and B) final design.

The capacity of the gas collection of the GLS was also improved ----------
---

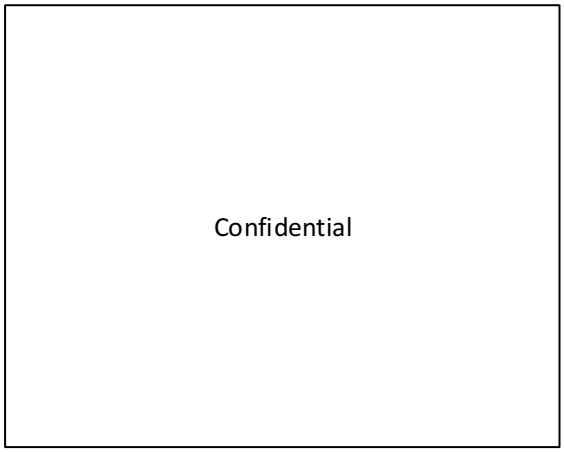

Figure 5.28. Conceptual design of the GLS of the anaerobic reactor. A) initial design and B) final design.

After installing all these modifications, the average daily concentration of methane in the water effluent of the anaerobic reactor was 28 ± 12 mg CH_4 L^{-1} at 20°C, which corresponds to 120% of oversaturation. Thus, the performed changes improved the collection of biogas from the anaerobic reactor, and proportionated the guidance for the detailed design of future installations.

5.5 Example of typical operation

This section illustrates the operation, monitoring and data collection of a typical period, which is selected as representative. It was chosen a period after start-up was successfully finalized. The selected week comprised from Monday (day 30) to Monday (day 36). This section exposes how the discontinuous and oscillating emissions impacted on the transitory performance. The scrubber configuration tested in the selected period was packed bed. The packing A was installed in the scrubber and there was not any pressure drop control implemented during the selected period.

5.5.1 Scrubber unit

The operational set-points in the selected week were: airflow through the scrubber of 660 m^3 h^{-1} and water flow of 3 m^3 h^{-1}, hence the liquid to air volume

ratio was $4.54 \cdot 10^{-3}$. Average air temperature at the inlet of the scrubber was 49 ± 7°C and inlet water temperature was 20 ± 1 °C. VOC concentration at the inlet and outlet air of the scrubber is plotted in Figure 5.29. Gas emission pattern varied depending upon the printing orders being processed, reaching maximum VOC concentration in the inlet air (2 867 mg-C Nm^{-3}) on day 33. The emissions were also linked to production time, with periods without VOC emission at closure periods of the facility (every night and from Saturday midday till Monday morning). In spite of this variation in the VOC inlet air concentration, daily average outlet air concentration at the scrubber ranged between 140 and 170 mg-C Nm^{-3} and average RE_{VOC} of the scrubber was quite stable (87.6 ± 1.0%).

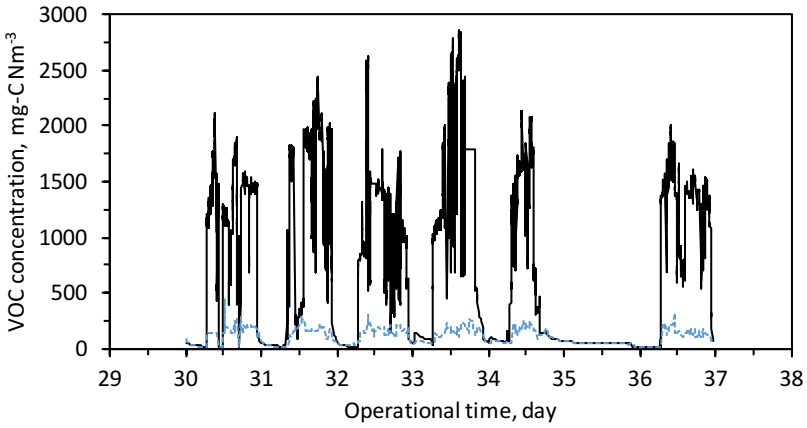

Figure 5.29. VOC concentration of the inlet (black line) and outlet (blue line) air of the scrubber since day 30 to day 36.

The RE_{VOC} achieved in this work was similar to those ones reported by on-site bioscrubber in the literature. Cloriec and Humeau (2013) studied a bioscrubber in an aluminum can manufacturer, whose emission was composed by ethanol, ethyl acetate, acetone, methyl ethyl ketone, isopropanol and ethoxypropanol. The flow of the gas emission was 31 000 m^3 h^{-1}. The VOC concentration at the inlet of the scrubber varied between 0 and 1 000 mg-C Nm^{-3} and the reported RE_{VOC} was 80% with an inlet VOC concentration of 900 mg m^{-3} (outlet VOC concentration of 150 mg m^{-3}). Granström et al. (2002) reported 99.6% of RE_{VOC} excluding evaporation losses by treating a waste gas mainly composed by ethanol, with smaller amounts of ethyl acetate, 1-propanol, 2-propanol, 1-methoxy-2-propanol and 3-methoxy-1-propanol. The flow of the waste gases varied from 1.68 to 3.73 m^3 h^{-1} and the water flow from 0.2 to 0.7 m^3 h^{-1}.

The on-line monitored pressure drop through the scrubber in the selected week is plotted in Figure 5.30. The pressure drop in production mode increased from 241 Pa (average value on day 30) to 503 Pa (average value on day 36), reaching the maximum values on day 34. This graph shows that the pressure drop will increase along the time if the pressure drop control protocol is not implemented, overpassing the recommended values for feasible energy consumption (200 Pa m^{-1}, Janssen et al. (2013)). Similar problem was stated by Malhautier et al. (2009) with an aerobic bioscrubber treating air emissions with a complex VOC mixture. The aerobic bioscrubber was equipped with a packed column scrubber. The clogging of the column by biofilm colonization of the packing material was observed after 20 weeks of test and pressure drop higher than 200 Pa m^{-1} was reached after two weeks of operation, even with a lamellar separator between the aerobic biological reactor and the packed bed. The results of Malhautier et al. (2009) suggest that the installation of a unit between the reactor and the scrubber to eliminate the suspended solids will not ensure the control of pressure drop at the packed bed. So, ---------- was selected in this thesis as the strategy to ensure a durable operation.

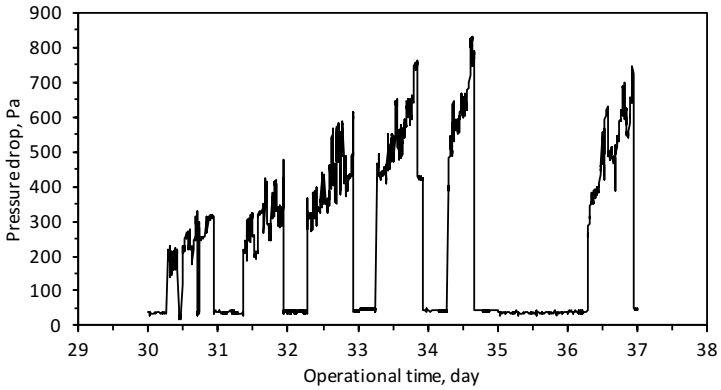

Figure 5.30. Pressure drop at the packed scrubber since day 30 to day 36.

5.5.2 Anaerobic reactor

The anaerobic reactor operational conditions in the selected week were an inlet water flow rate of 3 m^3 h^{-1} from the scrubber and a recirculation flow of 3 m^3 h^{-1}, resulting in a HRT of 2.9 h. The water temperature in the reactor was quite stable in the selected week, being the daily average temperature ranged between 19.4 and 20.7°C.

The OL fed to the anaerobic reactor is controlled by the performance of the scrubber. This fact is visualized in Figure 5.31, where the inlet and outlet air VOC concentration at the scrubber and the moving hourly average OL fed to the anaerobic reactor, calculated by equation (5.2), are plotted. The variations of VOC air emissions changed the OL fed to the anaerobic reactor, which was characterized as intermittent and fluctuating. The OL variation was buffered by using an intermediate tank ----------, as it can be seen in the upper part of the Figure 5.31. The OL in the selected week ranged between 0.02 (on day 31) and 6.9 kg COD h^{-1} (on day 33).

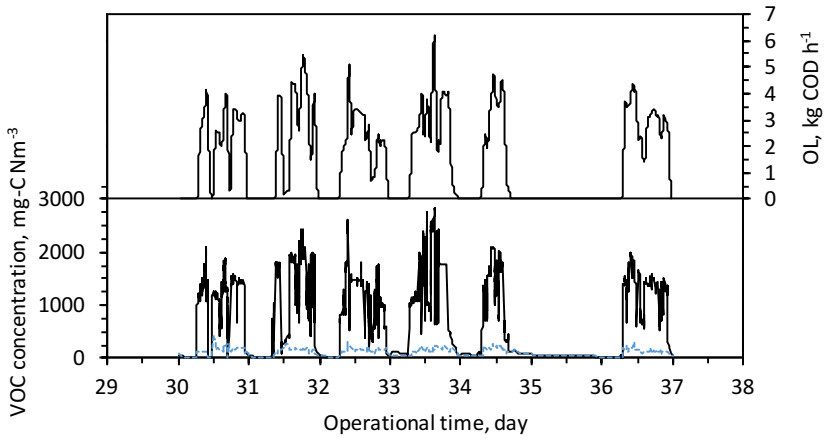

Figure 5.31. VOC concentration in the inlet (black line) and outlet (blue line) gas phase at the scrubber and moving hourly average OL applied to EGSB.

In spite of the variations in the OL, the biogas production rate kept almost constant during production hours, indicating that the substrate was degraded at the maximum rate, hence the load shocks were accumulated as a soluble non-degraded substrate, increasing the COD concentration in the water and degraded when the load fed to the anaerobic reactor decreased. This fact is shown in Figure 5.32, where the moving hourly average OL and the cumulative biogas production rate for the selected period are shown. The average biogas production rate for production and non-production hours from day 30 to 36 are summarized in Table 5.5. Biogas production kept quite stable during production hours, with an average of 0.69 $\pm$ 0.08 m^3 h^{-1} with OL of 2.86 $\pm$ 0.22 kg COD h^{-1} that corresponds to a COD degradation rate of 1.97 kg COD degraded h^{-1}. On the other hand, the average biogas production rate during non-production hours was negligible (0.06 $\pm$ 0.03 m^3 h^{-1}). The performance of the anaerobic reactor under shock loads matched with the results

of Leitão (2004). This researcher stated that the anaerobic reactor could not attenuate the imposed fluctuation in the influent load, hence the effluent COD concentration of the anaerobic reactor increased in the same range as the influent COD concentration produced by the organic shock load, indicating that the substrate was degraded at maximum rate.

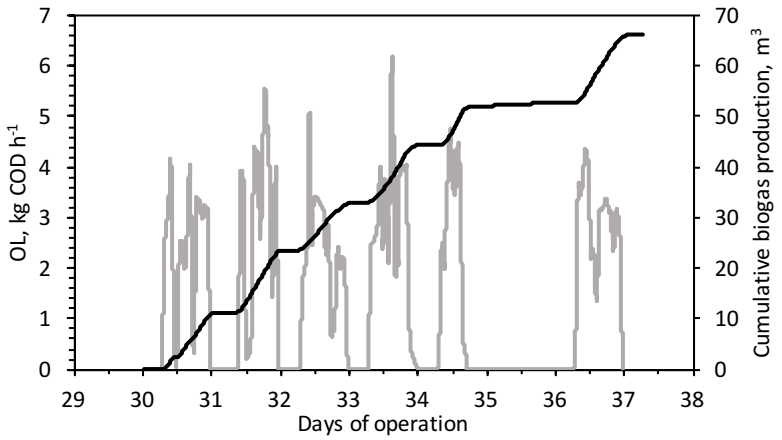

Figure 5.32. (▬) Cumulative biogas production rate and (▬) Moving hourly average OL applied to the EGSB.

Table 5.5. OL applied to the anaerobic reactor and the biogas production rate in the two operational modes from day 30 to day 36.

Days of operation	Daily average OL, kg COD h^{-1}	Biogas rate in production, m^3 h^{-1}	Biogas rate in non-production, m^3 h^{-1}
30	2.90	0.65	0.09
31	3.03	0.73	0.08
32	2.42	0.56	0.06
33	2.86	0.70	0.04
34	2.94	0.71	0.00
35	0	0	0
36	3.00	0.79	0.08

The stability of the anaerobic reactor was also evaluated by studying the delay of the start/stop of the biogas production with the start/stop of the production of the facility. The biogas production started one hour after the production of the facility began and stopped with a delay of one hour after the

production finished. These delays matched with the HRT of the buffer tank ---------- ---------- and HRT in the granular sludge bed (volume of 3 m^3 and HRT of 1 h), respectively. After the delay in the starting of the methane production, a pseudo-stable methane production was reached along the production time. This fact can be seen in Figure 5.33, where a zoom for day 33 is shown. The biogas production reached a constant rate of 0.70 m^3 h^{-1} from 10:00 to 20:00 (same performance occurred during the whole test).

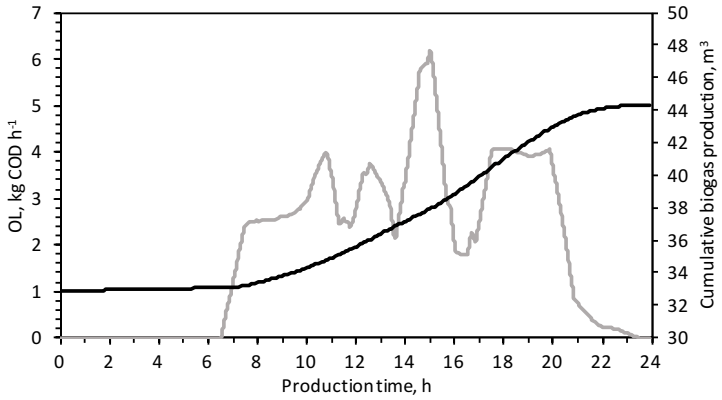

Figure 5.33. (—) Cumulative biogas production rate and (—) Moving hourly average OL applied to the EGSB on day 33.

On days with peak of production, the delay of stopping the biogas production was longer, indicating that the system was degrading the soluble non-degraded substrate accumulated in the water during production time. Overloading period did not occur in the selected week. As an example of overloading day, the biogas production and OL fed to reactor of day 52 is depicted in Figure 5.34. The average organic load was 6.13 kg COD h^{-1} and it was applied until 20:00, when the system changed to non-production to avoid acidification. The biogas production continued until 23:00 with a rate of 0.78 m^3 h^{-1}.

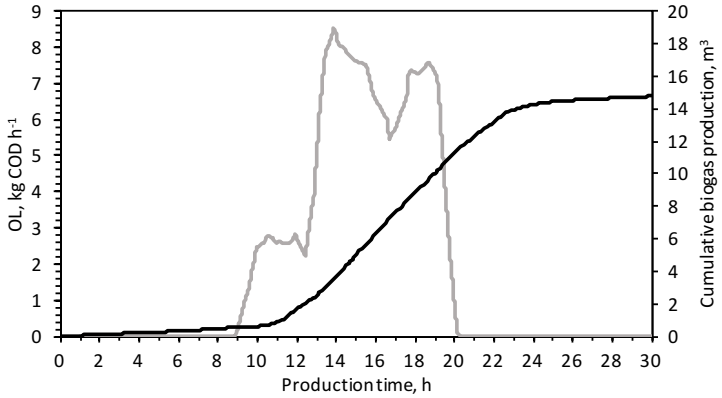

Figure 5.34. (▬) Cumulative biogas production rate and (▬) Moving hourly average OL applied to the EGSB on day 52.

The variations in the organic loading can also produce an accumulation of VFA concentration in water and a drop in the pH, due to the balance that exists between the primary processes (hydrolysis, acidogenesis and acetogenesis) and the conversion of the acid products by methanogenic bacteria into methane and carbon dioxide. The evolution of the on-line measured pH of the water effluent of the anaerobic reactor is depicted in Figure 5.35 along with the OL fed to it. The Table 5.6 summarizes the results of chemical analysis of the water effluent. The available bicarbonate alkalinity on the system ---------- kept the pH over 7 in the selected period, despite of the variation in the OL. The evolution of the pH shows that it decreased when the facility production started, indicating that there was a small ratio shift between VFA producers and consumers. The lowest pH value was reached on day 36 (Monday), at the beginning of production period, indicating that methanogenic activity is more negatively affected by feedless period during weekend. The adverse impact of the feedless periods on the methanogenic activity was previously pointed out by Lafita et al. (2005) by studying the methane yield in an EGSB reactor treating packaging wastewater. These researchers pointed out an increase in the methane yield during the first 6 hours after resumption of water supply after 8 hours of the feedless period. The negative impact in the methane yield was more remarkable on Monday, after 48 hours without supplying substrate. These researchers stated a methane yield reduction ranging between 15 and 30% on Monday in comparison to that measured during the first substrate supply hours after stopping 8 hours the feed of substrate. If Mondays are not taken into account, the lower values matched with production

peaks (days 33 and 34), indicating that the VFA producers were able to degrade the shock loads but the VFA were not degraded at same rate by the methanogenic bacteria (quite stable biogas rate production in production time, Figure 5.32). Same performance was reported by Borja and Banks (1995) who studied the response under shock loads of a fluidized bed reactor fed with synthetic ice-cream wastewater. They changed the OL by increasing the influent COD by 100 and 150% for 6 and 12 h. The response of the reactor was a drop in the pH with an increase of VFA in the effluent. Regarding the highest values of pH in Figure 5.35, those ones are reached in the non-production mode when the accumulated VFA in the water was degraded, producing an increase of pH due to the available alkalinity. The highest value was reached on day 33 at 8.2, this high value could be due to a slight over dosage of the alkali solution.

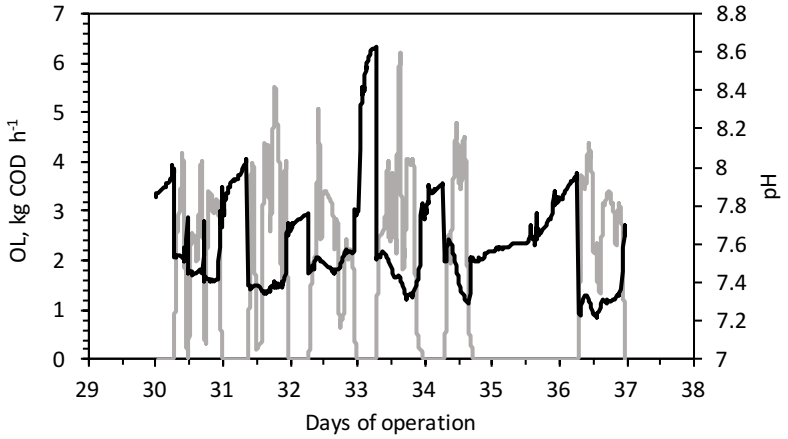

Figure 5.35. (**—**) pH at the outlet of the EGSB and (—) moving hourly average OL fed to the reactor.

The Table 5.6 shows the soluble organic matter concentration (COD units) at the effluent of the anaerobic reactor. The high values of COD reached on the system were due to the presence of 1-ethoxy-2-pronanol in the water. This compound was 9.1% of the VOC emissions of the flexographic facility. By other side, granular anaerobic sludge from water-brewery reactors needs 45 day at 25°C and more than 2 months at 18°C to start to degrade glycol ethers according to Lafita et al (2015). The long adaptation periods are related to the lack of enzymes for ether cleavage in the inoculum. The feedless periods (non-production time) could help to reduce this adaptation period, since the biomass had long periods in which the only available substrate is the glycol ether. In fact, the glycol ether was not accumulated

in the selected week because the COD eliminated with the daily purge (1 m^3 day^{-1}) was 2 ± 0.2 kg COD, which matched with the glycol ether fed to the system, thus indicating that it was required more than one month to start its biodegradation.

Table 5.6. Effluent water quality of the anaerobic reactor from day 30 to day 36.

Days of operation	----------	VFA, mg acetic acid L^{-1}	COD, mg O_2 L^{-1}	N-NH_4, mg L^{-1}	P-PO_4, mg L^{-1}
30	----------	109	2086	---	0.2
31	----------	77	2202	10.5	1.0
32	----------	73	1872	2.9	0.1
33	----------	116	1994	5.7	0.5
34	----------	---	---	---	---
35	----------	---	---	---	---
36	----------	147	1721	14.4	3.2

The Table 5.6 also shows the nutrient concentration at the liquid effluent of the anaerobic reactor. The presence of nutrients in the water effluent of the anaerobic reactor indicated that there were nutrients available for the growth of the biomass. At the same time, the dosing rules implemented in the PLC program avoided the accumulation over time.

5.5.3 Methane production

The total production of methane was calculated as the sum of the methane collected with the biogas and the methane removed from the anaerobic water effluent. The methane collected in the biogas was derived from the biogas production rate and the methane content calculated by the equation (1.12) accordingly to the pH and the bicarbonate alkalinity in the anaerobic reactor. The methane removed from the anaerobic water effluent was calculated by equation (5.3). The results are shown in Table 5.7.

Table 5.7. Methane collected ---------- from day 30 to day 36.

			Methane in biogas					Methane removed from the anaerobic reactor effluent				
Days of Operation	**pH**	**OL, kg COD h^{-1}**	**VFA, mg acetic acid L^{-1}**	**----------**	**Q_{Biogas}, m^3 h^{-1}**	**Cg_{CH4}, % CH_4**	**Q_{CH4}, m^3 h^{-1}**	**-------**	**-------**	**Q_{CH4}, m^3 h^{-1}**	**$Qtot_{CH4}$, m^3 h^{-1}**	**CH_4 yield, m^3 CH_4 kg^{-1} COD**
30	7.5	2.90	109	----------	0.65	89	0.58	-------	-------	0.24	0.82	0.28
31	7.38	3.03	77	----------	0.73	87	0.63	-------	-------	0.22	0.85	0.28
32	7.50	2.42	73	----------	0.56	90	0.50	-------	-------	0.26	0.76	0.31
33	7.40	2.86	116	----------	0.70	88	0.61	-------	-------	0.22	0.84	0.29
34	7.38	2.94	---	----------	0.71	---	---	-------	-------	---	---	---
35	---	0	---	----------		---	---	-------	-------	---	---	---
36	7.22	3	147	----------	0.79	82	0.64	-------	-------	0.27	0.91	0.30

The data of this table stated that the anaerobic reactor showed at high removal efficiency during the selected period, with an average RE_{COD} of 83 ± 3%. The RE_{COD} obtained in this work matched with the RE_{COD} reported by Lafita et al. (2015). These researchers stated a decrease in the RE_{COD} from 98% to 76% when the glycol ether was added to the substrate, which was previously composed only by ethanol. The solvent wastewater was treated in an EGSB reactor at 25°C. The OLR fed to the anaerobic rector was 46 kg COD m^{-3} day^{-1} and it was composed by ethanol and methoxy propanol in a mass ratio of 3:1. The gas chromatography analyses performed by these researchers showed the complete degradation of ethanol and a small degradation of methoxy propanol. The methane content in the biogas shown in Table 5.7 was over 87% except for one value in the selected week, thus indicating that the pH rules implemented in the PLC program allowed to obtain high-quality biogas. The methane yield was 0.29 ± 0.01 m^3 CH_4 kg^{-1} COD, which was close to the stoichiometric value (0.35 m^3 CH_4 kg^{-1} COD removed, Grady et al. 2011).

The methane concentration in the water effluent of the anaerobic reactor was also quite stable with an average dissolved methane concentration of 53 ± 5 mg CH_4 L^{-1}. This concentration corresponds to an oversaturation of 2.2 ± 0.2. The oversaturation value measured in the industrial prototype matched with the lowest oversaturation range summarized by Hartley and Lant (2006), who stablished oversaturation factors between 1.9 and 6.9. These researchers summarized data from a number of anaerobic studies (Table 5.8).

Table 5.8. Calculated degree of oversaturation of CH_4 from previous studies. Adapted from Hartley and Lant (2006).

Average Temperature, °C	Gas Flow rate, L day^{-1}	CH_4 conc. in the gas, %	Degree of oversaturation	Reference
29	0.52	82	3.8	Noyola et al. (1988)
28	30	66	6.9	Singh et al, (1996)
17	27.4	70	2.4	Lettinga et al (1983)
18	36	69	5	Barbosa and Sant' Anna (1989)
25	0.22	65	1.9	Kobayashi et al. (1983)

5.6 Conclusions

The prototype was installed in a flexographic facility, whose emission matched with the typical one of the flexographic sector (EC, 2007, Granström et al., 2002; Le Cloriec and Humeau, 2013; Sempere et al., 2012), indicating that the results obtained in this study can be extrapolated to the flexographic sector. The compounds in major proportions by weight were ethanol (60-65%), ethyl acetate (20-25%) and ethoxy propanol (10-15%). The VOC emission of the facility was intermittent and variable, since VOC emissions were not produced at closure periods and because VOC emissions depended upon the printing orders being processed. The OL fed to the reactor was controlled by the performance of the scrubber, hence the organic load had similar oscillating pattern of the VOC emissions.

The operation, monitoring and data collection, along with the calculations performed with the monitored and measured data, summarized in this chapter were implemented during the whole experimental study. The work explained in this chapter helped to run the prototype in the desired physical and chemical ranges without any disturbance. Moreover, and as it has been mentioned, the prototype kept running for more than a year, and it was only stopped to change the scrubber configuration. So, the commissioning, start-up, operation, monitoring and data collection protocols explained in this chapter should be performed in future industrial installations in order to ensure the applicability of the anaerobic bioscrubber as abatement VOC technology. Regarding the start-up protocol, the organic load applied during the start-up period were in the range proposed in the literature (Colussi et al., 2009). The used of granular sludge from a water-brewery reactor allowed to reduce the start-up period of the anaerobic reactor to less than 15 days, which was in the range found in the literature for continuous fed anaerobic reactor (Enright et al. 2005 and 2009). This is the first attempt of a successful start-up under intermittent and fluctuating loads, anyone else has been found in the literature.

Once the system was running, the scrubber column ----------, otherwise the pressure drop reach the maximum recommended value (200 Pa m^{-1}, Janssen et al. (2013)) ---------- with both commercial structured packing materials.

Regarding the anaerobic reactor, the biogas rate during production periods kept almost constant, despite of the variation of OL, indicating that the dissolved solvents are degraded at the maximum rate and the anaerobic reactor cannot

attenuate the imposed fluctuation in the influent load. Hence, the effluent COD concentration of the anaerobic reactor increased in the same range as the influent COD concentration. The average biogas rate in the non-production periods indicated if the anaerobic reactor was overloaded, since COD accumulated in production period was degraded during non-production period. Regarding the pH, a decreased was observed when the facility production started or when a shock load was applied, indicating that VFA formers are able to adapt to the variation of loads and methanogenic bacteria are more negatively affected by intermittent and oscillating loads. Same performance was reported in the literature by Lafita et al. (2005) and Borja and Banks (1995).

Average daily data from the on-line monitoring along with the daily and weekly chemical analysis will be used to demonstrate the steady state performance of the process. For doing that, daily production of methane (production plus non-production periods) will be used.

6 PROCESS PERFORMANCE OF THE ANAEROBIC BIOSCRUBBER

Part of this chapter has been published in:

Bravo, D., Ferrero, P., Penya-roja, J.M., Álvarez-Hornos, F.J. and Gabaldón, C. (2017). Control of VOCs from printing press air emissions by anaerobic bioscrubber: Performance and microbial community of an on-site pilot unit. Journal of Environmental Management 197: 287-295.

The experimental study of the anaerobic bioscrubber as a VOC abatement technology for the flexographic sector was carried out once the commissioning and the start-up, as well as, the retrofitting of the prototype were performed. The objective of this chapter is to establish the operational conditions and to provide a set of empirical parameters for the scale-up, in order to make the anaerobic bioscrubber technology economically and technically feasible for air emissions treatment of the mentioned sector.

To achieve this goal, the performance of the two main units of the industrial prototype were investigated. The study of the scrubber aimed to determine the best scrubber configuration and the best hydraulic conditions for the abatement of the flexographic VOC emission. The results of this research established the best working conditions that would permit to obtain the maximum VOCs removal efficiency with a feasible pressure drop through the scrubber and by applying the minimum scrubbing liquid flow. On the other hand, the study of the anaerobic reactor aimed to determine the maximum organic load that the reactor can treat under intermittent and variable solvent loads. This parameter, along with the liquid flow, determined the design criteria and operational protocols of the anaerobic reactor for future industrial installations. It was also evaluated the nutrient dosing rule and the pH control rule implemented in the PLC program by studying the variation of the nutrient concentration and the pH of the water effluent of the anaerobic reactor along the whole experimental period.

6.1 Working plan

The study of the feasibility of the anaerobic bioscrubber was performed with the on-site industrial prototype, which treated real emissions from a flexographic facility. The whole plant (scrubber and anaerobic reactor) was tested at once, which means that the anaerobic reactor was degrading the scrubbing liquid for the whole experimental period. Therefore, every change in the working conditions or in the configuration at the scrubber involved a modification of the operational conditions for the anaerobic reactor. The organic load fed to the anaerobic reactor is related to the performance of the scrubber, as it has been stated in the previous chapter. In this chapter, the performance of the scrubber is initially evaluated. Afterwards, the performance of the anaerobic reactor is introduced and discussed.

6.1.1 Study of the scrubber configuration

The objective of this study was to determine the best configuration and the best working conditions of the scrubber. One key parameter for the design of absorption operations is the liquid-to-gas ratio. This ratio is determined by the solubility of the gas pollutants, the abundance of pollutants and the mass transfer characteristics of the scrubber. Increasing L/G increases the collection efficiency of the system but increases the volume of the anaerobic reactor and the energy costs of the installation, since the water flow rate would be higher resulting in greater pumping energy consumption. So, finding the optimum ratio is important for balancing performance with design and operating costs. Three scrubber configurations were tested at the prototype. The scrubber was evaluated as a packed bed configuration by installing two commercial packing materials (Packing A and Packing B) and as a spray tower by installing three nozzles spaced 55 cm. The characteristics of the packing materials were summarized in chapter 4 and the main differences between them were the specific surface area and the water pathway.

The performance of the scrubber configuration was evaluated in two ways. Firstly, it was evaluated in terms of removal efficiency of each of the three main solvents of the gas emissions -ethanol (EtOH), ethyl acetate (EA) and 1-ethoxy-2-propanol (ET2Pr)-. Afterwards, the performance of the scrubber was evaluated in terms of overall VOC removal efficiency (RE_{VOC}). The working plan followed in each study is explained hereafter.

6.1.1.1 *Effect of the scrubber configuration on the removal efficiency of each solvent*

The experiments to evaluate the influence of the scrubber configuration and the applied liquid-to-air ratio in the removal efficiency of each solvent from the air emission were performed when a new scrubber configuration was installed at the prototype. These experiments were based on the measurement of the composition of the gas phase at the inlet and outlet of the scrubber. The composition was measured following the protocol explained in section 4.3.1.2 and the experiments were carried out at different liquid-to-air ratios in order to cover a wide range, that were afterwards tested during the prototype operation. The Table 6.1 shows the working conditions of the different experiments performed.

Table 6.1. Experimental conditions to evaluate the performance of the scrubber in terms of the removal efficiency of each solvent.

Configuration	v_G m s^{-1}	v_L m h^{-1}	L/G $\cdot 10^3$ m^3 water m^{-3} air	$T_{air, in}$ °C	$T_{water, in}$ °C
Packing A	2.1	12.6	1.6	40	25
Packing A	1.8	15.1	2.3	40	25
Packing A	1.0	13.0	3.7	40	25
Packing A	0.9	25.2	7.6	40	25
Spray column	1.0	10.1	2.7	40	25
Packing B	1.8	15.5	2.3	53	17
Packing B	1.2	10.4	2.4	52	17
Packing B	1.2	15.1	3.5	50	17
Packing B	1.2	25.6	5.9	51	19

6.1.1.2 *Influence of the scrubber configuration in the overall performance*

The overall RE_{VOC} of the scrubber was evaluated in 5 stages. Packing material A was used in stages I and V and packing material B in stages II and IV. Both packing materials were tested two times because the pressure drop control method was not implemented in stage I and II, on the other hand it was implemented in stages IV and V. The evolution of the pressure drop through the scrubber in stages I, II, IV and V and the influence of the pressure drop control protocol on the overall performance of the scrubber have been also studied. The scrubber was tested as a spray column on stage III. The working conditions at each stage are shown in Table 6.2, this table shows the specific surface area of each packing material and the range of liquid-to-air ratios tested.

Table 6.2. Experimental conditions of each stage at the scrubber.

	Stage I	Stage II	Stage III	Stage IV	Stage V
Days	0 - 95	96 - 130	131 - 180	181 - 265	266 - 484
Packing material	Packing A	Packing B	Spray column	Packing B	Packing A
Specific area, m^{-1}	150	125	---	125	150
Liquid/air volume ratios $\cdot 10^3$, m^3 water m^{-3} air	3.5 - 9.1	7.6, 10.1	1.9, 3.7	3.8 - 8.0	4.3 - 7.9

6.1.2 Evaluation of the performance of the anaerobic reactor

The objective of this study was to evaluate the long-term operation of the anaerobic reactor fed with intermittent and oscillating loads and at the same time, to stablish the maximum load that can be treated by the anaerobic reactor running in a closed water loop. This organic load will fix the design criteria of future industrial installation.

The nutrient concentration and the pH evolution of the liquid effluent of the anaerobic reactor were also evaluated with the aim of corroborating the feasibility of the dosing rules of nutrients and alkali solution for their implementation at future industrial installations.

To achieve these goals, the anaerobic reactor treated the scrubbing liquid during the whole experimental period. The Table 6.3 shows the average, maximum and minimum values of the organic load fed to the anaerobic reactor in the different stages, which were characterized by a different scrubber configuration.

Table 6.3. Organic load fed the anaerobic reactor in the different stages.

		Stage I	**Stage II**	**Stage III**	**Stage IV**	**Stage V**
Days		0 - 95	96 - 130	131 - 180	181 -265	266 - 484
OL, Kg COD h^{-1}	Av	2.45	1.79	2.32	2.09	1,75
	STD	1.19	0.66	1.07	1.30	0.90
	Max	6.96	3.01	5.06	5.78	4.61
	Min	0.86	0.54	0.24	0.37	0.42

Av: Average. STD: Standard deviation. Max: Maximum. Min: Minimum

6.2 Results and discussion

6.2.1 Performance of the scrubber treating VOC emissions from a flexographic facility

The scrubber was studied in terms of the removal efficiency of each solvent and the overall RE_{VOC} of the emissions of a flexographic facility. The evolution of the pressure drop along the packed bed and the application of a pressure drop control protocol and its influence in the overall performance were also evaluated.

6.2.1.1 *Influence of the scrubber configuration in the removal efficiency of each compound*

The removal efficiency of each solvent was evaluated with the different configurations tested in the prototype. The Table 6.4 shows the composition of the inlet and outlet gas phase of the scrubber with the different tested configurations, along with the inlet and the outlet total VOC concentration. The liquid-to-air volume ratio and the inlet temperature of air and water are also summarized. As fresh water was used as scrubbing liquid, the inlet solvent concentration was considered zero.

Table 6.4. Composition of the inlet and the outlet gas streams at the scrubber with the tested configurations.

Configuration	**L/G* ·10^3**	**T_{air}**	**T_{water}**	**EtOH**	**EA**	**Et2Pr**	**EtOH**	**EA**	**Et2Pr**
		Inlet T, °C		**Inlet composition,** % weight			**Outlet composition,** % weight		
Packing A	1.6	40	25	71.0	22.0	7.0	23.2	75.8	1.1
Packing A	2.3	40	25	63.5	15.3	21.2	17.7	72.6	1.2
Packing A	3.7	40	25	66.3	27.5	6.2	22.8	76.0	2.3
Packing A	7.6	40	25	62.3	33.6	4.1	25.7	72.1	9.7
Spray column	2.7	40	25	66.2	21.6	12.2	35.4	59.2	5.4
Packing B	2.3	53	17	68.8	26.1	5.1	37.2	59.8	3.0
Packing B	2.4	52	17	66.9	28.0	5.1	51.6	46.0	2.3
Packing B	3.5	50	17	66.9	28.0	5.1	48.6	49.2	2.3
Packing B	5.9	51	19	68.8	26.1	5.1	56.1	41.3	2.5

* m^3 water m^{-3} air

Table 6.4cont. Composition of the inlet and the outlet gas streams at the scrubber with the tested configurations.

Configuration	L/G* ·10^3	Cg_{in}, mg-C Nm^{-3}	Cg_{out}, mg-C Nm^{-3}
Packing A	1.6	1272	274
Packing A	2.3	2261	309
Packing A	3.7	443	85
Packing A	7.6	2943	366
Spray column	2.7	870	268
Packing B	2.3	885	226
Packing B	2.4	968	224
Packing B	3.5	503	136
Packing B	5.9	945	232

* m^3 water m^{-3} air

The table shows that EA was the major compound in the outlet gas phase for all configurations, since it is the less water soluble solvent, with a Henry Constant (gas/liquid dimensionless) of $6.9 \cdot 10^{-3}$ (Sander, 2015). The concentration of this compound in the outlet emission varied from 76%, which was achieved with packing A working with a volumetric liquid to air ratio of $3.7 \cdot 10^{-3}$, to 41.3% with packing B when the liquid-to-air ratio was $5.9 \cdot 10^{-3}$. The fact that the EA is less soluble than EtOH and Et2PR makes EA the key component in the design of the scrubber, since it will be the major compound emitted in the cleaned gas. Regarding the composition of EtOH, it was quite constant when packing material A was installed in the scrubber, despite of the wide range of tested liquid-to-air ratio (between $1.6 \cdot 10^{-3}$ and $7.6 \cdot 10^{-3}$). This can be observed in detailed in Figure 6.1a where the RE of each solvent is plotted against the volumetric liquid-to-air ratio. The Figure 6.1b shows the same information for Packing B.

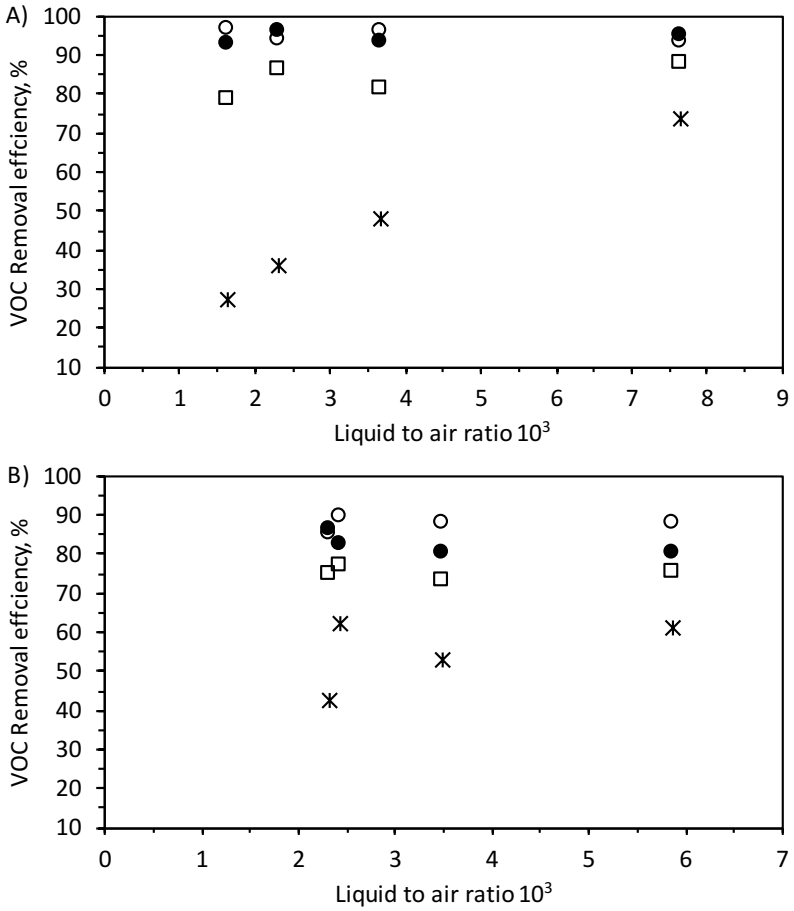

Figure 6.1. RE of the scrubber for each of the three major solvents. A) Packing A and B) Packing B. (●) EtOH, (x) EA, (○) Et2Pr and (□) overall RE.

The removal efficiency of EtOH and Et2Pr with packing A ranged between 93-96% and 93-97%, respectively. In the case of packing B, removal efficiency of EtOH and Et2Pr was between 80-86% and 85-90%, respectively. The results obtained with both packing materials stated that the absorption of these compounds were not influenced by the liquid-to-air ratios due to the very high solubility in water. Same explanation was pointed out by Le Cloriec et al. (2001), who studied the performance of a bioscrubber treating an EtOH emission with volumetric liquid to air ratios varying from $0.6 \cdot 10^{-3}$ to $2.0 \cdot 10^{-3}$, resulting in removal efficiency that varied between 90.1 and 100%.

On the other hand, the removal efficiency of EA with both packing materials was influenced by the applied liquid-to-air ratios. The removal efficiency of EA with packing material A ranged between 27% and 74% with liquid-to-air ratios between 1.6 and $7.6 \cdot 10^{-3}$. The removal efficiency of EA with Packing B varied from 42% to 62% with liquid-to-air ratios between $2.3 \cdot 10^{-3}$ and $5.9 \cdot 10^{-3}$. It should be mentioned that EA removal efficiency obtained in Packing B with liquid-to-air ratio of $2.4 \cdot 10^{-3}$ of was out of the trend; the reason could be a sudden change in the experimental conditions probably in the inlet gas composition.

Comparing both packing materials, EtOH and Et2Pr removal efficiency with packing A was higher than those achieved by packing B, due to the higher specific surface area and the more complex water pathway within Packing A, which enhanced the mass transfer of pollutants between both phases. Comparing EA removal efficiency with both packing materials, the EA did not follow the expected trend, since the removal efficiency of Packing B with liquid-to-air ratios of $2.4 \cdot 10^{-3}$ and $3.5 \cdot 10^{-3}$ were 52% and 53%, which were higher than those achieved with Packing A with similar ratios (36% and 48%). This result can be explained by a change in the inlet composition when the experiments of packing B were performed or due to the lower temperature of water in the experiments with Packing B, since the absorption is an exothermic process and it is enhanced by lower temperatures.

If both packing materials are evaluated in the liquid-to-air ratios suggested by Kennes et al. (2009) ($2 \cdot 10^{-3}$-$3.33 \cdot 10^{-3}$), the packing materials showed high overall removal efficiencies, ranging between 79-87% and 73-77% with Packing A and Packing B, respectively. These removal efficiencies are close to the ranges suggested by Delhoménie and Heitz (2005), who recommended removal efficiencies for absorption technologies ranged between 90% and 98%. The removal efficiency achieved by the packed bed configuration makes these configurations economically and operational viable for the scale-up of the technology.

The removal efficiency of the spray tower was 85% for EtOH, 22% for EA and 87% for Et2Pr. The EA removal efficiency with this configuration was lower than those achieved by both packed beds, indicating that higher water flows are needed to abate the VOC emissions, doing this configuration economically inviable due to the energy cost for water pumping and the impact to increase the surface of the anaerobic reactor to treat the scrubbing liquid.

6.2.1.2 *Influence of the scrubber configuration on the overall performance*

The three configurations were investigated in terms of overall RE_{VOC} and pressure drop. The Table 6.5 shows the working conditions and the parameters that affect the performance of the scrubber in stage I and the inlet and outlet gas VOC concentration. The RE_{VOC} of this stage is plotted in Figure 6.2, along with the VOC concentration at the inlet and at the outlet gas phase of the scrubber. The scrubber was operated with liquid-to-air volumetric ratios ranged between $3.5 \cdot 10^{-3}$ and $9.1 \cdot 10^{-3}$, achieving RE_{VOC} up to 97% (day 75) at the maximum tested liquid-to-air ratio, when the gas inlet VOC concentration was 2 000 mg-C Nm^{-3}. The overall RE_{VOC} was high (usually over 83%) and quite constant at each tested liquid to air ratio, indicating that the overall performance of the scrubber was stable despite of the changes in the inlet concentration. The outlet air temperature was quite constant in the stage I, with an average value of 22°C, being the minimum value 18°C. The maximum pressure drop for scrubber operation recommended in the literature is 200 Pa m^{-1} (Janssen et al. 2013), which corresponds to 400 Pa in the studied industrial prototype taking into account the 2 m of packing material. The pressure drop increased since the beginning, reaching the maximum recommended value on day 32 (pressure drop 414 Pa), indicating that a control pressure protocol should be implemented to ensure the long-term operation.

RE_{VOC} achieved by Packing A is similar to those reported in the literature. Le Cloriec and Humeau (2013) investigated a bioscrubber treating a gaseous emission from a paint workshop. The RE_{VOC} of the bioscrubber was 80% with a gas inlet concentration of 900 mg m^{-3} and a gas outlet concentration of 150 mg m^{-3}. Dobslaw et al. (2007) studied a bioscrubber working in a printing company. The waste gas concentrations were up to 1 200 mg-C m^{-3} and the concentration in the treated air did not reach 150 mg-C m^{-3}, which corresponds to a RE_{VOC} of 88%. Granström et al. (2002) ran an experiment to treat the air emissions from a printing process, average exhaust gas flow rate to the scrubber unit ranged between 1.68 and 3.72 m^3 h^{-1} and liquid flow rate varied from 3.2 to 12 L min^{-1}. After bioscrubber column VOC concentration dropped down to a level of 20 mg of carbon VOC m^{-3} being only 0.6% of the original carbon amount.

Table 6.5. Working conditions and overall performance of the scrubber filled with packing A during stage I (no pressure drop control).

Day		**0-24**	**25-37**	**38-50**	**51-56**	**57-62**	**63-95**
Airflow, $m^3\ h^{-1}$		397	660	853	759	794	348
Water flow, $m^3\ h^{-1}$		3	3	3	3	3	3
$L/G \cdot 10^3$*		7.5	4.5	3.5	4.0	3.8	9.1
T_{air} in, °C	AV	39	49	50	53	45	42
	STD	2	6	5	4	4	7
T_{air} out, °C	AV	22	21	21	22	21	22
	STD	2	2	2	1	0	2
Gas inlet conc., mg-C Nm^{-3}	AV	1371	1175	1425	1458	1349	1327
	STD	334	286	499	580	253	308
Gas outlet conc., mg-C Nm^{-3}	AV	131	154	234	227	231	107
	STD	38	33	62	55	30	51
RE_{VOC}, %	AV	90	87	83	83	83	92
	STD	3	2	3	4	1	3
ΔP, Pa	AV	---	424	543	633	658	625
	STD	---	137	121	155	129	338
ΔP_{max}, Pa		---	624	750	848	872	1382

AV: average. STD standard deviation.
* m^3 water m^{-3} air

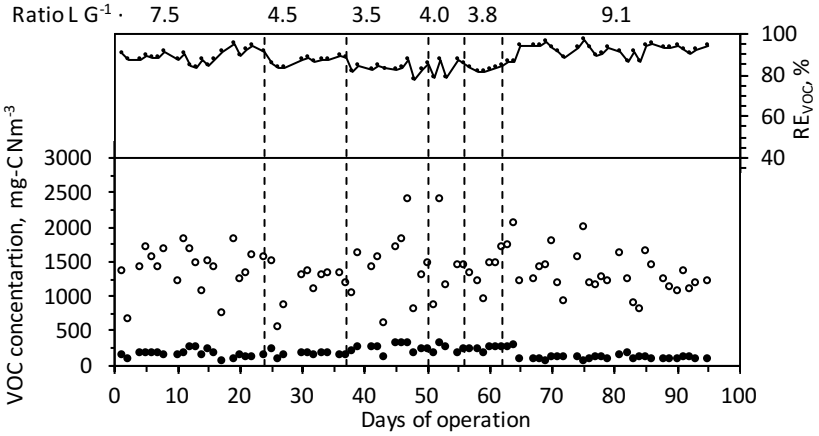

Figure 6.2. Inlet (○) and outlet (●) VOC concentration at the gas phase of the scrubber and RE_{VOC} of the scrubber with packing A (stage I).

Stage II was characterized by the installation of packing B in the scrubber without pressure drop control. The working conditions in this stage are summarized in Table 6.6. Inlet and outlet gas VOC concentration and RE_{VOC} in this stage are plotted in Figure 6.3.

Packing B showed a constant average RE_{VOC} along the trial, with an average of 83 ± 3%, varying from 77% on day 125 to 88% on day 129. This result indicated that packing B is less influenced by the liquid-to-air ratio than Packing A. VOC outlet gas concentration from the scrubber was higher with Packing B than with Packing A, even if higher liquid to air ratios would be applied. The maximum VOC concentration in the outlet gas was 370 mg-C Nm^{-3} (day 120), while in stage I was 310 mg-C Nm^{-3} (day 46 and 52).

Table 6.6. Working conditions and overall performance of the scrubber filled with packing B during stage II (no pressure drop control).

Day	**96-105 & 116-130**	**106-110**
Airflow, $m^3\ h^{-1}$	395	396
Water flow, $m^3\ h^{-1}$	3	4
$L/G \cdot 10^3$*	7.6	10.1
T_{air} in, °C	38 ± 3	37 ± 2
T_{air} out, °C	23 ± 2	22 ± 1
Gas inlet conc., mg-C Nm^{-3}	826 ± 700	1525 ± 457
Gas outlet conc., mg-C Nm^{-3}	213 ± 93	220 ± 69
RE_{VOC}, %	84 ± 4	85 ± 2
ΔP, Pa	62 ± 14 & 200 ± 131	51 ± 2
ΔP_{max}, Pa	96 & 386	53

* m^3 water m^{-3} air

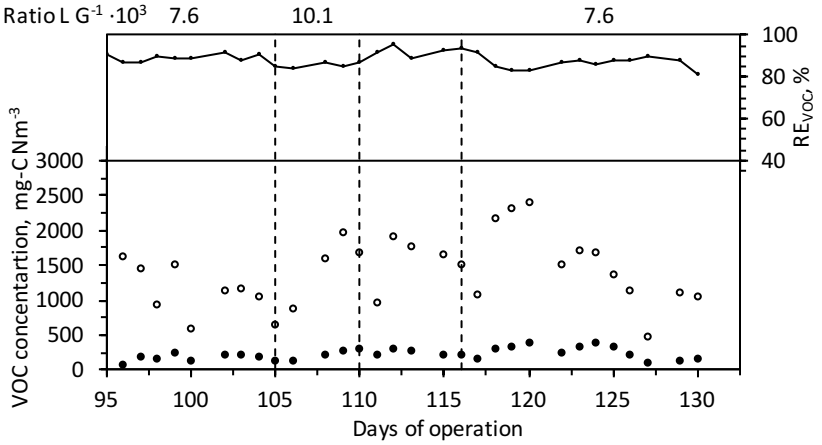

Figure 6.3 Inlet (○) and outlet (●) VOC concentration in the gas phase of the scrubber and RE_{VOC} of the scrubber with packing B (stage II).

Temperature of both phases was quite constant with averages of 38°C and 31°C at the inlet and the outlet gas, respectively. The clogging of this packing material occurred within one month of operation. Pressure drop started with average value of 62 Pa from day 96 to 105 and finished with an average value of 200 Pa from day 116 to 130 (maximum value of 386 Pa). These results indicated that the system requires more time to reach values that could be considered non-feasible to ensure the robustness of the process with less complex pathway of water in Packing B.

The study of stages I and II pointed out that packed bed configuration cannot be feasibly applied for the abatement of VOC if a pressure drop control protocol is not implemented. Spray column configuration was tested afterwards, since this configuration will not be clogged. The working conditions of this stage are introduced in Table 6.7. Inlet and outlet gas VOC concentration and RE_{VOC} in stage III are shown in Figure 6.4.

Table 6.7. Working conditions and overall performance of the spray column (stage III).

Day	**131-173**	**174-180**
Airflow, $m^3\ h^{-1}$	1065	1080
Water flow, $m^3\ h^{-1}$	2	4
$L/G \cdot 10^3$*	1.9	3.7
T_{air} in, °C	42 ± 3	37 ± 4
T_{air} out, °C	25 ± 2	25 ± 2
Gas inlet conc., mg-C Nm^{-3}	1034 ± 423	838 ± 258
Gas outlet conc., mg-C Nm^{-3}	459 ± 187	399 ± 120
RE_{VOC}, %	56 ± 4	52 ± 1
ΔP, Pa	206 ± 29	223 ± 13
ΔP_{max}, Pa	275	243

* m^3 water m^{-3} air

RE_{VOC} efficiency dropped to an average of 55% with this configuration, being the maximum outlet gas VOC concentration 798 mg-C Nm^{-3}, reached on day 171 when gas inlet VOC concentration was 1 715 mg-C Nm^{-3}. Although the pressure drop was quite constant during the whole stage, RE_{VOC} achieved in this stage was quite low, making this configuration technologically unviable for the treatment of VOC emissions from flexographic facilities. Unfeasible high water flow rates would be required in order to fulfill the compliance levels. In addition, RE_{VOC} of this configuration was more variable, since it is more dependent on the VOC composition because the RE of EA is approx. 20% with $2.7 \cdot 10^{-3}$ liquid-to-air ratio.

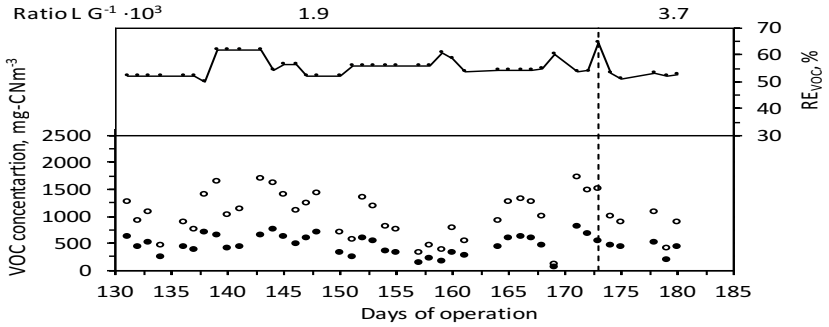

Figure 6.4. Inlet (○) and outlet (●) VOC concentration in the gas phase and RE_{VOC} of the spray column (stage III).

The packed bed configuration was tested again in the stages IV and V. The pressure drop control protocol detailed in Chapter 5 was implemented in these stages. The evolution of the pressure drop along the packed bed and the influence of the pressure drop control system in the overall performance is evaluated herein. The running conditions of stage IV (Packing B installed in the scrubber) are presented in Table 6.8. Inlet and outlet VOC gas concentration and RE_{VOC} of the scrubber are plotted in Figure 6.5:

Table 6.8. Working conditions and overall performance of the scrubber filled with packing B during stage IV (with pressure drop control protocol).

Day	**181-187**	**188-202**	**203-230**	**231-265**
Airflow, $m^3\ h^{-1}$	806	1030	649	405
Water flow, $m^3\ h^{-1}$	4	4	4	3.2
$L/G \cdot 10^3$*	5.0	3.9	6,2	8,0
T_{air} in, °C	36 ± 3	39 ± 2	37 ± 4	39 ± 7
T_{air} out, °C	23 ± 1	23 ± 1	21 ± 1	20 ± 1
Gas inlet conc., mg-C Nm^{-3}	1000 ± 315	1202 ± 461	1173 ± 359	755 ± 376
Gas outlet conc., mg-C Nm^{-3}	276 ± 114	265 ± 102	241 ± 93	138 ± 68
RE_{VOC}, %	75 ± 4	77 ± 4	82 ± 12	83 ± 4
ΔP, Pa	161± 4	266 ± 35	218 ± 98	105 ± 24
ΔP_{max}, Pa	166	322	493	171

* m^3 water m^{-3} air

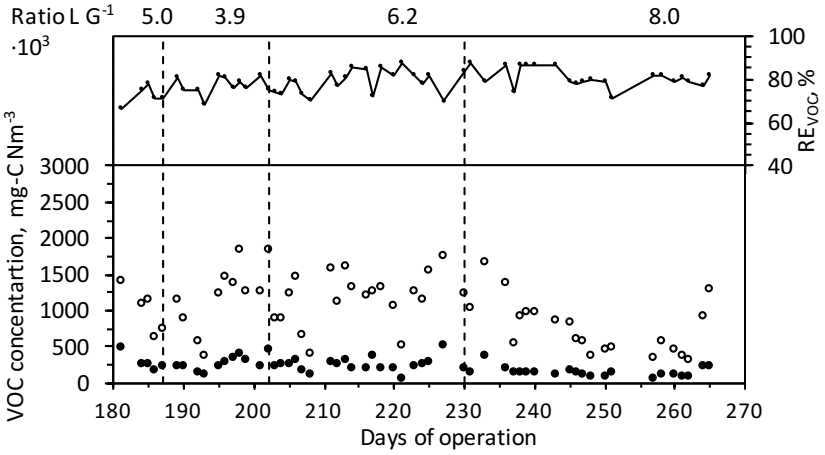

Figure 6.5. Inlet (○) and outlet (●) VOC concentration in the gas phase of the scrubber and the RE_{VOC} of the scrubber with packing B (stage IV).

RE_{VOC} of the packing B in Stage IV was slightly lower than the RE_{VOC} achieved in Stage II. RE_{VOC} was higher than 80% when liquid to air ratio was $7.6 \cdot 10^{-3}$ in stage II, but this value was achieved in stage IV at slightly higher ratio ($8.0 \cdot 10^{-3}$). The maximum RE_{VOC} was 87% on day 221, when the liquid to air ratio was $6.2 \cdot 10^{-3}$. These variations could be due to a change in the air emission composition. The pressure drop values ranged between 166 Pa (83 Pa m^{-1}) and 493 (247 Pa m^{-1}), indicating that the protocol implemented in this thesis was able to control the pressure drop in the scrubber when the packing material B was installed.

Packing A was installed and tested in the scrubber in the last stage. The running conditions and results obtained in this period are shown in Table 6.9. VOC concentration at the inlet and outlet gas and RE_{VOC} of the scrubber are plotted in Figure 6.6. The RE_{VOC} achieved in stage V was 10% lower in comparison with stage I at similar liquid-to-air ratios. This result was attributed to the creation of preferential pathways, probably due to the difficulties associated to the self-assembly of the packing on day 266. The pressure drop remained at values lower than 400 Pa except some days.

Table 6.9. Working conditions and overall performance of the scrubber filled with packing A during stage V (with pressure drop control protocol).

Day	**266-383**	**384-397**	**398-428**	**429-484**
Airflow, $m^3\ h^{-1}$	411	602	651	756
Water flow, $m^3\ h^{-1}$	3.2	3.2	3.2	3.2
L/G 10^3	7.9	5.3	4.9	4.3
T_{air} in, °C	39 ± 5	38 ± 3	41 ± 1	39 ± 3
T_{air} out, °C	22 ± 2	24 ± 1	27 ± 1	25 ± 1
Gas inlet conc., mg-C Nm^{-3}	1035 ± 540	819 ± 280	1133 ± 387	988 ± 366
Gas outlet conc., mg-C Nm^{-3}	161 ± 79	150 ± 66	219 ± 82	202± 80
RE, %	82 ± 12	82 ± 4	80 ± 6	79 ± 5
ΔP, Pa	188 ± 73	298 ± 71	503 ± 388	442 ± 148
ΔP_{max}, Pa	382	386	1362	771

* m^3 water m^{-3} air

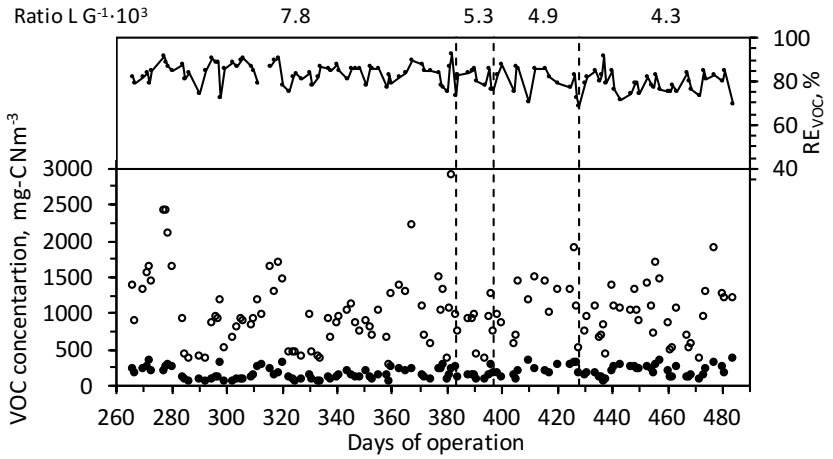

Figure 6.6. Inlet (○) and outlet (●) VOC concentration in the gas phase of the scrubber and the RE_{VOC} of the scrubber with packing A (stage V).

The comparison between both packing materials is shown in Figure 6.7, where the average RE_{VOC} versus the applied liquid to air ratio for packing A (stage I) and packing B (stage II and IV) are plotted. In case of Packing A, stage V was discarded due to the re-installation problem. The positive effect of increasing the liquid to air ratio can be observed for both packings. In case of Packing A, RE_{VOC} increased from 83 to 92% by increasing the ratio from $3.5 \cdot 10^{-3}$ to $9.1 \cdot 10^{-3}$. For packing B, RE_{VOC} increased from 75 to 85% as the ratio increased from $3.9 \cdot 10^{-3}$ to $10.1 \cdot 10^{-3}$. Comparing both packing materials, higher RE_{VOC} were achieved by packing A due to the higher specific surface and the more complex path-water, which favored the contact between both phases enhancing the mass transfer. With packing B, liquid to air ratio higher than $6 \cdot 10^{-3}$ was required to achieve RE_{VOC} over 80%, while this RE_{VOC} could be reached by applying nearly half ratio ($3.5 \cdot 10^{-3}$) in packing A. Results indicates that packing A is the best alternative for industrial applications, as long as clogging problem associated to solid accumulation is prevented by active control of pressure drop.

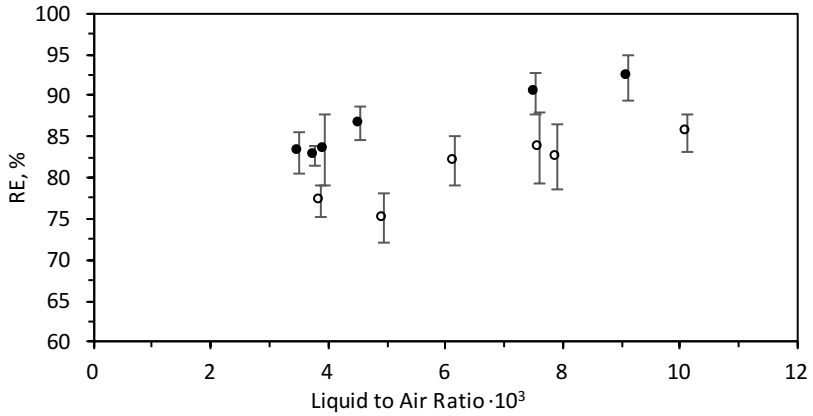

Figure 6.7. Influence of the liquid to air ratio on the RE_{VOC} of the scrubber unit. (●) Packing A, stage I, and (○) packing B, stages II and IV.

6.2.1.3 *Pressure drop evolution in the packed bed and its influence in the overall performance*

Pressure drop problems were reported in the literature when the bioscrubber technology was selected for the treatment of VOC air emissions. Granström et al. (2002) reported strong wall growth of biomass which blocked the air stream flow into the packed bed of an aerobic bioscrubber treating VOCs from printing press air. Same problem was reported by Malhautier et al. (2009) when they studied the performance of an aerobic bioscrubber treating a complex VOC mixture. The clogging of the column by biofilm development on the packing material was observed after 20 weeks of trial and pressure drop was over 200 Pa m^{-1} within two weeks.

The scrubber tested in this thesis also showed pressure drop problems due to the solid accumulation, which resulted in an increase of the pressure drop in the scrubber in stages I and II, when packing materials without any pressure control protocol were implemented. The Figure 6.8 shows the pressure drop evolution along with the airflow with both packing materials. The Figure also shows with a horizontal broken line the value of 400 Pa, selected as the maximum desired pressure drop in the 2-m scrubber.

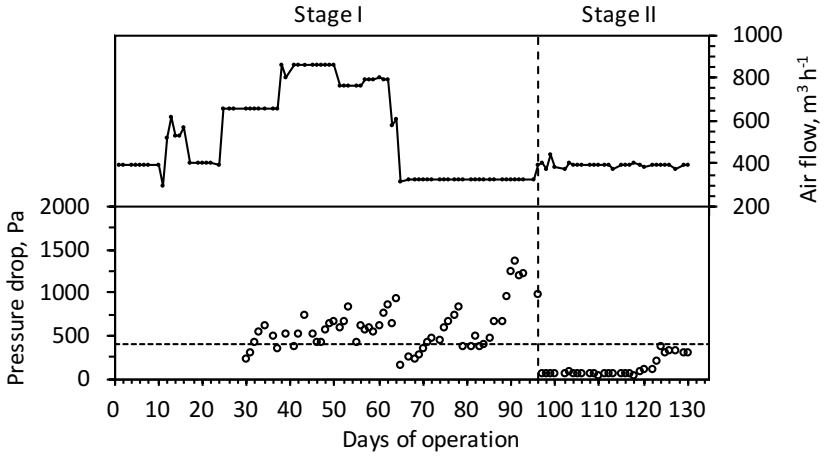

Figure 6.8. Evolution of the pressure drop and the airflow rate through the scrubber in Stages I and II. Stages without pressure drop control.

The value of 400 Pa was reached with both packing materials within one month of operation, indicating that a pressure drop control protocol should be implemented. The pressure control system developed in this thesis was implemented in stage IV and V in order to keep under control the solid accumulation on the packing materials (B and A, respectively). The average daily pressure drop and airflow rate through the scrubber in stages IV and V are plotted against the operational days in Figure 6.9. The horizontal broken line indicates the recommended limit pressure drop of 400 Pa.

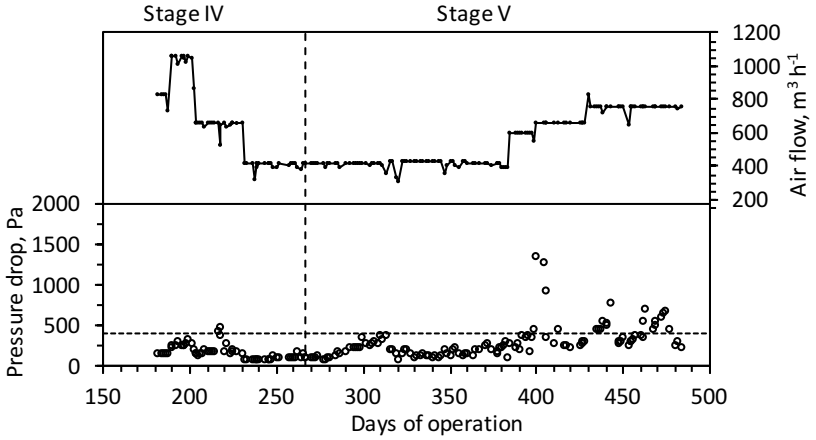

Figure 6.9. Evolution of the pressure drop and the airflow rate through the scrubber in Stages IV and V.

The Figure 6.9 states that the pressure drop control protocol implemented in this thesis was able to keep the pressure drop below the selected value of 400 Pa. This value was overpassed some days associated to specific days when the pressure drop control protocol was being adapted and updated. Hence, the stable pressure drop values achieved during more than 200 days without interruption with the developed protocol demonstrates the successful implementation and the robustness of the process.

The results presented in this section indicate that packing A is the best alternative for industrial application if accumulation of solids is prevented by active control of pressure drop. In addition, the pressure drop control developed in the framework of this thesis does not interfere in the overall performance of the scrubber and its regular application in industrial installations will ensure the long-term operation as it has been stated in stage V.

6.2.2 Performance of the anaerobic reactor treating solvents from flexographic sector.

The scrubbing liquid with the dissolved solvents was pumped to the anaerobic reactor for solvent degradation prior recirculation to the scrubber. OL fed to the anaerobic reactor varied along the day, since it derived from the difference between the inlet and outlet VOC concentration in the gas phase at the scrubber. The fluctuations of the inlet concentration were associated with the number of printing press in operation and the printed jobs. This section shows the performance of the anaerobic reactor working under variable and intermittent feed. Table 6.10 shows the general performance of the anaerobic reactor: organic load, removal efficiency, biogas production and its composition in methane along with the water parameters, such as pH, temperature, VFA and COD concentration at the liquid effluent of the anaerobic reactor. The data introduced in Table 6.10 is divided according to the stages of the scrubber. RE_{COD} of the anaerobic reactor was calculated from the solvent mass balance (expressed in COD units) on weekly basis:

$$RE_{COD}\ (\%) = \frac{OL_W\text{-Acum-Purge}}{OL_W} \cdot 100 \qquad (6.1)$$

Where OL_W is the cumulative organic load applied to the EGSB during a week, ACUM is the intra-week accumulated solvents in water, and Purge is the total

amount of purged solvents during a week. Acum and Purge derived from COD water analysis. The composition of methane in the biogas was calculated by the equation (1.12).

Table 6.10. Daily average, maximum and minimum parameters of the performance of the anaerobic reactor along with water quality of the effluent.

		Stage I	**Stage II**	**Stage III**	**Stage IV**	**Stage V**
Days		0 - 95	96 - 130	131 - 180	181 -265	266 - 484
OL, kg COD h^{-1}	Av	2.45	1.79	2.32	2.09	1.75
	STD	1.19	0.66	1.07	1.30	0.90
	Max	6.96	3.01	5.06	5.78	4.61
	Min	0.86	0.54	0.43	0.37	0.42
RE_{COD}, %	Av	92	86	89	91	94
	STD	4	7	3	2	4
	Max	99	95	93	95	99
	Min	84	77	83	86	85
T, °C	Av	22	25	27	22	26
	STD	2	2	2	2	2
	Max	26	29	31	26	31
	Min	18	21	22	19	21
pH	Av	7.51	7.47	7.41	7.39	7.41
	STD	0.20	0.23	0.16	0.24	0.40
	Max	8.25	8.41	7.71	8.12	8.75
	Min	7.09	7.14	7.09	6.83	6.85
VFA, mg acetic acid L^{-1}	Av	187	113	249	526	153
	STD	198	16	215	383	139
	Max	934	135	815	1154	615
	Min	43	85	58	47	44
Soluble organic matter, mg COD L^{-1}	Av.	1957	1367	1848	2697	948
	STD	1143	279	773	1466	631
	Max	5684	1847	3375	5252	2768
	Min	676	971	890	503	330

Av: Average. STD: Standard deviation. Max: Maximum. Min: Minimum

Table 6.10cont. Daily average, maximum and minimum parameters of the performance of the anaerobic reactor along with water quality of the effluent.

		Stage I	**Stage II**	**Stage III**	**Stage IV**	**Stage V**
Days		0 - 95	96 - 130	131 - 180	181 -265	266 - 484
Biogas, $m^3\ h^{-1}$	Av	0.49	0.32	0.87	0.74	0.41
	STD	0.27	0.32	0.25	0.30	0.26
	Max	1.13	0.52	1.21	1.32	0.89
	Min	0.08	0.07	0.42	0.30	0.10
CH_4 in biogas, % Volume	Av	90	91	83	84	89
	STD	4	3	6	5	7
	Max	98	96	93	93	99
	Min	79	84	74	78	74

Av: Average. STD: Standard deviation. Max: Maximum. Min: Minimum

The OL fed to the reactor was quite fluctuating due to the production of the facility and the performance of the scrubber. The Figure 6.10a compiles the inlet and the outlet VOC gas concentration and the RE_{VOC} of the scrubber for the whole experimental period (484 days). OL fed to the reactor and its RE_{COD} are plotted in Figure 6.10b. OL ranged between 0.37 kg COD h^{-1} (on day 262) to 6.96 kg COD h^{-1} (on day 169). Despite OL fluctuations, RE_{COD} of the anaerobic reactor was stable at 93 ± 5%, even working at psychrophilic conditions (minimum temperature was 18°C on day 65), proving the feasibility of the anaerobic biodegradation of a mixture of solvents containing mainly EtOH, EA and Et2Pr.

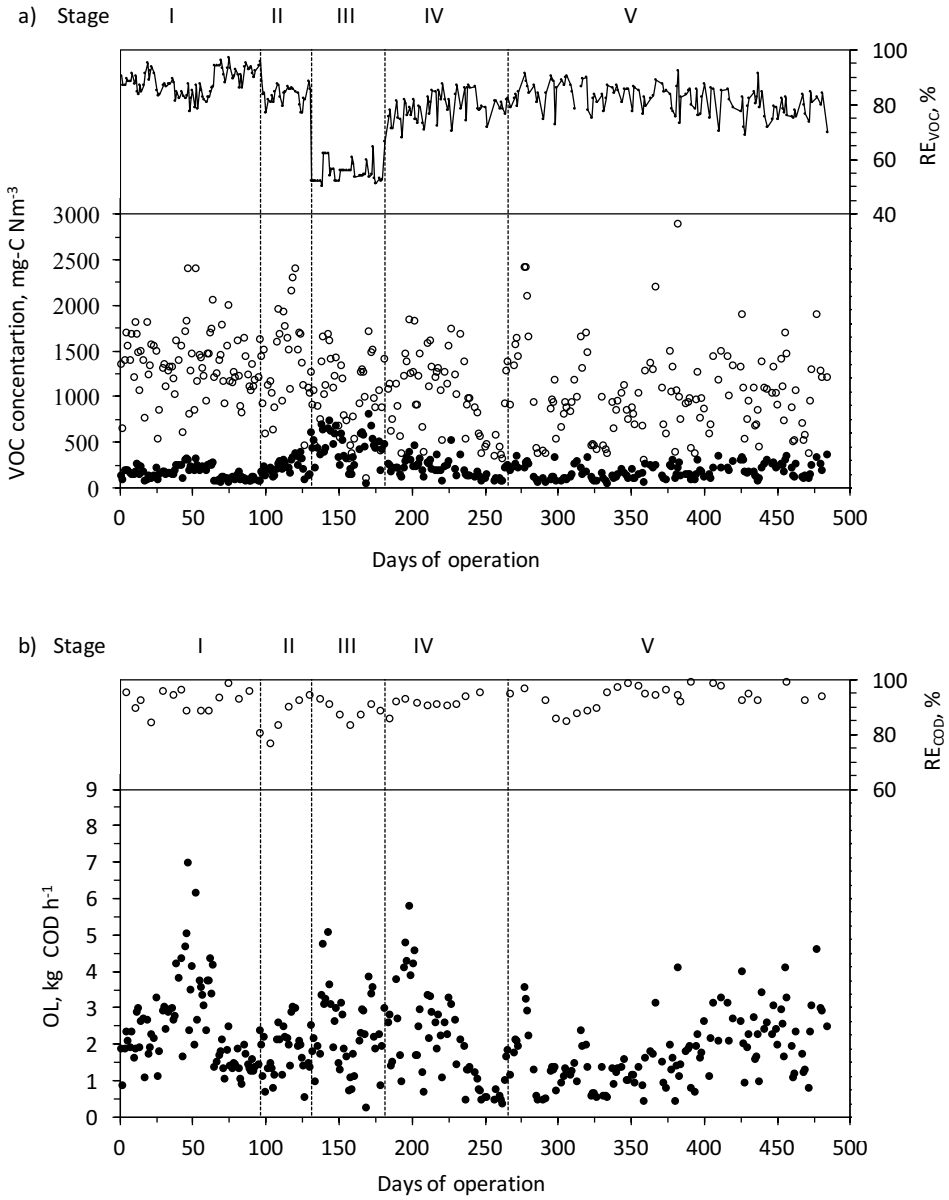

Figure 6.10. Performance of the industrial prototype of anaerobic bioscrubber. (A) Daily average of: (—) RE_{VOC}, (○) Inlet VOC and (●) Outlet VOC concentration in the gas phase of the scrubber. (b) Daily average OL (●) and weekly RE_{COD} (○) of the anaerobic reactor.

The capability of the anaerobic reactor to reach high RE_{COD} at psychrophilic conditions has been widely reported in the literature, even in the treatment of packaging wastewater. Lafita et al. (2015) studied an EGSB reactor operated at 18°C treating packaging wastewater. The reactor was fed with a mixture of ethanol and methyl-2-propanol (mass ratio 3:1). The RE_{COD} reported by these authors was up to 94% operating with continuous supply of wastewater, similar to the RE_{COD} achieved in this study with intermittent and fluctuating loads. The novelty of this thesis is that this is the first attempt to show the robustness of the process for a long-term operation and under industrial air emissions (with its variation in concentration and composition). The importance of this research lies on demonstrating the feasibility of the process at industrial scale as last stage to design commercial units.

VFA concentrations at the liquid effluent of the anaerobic reactor are plotted against OL in Figure 6.11. As it can be seen, the anaerobic reactor showed a good balance between acidogenesis and methanogenesis, since VFA concentration was kept in values lower than 300 mg acetic acid L^{-1} when OL was lower than 3 kg COD L^{-1}, except for 4 exceptional days. The accumulation of VFA with OL higher than 3 kg COD h^{-1} indicates that the slowly growing methanogens cannot sufficiently and rapidly metabolize the intermediate products from VFA producers (acidogens and acetogens population). This imbalanced situation could derive, if keep over time, in the destabilization of the reactor. Considering the biomass volume of the reactor, the design organic load should be less than 24 kg COD m^{-3} bed d^{-1} for ensuring stable RE_{COD} over 94% and VFA concentration below 300 mg acetic acid L^{-1}. The stable performance of the EGSB reactor is also shown when the methane production is evaluated. Figure 6.12 shows the methane production (in biogas plus dissolved in the water effluent) against the OL. As it can be seen, the reactor had a similar performance during nearly 500 days of operation. The shape of the curve is the typical Monod-kinetic, reaching a maximum of 1.3 m^3 CH_4 h^{-1} for OL higher than 4 kg COD h^{-1}.

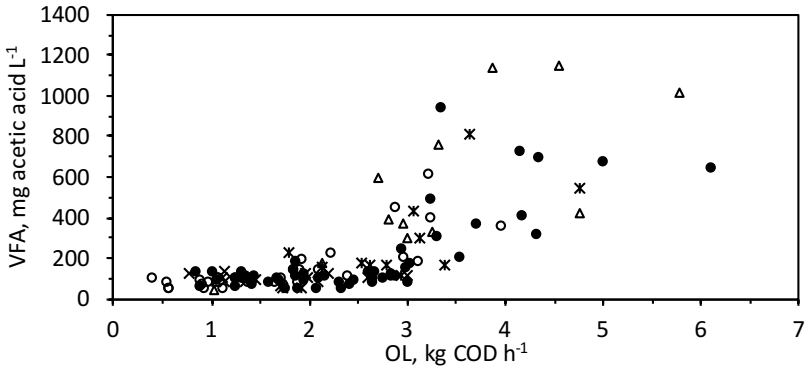

Figure 6.11. Effect of the OL on the water effluent VFA concentration of the EGSB. VFA concentration in Stage I (•), Stage II (x), Stage III (∗), Stage IV (Δ) and Stage V (o).

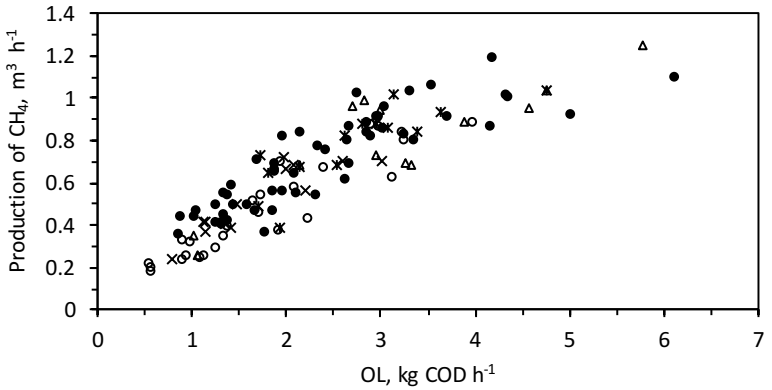

Figure 6.12. Effect of the OL on the produced methane. Methane produced in Stage I (•), Stage II (x), Stage III (∗), Stage IV (Δ) and Stage V (o).

COD concentration at the effluent of the reactor and the OL over time is plotted in Figure 6.13. The soluble organic matter concentration at the liquid effluent of the anaerobic reactor varied between 330 and 5 684 mg COD L^{-1}, reaching higher values the days with higher OL or after several days working with high OL. The broken lines in the graph indicate when the configuration of the scrubber was changed. These changes produced a variation in the fed OL, which caused a change in the COD effluent concentration. Leitão (2004) also stated that the COD effluent concentration from pilot-scale UASB varied in the same range of the inlet COD concentration. This fact was specially pointed out in stage I, when the airflow was increased stepwise. Figure 6.14 shows the COD concentration of the effluent of the anaerobic reactor and the OL in this stage, continuous line indicated when the airflow rate in the scrubber was changed. As it can be seen, the OL fed to

the reactor increased when the airflow was increased, resulting in an increase in the COD concentration at the liquid effluent of the reactor. For example, when the airflow rate was increased approx. two times (from 397 to 853 $m^3\ h^{-1}$), the COD effluent concentration rose from values of 1 000 mg COD L^{-1} to values of 3 000 mg COD L^{-1}.

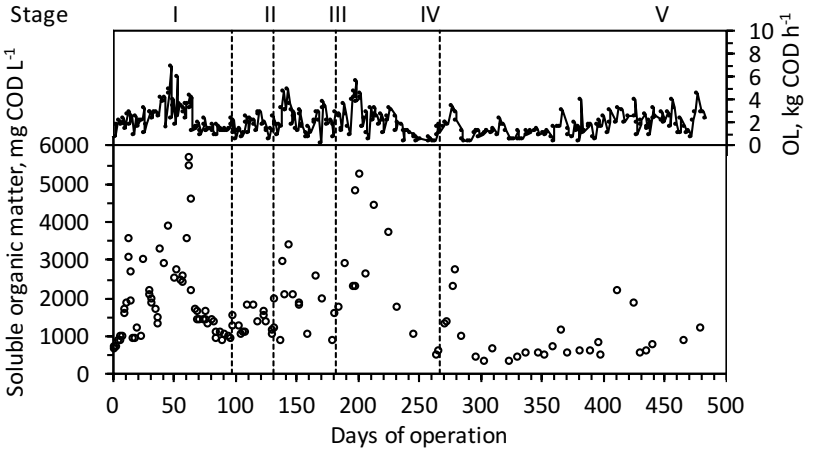

Figure 6.13. (○) COD concentration at the effluent of the anaerobic reactor and (●) OL. Broken lines indicate a change in the scrubber configuration.

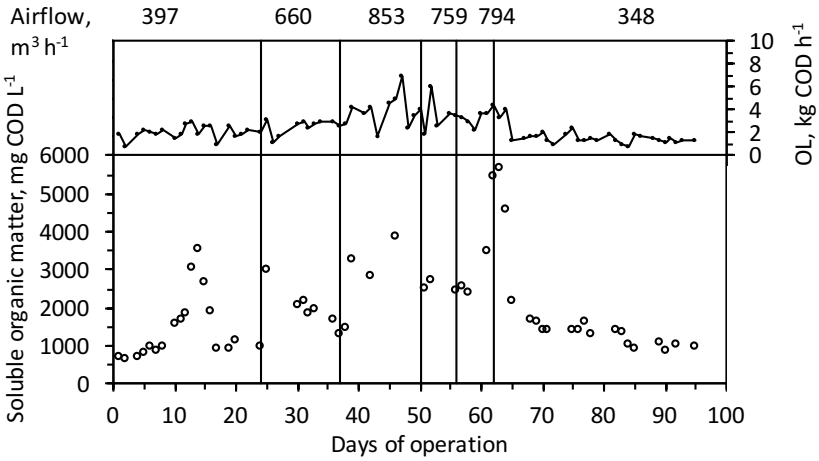

Figure 6.14. (○) COD concentration at the effluent of the anaerobic reactor in the stage I and (●) OL. Vertical lines indicate a change in the airflow rate in the scrubber.

Other important aspect is the minimum soluble organic matter concentration in the liquid effluent of the anaerobic reactor. As it can be seen in Figure 6.13, the minimum COD concentration was higher at the beginning of the study, due to the accumulation of 1-ethoxy-2-pronanol in the water. A similar granular anaerobic sludge coming from a brewery WWTP required 45 day at 25°C and more than 2 months at 18°C to start to degrade glycol ethers according to Lafita et al (2015). The long adaptation periods are related to the lack of enzymes for ether cleavage in the inoculum. In this way, the adaptation period could be reduced thanks to feedless periods, since the only available substrate was Et2Pr, forcing the biomass to adapt to this compound. Figure 6.15 shows the evolution of the COD concentration associated to Et2PR in the water effluent of the anaerobic reactor, along with the OL. The adaptation period for this solvent was between 40 and 75 days, unfortunately, intermediate values are not available to better define this time interval. The concentration of Et2Pr in the system was controlled with the daily purge, in order to avoid the accumulation of this compound in the system. Once, it was detected that the solvent started to degrade, the daily purge was reduced from 1 m^3 to 0.5 m^3, being the residence time of the system increased from 16 days to 32 days. According to the mechanism proposed by Speranza et al (2002), ET2Pr is assumed to degraded to EtOH and acetone. Acetone was not detected in the water composition analyses, indicating that the limit step in the degradation of Et2Pr is the ether cleavage, the formed acetone seemed to be immediately degraded to acetic acid. Ethanol was only detected in the water effluent on punctual days when COD concentration was significantly high, while ethyl acetate was never detected, indicating that this compound was fully degraded to ethanol according to the route proposed by Yanti et al. (2014).

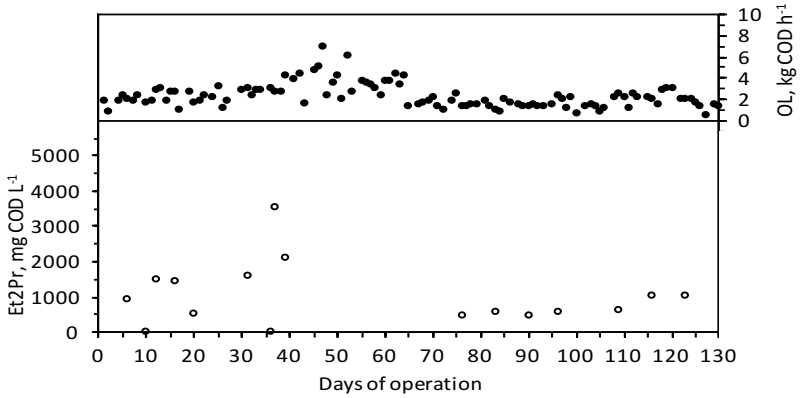

Figure 6.15. (○) Et2Pr concentration at the effluent of and (•) OL fed to the anaerobic reactor.

The water quality of the system was controlled to keep the stability of the anaerobic process. The OL evolution during the experimental period is shown in Figure 6.16, along with the VFA concentration, the pH and the methane content in the biogas stream. pH was chemically controlled by adding sodium carbonate and following the dosing control rules developed in this thesis (chapter 5). pH was kept above the minimum value for optimal growth of methanogens (6.8; Grady et al., 2011), reaching minimum values on days when the OL was high and VFA was accumulated in water. The lowest value was reached on day 199 (daily average pH of 6.83) after 4 days running with OL higher than 4 kg COD h^{-1}, resulting in the maximum VFA concentration (1 154 mg acetic acid L^{-1}). Average methane content in the biogas was 88 ± 6% Vol., signifying that the chemical conditions kept in the anaerobic reactor allows to obtain a biogas with a high content of methane, which does not need further upgrading. The methane yield was 0.32 Nm^3 CH_4 kg^{-1} removed COD, close to the stoichiometric value (0.35 Nm^3 CH_4 kg^{-1} removed COD; Grady et al., 2011), signifying that growth yield coefficient was 0.06 mg-VSS mg-COD^{-1}. In spite of microbial growth, the volume of the granular sludge bed kept constant at 3 m^3. The reason was the design of the anaerobic reactor, in particular the distance from the top part of the sludge bed and the GLS. The hydraulic characteristics did not allow the increase of the volume of the sludge bed. The biomass washed out from the reactor was eliminated from the system in the water purge.

The relation of pH of the liquid effluent of the anaerobic reactor and the biogas methane content with the OL is shown in Figure 6.17. The pH decreased slightly from OLs higher than 3 kg COD h^{-1}, due to the accumulation of VFA since methanogenic bacteria cannot metabolize at the same rate the products generated by acidogens and acetogens population. The methane content in the biogas was lower for those days with high OL, since the content of CO_2 increases at lower pHs.

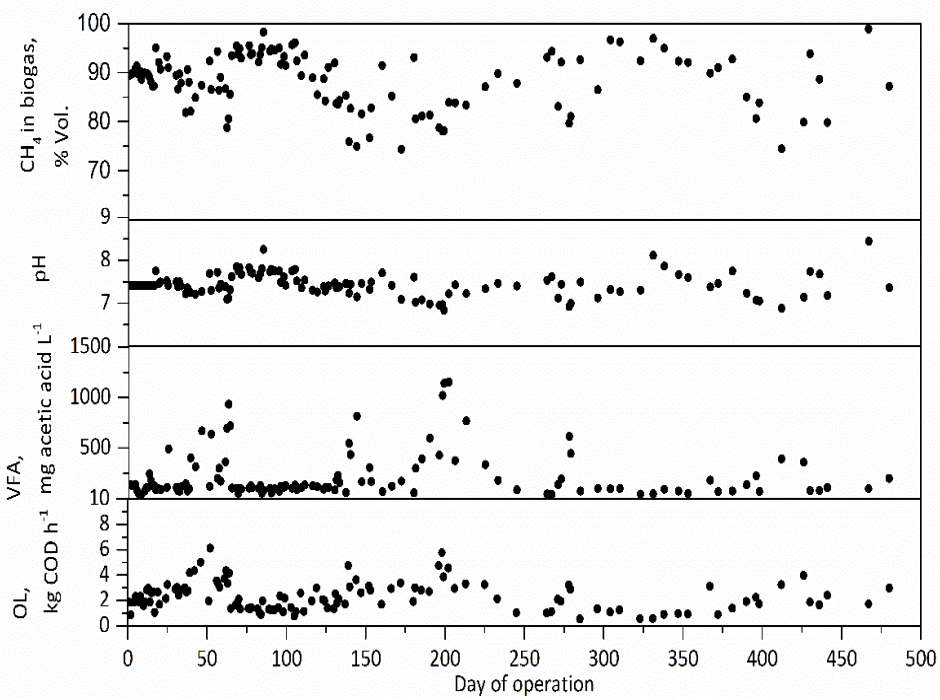

Figure 6.16. Evolution during experimental period of the OL, the VFA concentration and the pH of the water effluent and the methane content in the biogas.

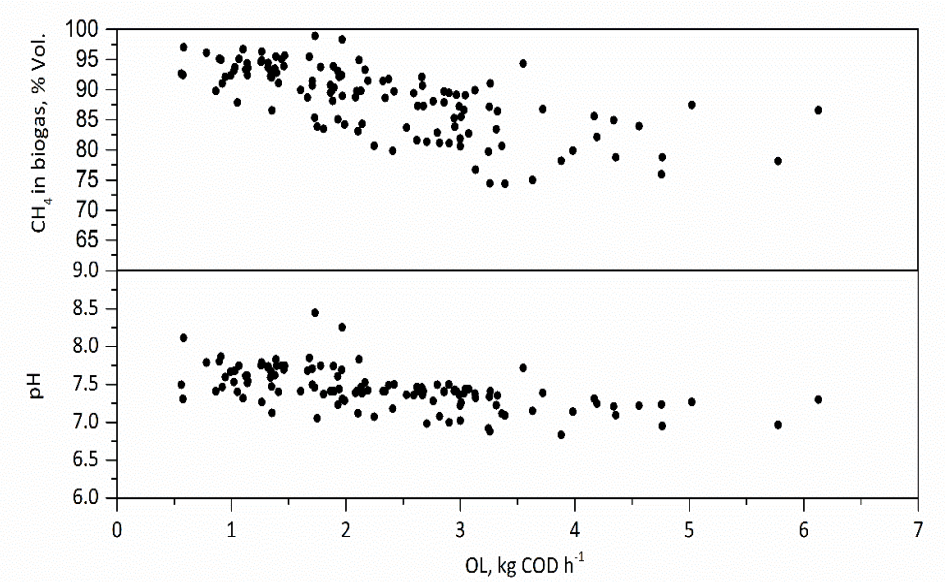

Figure 6.17. Dependency between the methane content in the biogas and the pH of the water effluent with the OL.

Nutrients were supplemented to the system, since they are essential components of the biomass. The rules implemented in the software tried to avoid the accumulation of ions in the system by providing the requirements for biomass growth based on the organic substrate fed to the anaerobic reactor. Table 6.11 summarizes the concentration of the ions at the water effluent of the anaerobic reactor. The evolution of the anions and cations concentration along the time is plotted in Figure 6.18 and Figure 6.19, respectively.

Table 6.11. Nutrient concentration at the water effluent of the anaerobic reactor.

		Stage I	**Stage II**	**Stage III**	**Stage IV**	**Stage V**
Days		0 - 95	96 - 130	131 - 180	181 - 265	266 - 484
$N\text{-}NH_4^+$, mg L^{-1}	Av	3.43	1.72	0.60	2.31	4.17
	STD	4.41	2.54	1.01	5.30	7.84
	n	56	14	21	13	28
$P\text{-}PO_4^{3-}$, mg L^{-1}	Av	1.71	3.95	0.48	0.66	1.82
	STD	1.55	1.15	0.71	0.91	2.36
	n	56	14	21	13	28
Ca^{2+}, mg L^{-1}	Av	37.53	52.95	10.04	29.86	23.46
	STD	14.81	5.80	---	13.91	1.60
	n	12	4	1	8	2
Mg^{2+}, mg L^{-1}	Av	7.05	5.49	0.47	6.37	6.67
	STD	0.51	3.12	---	2.29	0.91
	n	12	4	1	8	2
Na^+, mg L^{-1}	Av	879.84	658.13	1060.94	790.36	997.88
	STD	109.18	58.38	---	331.13	221.85
	n	12	4	1	8	2
K^+, mg L^{-1}	Av	12.26	10.65	0.00	15.73	8.32
	STD	6.24	6.88	---	21.46	6.45
	n	12	4	1	8	2
$S\text{-}SO_4^{2-}$, mg L^{-1}	Av	1.01	0.89	2.73	6.93	1.78
	STD	1.05	0.20	---	15.48	0.37
	n	12	4	1	8	2
Cl^{-1}, mg L^{-1}	Av	238.74	258.01	297.62	240.41	115.54
	STD	51.72	23.51	---	36.89	6.31
	n	12	4	1	8	2

Av: average. STD: standard deviation. n: number of measurements

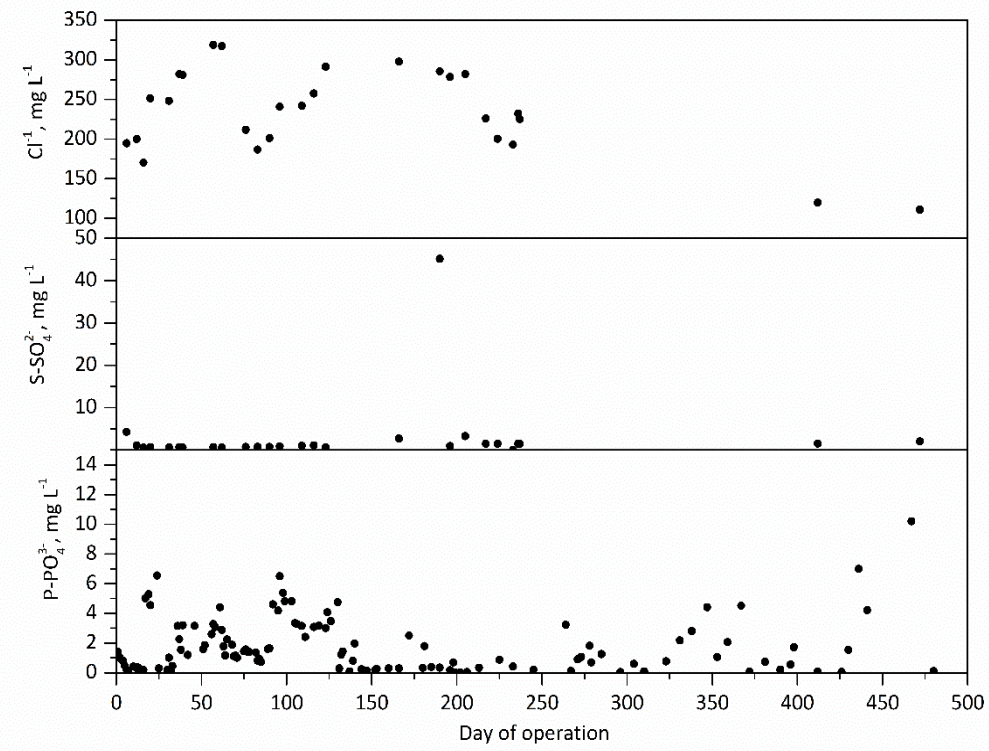

Figure 6.18. Anion concentration at the water effluent of the anaerobic reactor.

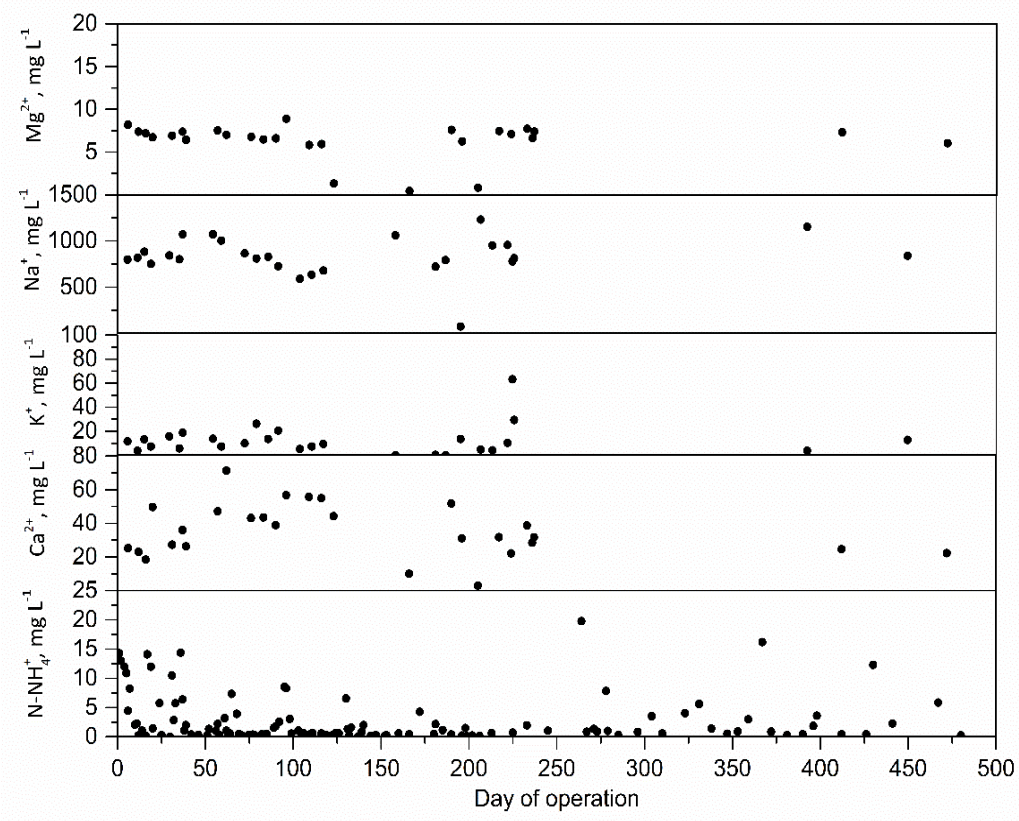

Figure 6.19. Cation concentration at the water effluent of the anaerobic reactor.

Data from Figure 6.18 and Figure 6.19 indicate that there were always nutrients available at the reactor and there was not accumulation of them in the system, since high concentrations of nutrients were not reached at the effluent of the reactor. The high concentration reached on day 190 for S-SO_4^{2-} (45 mg L^{-1}) could be an analysis error, since the concentration reduced to 0.92 mg L^{-1} on day 196, being the purged water between days 190 and 196 kept at regular values (0.5 m^3 day^{-1}) and without stopping the dose of nutrients. The average concentration for N and P were 2.85 $\pm$ 5.07 and 1.67 $\pm$ 1.82 mg L^{-1}, respectively. The concentration of sulfate was kept at low values to avoid the formation of H_2S, so the maximum H_2S concentration measured at the biogas was 12 ppm on day 285. Sodium is required for both growth and methane production and its optimal concentration varies widely amongst the different methanogens, being 100-200 mg Na^+ L^{-1} (for the growth of mesophilic anaerobes), 230 mg L^{-1} for mesophilic aceticlastic

methanogens and 350 mg L^{-1} for mesophilic hydrogenotrophic methanogens. Sodium is moderately inhibitory at concentrations of 2.5-4.5 g L^{-1} (Hayes and Theis, 1978). Microorganisms require potassium for their normal growth, 400 mg L^{-1} of potassium can enhance the performance and it is moderately inhibitory at concentrations of 2.5 to 4.5 g·L^{-1} (Hayes and Theis, 1978). Inhibitory concentrations for sodium and potassium were not reached during the experimental period. The presence of divalent cations (Ca^{2+} and Mg^{2+}) induces the production of single cells, but their concentration should be controlled to avoid phosphate precipitation. The arbitrary maximum selected concentration (100 mg L^{-1}) for both cations were not reached during the experimental period.

Figure 6.20 shows the granule size distribution of biomass samples took on days 0, 238 and 430. The biomass samples showed a narrow range of granule size distribution for the whole experimental period due to the adequate conditions maintained in the anaerobic reactor, despite of the variable and intermittent organic load. The large De Brouckere mean diameters were 0.78, 0.95 and 1.03 mm for samples took on days 0, 238 and 430, respectively. The results demonstrated that the shift of the substrate from complex wastewater from brewery production (sample took on day 0) to a mixture of EtOH, EA and Et2Pr, in which EtOH was the major component, did not show a marked difference in the granular size; a small increase in particle size was observed. This result contrasts with that previously reported by Lafita et al. (2015). These authors indicated a progressively deterioration in methane production and granule disintegration by working at OLR of 35 kg COD m^{-3} d^{-1} with a mixture of EtOH and 1-methoxy-2-propanol (4:1 in mass) applied intermittently (16 hours per day, 5 days per week) to a 4-L EGSB reactor. Although the carbon source and the type of sludge were similar for both studies, the fluffy granule formation reported by these authors could be related to an excessive granular growth, with abundant extra polymeric substances (EPS) production that inhibits the release of gases.

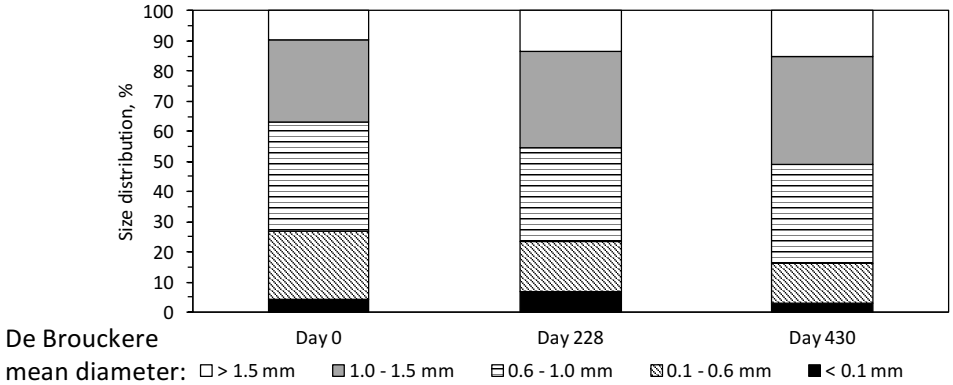

Figure 6.20. Size distribution of biomass samples took on days 0, 238 and 430.

6.3 Conclusions

The results of this chapter demonstrated that the anaerobic bioscrubber was an effective solution for the VOC emissions control coming from the flexographic sector. The optimization of the industrial prototype ensured high VOC removal, while at the same time biogas with a high content of methane was produced in the anaerobic reactor.

From the performance of the scrubber, it can be derived that EA was the major compound in the outlet gas for all configurations, making this compound the key component in the design of the scrubber. The removal efficiency of EtOH and ET2PR with packing A and B was not influenced by the liquid-to-air ratio due to their high solubility in water. The results obtained with the spray column indicated that high water flows are needed to abate the VOC emissions of a flexographic facility, doing this configuration economically unviable at industrial scale.

From the two tested packing materials in the scrubber, Packing A was the best option. Higher RE_{VOC} were achieved with packing material A, due to its higher specific surface and the more complex path-water through the packing in comparison with the packing B. The overall RE_{VOC} with this configuration was over 83% for liquid-to-air ratios ranged between $3.5 \cdot 10^{-3}$ and $9.1 \cdot 10^{-3}$ m^3 water m^{-3} air.

The long-term operation of the anaerobic bioscrubber also pointed out that clogging problem associated to solid accumulation can be prevented by active control of the pressure drop. The pressure drop did not reach the arbitrarily value of 400 Pa (200 Pa m^{-1}) for more than a year of continuous operation, independently

of the packing material used when the pressure drop control protocol was implemented.

Regarding the anaerobic reactor, a stable conversion of alcohols, esters and glycol ethers to enriched methane biogas (RE_{COD} was 93 ± 5%) was demonstrated, despite of the fluctuations of the organic load fed to the anaerobic reactor and the temperature oscillations. From the results of the performance of the anaerobic reactor, an organic load limit of 24 kg COD m^{-3} bed d^{-1} could be stablished to assure a stable behavior of the anaerobic reactor. In fact, when organic loads higher than this limit were applied, an accumulation of VFA in the effluent of the anaerobic reactor was observed, since the methanogenic bacteria cannot degrade the formed VFA.

The methane yield derived from the production of biogas and removal of soluble organic matter during the 484 days of operation was 0.32 Nm^3 CH_4 kg^{-1} COD removed, thus resulting in a growth yield coefficient of 0.06 mg-VSS mg-COD^{-1}. Although biomass growth has been estimated, the volume of the granular sludge bed kept at 3 m^3 along the study mainly due to the hydraulic conditions kept in the reactor.

The dosing rules tested in this thesis ensured the control of the pH and the nutrient concentration within optimal values for anaerobic biodegradation. The pH was kept over the minimum value for optimal growth of methanogens and the dosing rules of nutrients avoided the accumulation of ions in the system. Moreover, the chemical conditions kept in the system allowed to obtain a biogas whose methane content was 88 ± 6%, with a H_2S concentration lower than 12 ppm.

7 ANAEROBIC BIOSCRUBBER MODEL

Part of this chapter has been recently submitted to Journal of Environmental Management as:

Bravo, D., Álvarez-Hornos, F. J., Penya-roja, J.M., San-Valero, P. and Gabaldón, C. Aspen Plus process-simulation model: Producing biogas from VOC emissions in an anaerobic bioscrubber.

This chapter introduces the process simulation model developed for the anaerobic bioscrubber technology, which has been calibrated and validated using the experimental data presented in chapter 6. The process simulation models are well appreciated by researchers and industries, since aims to simulate the process at different conditions and provide a tool to the industry for the design and process optimization.

To achieve these goals, two models for the two main units were developed. The model of the scrubber predicted the VOC concentration at the gas effluent of the scrubber based on the operational conditions and the scrubber configuration. The model of the expanded granular sludge bed anaerobic reactor provided the biogas rate production and its methane content along with the water effluent characteristics (solvent content, pH, VFA and alkalinity) based on the characteristics of the substrate fed (solvent content, pH, VFA and alkalinity) and the kinetic of biodegradation of the solvents.

7.1 Description of the process simulation model

The developed process simulation model was created in the simulator Aspen Plus® V8.0. This commercial simulator was selected due to the availability of the thermodynamic model Electrolyte NRTL (ELECNRTL), which is an extension of the model NRTL for its application in aqueous solutions with electrolyte species. This extension allows to simulate the pH in the anaerobic reactor and accurately simulates the equilibrium of carbonate species (CO_2, HCO_3^- and CO_3^{2-}), which allows to predict the methane content in the biogas stream. After selecting the thermodynamic model, next step consisted in the specification of the conventional components: O_2, N_2, H_2O, CO_2, CH_4, H_2, ethanol (EtOH), ethyl acetate (EA), 1-ethoxy-2-propanol (Et2Pr), acetic acid, Na_2CO_3 and the subsequent electrolytes with their equilibrium constants defined by the Aspen Plus® database. Afterwards, the component approach should be selected between true or apparent. This decision defines how Aspen Plus® reports the simulation results, which are reported in terms of the ions, salts, and molecular components (true component approach) that are actually present, or in terms of the total composition associated to the defined chemical species (apparent approach). The apparent component approach was selected because the scrubber operation unit can only deal with this approach. In spite of the fact that the apparent component approach was selected, Aspen Plus® allows to visualize the ions salts concentration in the liquid phase. The model

implemented in Aspen Plus® has been linked to the software MATLAB® R2016a (Mathworks, Natick, USA). This connection allowed the creation of an interface for the transference of data between both software and the use of Matlab® toolboxes (optimization algorithms as example) for the model calibration and validation.

The creation of the process simulation model in Aspen Plus® can be divided in two steps. Firstly, the scrubber model was implemented in Aspen Plus®, and it was calibrated and validated for the two tested packing materials. The data of the spray column was not used, since the application of this configuration at industrial scale is unfeasible. Secondly, an original approach for modeling the anaerobic reactor was developed, where the kinetics of the acidogenesis and methanogenesis reactions have been assumed as Monod-type expressions. The details of the assumptions to implement the anaerobic bioscrubber in Aspen Plus® are presented in the following sections.

7.1.1 Description of the scrubber model

The scrubber unit was modelled using Radfrac Aspen Plus® Module. This module is the rigorous one for all types of multistage vapor-liquid fractionation operations, including absorption. The equations implemented in this module were explained in Chapter 4, hereafter a detailed explanation of the flowsheet created in the simulator is presented. The simulation program created in Aspen Plus® for the scrubber is shown in Figure 7.1. As can be seen, the gas stream polluted with the solvents (VOC-AIR) entered by the bottom of the column and the scrubbing water stream (WATER-SC) was sprayed from the top. Two outlet steams were calculated by the scrubber block: a solvent cleaned gas stream (CLEANAIR) and a solvent contaminated water stream (VOCWATER), which went to the anaerobic reactor. The flowrate of the VOCAIR stream was set by adjusting the flowrate of the AIR stream, its humidity by the mass-flow of the HUMIDITY stream, and the VOC concentration by specifying the mass-flows of the three solvent streams: ethanol (ET-IN), ethyl acetate (EA-IN) and 1-ethoxy-2-propanol (E2P-IN). The heater (HE-A01) was used to establish the temperature of the polluted inlet air. The required parameters to run the absorber were the pressure drop profile inside the column, the number of equilibrium stages, and the liquid and gas phase feed stage, which were the top one and the bottom one for liquid and gas, respectively. The output results calculated by this model were used as input values for the anaerobic reactor model.

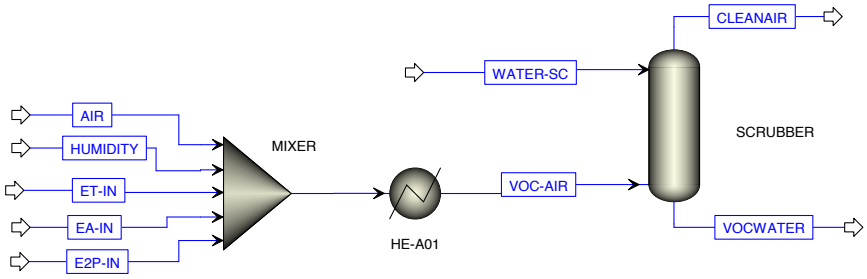

Figure 7.1. Process flowsheet for describing the scrubber unit in Aspen Plus®.

7.1.2 Description of the anaerobic reactor unit model

The model developed in the framework of this thesis is a simplified anaerobic degradation model based on the ADM1 model. However, one of the main drawbacks of this model is its complexity, being the application of this model limited by the parameters required to describe it (Razaviarani and Buchanan, 2015). For this reason, following phenomena were considered negligible due to operation conditions and observations during the experimental period. The processes omitted were: (i) sulphate and nitrate reduction due to the low concentration values of these anions in the liquid influent of the anaerobic reactor; (ii) nutrient limitation because of adequate supplementation of macro and micro nutrients; (iii) inhibition by pH and other compounds due to the control of pH and VFA within the ranges of 6.83 and 8.75 for pH and 43 and 1154 mg acetic acid L^{-1} for VFA; and (iv) biomass growth and decay since the volume of the granular sludge in the reactor was stable at 3.5 m^3 despite of biomass growth.

The reaction set for the degradation of the three solvents was defined according to the literature. Regarding acidogenesis step, Kalyuzhnyi et al. (1997) reported that ethanol is decomposed to acetic acid and hydrogen. Ethyl acetate was assumed to be fully transformed to ethanol and acetic acid, following the mechanism proposed by Yanti et al. (2014) for other esters. The degradation of 1-ethoxy-2-propanol should result in ethanol and acetone. Following the mechanism proposed by Platen and Schink (1987), acetone is further degraded to acetic acid. The analyses of the solvent composition of the liquid effluent of the anaerobic reactor did not detect acetone, hence the acetone was not included in the model and Et2Pr acidogenesis was simulated as one step to produce ethanol and acetic

acid. The acidogenic and methanogenic set of reactions are detailed in the equations (7.1) to (7.5).

Ethanol	$C_2H_5OH + H_2O \rightarrow CH_3COOH + 2H_2$	(7.1)
Ethyl acetate	$C_4H_8O_2 + H_2O \rightarrow CH_3COOH + C_2H_5OH$	(7.2)
1-Ethoxy-2-propanol	$C_5H_{12}O_2 + H_2O + CO_2 \rightarrow 2\,CH_3COOH + C_2H_5OH$	(7.3)
Acetic acid	$CH_3COOH \rightarrow CO_2 + CH_4$	(7.4)
Hydrogen	$4H_2 + CO_2 \rightarrow 2H_2O + CH_4$	(7.5)

The model developed in Aspen Plus® for the simulation of the anaerobic reactor is shown in Figure 7.2.

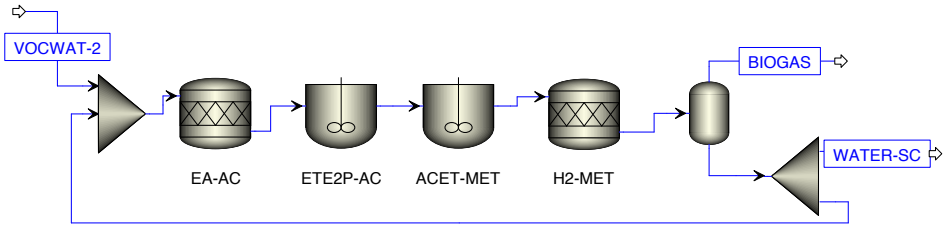

Figure 7.2. Process flowsheet for describing the anaerobic reactor in Aspen Plus®.

The simulation model of the anaerobic reactor has been developed by using several Aspen Plus® reactor blocks, whose selection depended on the type of reaction to be modelled. The Aspen Plus® blocks were connected in series. The reaction temperature was set to the required value by specifying it in each reactor block. The water stream (VOCWAT-2) was defined using the stream coming from the scrubber (VOCWATER) to which it was adjusted the soluble organic matter concentration (in COD units) using the water solvent content from the scrubber simulation and the carbonate species according to the experimental values of total alkalinity and pH. The stream VOCWAT-2 entered in the EA-ACI stoichiometric reactor, in which 100% of ethyl acetate is converted to ethanol and acetic acid. The stoichiometric reaction was modelled in Aspen Plus® by RStoic Block, which is the simplest Module of Aspen Plus®. It permits the molar extent of conversion or fractional conversion of a component. The required variables to run the Rstoic Module are temperature, pressure and valid phases. The pressure was considered the atmospheric. Valid phases are the phases taken into account for chemical equilibrium calculations, being vapor-liquid selected for this model. The outlet stream from the EA-AC unit is connected to a series of two reactors modelled with the RCSTR block, which is a rigorous reactor with rate-controlled reactions based on

specified kinetics. In the ETE2P-AC reactor, the acidogenesis of ethanol and 1-ethoxy-2-propanol was simulated and in the ACET-MET, the production of biogas from acetic acid was modelled. The design parameters for the block RCSTR are pressure, temperature (or heat duty) and specification of the valid phases. The set valid phases in the reactor were vapor and liquid. Regarding the Monod kinetics, Aspen Plus® does not include it, hence the kinetic has been defined in Aspen Plus® using Langmuir-Hinshelwood Hougen-Watson (LHHW) reaction type:

$$r=\frac{(\text{kinetic factor})(\text{driving force})}{(\text{adsorption expression})} \qquad (7.6)$$

Where kinetic factor is expressed as kmol m^{-3} h^{-1}, driving force was the reactant concentration expressed as kg m^{-3} and adsorption expression has units of kg m^{-3} and its mathematical expression is:

$$\left[\sum_{i=1}^{M} K_i \left(\prod_{j=1}^{N} C_j^{\alpha j}\right)\right]^m \qquad (7.7)$$

Where $\ln(k_i)=A_i+{}^{B_i}/_{T}+C_i\ln(T)+D_iT$

Here m is the adsorption expression exponent, M the number of terms in adsorption expression, N the number of components, α_j the concentration exponent, C the concentration of the compounds and K_i the equilibrium constant.

The definition of the different terms of LHHW reaction type to obtain a Monod kinetic expression is described hereafter. The kinetic factor is defined as $\frac{\mu_{max}X}{Y}$, where X is the biomass concentration and Y is the biomass growth yield coefficient. The driving force is defined as the concentration of the limiting substrate for growth, S. The adsorption expression should be defined as K_S +S, as an example the equations for the Monod substrate A, whose $K_S = K_{SA}$ is presented in Table 7.1.

Table 7.1. Values of parameters in the absorption expression of LHHW kinetics to mimic Monod kinetics.

	m	M	A	B	C	D	N	α
K_{SA}:	1	1	$\ln K_{sA}$	0	0	0	1	0
[A]:	1	2	0	0	0	0	1	1

The outlet stream from the ACET-MET reactor went to the H2-MET stoichiometric reactor where hydrogen was fully converted to methane. The model of the anaerobic reactor in Aspen Plus® is completed with the simulation of the separation of biogas and water that occurred in the GLS. The GLS had been modelled with Flash2 Aspen Block, which is designed to produce a single vapor phase and a single liquid phase that are in equilibrium when the flash conditions are specified (pressure and temperature). The vapor phase was the BIOGAS stream in Figure 7.2, and it contains as major compounds CH_4 and CO_2, and the liquid phase was WATER-SC stream in Figure 7.2. This last stream passed through a split block to recirculate, if necessary, a part to be mixed with the VOCWATER stream.

7.1.3 Estimation of the parameters of the model

Models should be calibrated and validated as previous steps for its possible application. The calibration step consists in the estimation of the model parameters that permits to predict accurately the experimental data. The parameters estimated in the calibration of the scrubber model were the number of theoretical stages for every solvent (N_{ET}, N_{EA} and N_{E2P}). The parameters estimation was conducted by the Matlab® algorithm *fminsearch* that minimized the objective function defined as the sum of the squared deviation between the model prediction and the experimental values.

In the case of the anaerobic reactor model, the estimated parameters were the six kinetic parameters: the volumetric maximum growth rate and the half saturation constant for EtOH, Et2Pr and acetic acid. These parameters were preliminary estimated by fitting the methane gas flowrate and the VFA concentration in the water effluent predicted by the simulation model against a set of experimental data, which covered a wide range of operational conditions. The weighted objective function -equation (7.8)- was defined as the sum of the squared relative deviation between the model prediction for methane production ($Q\text{-}CH_{4,mod}$) and VFA concentration (VFA_{mod}) and the experimental one for both ($Q\text{-}CH_{4,exp}$ and VFA_{exp}). The weight of the relative error of methane in this function was increased ten times in order to give the same importance to both anaerobic processes (acidogenesis and methanogenesis steps).

$$O.F. = 10 \cdot \left(\frac{CH_{4,\,exp} - CH_{4,mod}}{CH_{4,exp}} \right)^2 + \left(\frac{VFA_{\,exp} - VFA_{mod}}{VFA_{exp}} \right)^2 \qquad (7.8)$$

A sensitivity analysis with the preliminary fitted values of the six kinetic parameters was previously carried out to stablish which of those parameters will be

determined during the calibration step by minimizing the previous objective function with the Matlab® algorithm *fmincon*.

The validation step is the process of determining the degree to which a model is an accurate representation of the real process. The next sections explain the calibration and the validation of the two models (scrubber and anaerobic reactor).

7.2 Calibration and validation of the scrubber model

7.2.1 Experimental data

The experimental data used for the calibration of the scrubber model were those data from the removal efficiency of each solvent for each scrubber configuration, which were exposed in section 6.2.1.1. These experiments were carried out with fresh water as scrubbing liquid. The air to liquid ratios tested in these experiments covered the whole range of operating conditions tested at the prototype. The parameters for the calibration of the model were: the temperature and the flow rates of air and liquid streams and the gas composition at the inlet and at the outlet gas phase of the scrubber, being the calibrated parameters the number of theoretical equilibrium stages (N) for each solvent and for each experiment. The conditions of those experiments are summarized in Table 7.2 and Table 7.3 for packing A and packing B, respectively. These tables show the liquid and gas velocity, the liquid to air volume ratio, the temperature of the both phases and the gas load factor (F, m s^{-1} (kg m^{-3})$^{0.5}$), whose mathematical expression is introduced in equation (7.9).

$$F = \frac{Q_{air}\sqrt{\rho}}{3600 \cdot A} \qquad (7.9)$$

Where Q_{air} is the air flow (m^3 h^{-1}), ρ is the air density (kg m^{-3}) and A is the cross-sectional area of the scrubber (m^2).

Table 7.2. Experiments for the calibration of Packing A.

F, $m\ s^{-1}\ (Kg\ m^{-3})^{0.5}$	v_{air}, $m\ h^{-1}$	v_{water}, $m\ h^{-1}$	$L/G \cdot 10^3$	T_{air}, °C	T_{water}, °C
2.3	7637	12.6	1.6	40	25
2.0	6608	15.3	2.3	40	25
1.1	3565	13.0	3.7	40	25
1.0	3308	25.3	7.6	40	25

Table 7.3. Experiments for the calibration of Packing B.

F, $m\ s^{-1}\ (Kg\ m^{-3})^{0.5}$	v_{air}, $m\ h^{-1}$	v_{water}, $m\ h^{-1}$	$L/G \cdot 10^3$	T_{air}, °C	T_{water}, °C
2.0	6644	15.4	2.3	53	17
1.3	4321	10.5	2.4	52	17
1.3	4316	15.1	3.5	50	17
1.3	4326	25.5	5.9	51	19

The validation of the scrubber model was carried out by using the whole set of experimental data obtained in the stage I and V for the packing A, and the stages II and IV for packing B, which corresponds to a total of 291 days of operation. The temperature, the flow and the composition of the gas and the water inlet streams of the scrubber should be specified. The specified temperature and flow of both streams were the average value measured during production time. The gas composition used for the validation of the model was the average one obtained from 14 measurements of the inlet gas composition done along the 484 days of the prototype operation (65.5%, 25.4% and 9.1% for EtOH, EA and Et2Pr, respectively, Table 5.1). By using this solvent composition and the average daily VOC concentration, monitored as mg-C Nm^{-3}, it was estimated the corresponding inlet concentration for each solvent. The inlet liquid stream was assumed to be only composed by water, since low solvent concentration was measured in the analyses of the water effluent of the anaerobic reactor.

7.2.2 Calibration of the scrubber model

The calibration of the scrubber was done by adjusting the number of theoretical stages to minimize the deviations between the experimental VOC outlet gas concentration and the modelled one. The Murphree efficiency -(equation (4.9)- was used to refine the number of stages per compound, since Radfrac module only

allows to type entire number of theoretical stage, being necessary to define more accurately the theoretical stages to achieve the experimental separation. The number of theoretical stages obtained from the calibration process for each experiment are shown in Table 7.4 and Table 7.5 for packing A and B, respectively. The experimental VOC outlet gas concentration of each solvent at each experiment and the pertinent simulated values are summarized in Table 7.6.

Table 7.4. Theoretical stages for Packing A per solvent.

F, $m\ s^{-1}\ (Kg\ m^{-3})^{0.5}$	v_{air}, $m\ h^{-1}$	v_{water}, $m\ h^{-1}$	$L/G \cdot 10^3$	T_{air}, °C	T_{water}, °C	N_{EtOH} [a]	N_{EA} [a]	N_{Et2Pr} [a]
2.3	7637	12.6	1.6	40	25	1.00	0.85	0.98
2.0	6608	15.3	2.3	40	25	1.08	0.95	0.91
1.1	3565	13.0	3.7	40	25	0.90	0.90	0.97
1.0	3308	25.3	7.6	40	25	0.98	1.10	0.90

[a] Number of equilibrium stages per meter

Table 7.5. Theoretical stages for Packing B per solvent.

F, $m\ s^{-1}\ (Kg\ m^{-3})^{0.5}$	v_{air}, $m\ h^{-1}$	v_{water}, $m\ h^{-1}$	$L/G \cdot 10^3$	T_{air}, °C	T_{water}, °C	N_{EtOH} [a]	N_{EA} [a]	N_{Et2Pr} [a]
2.0	6644	15.4	2.3	53	17	0.78	0.79	0.75
1.3	4321	10.5	2.4	52	17	0.70	0.77	0.81
1.3	4316	15.1	3.5	50	17	0.67	0.69	0.77
1.3	4326	25.5	5.9	51	19	0.64	0.68	0.77

[a] Number of equilibrium stages per meter

Table 7.6. Set of experimental data and their model predictions for the calibration of the scrubber unit.

F^a	$v_L{}^b$	$C_{in,\,EtOH}{}^c$	$C_{in,\,EA}{}^c$	$C_{in,\,Et2Pr}{}^c$	$C_{in,tot}{}^c$	$C_{out,\,EtOH}{}^c$	$C_{out,\,EA}{}^c$	$C_{out,\,Et2Pr}{}^c$	$C_{out,\,tot}{}^c$	$C_{out,\,EtOH}{}^d$	$C_{out,\,EA}{}^d$	$C_{out,\,Et2Pr}{}^d$	$C_{out,\,tot}{}^d$
Packing A													
2.3	12.6	887	287	97	1271	61	210	3	274	60	209	4	273
2.0	15.3	1395	352	514	2261	52	225	32	309	57	227	12	296
1.1	13.0	288	125	30	443	19	65	1	85	24	65	2	91
1.0	25.3	1797	1014	132	2943	91	267	9	367	89	267	6	362
Packing B													
2.0	15.4	599	238	49	886	81	137	7	225	81	161	7	249
1.3	10.5	635	279	54	968	113	105	6	224	113	154	6	273
1.3	15.1	330	145	28	503	65	68	3	136	61	68	3	132
1.3	25.4	639	253	52	944	127	98	6	231	128	98	6	232

[a] F: gas load factor ($m\ s^{-1}\ (kg\ m^{-3})^{0.5}$)
[b] v_L superficial liquid velocity, ($m\ h^{-1}$)
[c] Experimental concentrations, ($mg\text{-}C\ Nm^{-3}$)
[d] Predicted concentrations, ($mg\text{-}C\ Nm^{-3}$)

The average number of theoretical stages per meter for each solvent with packing A were 0.99 ± 0.07, 0.95 ± 0.10 and 0.94 ± 0.04 m^{-1} for EtOH, EA and Et2Pr, respectively. The number of theoretical stages per meter for EA was lower than EtOH because it is the less soluble solvent. On the other hand, this expected performance was not follow with packing material B, since the average number of theoretical stages per meter for each solvent were 0.70 ± 0.06, 0.73 ± 0.06 and 0.78 ± 0.03 m^{-1} for EtOH, EA and Et2Pr, respectively.

Table 7.4 and Table 7.5 show that the theoretical number of stages per meter at the tested conditions are quite stable for both packing materials, being the average 0.96 ± 0.08 and 0.74 ± 0.06 m^{-1} for packing A and packing B, respectively. The number of theoretical stages per meter in Packing A is higher than in Packing B, since the higher specific surface area and the more complex created path-water of packing material A enhance the mass transfer between both phases. The result is in concordance with the experimental results, higher RE_{VOC} were achieved with packing A in comparison with packing B at same operational conditions. With the aim of simplifying the process simulation model, it was decided to use the average value as a calibration value. The average number of equilibrium stages for the three solvents for both packing materials were transformed to a more engineering concept as HETP: 1.05 $\pm$ 0.08 and 1.37 ± 0.11 m, respectively.

For each experiment, Table 7.6 shows the experimental VOC inlet concentration and the experimental and predicted VOC outlet concentration of each solvent. As it can be observed, the model is able to simulate the data accurately. The model prediction fitted the experimental data with an average deviation between the observed and the predicted outlet concentrations of solvents of 12.9 $\pm$ 16.5 mg-C Nm^{-3}, and with an average relative error between the observed and the predicted total outlet concentrations of 6.1 $\pm$ 7.3%.

For each experiment, the experimental and simulated removal efficiency is shown in Table 7.7 and Table 7.8 for packing A and packing B, respectively. The maximum relative error found in the simulated removal efficiency of packing A was 2%, 2% and 4% for EtOH, EA and Et2Pr, respectively. The maximum relative errors achieved with packing B were 2%, 28% and 1% for EtOH, EA and Et2Pr, respectively. The 28% of relative error was achieved in the experiment that did not follow the expected trend in the RE_{VOC} of EA (section 6.2.1.1, chapter 6).

Table 7.7. Experimental and simulated RE_{VOC} of packing A.

F, $m\ s^{-1}\ (Kg\ m^{-3})^{0.5}$	RE_{exp} EtOH, %	RE_{exp} EA, %	RE_{exp} Et2Pr, %	RE_{mod} EtOH, %	RE_{mod} EA, %	RE_{mod} Et2Pr, %
2.3	93	27	97	93	27	96
2.0	96	36	94	96	35	98
1.1	94	48	96	92	48	93
1.0	95	74	93	95	74	96

Table 7.8. Experimental and simulated RE_{VOC} of packing B.

F, $m\ s^{-1}\ (Kg\ m^{-3})^{0.5}$	RE_{exp} EtOH, %	RE_{exp} EA, %	RE_{exp} Et2Pr, %	RE_{mod} EtOH, %	RE_{mod} EA, %	RE_{mod} Et2Pr, %
2.0	86	42	85	86	32	86
1.3	82	62	89	82	45	90
1.3	80	53	88	82	53	88
1.3	80	61	88	80	61	88

7.2.3 Sensitivity analysis of the scrubber model

The sensitivity analysis of a model investigates how the variation in the output of a numerical model can be attributed to variations of its inputs factors. This investigation is performed by studying the results of several simulations where only one variable under study changed, while the rest of target variables keep constant.

The sensitivity analyses in this case consist in the determination of the influence of the variation of two parameters: the number of equilibrium stages, N, and the VOC composition of the inlet gas on the RE_{VOC} of the scrubber. These analyses have been carried out for both packing materials by changing ±5, 10, 15 and 20% the mentioned parameters. The selected conditions for the sensitivity analyses were an airflow rate of 619 $m^3\ h^{-1}$, which corresponds to a F of 0.96 $m\ s^{-1}$ $(kg\ m^{-3})^{0.5}$, water flow rate of 3 $m^3\ h^{-1}$, inlet gas VOC concentration of 1 129 mg-C Nm^{-3}, inlet gas and water temperature of 47°C and 21°C, respectively. The inlet gas VOC composition was 65.5%, 25.4% and 9.1% for EtOH, EA and Et2Pr, respectively. The result of changing the value of N and its influence on the overall RE_{VOC} of the scrubber for packing A is introduced in Figure 7.3. This Figure shows that the RE_{VOC} of the scrubber is affected by the change of N, since the RE_{VOC} is reduced 8% when the number of the stages is reduced 20% and the RE_{VOC} increased 5% when N increased up to 20%.

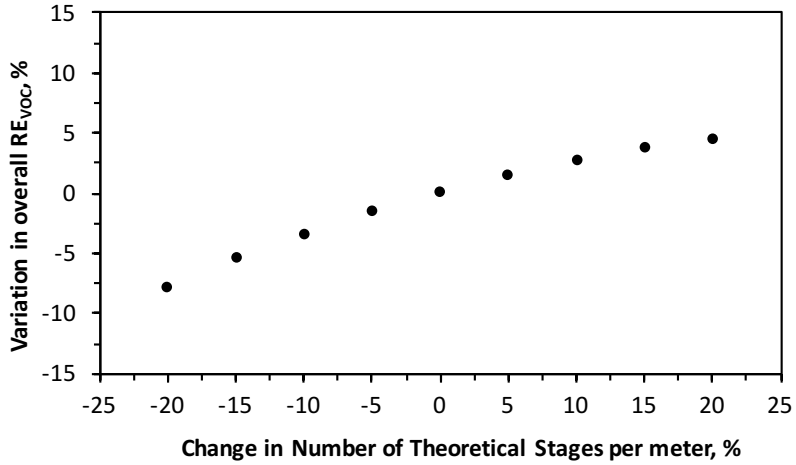

Figure 7.3. Sensitivity analysis of Packing A. Influence of changing the number of theoretical stages on the overall RE_{VOC}.

Figure 7.4 shows the influence of changing N on the RE of each solvent. The influence of increasing N is less evident than its decrease, since the RE of EtOH and Et2Pr slightly change with higher values of N. The RE of those compounds is almost 100% when N increases, while decreases when N decreases. On the other hand, the RE of EA is more influenced by the change of N, but this influence is vaguely reflected on the overall RE_{VOC} because the concentration of EA in the inlet gas stream is only 25.4%.

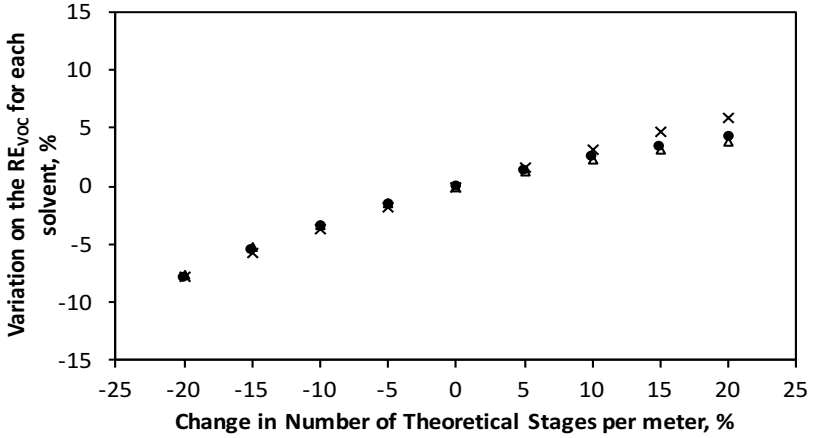

Figure 7.4. Sensitivity analysis of Packing A. Influence of changing the number of theoretical stages on the RE of each solvent. (•) Ethanol, (x) Ethyl acetate and (Δ) ethoxy-2-propanol.

Figure 7.5 shows the influence of changing the composition of one solvent in the inlet gas VOC composition on the overall RE_{VOC} for the packing A. The overall RE_{VOC} increases 4% when EtOH concentration increases 20% and it decreases 4% when the EtOH decreases 20%. The effect of the other two solvents is less evident because its percentage is lower in the inlet emission. The RE_{VOC} varies ±2% when the concentration of EA changes ±20%, decreasing the overall RE_{VOC} when the concentration of EA increases. Regarding Et2Pr, the RE_{VOC} changes ±0.2% when the concentration of Et2Pr changes ±20%, due to the low percentage in the emission (<10%). From the experimental analyses, the variation in the solvent composition of the polluted gas stream during the whole testing period (484 days) was ±10%, corresponding to changes in the overall scrubber performance below ±2%, thus demonstrating the robustness of the proposed approach to satisfactorily model the performance of the scrubber.

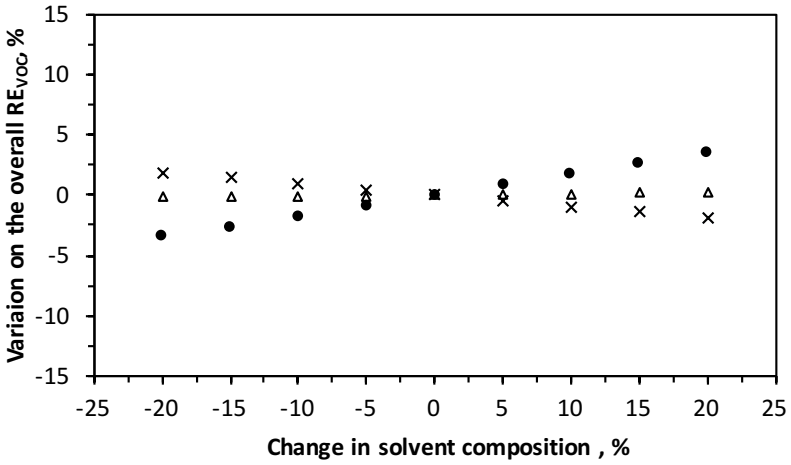

Figure 7.5. Sensitivity analysis of Packing A. Influence of changing the inlet gas VOC composition on the overall RE_{VOC}. Solvent composition changed: (•) Ethanol, (x) Ethyl acetate and (Δ) ethoxy-2-propanol.

The same sensitivity analyses were performed for the packing B. Figure 7.6 shows the effect of changing N. The Packing B is more influenced by the change of N than Packing A, due to its lower absorption efficiency. The RE_{VOC} increases 7% when N increases 20% and decreases 11% when N decreases 20%. By studying the effect of changing N per solvent, EtOH is the most affected by changing N with Packing B. This effect is shown in Figure 7.7, where the single RE for each solvent is plotted against the variation in N.

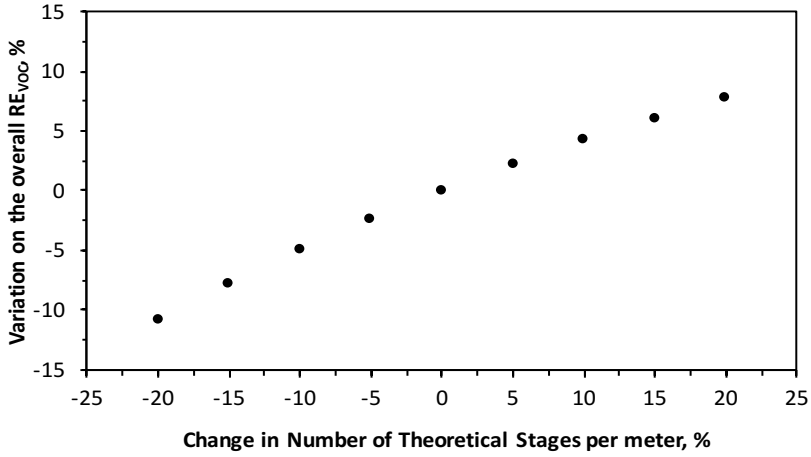

Figure 7.6. Sensitivity analysis of Packing B. Influence of changing the number of theoretical stages on the overall RE_{VOC}.

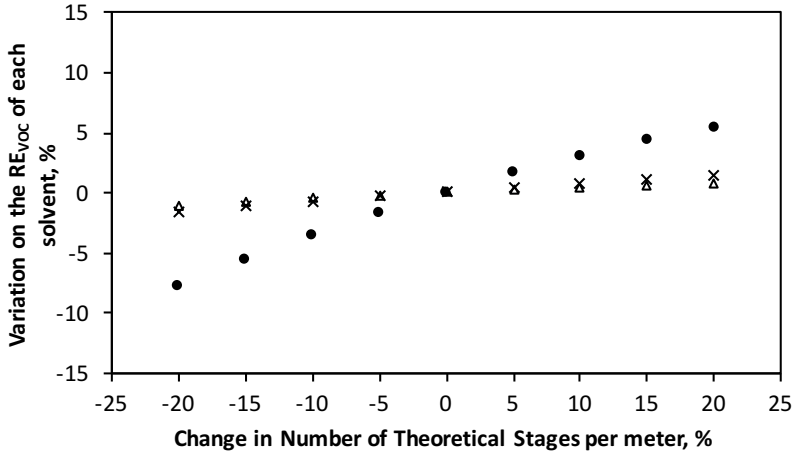

Figure 7.7. Sensitivity analysis of Packing B. Influence of changing the number of theoretical stages on the RE of each solvent. (•) Ethanol, (x) Ethyl acetate and (Δ) ethoxy-2-propanol.

The sensitivity analysis based on the change of the VOC composition in the inlet gas stream is plotted in Figure 7.8. The packing material B showed a similar response of Packing A. The overall RE_{VOC} was linearly influenced by changes in composition of EtOH and EA, varying ±3.5% and ±1.8% with a change of ±20% in EtOH and EA composition, respectively. In contrast, the variation of Et2Pr composition did not altered the overall RE_{VOC} due to its low concentration in the industrial VOC emission.

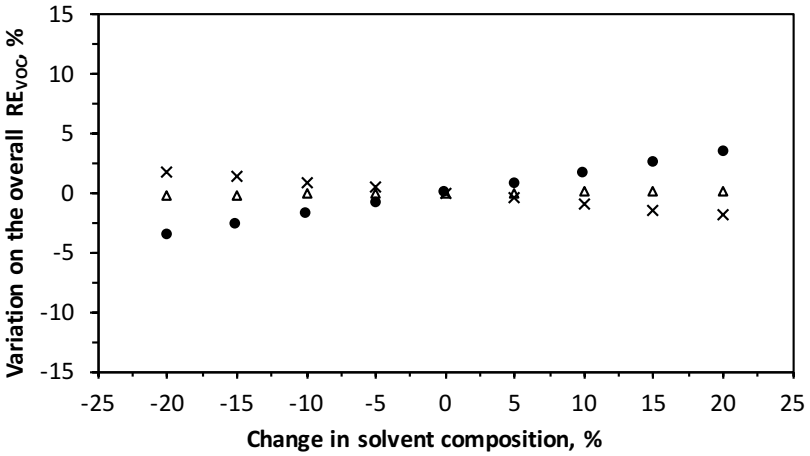

Figure 7.8. Sensitivity analysis of Packing B. Influence of changing the inlet gas VOC composition on the overall RE_{VOC}. Solvent composition changed: (•) Ethanol, (x) Ethyl acetate and (Δ) ethoxy-2-propanol.

7.2.4 Validation of the scrubber model

The model was validated by using the whole set of experimental data of the stages I, II, IV and V, which corresponds to 291 days by excluding non-working days. The validation of the model is shown in Figure 7.9, where the experimental and predicted VOC concentration at the outlet gas phase of the scrubber are plotted. The Figure also shows the inlet VOC concentration at the inlet air stream of the scrubber and the gas load factor (F) of the gas phase. Vertical broken lines indicate a change in the scrubber configuration.

The graph shows that the model accurately predicts the outlet VOC concentration, with an average relative error lower than 5% for stages I and II. Table 7.9 includes the average and the maximum relative error for each stage. The difference between the predicted outlet VOC concentration by the model and the experimental value could be due to a discrepancy between the average inlet composition and the actual one, since as it was mentioned above the validation was performed by using the average concentration for the inlet gas. The relative error in stages IV and V were slightly higher. In these stages, some data points deviate from the model predictions, thus indicating that the performance of the scrubber could be affected by factors such as the creation of pathways after the self-assembly and/or the biomass accumulation onto the packing surface during long-term operation.

The assumption of considering the average value for the number of equilibrium stage per packing, independently of the solvent, can be assumed as valid, since the model was able to accurately predict the performance of the scrubber unit treating VOC emission during 291 days with considerably low differences between experimental and predicted data.

Table 7.9. Average and maximum relative error obtained during the validation of the scrubber model.

	Average relative error, %	Maximum relative error, %
Stage I	2.68 ± 1.93	8.05
Stage II	4.45 ± 3.15	15.66
Stage IV	5.38 ± 4.04	4.04
Stage V	6.91 ± 5.87	28.44

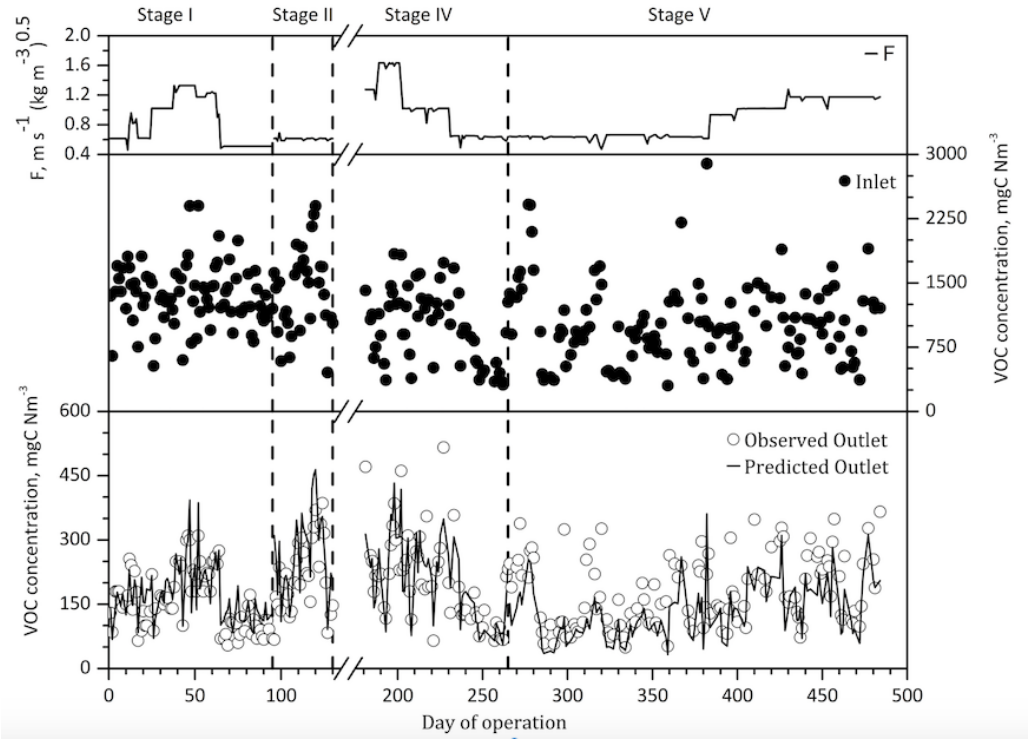

Figure 7.9. Validation of the scrubber model. Packing A was assembled in Stage I and V and Packing B in stages II and IV

Once the model of the scrubber was calibrated and validated, the outlet liquid stream of the scrubber model, which was named as VOCWATER in Figure 7.1, was used to define the input data for the anaerobic reactor model, whose calibration and validation is explained hereafter.

7.3 Calibration and validation of the anaerobic reactor model

7.3.1 Experimental data

The calibration of the anaerobic reactor model was carried out using those experimental data obtained during stage I. Parameters required for the calibration of the model were the VFA and total alkalinity concentrations of the liquid effluent of the anaerobic reactor, which were frequently monitored in stage I. These parameters were used to determine the methane content of the biogas stream (eq. 1.12). The daily average pH of the liquid influent and effluent along with the biogas flow rate were also used. It is important to indicate that organic load input data for the calibration corresponded to experimental values. The solvent composition of the influent was set as the output values of water outlet of the scrubber model effluent predicted in the validation step.

The first 95 days of operation were selected for the calibration of the anaerobic reactor model. The data comprised organic loads ranged between 0.86 and 6.12 kg COD h^{-1}. The pH varied between 7.09 and 8.25, being the minimum and maximum VFA concentration of the liquid effluent of the anaerobic reactor 43 and 934 mg acetic acid L^{-1}, respectively. The methane concentration fluctuated between 79% and 98%. So, the data selected for calibration included the whole range of the tested OLs in the industrial prototype.

The validation of the model was performed by using the experimental data from day 96 to 484, so that the validity of the model has been checked with 211 data points (excluding non-working days and days without in-situ water quality analysis). The experimental OL was the input for the model and the solvent composition of the water influent was equal to that obtained with the scrubber model for the water outlet stream. The OL varied from 0.37 to 5.78 kg COD h^{-1}, with pH of the liquid effluent of the anaerobic reactor ranging between 6.83 and 8.75. The VFA concentration at the liquid effluent varied between 44 and 1 154 mg acetic acid L^{-1}. The methane concentration in the biogas ranged between 74% and 99%. These data were used to corroborate that the anaerobic reactor model is able to

simulate the biodegradation of the solvents, the biogas production rate, the methane production and the characteristics of the liquid effluent of the anaerobic reactor, in terms of VFA and pH.

7.3.2 Calibration of the anaerobic reactor model

The set of degradation reactions included in the anaerobic reactor model were the equations (7.1) to (7.5). The initial parameters to be calibrated in the model were: the Monod kinetic parameters of the acidogenesis step of ethanol and 1-ethoxy-2-propanol and the acetoclastic step: the volumetric growth rates ($\nu_{max, EtOH}$, $\nu_{max, Et2Pr}$ and $\nu_{max, acetic\ acid}$) and the half saturation constants ($K_{s,EtOH}$, $K_{s,Et2Pr}$ and $K_{s,acetic\ acid}$).

The estimation of all parameters would require a significantly broader pool of experimental results to avoid ill-conditioning of the parameter estimation problem (Kesavan and Law, 2005). The problem of ill-conditioning can be avoided by reducing the number of identifiable parameters. Sensitivity analysis has been widely applied to reduce model complexity, by determining the significance of model parameters and identifying dominant parameters. The significance of the parameters was quantified in terms of the variation of measurable process variables under the perturbation of model parameters in their neighborhood domain. The sensitivity analysis should be performed to a set of initial values of the parameters. The set of initial values were obtained by minimizing the objective function (7.8) for some selected days from the first 95 days of operation of the anaerobic reactor. The experimental OLs, production of methane and VFA concentration of the selected data are summarized in Table 7.10. They were chosen in order to cover the wide range of experimental OLs.

Table 7.10. Set of experimental data for the preliminary calibration of the anaerobic reactor model.

Day	OL, kg COD h^{-1}	VFA concentration, mg acetic acid L^{-1}	Production of CH_4, m^3 h^{-1}
10	1.61	73.7	0.5
30	2.89	109	0.81
42	4.34	315	1.02
46	5.02	671	1.02
52	6.13	640	1.14

For this first approach, the COD inlet water composition was established in 73.5% of ethanol, 17% ethyl acetate and 9.5% of 1-ethoxy-2-propanol as average values from the application of the scrubber model. The following assumptions prior to this pre-optimization step were done:

- The maximum specific uptake rate of the 1-ethoxy-2-propanol acidogenesis was adopted as 8.26 times lower than the volumetric maximum rate of ethanol ($\nu_{max,\ EtOH}$). This factor was obtained as the reverse ratio of the Specific Methanogenic Activity (SMA) values of ethanol and 1-methoxy-2-propanol (Lafita et al. 2015).
- The half-saturation constants of acidogenesis of EtOH and Et2Pr and acetoclastic methanogenesis steps were assumed to have the same value: 50 mg L^{-3} (in COD units). This assumption was adopted on the basis of the typical ranges of the half-saturation constants for acidogenic reactions (20-500 mg L^{-1}), and methanogenic ones (30-300 mg L^{-1}) (Grady et al., 2011).

By using these assumptions, the initial six kinetic parameters of the anaerobic reactor model were reduced to two: the volumetric maximum rate of EtOH and acetic acid, $\nu_{max,\ EtOH}$ and $\nu_{max,\ acetic\ acid}$, respectively. The preliminary values of these parameters were obtained by minimizing the objective function of equation (7.8).

The estimated values of the initial parameters of the model are introduced in Table 7.11, along with the value of the objective function after the optimization.

Table 7.11. Preliminary kinetic parameters of the anaerobic reactor model.

	Kinetic constants	**Reaction**
$\nu_{max,\ EtOH}$, kg COD_{EtOH} m^{-3} h^{-1}	0.490	Acidogenesis EthOH
$K_{S,\ EtOH}$, g COD_{EtOH} m^{-3}	50	
$\nu_{max,\ Et2Pr}$, kg COD_{Et2Pr} m^{-3} h^{-1}	0.059	Acidogenesis Et2Pr
$K_{s,\ Et2Pr}$, g COD_{Et2Pr} m^{-3}	50	
$\nu_{max,\ acetic\ acid}$, m^3 CH_4 h^{-1} m^{-3} reactor	0.105	Methanogenesis
$K_{S,\ acetic\ acid}$, g COD_{CH4} m^{-3}	50	
Objective Funtion = 0.71		

The relative error for each selected day is shown in Table 7.12, along with the experimental and the predicted methane production and effluent VFA

concentration. The average relative error of methane production and the VFA concentration were 8.01 ± 8.18% and 12.95 ± 10.25%, being the maximum error found on day 10 when the relative errors were 21.40% and 24.51%, respectively.

Table 7.12. Experimental data used to obtain an initial estimation of the kinetic parameters of the model.

Day	CH_4 Production[a], $m^3\ h^{-1}$	CH_4 Production[b], $m^3\ h^{-1}$	CH_4 relative error, %	VFA[a], mg acetic acid L^{-1}	VFA[b], mg acetic acid L^{-1}	VFA relative error, %
10	0.50	0.60	21.40	73.7	55.6	24.51
30	0.81	0.83	1.85	109	118.5	8.75
42	1.02	1.05	3.16	315	330.3	4.86
46	1.02	1.12	10.26	671	514.1	23.38
52	1.14	1.18	3.35	640	660.7	3.23

[a]Experimental data. [b]Predicted values

Once the preliminary parameters of the model were fitted, a sensitivity analysis was performed for OLs of 1, 3 and 6 kg COD h^{-1} in order to cover the whole range of experimental loads, including those associated with overloading of the reactor. The effect on the VFA concentration of the liquid effluent of the reactor and the methane production was assessed. Results are shown in Figures 7.10 and 7.11 for the three tested OLs (1, 3 and 6 kg COD h^{-1}) and for the two evaluated parameters. The sensitivity analysis was completed by verifying the influence of changing the volumetric maximum uptake rate of Et2Pr (Figure 7.12).

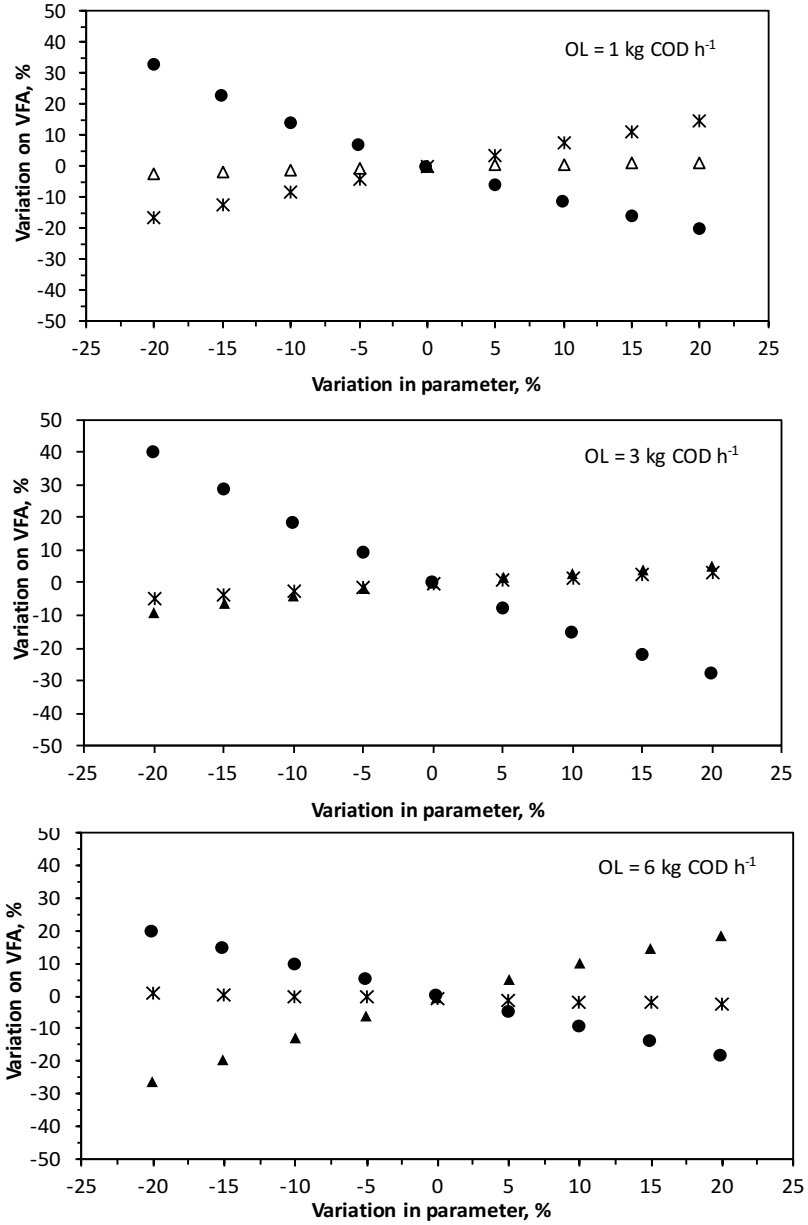

Figure 7.10. Sensitivity analysis of the initial fitted kinetic parameters. Influence on the VFA concentration of the liquid effluent of the anaerobic reactor. (•) acetoclastic methanogenesis $\nu_{max,\ acetic\ acid}$, (▲) uptake of ethanol $\nu_{max,\ EtOH}$ and (*) half-saturation constant K_S.

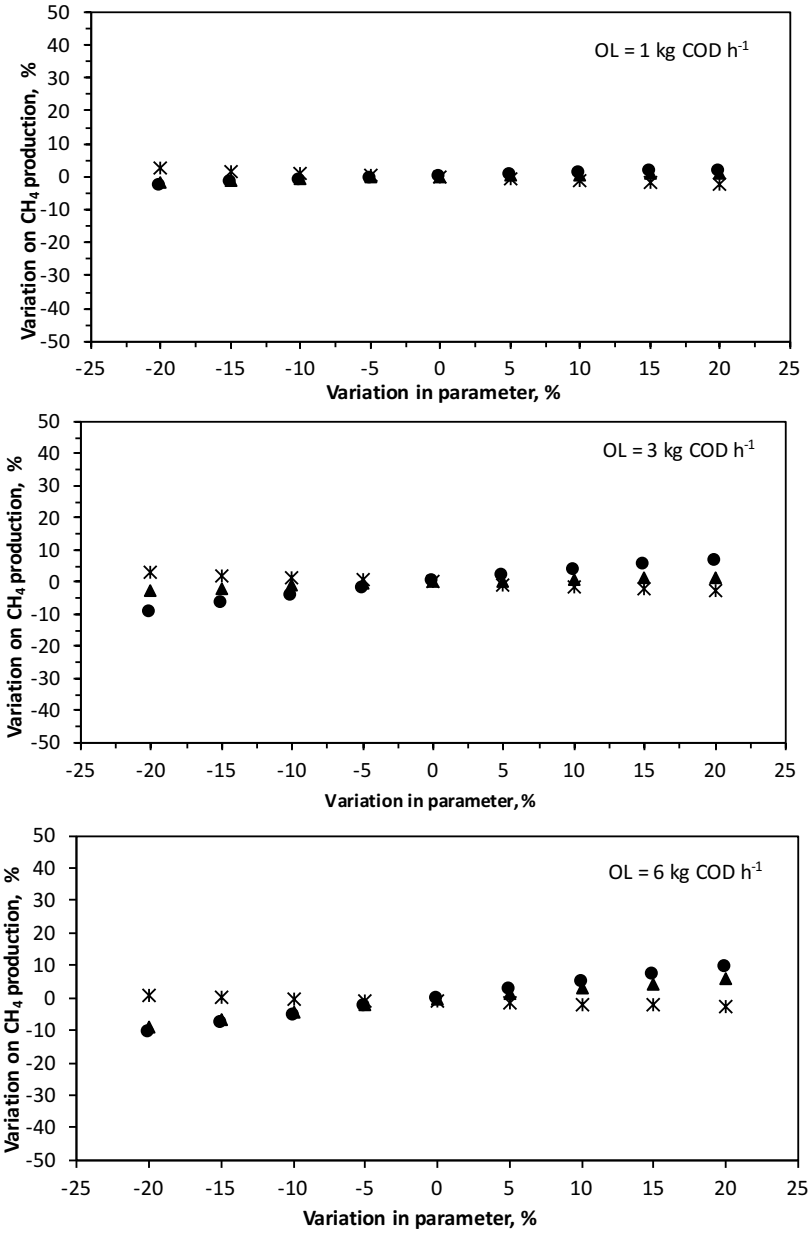

Figure 7.11. Sensitivity analysis of the initial fitted kinetic parameters. Influence on methane production of the anaerobic reactor. (•) acetoclastic methanogenesis $\nu_{max,\ acetic\ acid}$, (▲) uptake of ethanol $\nu_{max,\ EtOH}$ and (*) half-saturation constant K_S.

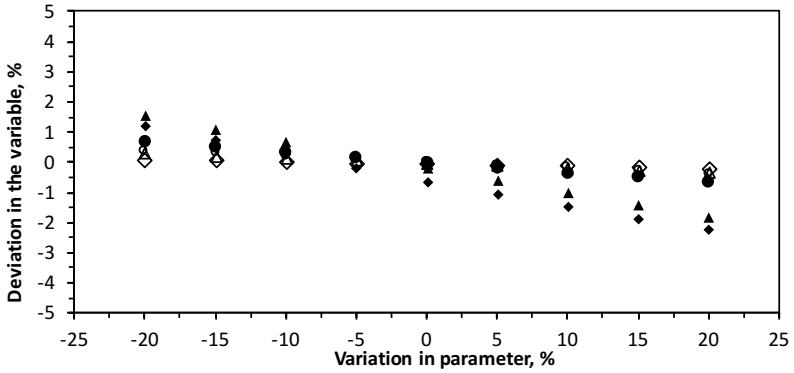

Figure 7.12. Sensitivity analysis of the initial fitted kinetic parameters. Influence of maximum uptake rate of 1-ethoxy-2-propanol on methane production and VFA concentration of the liquid effluent of the anaerobic reactor with OLs of 1, 3 and 6 kg COD h^{-1}. Influence on:(•) VFA concentration with OL 1 kg COD h^{-1}, (▲) VFA concentration with OL 3 kg COD h^{-1}, (♦) VFA concentration with OL 6 kg COD h^{-1}, (o) methane production with OL 1 kg COD h^{-1}, (Δ) methane production with OL 3 kg COD h^{-1} and (◊) methane production with 6 kg COD h^{-1}.

The results of the sensitivity analysis allow to corroborate the assumptions adopted regarding which kinetic parameters should be further refining in the calibration step. The parameters with the largest impact in the prediction of VFA concentration of the liquid effluent of the reactor and the methane production would be the maximum uptake rates of ethanol ($\nu_{max,\ EtOH}$) and acetogenic methanogenesis step ($\nu_{max,\ acetic\ acid}$). For example, when one of these parameters were changed by ±20%, the variations in the VFA concentration achieved up to 40% for an OL of 3 kg COD h^{-1}, whereas in the methane production achieved up to 10% for an OL of 6 kg COD h^{-1}. The half-saturation constant had impact in the VFA concentration only at loads of 1 kg COD h^{-1} (Figure 7.10), but the impact was negligible at higher loads, presenting variations lower than 5% for OLS of 3 and 6 kg COD h^{-1}. Therefore, it was decided that the assumption of a constant value of 50 g COD m^{-3} for all the kinetic reactions is a good approach to reproduce the experimental performance of the anaerobic process. Regarding the maximum uptake rate of 1-ethoxy-2-propanol, it did not have impact on any variable at any load (Figure 7.12), hence the assumption regarding to its value was also considered adequate for the scope of this modelation process. The results obtained in this sensitivity analysis are in contrast with the results of Tartakovsky et al. (2008), who found that the maximum uptake rates and the half saturation constants of acetate, propionate and butyrate/valerate were the largest impact parameters in the

validation of the ADM1 model for an UASB reactor treating synthetic wastewater composed by sucrose, butyric acid, yeast extract and ethanol. In this study, the half saturation constant was a non-sensitive parameter.

The calibration of the anaerobic reactor model was carried out by using the first 95 days of the experimental data, including: water flow rate, organic load, temperature, pH and alkalinity of the liquid influent, pH and VFA concentration of the liquid effluent of the anaerobic reactor, and the biogas production. The solvent composition of the inlet stream to the anaerobic reactor (VOCWAT-2 in Figure 7.2) was set to the values of composition of the exit stream obtained with the scrubber model (VOCWATER in Figure 7.1). The value of the two calibration parameters ($\nu_{max,\ EtOH}$ and $\nu_{max,\ acetic\ acid}$) were obtained by minimizing the objective function defined in equation (7.8) with the Matlab® algorithm fmincon, which finds the minimum of constrained nonlinear multivariable function. The optimization was restricted to positive values of the parameters. The initial values were summarized in Table 7.11 (0.49 kg COD m^{-3} reactor h^{-1} and 0.105 m^3 CH_4 m^{-3} reactor h^{-1}). The results of the optimization problem are shown in the Table 7.13, where the optimized calibration parameters appear in bold.

The experimental data and the predicted values by the model are shown in Figure 7.13 and Figure 7.14, for the methane production and the VFA concentration of the liquid effluent of the anaerobic reactor, respectively.

Table 7.13. Optimized kinetic parameters for the anaerobic reactor model.

	Initial parameters	**Optimized parameters**	**Reaction**
$\nu_{max,\ EtOH}$, kg COD m^{-3} reactor h^{-1}	0.490	**0.520**	Acidogenesis EthOH
$K_{S,\ EtOH}$, g COD m^{-3}	50	50	
$\nu_{max,\ Et2Pr}$, kg COD m^{-3} reactor h^{-1}	0.060	0.072	Acidogenesis Et2Pr
$K_{S,\ Et2Pr}$, g COD m^{-3}	50	50	
$\nu_{max\ acetic\ acid}$, m^3 CH_4 h^{-1} m^{-3} reactor	0.105	**0.060**	Methanogenesis step
$K_{S\ acetic\ acid}$, g COD m^{-3}	50	50	

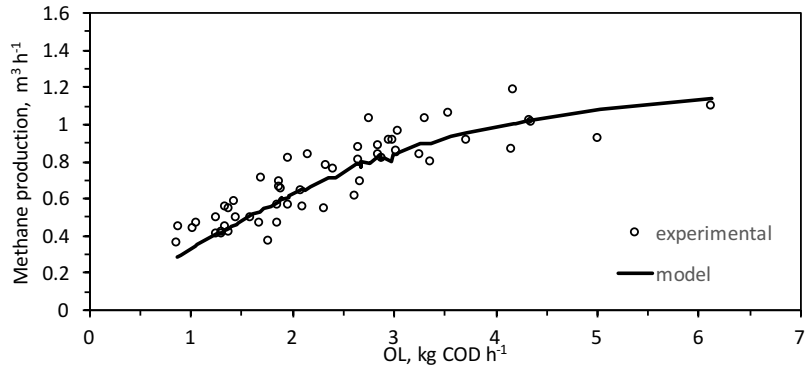

Figure 7.13. Methane production predicted by the anaerobic reactor model in the calibration step.

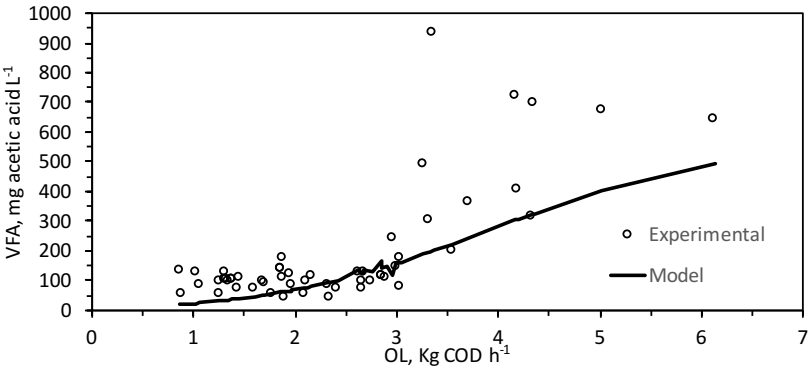

Figure 7.14. VFA liquid effluent concentration predicted by the anaerobic reactor model in the calibration step.

The model was able to predict accurately the methane production, taking into account that the data come from an industrial installation working under high variability accordingly to the VOC emission of the industrial site. Moreover, the chemical parameters of the water measured on-site corresponded to instantaneous analysis, which were assumed to be average representative of a particular day, increasing the source of error in the model.

The average relative error found in the methane production was 13 $\pm$ 10%, being the maximum error 50%, this error occurred on day 69 when the experimental methane production was 0.36 $m^3 h^{-1}$ and the predicted value by the model was 0.56 $m^3 h^{-1}$. If this anomaly is discarded, the maximum error decreased to 32%. In spite of the error, the model showed the same trend as the experimental data.

Regarding the VFA concentration of the liquid effluent of the anaerobic reactor, it seems that the model is able to predict the maximum recommended OL from which acidification due to overloading was empirically detected (approx. 3 kg COD h^{-1}). The model results showed that loads higher than 3 kg COD h^{-1} will produce an accumulation of VFA in the liquid effluent of the anaerobic reactor. The model can simulate the trend of acidification due to overloading (increases from 150 mg acetic acid L^{-1} at OL of 3 kg COD h^{-1} to 450 mg acetic acid L^{-1} at OL of 6 kg COD h^{-1}), but it cannot predict accurately the accumulation of the VFA in the system (closed-recirculation water loop) because of intra days accumulation. The model was developed to solve the steady state daily conditions, not the intra-day accumulation. Thus, it would be necessary a dynamic model in order to simulate this transient behaviour.

The Figure 7.15 shows the pH and the methane content of the biogas predicted by the model versus the daily average OL, along with the experimental values. The Figure shows that the pH predicted by the model is slightly lower than the experimental one (average relative error 2 $\pm$ 2%). The reason could be the defined electrolyte chemistry in the system, so that other acid/base species with impact in the anaerobic digestion such as propionate and butyrate should be included in future version of the process simulation model to better prediction of the pH. Other authors have also observed greater deviations in the prediction of pH in the modeling of anaerobic process (Chen et al., 2009). In spite of this difference, the model is able to well predict the methane content of the biogas.

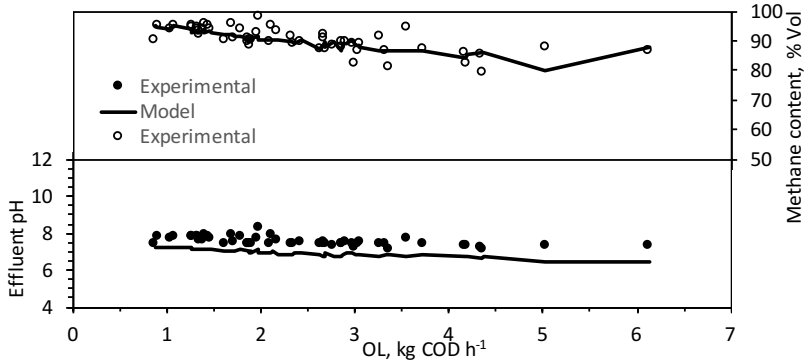

Figure 7.15. pH at the liquid effluent of the anaerobic reactor and methane content in biogas predicted by the model in the calibration step.

Once the model was calibrated with the experimental data of the stage I, the validation was done with the data of stage II, IV and V. The validation is explained in the next section.

7.3.3 Validation of the anaerobic reactor model

The validation was done with the data from days between 96 and 484, by using only the days when the chemical parameters of the liquid effluent of the anaerobic reactor were measured (n=211). The required experimental data were: water flow rate, organic load, temperature, pH and alkalinity of the liquid influent, pH and VFA concentration of the liquid effluent of the anaerobic reactor, and the biogas production. The load fed to the anaerobic reactor model was the experimental one and its solvent composition was set to the values of composition of the water outlet stream of the scrubber model.

The Figure 7.16 shows the predicted and the experimental methane production against the organic load fed to the anaerobic reactor. The average relative errors in the validation of the model for each stage are shown in Table 7.14. The average relative error was 23 $\pm$ 20%, with higher errors in stage IV and V due to the higher discrepancy in the scrubber model predictions for these stages. From these results, it can be concluded that the model is able to predict the methane production, considering the scope of the model that was to develop a design tool for industrial scale-up.

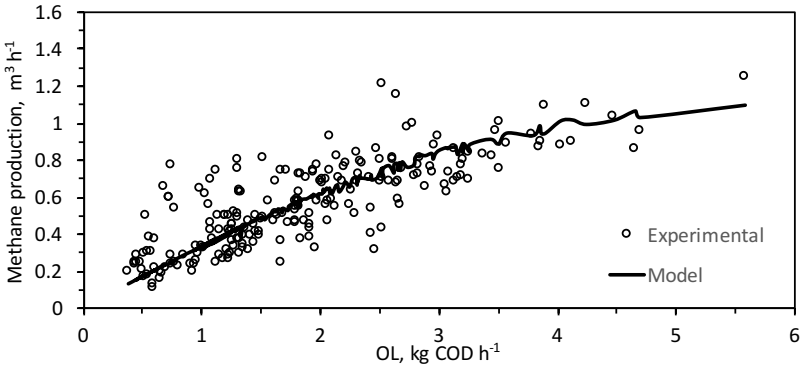

Figure 7.16. Methane production predicted by the anaerobic reactor model in the validation step.

Table 7.14. Relative error in the methane production of the anaerobic reactor model.

	Average relative error, %
Stage II	14.53 ± 13.20
Stage IV	27.88 ± 22.63
Stage V	22.63 ± 19.69

The predicted VFA concentration of the liquid effluent of the anaerobic reactor is plotted against the organic load fed to the anaerobic reactor in Figure 7.17, along with the experimental values. The model can simulate the overproduction of VFA when reactor is overloaded (OL higher than 3 kg COD h^{-1}) but it cannot simulate the accumulation of the VFA in the system due to the steady-state nature of the model.

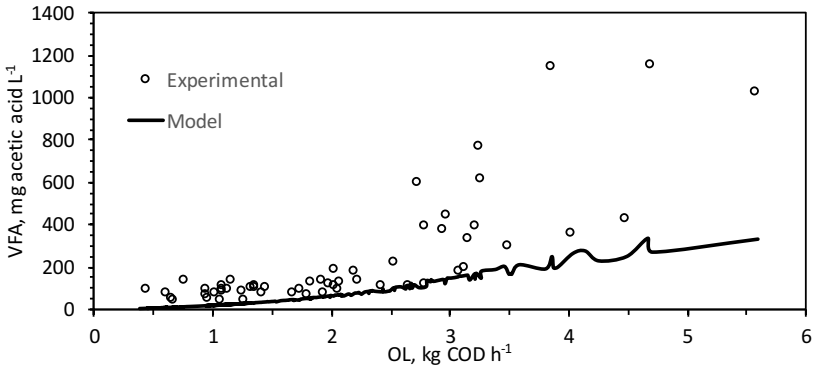

Figure 7.17. VFA liquid effluent concentration predicted by anaerobic reactor model in the validation step.

The pH of the liquid effluent of the anaerobic reactor and the methane content of the biogas are depicted against the organic load in Figure 7.18. The average error found in the methane content of the biogas was 5 ± 4%, being the maximum error 16% on day 412 with an organic load of 3.26 kg COD h^{-1}. Regarding the pH, the value predicted by the model is slightly lower than the actual one, as it was obtained during calibration.

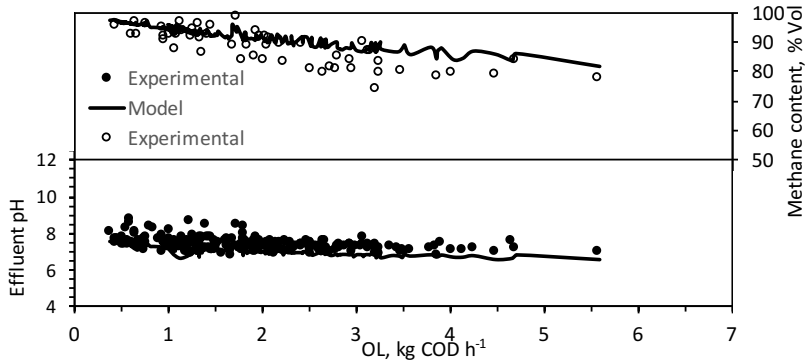

Figure 7.18. pH of the liquid effluent of the reactor and methane content in the biogas predicted by the anaerobic reactor model in the validation step.

7.4 Anaerobic bioscrubber model: Linking scrubber and anaerobic reactor models

7.4.1 Experimental data

Both models developed in this study have been linked and checked with the whole set of data, except the data of stage III when the spray column was tested. Therefore, the validity of the anaerobic bioscrubber model was checked with 291 data points. The model was applied with the previous calibrated parameters of both models: number of equilibrium stages in the scrubber for packing A and packing B and the Monod kinetic parameters for the anaerobic process. By doing this, the only set of experimental data corresponds to the inlet air emission along with the experimental conditions (temperature, liquid flow rate, alkalinity and pH) of the influent liquid to the anaerobic reactor. So, in this case the feasibility of the model to be used as a design tool will be demonstrated.

7.4.2 Connecting scrubber and anaerobic reactor models

Both models are connected via the estimated OL to the anaerobic reactor coming from the scrubber model predictions. The Figure 7.19 shows the experimental and predicted OLs against the operational time. The scrubber model is able to predict the organic load fed to the anaerobic reactor, being the average relative error for the whole experimental period of 5 $\pm$ 5%. Results for each stage are summarized in Table 7.15. The highest relative error was obtained in stage V

(average value 6.90 ± 6.49% and maximum of 31.78% on day 405), probably because of self-assembly of the packing and the biomass accumulation onto the packing surface, as already motioned in chapter 6.

Table 7.15. Relative error in the OL predicted by the scrubber model.

	Average relative error, %	**Maximum relative error, %**
Stage I	2.81 ± 1.97	7.75
Stage II	4.86 ± 3.24	16.17
Stage IV	5.28 ± 3.93	16.49
Stage V	6.90 ± 6.49	31.78

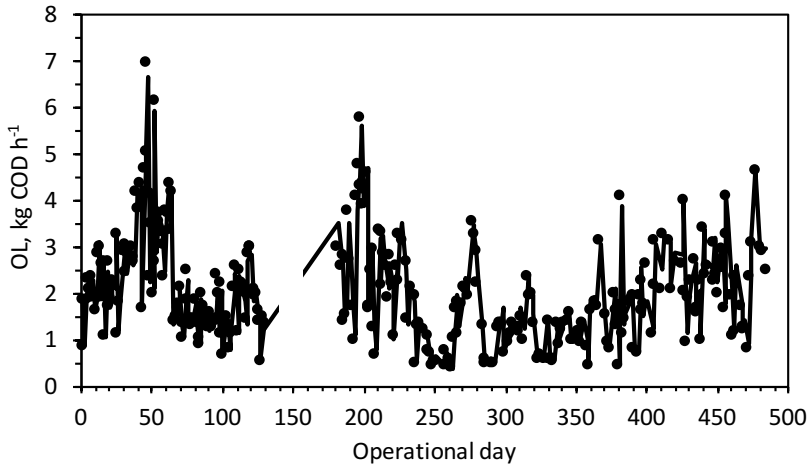

Figure 7.19. Comparison between experimental and predicted organic load by the scrubber model.

The predicted OL by the scrubber model was used as the input data for the anaerobic model instead of the experimental values. The Figure 7.20 shows the methane production against the organic load. The average relative error between the experimental and the predicted methane production is shown in Table 7.16, along with the maximum errors for each stage. As can be observed, the relative errors were nearly identical to that obtained by using experimental data.

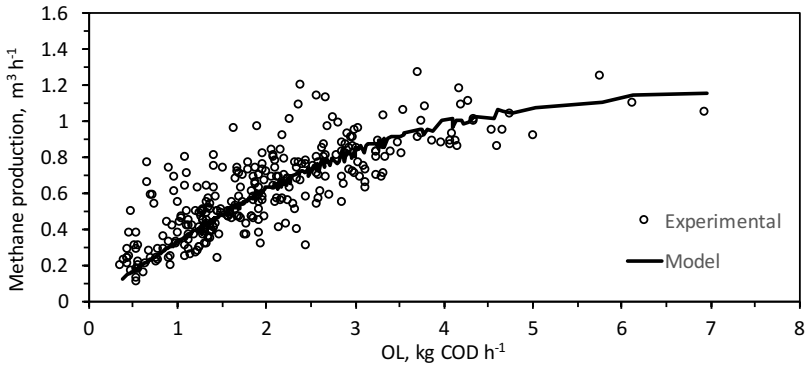

Figure 7.20. Methane production predicted by linking both models.

Table 7.16. Relative error in the methane production of the anaerobic bioscrubber model.

	Average relative error, %
Stage I	14.35 ± 11.26
Stage II	14.25 ± 12.95
Stage IV	27.36 ± 21.79
Stage V	23.29 ± 20.89

The Figure 7.21 shows the VFA concentration of the liquid effluent of the anaerobic reactor. Model results showed similar tendency than in Figure 7.17, slightly higher VFA concentration simulated at high OLs. The performance of the anaerobic reactor, in terms of removal of soluble organic matter for OLs lower than 3 kg COD $h^{-1}$and the effluent pH of the anaerobic reactor, was predicted with similar precision.

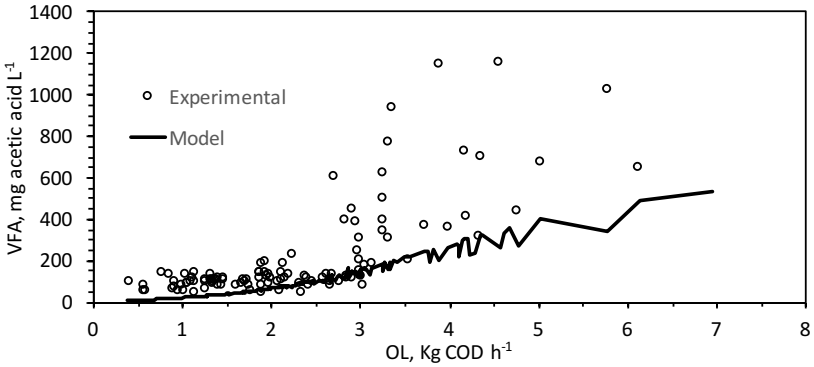

Figure 7.21. Experimental and predicted VFA concentrations in the effluent of the anaerobic reactor with the anaerobic bioscrubber.

The process simulation model developed in this study demonstrated a great potential to predict and simulate the performance of the anaerobic bioscrubber technology. In addition, the connection between Matlab® and Aspen Plus® provided the possibility of running a huge number of simulation events in short period of time. This possibility has been used to create a design tool for sizing the anaerobic bioscrubber.

7.5 Design tool of anaerobic bioscrubber technology

The case of study is a facility whose average waste gas VOC emission is 1 126 mg-C Nm^{-3} and its composition is 65.5% EtOH, 25.4% and 9.1% of Et2Pr. The result are 3D figures that were created to be used as tool for design purpose. The diagrams shown in this section were created by simulating scrubbers of 2,4 8 and 10 m of height, F factor of 0.5, 1, 1.5, 2 and 2.5 m s^{-1} $(kg\ m^{-3})^{0.5}$ and liquid velocities of 10.2, 15.3, 20.4, and 25.5 m h^{-1}.

The Figure 7.22 shows the relationship between the predicted removal efficiency of the scrubber, the gas load factor, the height of the packing material and the superficial velocity of the scrubbing liquid in a 3D mesh. The figure shows the expected performance, because for a specific height, if the water flow rate increases the RE_{VOC} increases.

By using this Figure, it is possible to design the scrubber unit. The airflow, the VOC concentration and the desired removal efficiency are known parameters; hence two parameters of: the scrubber diameter, water flow rate or height of the scrubber, should be defined to obtain the third one. For example, the scrubber diameter can be defined, obtaining the F factor, the liquid velocity is established when the water flow rate is selected. The height of the packing material is estimated by using the Figure 7.22 in order to achieve the desired removal efficiency.

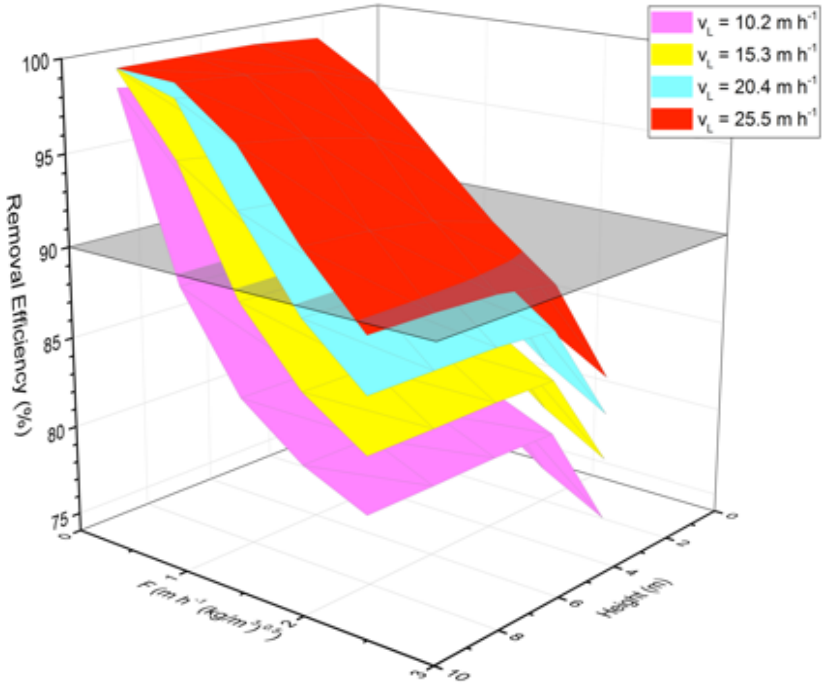

Figure 7.22. Example of design for a certain VOC waste gas emission.

Once the water flow rate has been established, the model permits to obtain the different pictures when different height of the scrubber and the different waste gas composition are defined. The Figure 7.23 shows the removal efficiency against the F factor and the height of the scrubber at different ethanol content in the inlet waste gas ranged between 62% and 69%, when the liquid velocity is 15.3 m h^{-1}. The figure shows how the removal efficiency increases with the concentration of ethanol (the most soluble solvent) for a specific airflow rate and a height.

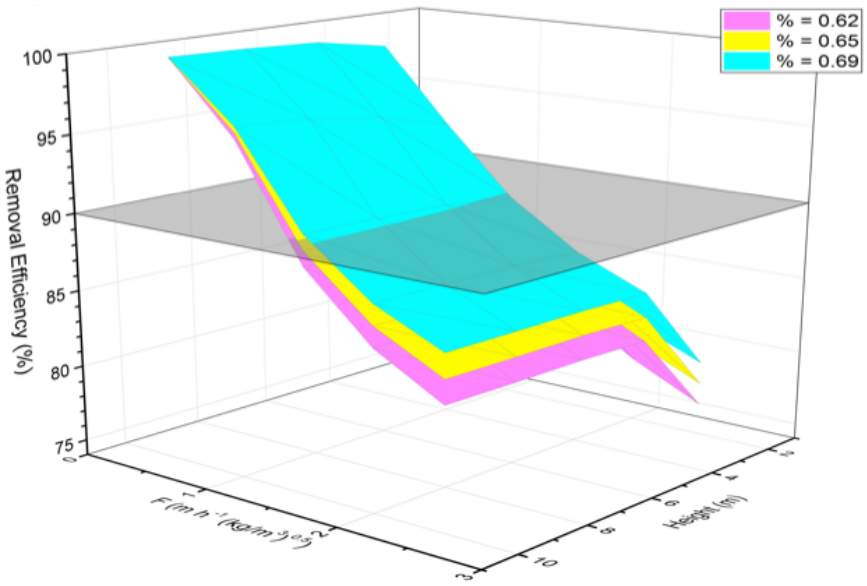

Figure 7.23. Influence of the ethanol composition in the design of the scrubber.

The scrubber model allows to obtain the range of organic the load fed to the anaerobic reactor depending on the VOC waste gas concentration, RE_{VOC}, the height of the packed bed and the airflow velocity. As example, this relationship is shown in Figure 7.24. for three inlet VOC concentrations of 656, 1 126 and 1 596 mg-C Nm^{-3} and a liquid velocity of 15.3 m h^{-1}. As can be observed, the OL increases with the increase of the airflow rate and the VOC waste gas concentration.

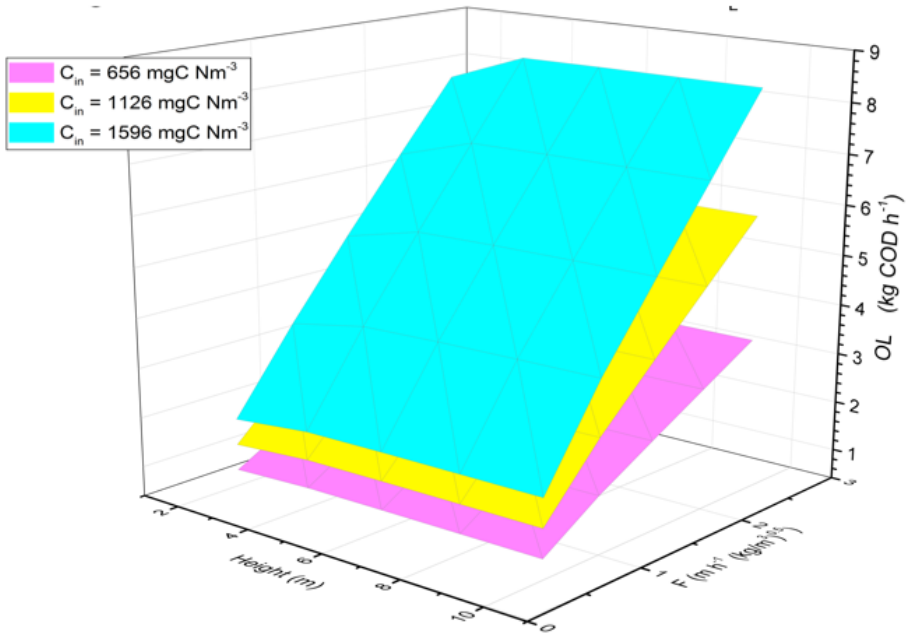

Figure 7.24. Influence of the inlet concentration with a liquid velocity of 15.3 m h^{-1} on OL.

Similar graphs can be plotted for the anaerobic reactor. The Figure 7.25 shows the relationship between the HRT, the OLR fed and the VFA effluent liquid concentration of the anaerobic reactor. This Figure could be used for design purpose as follow. The organic load can be obtained from the mass balance of the scrubber by using equation (5.2). Afterwards, from Figure 7.25 and defining a maximum value of VFA concentration at the effluent stream (here 300 mg L^{-1}, grey plane in Figure 7.25) and using the water flow rate derived from Figure 7.22, the reactor volume can be obtained from resulted pairs of OLR and HRT. The flow rate of the scrubbing liquid (the anaerobic reactor operates in water-loop) would be changed to modify the HRT, thus the OLR. This changed on the water flow rate of the scrubbing liquid will change the RE_{VOC}; hence an iteration process between Figure 7.22 and Figure 7.25, should be performed to keep RE_{VOC}. Once the iteration process has been finalized, the biogas rate production can be obtained by using Figure 7.26, since the OLR and HRT are fixed by Figure 7.25.

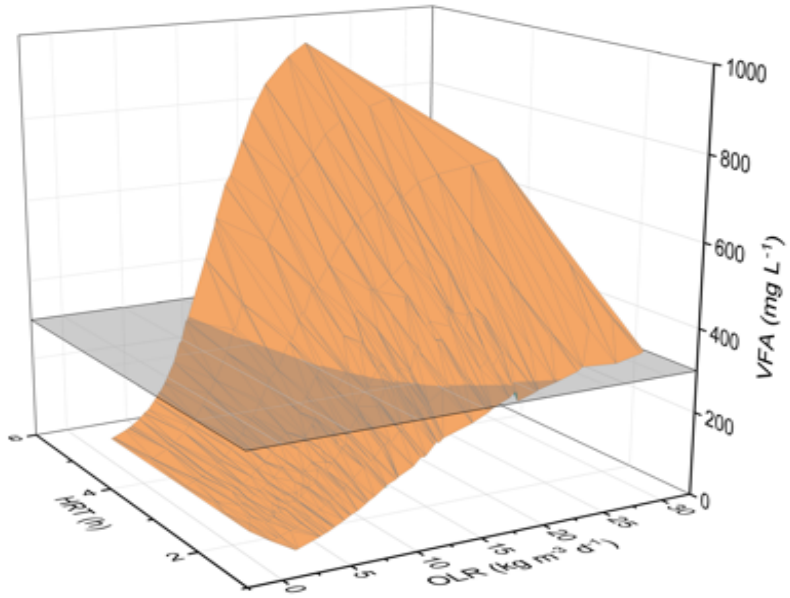

Figure 7.25. Anaerobic reactor: 3D mesh for the VFA concentration against the OLR and the HRT.

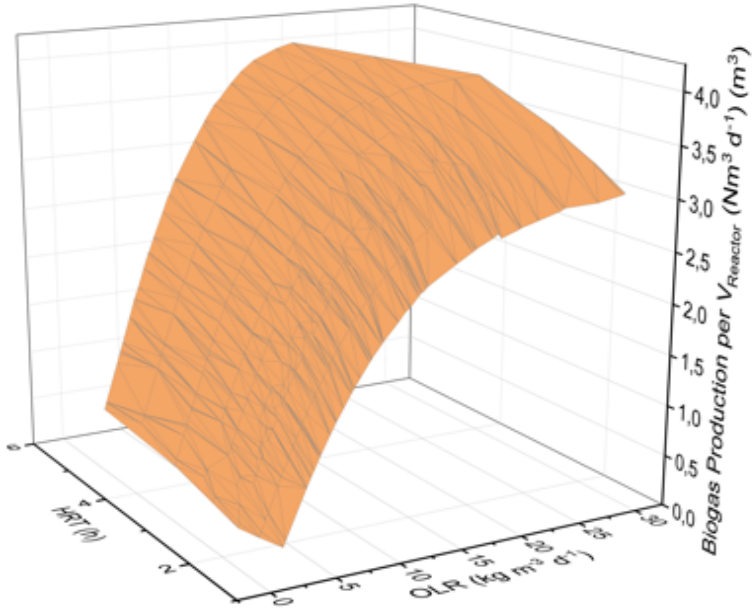

Figure 7.26. Anaerobic reactor: 3D mesh for the biogas production against the OLR and the HRT.

This section has exposed a case study of the developed model that can be used as design tool. The execution time for obtaining this kind of graph is really short and the information available in them are really useful for the design and for the operation of the anaerobic bioscrubber. The design tool allows determining the diameter and the height of the scrubber, the flow rate of the scrubbing liquid and the anaerobic reactor volume as the main parameters of the process.

7.6 Conclusions

The results discussed in this chapter demonstrated that the developed model is able to adequately predict the performance of the anaerobic bioscrubber technology. The scrubber unit was modelled using a constant height of theoretical plate for two commercial packing materials. A novelty approach to model the anaerobic reactor was implemented by using a series of stoichiometric and kinetic reactors with the aim to minimize the number of kinetic reactions which could simulate the process performance. The connection of Matlab® and Aspen Plus® allowed to use the strength of both software: the availability of thermodynamic models in the simulator plus the optimization tools of the mathematical tool. Moreover, the linked between both software allows running a huge number of simulation events, saving time processing.

The scrubber model was able to predict the outlet VOC concentration with an average relative error below 10% for the whole experimental period (more than a year), which also allowed the simulation of the organic load fed to the anaerobic reactor with a relative error below 5%. The anaerobic reactor model proposed herein simulated the methane production with a relative error of 15% for the stages I and II and up to 30% for the stages IV and V. This discrepancy could be due to the steady state nature of the model, which cannot simulate the accumulation of solvents and VFA in the system, and to the nature of the data, which comes from an industrial experimentation, treating on-site variable emissions in concentration and composition. Any case, the model is able to predict the general performance of the anaerobic reactor, in terms of removal of soluble organic matter and methane production, and reproduces the recommended maximum organic load for this process. The selected thermodynamic model of Aspen simulator predicted the methane content in the biogas and the predicted pH in the effluent of the anaerobic reactor was slightly lower than the experimental ones. The presence of other ions

and acid/bases species in the water moreover than carbonate alkalinity and acetic acid could be included to improve this estimation.

It has been shown the capability of the model to be used as predicting tool and, furthermore, as an assisting tool in design, resulting in time and money saving for practitioners. The approach proposed here can be expanded to other solvents of industrial interest (e.g. isopropanol) or to other bioprocesses that need to be linked with unit operations.

8 CONCLUSIONS

The general objective of this work was to optimize the performance and to demonstrate the stability of the anaerobic bioscrubber, a new technology that recycles the VOC air emissions from the packaging sector to bioenergy. The main conclusions drawn from the obtained results of this study are summarized in this section

The first part of the study was the **commissioning and start-up of the industrial prototype.** The industrial protocols to be used in the commissioning, the start-up and the operation and the control rules of the future installations of anaerobic bioscrubber were developed. Additionally, the anaerobic reactor was redesigned during commissioning period. The results obtained during the commissioning step showed the necessary retrofitting of the anaerobic reactor (to reduce the dissolved methane in the effluent and to improve the recovery of methane in the biogas). These objectives were achieved after making the proposed changes in the reactor design.

Granular sludge from high-rate reactor treating brewery wastewaters was demonstrated to be a suitable source of biomass for the start-up of the anaerobic reactor. The use of an average organic load rate of 3.2 kg COD m^{-3} d^{-1} –value in the range proposed by Colussi et al. (2009)- during the start-up enabled to achieve removal efficiencies of organic substrate higher than 80% in 15 days. In addition, during this period the pH and the VFA concentration of the water effluent of the reactor kept over 7.0 and below 200 mg acetic acid L^{-1}, respectively. This successfully start-up of the anaerobic reactor under intermittent and variable load is the first example found in the literature.

The second part was the study of the **process performance of the prototype**, the results obtained in this stage demonstrated the stability of the anaerobic bioscrubber for the abatement of VOC air emissions. The cross-flow packing material was found the best scrubber configuration for the industrial application. The VOC removal efficiency achieved with this packing ranged between 83% and 93% for liquid to air volumetric ratios between $3.5 \cdot 10^{-3}$ and $9.1 \cdot 10^{-3}$. The long-term operation of the prototype gave some insight on the importance of implementing a pressure drop control protocol in the scrubber. The developed pressure control protocol maintained the pressure drop through the scrubber below the recommended limit during 218 days.

A stable conversion of alcohols, esters and glycol ethers to biogas, with an average COD removal efficiency of 93 ± 5% was observed in the anaerobic reactor.

A limit value of 24 Kg COD m^{-3} bed d^{-1} for the organic loading rate was found to maintain stable performance of the anaerobic reactor, being this value the selected as a design criteria of future industrial installations. The VFA concentration at the effluent was below 300 mg acetic acid L^{-1} when the OLR was below this limit, while higher concentrations were reached when higher loads were fed to the anaerobic reactor. This accumulation indicates that methanogens cannot sufficiently and rapidly degrade the VFA. This situation could derive in the destabilization of the reactor if keep over time.

The long-term operation of the industrial prototype enabled to evaluate the industrial application of the pH control rules and the control rules for nutrients dosage. These rules demonstrated their robustness, since the pH was over 6.83 and it was not observed an accumulation of ions in the system that worked in water-closed recirculation, with daily water renewal lower than 10%. The chemical conditions established in the system allowed to obtain a biogas stream whose methane content was 88 ± 6% Vol. These rules have been adopted to be used in the future industrial installations to guarantee their long-term operation.

The third part of the thesis consisted in the development of a **process simulation model** of the anaerobic bioscrubber process in the commercial simulator Aspen Plus®. This implementation in the commercial simulator was carried out by creating two models in steady-state for the two units: scrubber and anaerobic reactor. The selected thermodynamic package for both models was the electrolyte NRTL (ELECNRTL), since it is appropriate for the application in systems with aqueous solutions with electrolyte. The scrubber column was modelled by using the rigorous distillation method Radfrac and the anaerobic has been developed by using several Aspen Plus® reactor blocks connected in series. This approach to implement the anaerobic reactor in Aspen Plus® can be expanded to other solvents and to other bioprocess in order to integrate anaerobic systems with other unit operations. The model implemented in Aspen Plus® has been linked to the software Matlab®. This connection allowed the transference of data between both software and the use of Matlab® toolboxes for the model calibration and validation.

The calibration of the scrubber was performed by fitting the experimental concentration and the model predictions of each solvent at the outlet air stream for a set of experimental data for each structured packing material (cross-flow and vertical flow packing material). The calibration procedure resulted in values of the number of equilibrium stages per meter within 0.90-1.10 and 0.64-0.79 for cross-flow and vertical flow packing material, respectively. As similar values were obtained per packing material, it was decided to use the average value of the

number of equilibrium stages per each packing material: 0.96 ± 0.08 m^{-1} and 0.74 ± 0.06 m^{-1} for cross-flow and vertical flow packing material, respectively. The validation of the scrubber model was carried out by using the experimental data obtained from the scrubber of the prototype where the two structured packing materials were used. The validation step stated that the scrubber model accurately predicted the experimental results, with an average relative error below 10%.

The anaerobic reactor model was calibrated in two steps. Firstly, the kinetic parameters from Monod-type kinetic expressions were preliminary fitted by using a set of experimental data, which covered a wide range of inlet organic loading rate, from the first 95 days of operation of the anaerobic reactor. A sensitivity analysis of the adjusted parameters was performed by varying their values up to ±20% to discern their impact on the predicted methane production and VFA concentrations. The results of this analysis stated that the most sensitive parameters were the volumetric maximum growth rate of ethanol and acetic acid up-take. Therefore, these parameters were chosen as the parameters to determine by model calibration using the first 95 days of experimental data obtained in the industrial prototype. After obtaining the calibration parameters, the validation of the model was performed. The validation of the anaerobic reactor model was conducted by using the experimental data from days 96 to 484. The anaerobic reactor model simulated the methane production with a relative error of 23 ± 20%. This discrepancy is due to steady state nature, since it could not simulate the accumulation of the VFA in the system due to intra days accumulation. In spite of this fact, the model of the anaerobic reactor accurately predicted the experimental performance, since it was able to predict the maximum recommended OLR obtained in the performance study of the industrial prototype. Finally, the selected thermodynamical model was able to predict the methane content of the biogas stream with an average error of 5 ± 4%. However, the predicted pH was slightly lower than the experimental one. The deviations observed in the pH could be associated that only acetic acid and carbonate alkalinity were defined in the electrolyte chemistry in the system.

The process simulation model has shown its potential to be used as a tool for design the anaerobic bioscrubber technology. The connection of Aspen Plus® and Matlab® permitted to obtain 3D diagrams that can be used for design purpose. For the scrubber design, 3D mesh that related the predicted removal efficiency of the scrubber with the gas load factor, the height of packing material and the superficial liquid velocity for a determinate VOC gas emission can be obtained. For the anaerobic reactor design, 3D diagrams that correlates the VFA effluent

concentration with the HRT and the OLR of the anaerobic reactor can be plotted. This developed tool can be also used in a wide range of practical applications such as: (i) the study of the operational parameters affecting the performance of the system and obtaining the response of the system to their changes; (ii) and the optimization of the system. However, the results obtained in this work has showed some limitations related to the simulation of transient behavior and pH predictions. Therefore, the Aspen Plus® model can be improved in future with the extension of more components in the electrolyte chemistry and its conversion to a dynamic simulation, allowing to reduce the slightly error in pH prediction and to study the transient response and stability of the system to perturbations in the operational parameters.

9 NOMENCLATURE

Acronyms

ADM1 Anaerobic Digestion Model 1

AF Anaerobic Filter

BAT Best Available Techniques

BTF Biotrickling filter

COD Chemical Oxygen Demand

EA ethyl acetate

EGSB Expanded Granular Sludge Bed

EPS extra polymeric substances

EtOH Ethanol

Et2Pr Ethoxy-2-propanol

FB Fluidized Bed

FID Flame Ionization Detector

GLS Gas Liquid Solid Separator

HETP Height Equivalent to Theoretical Plate

HRT Hydraulic Residence Time

HTU Height of Transfer Unit

IBC Intermediate Bulk Container

IC Internal Circulation

LHHW Langmuir-Hinshelwood Hougen-Watson

N Number of Theoretical Stages

NMVOC Non-Methanics Volatile Organic Compounds

NTU Number of Transfer Unit

PLC Programmable Logic Controller

OL Organic Load

OLR Organic Loading Rate

RE Removal Efficiency

RE_{COD} Removal Efficiency of Chemical Oxygen Demand

RE_{VOC} Removal efficiency of Volatile Organic Compound

RTU Remote Terminal Unit

SRT Sludge Retention Time

TS Total Solids

UASB Upflow Anaerobic Sludge Blanket

VFA Volatile Fatty Acids

VOC Volatile Organic Compound

VSS Volatile Suspended Solids

WHO World Health Organization

Variables

ACUM intra-week accumulated solvents in water (kg COD $week^{-1}$)

$C_{A,L}$ Concentration of component A in liquid phase (mol L^{-1})

$C_{A,g}$ Concentration of component A in liquid phase (mol L^{-1})

C_{g,CH_4} is the methane concentration in the gas phase at the outlet of the stripper (mg-C Nm^{-3})

$Cg_{VOC,in}$ VOC concentration at air inlet of the scrubber (mg-C Nm^{-3})

$Cg_{VOC,out}$ VOC concentration at air outof the scrubber (mg-C Nm^{-3})

C_{L,CH_4} concentration of methane in the water effluent of the reactor (mg CH_4 L^{-1})

D inner diameter of the pipe (m)

$E_{i,j}^{MV}$ Murphree vapor efficiency for the component i on stage j (dimensionless)

F_{CH_4} is the conversion factor from mg-C to mg-CH_4 (mg-CH_4 mg^{-1}-C)

F_{COD} conversion factor from mg-C to COD (g COD g^{-1}-C)

F_j Feed stream entering in stage j (m^3 h^{-1})

F_P packing factor, characteristic of the size and type of packing (m^{-1})

H height of packed bed (m)

H_{cc} Henry constant (gas concentration / liquid concentration)

H_{cp} Henry constant (M atm^{-1})

k_G gas phase mass transfer coefficient on partial pressures (moles m^{-2} s^{-1} Pa^{-1})

k_L individual liquid mass transfer coefficient based on concentration (m s^{-1})

k_x individual liquid mass transfer coefficient based on mole fractions (mol s^{-1} m^{-2})

k_y gas mass transfer coefficient based on mole fractions (mol s^{-1} m^{-2})

Ks half-saturation constant (mg COD L^{-1})

L_j flow rate of liquid leaving stage j (m^3 h^{-1})

L_W^* liquid mass flow rate per unit area column cross-sectional area (kg m^{-2} s^{-1})

V_W^* gas mass flow rate per unit area column cross-sectional area (kg m^{-2} s^{-1})

MW_{CH_4} molecular weight of methane (g mol^{-1})

MW_C molecular weight of carbon (g mol^{-1})

N number of theoretical stages (dimensionless)

N_A mass transfer rate (mol s^{-1} m^{-2})

OL_W cumulative organic load applied to the EGSB during a week (kg COD $week^{-1}$)

P_{AG} partial pressure of A in the bulk of gas phase (Pa)

P_{Ai} partial pressure of A at the interface the gas phase (Pa)

P_{CO_2} is the partial pressure of carbon dioxide in the gas space (atm)

Purge total amount of purged solvents during a week (kg COD $week^{-1}$)

Q influent flow rate of the reactor (m^3 h^{-1})

$Q_{air,SC}$ Airflow through the scrubber (m^3 h^{-1})

$Q_{air,ST}$ Airflow through the stripper (m^3 h^{-1})

Q_{evap} daily water volume lost as evaporation (m^3 d^{-1})

$Q_{fresh\ water}$ volume of fresh water added to the system (m^3 d^{-1})

Q_L is the water flow rate through the stripper (m^3 h^{-1})

Q_{Nut} flow rate of the nutrient solution (L day^{-1})

Q_{purge} daily water volume purged (m^3 d^{-1})

RE_{COD} Removal Efficiency of Chemical Oxygen Demand (%)

RE_{VOC} Removal efficiency of Volatile Organic Compound (%)

S concentration of the limiting substrate for growth (mg COD L^{-1})

S_O substrate concentration at the liquid inlet of the anaerobic reactor (mg COD L^{-1})

S_{BALK} Bicarbonate alkalinity concentration (mg $CaCO_3$ L^{-1})

S_{TALK} Total alkalinity concentration (mg $CaCO_3$ L^{-1})

S_{VFA} Volatile fatty acids concentration (mg acetic acid L^{-1})

V liquid velocity assuming full pipe (m s^{-1})

V_j flow rate of gas leaving stage j (m^3 h^{-1})

V_L total liquid volume of the reactor (m^3)

V_m^* gas mass flow rate per unit column cross- sectional area (kg m^{-2} s^{-1})

V_N effective liquid volume of the reactor (m^3)

V_W^* gas mass flow rate per unit area column cross-sectional area (kg m^{-2} s^{-1})

Y bacterial growth (VSS g^{-1}-$COD_{removed}$)

X biomass concentration (kg m^{-3})

x_{Ai} mole fraction of A in the liquid phase at the interface of the liquid phase (dimensionless)

x_{AL} mole fraction of A in the liquid phase in the bulk of the liquid phase (dimensionless)

$x_{i,j}$ molar composition of component i in liquid phase leaving stage j (dimensionless)

y_{AG} mole fraction of A in the bulk of gas phase (dimensionless)

y_{Ai} mole fraction of A at the interface the gas phase (dimensionless)

$y_{i,j}$ molar composition of component i in gas phase leaving stage j (dimensionless)

[Z] concentration of the element Z in the nutrient solutions (g L^{-1})

$[Z]_{methanogenic\ bacteria}$ concentration of element Z methane bacteria (mg kg^{-1})

$[Z]_{residual}$ residual concentration of element Z at liquid phase of the system (g L^{-1})

$[Z]_{tap}$ concentration of element Z in the tap water. (g L^{-1})

zj molar composition of component i in in feed stream entering to stage j (dimensionless)

δ molar extent of reaction

μ specific growth rate of the microorganism (kg m^{-3} h^{-1})

μ_L is the liquid viscosity (Ns·m^{-2})

μ_{max} specific growth rate of the microorganismρ_L are liquid density (kg m^{-3})

ρ_V are vapor density (kg m^{-3})

10 REFERENCES

Aidan, A., Alnaizy, R., Nenov, V. and Abdelrahman, O. (2011). Process design of waste gas treatment from Emirates Gold Refinery. Clean Technology and Environmental Policy, 13 (3): 447-457.

Alves, M., Cavaleiro, A.J., Ferreira, E.C., Amaral, A.L., Mota, M., Da Motta, M., Vivier, H. and Pons, M.N. (2000). Characterization by image analysis of anaerobic sludge under shock conditions. Water Science and Technology, 41 (12): 207-214.

Alphenaar, P.A., Pérez, M.C. and Lettinga, G. (1993). The influence of substrate transport limitation on porosity and methanogenic activity of anaerobic sludge granules. Applied Microbiology and Biotechnology, 39 (2): 276-280.

Aspen Technology (2013). Getting started Modeling Processes with Electrolytes Aspen Plus

Astals, S., Esteban-Gutiérrez, M., Fernández-Arévalo, T., Aymerich, E., García-Heras, J.L. and Mata-Alvarez, J. (2013). Anaerobic digestion of seven different sewage sludges: A biodegradability and modelling study. Water Research, 47 (16): 6033–6043.

Atuman, S.J., Wang, M. and Ramshaw, C. (2015). Modelling and simulation of intensified absorber for post-combustion CO_2 capture using different mass transfer correlations. Applied Thermal Engineering, 74 (5): 47-53.

Bae, H.K., Kim, S.Y. and Lee, B. (2011). Simulation of CO_2 removal in a split-flow gas sweetening process. Korean Journal of Chemical Engineering, 28 (3): 643-648.

Barbosa, R.A. and Sant'Anna, G.L. (1989). Treatment of raw domestic sewage in an UASB reactor. Water Research, 23 (12): 1483-1490.

Barkley, R.W. and Motard, R.L. (1972). Decomposition of nets. Chemical Engineering Journal, 3 (C): 265-275.

Barta, Z., Reczey, K. and Zacchi, G. (2010). Techno-economic evaluation of stillage treatment with anaerobic digestion in a softwood-to-ethanol process. Biotechnology for Biofuels 3 (21): 1-11.

Batstone, D.J., Keller, J., Angelidaki, I., Kalyuzhnyi, S. Pavlostathis, S.G., Rozzi, A., Sanders, W., Siegrist, H. and Vavilin, V. (2002). The Anaerobic Digestion Model No 1 (ADM1). Water Science and Technology, 45 (10): 65-73.

Batstone, D.J. and Keller, J. (2003). Industrial applications of the IWA anaerobic digestion model No.1 (ADM1). Water Science and Technology, 47 (12): 199–206.

Berenjian, A., Chan, N. and Malmiri, H.J. (2012). Volatile organic compounds removal methods: A review. American Journal of Biochemistry and Biotechnology, 8 (4): 220-229.

Bhatia, D., Vieth, W.R. and Venkatasubramaniam. K. (1985). Steady-state and transient behavior in microbial methanification: I. Experimental results. Biotechnology and Bioengineering, 27 (8): 1192-1198.

Bhatti, Z.I., Furukawa, K and Fujita, M. (1995). Comparative composition and characteristics of methanogenic granular sludges treating industrial wastes under different conditions. Journal of Fermentation and Bioengineering, 79 (3): 273-280.

Bhoi, P.R., Huhnke, R.L., Kumar, A., Patil, K.N. and Whiteley, J.R. (2015). Equilibrium stage based model of a vegetable oil based wet packed bed scrubbing system for removing producer gas tar compounds. Separation and Purification Technology, 142 (4): 196-202.

Blumensaat, F. and Keller, J. (2005). Modelling of two-stage anaerobic digestion using the IWA Anaerobic Digestion Model No. 1 (ADM1). Water Research, 39 (1): 171-183.

Borja, R. and Banks, C.J. (1995). Response of an anaerobic fluidized bed reactor treating ice-cream wastewater to organic, hydraulic, temperature, and pH shocks. Journal of Biotechnology, 39 (3): 251-259.

Brunet, R., Guillén-Gosálbez, G. and Jiménez, L. (2012a). Cleaner design of single-product biotechnological facilities through the integration of process simulation, multiobjective optimization, life cycle assessment, and principal component analysis. Industrial & Engineering Chemistry Research, 51 (1): 410-424.

Brunet, R., Guillén-Gosálbez, G., Pérez-Correa, J.R., Caballero, J.A. and Jiménez, L. (2012b). Hybrid simulation-optimization based approach for the optimal design of single-product biotechnological processes. Computers and Chemical Engineering, 37 (10): 125-135.

Cimini, S., Prisciandaro, M. and Barba, D. (2005). Simulation of a waste incineration process with flue-gas cleaning and heat recovery sections using Aspen Plus. Waste Management, 25 (2): 171-175.

Chen, Y., Cheng, J.J. and Creamer, K.S. (2008). Inhibition of anaerobic digestion process: a review. Bioresource Technology, 99 (10): 4044-4064.

Chen, Z., hu, D., Zhang, Z., Ren, N. and Zhu, H. (2009). Modeling of two-phase anaerobic process treating traditional Chinise medicine wastewater with the IWA Anaerobic Digestion Model No. 1. Biorsource Technology, 100 (20): 4623-4631.

Christensen, J.H. and Rudd, D.F. (1969). Structuring design computations. AIChE Journal, 15 (1): 94-100.

Chong, S., Sen, T.K., Kayaalp, A. and Ang, H.M. (2012). The performance enhancements of upflow anaerobic sludge blanket (UASB) reactors for domestic sludge treatment - A State-of-the-art review. Water Research, 46 (11): 3434-3470.

Colussi, I., Cortesi, A., Della Vedova, L., Gallo, V. and Robles, C. (2009). Start-up procedures and analysis of heavy metals inhibition on methanogenic activity in EGSB reactor. Bioresource Technology, 100 (24): 6290-6294.

Colussi, I., Cortesi, A., Gallo, V., Rubesa Fernandez, A.S. and Vitanza, R. (2012). Modelling of an anaerobic process producing biogas from winery wastes. Chemical Engineering Transactions, 27: 301-306.

Cooper, C.D. and Alley, F.C. (2011). Air pollution control. A design approach (4th edition). *Wavelland Press*, USA.

Cox, H.H. and Deshusses, M.A. (1998). Biological Waste Air Treatment in Biotrickling Filters. Current Opinion in Biotechnology, 9 (3): 256-262.

Cox, H.H. and Deshusses, M.A. (1999). Biomass Control in waste air biotrickling filters by Protozoan Predation. Biotechnology and Bioengineering, 62 (2): 216-224.

DeHollander, G.R., Overcamp, T.J. and Grady, C.P.L. (1998) Performance of Suspended Growth Bioscrubber for the control of methanol. Journal of the Air & Waste Management Association, 48 (9): 872-876.

Delhoménie, M.C. and Heitz, M. (2005). Biofiltration of air: A review. Critical Reviews in Biotechnology, 25 (1-2): 53-72.

Devinny, J.S. and Deshusses, M.A., Webster, T.S. (1999). Biofiltration for Air Pollution Control. *Lewis Publishers*, USA.

Díaz, C., Baena, S., Patel B.K.C. and Fardeau, M.L. (2010). Peptidolytic microbial community of methanogenic reactors from two modified UASBs of brewery industries. Brazilian Journal of Microbiology, 41 (3): 707-717.

Directive 2008/50/EC, 21 May 2008 on ambient air quality and cleaner air for Europe. OJ L 152 June 2008.

Directive 2010/75/EU, 24 November 2010 on industrial emissions (integrated pollution prevention and control). OJ L334, 17 December 2010.

Dobslaw, D., Dobslaw, C., Fütterer, N. and Engesser, K. (2007). Optimisation of a Biological waste air purification plant in printing industry for treatment of crude air containing alcohols and ethers. Biospectrum Tagungsband Osnabrück. P.2.

Eichler, B. and Schink, B. (1985). Fermentation of primary alcohols and diols and pure culture of syntrophically alcohol-oxidizing anaerobes. Archives of Microbiology, 143 (1): 60-66.

Enright, A. M., McGrath, V., Gill, D., Collins, G. and O'Flaherty, V. (2009). Effect of seed sludge and operation conditions on performance and archaeal community structure of low-temperature anaerobic solvent-degrading bioreactors. Systematic and Applied Microbiology, 32 (1): 65-79.

Enright, A.M., McHugh, S., Collins, G. and O'Flaherty, V. (2005). Low-temperature anaerobic biological treatment of solvent-containing pharmaceutical wastewater. Water Research, 39 (19): 4587- 4596.

Ernst and Young (2007). Competitiveness of the European Graphic Industry. Prospects for the EU printing sector to respond to its structural and technological challenges. Brussels, Belgium.

European Commission (EC) (2007). Reference Document on Best Available Techniques on Surface Treatment using Organic Solvents. Seville, Spain

European Commission (EC) (2013). Communication from the commission to the European Parliament, the council, the European economic and social committee and the committee of the regions. A policy framework for climate and energy period from 2020 to 2030. Brussels, Belgium

European Commission (EC) (2016). Best Available Techniques (BAT) Reference Document for Common Waste Water and Waste Gas Treatment/Manage Systems in the chemical sector. Seville, Spain.

European Environment Agency (EEA) (2010). The European environment. State and outlook 2010: synthesis. Copenhagen, Denmark.

European Environment Agency (EEA) (2013). Air quality in Europe – 2013 report. Copenhagen, Denmark.

European Environment Agency (EEA) (2016). Air quality in Europe – 2014 report. Copenhagen, Denmark.

European Environment Agency (EEA) (2014). European Union emission inventory report 1990-2012 under the UNECE Convention on Long-range Transboundary Air Pollution (LRTAP). Copenhagen, Denmark.

European Environment Agency (EEA) (2016). European Union emission inventory report 1990-2014 under the UNECE Convention on Long-range Transboundary Air Pollution (LRTAP). Copenhagen, Denmark.

European Solvents Industry Group (ESIG) (2015). Available on-line at http://www.esig.org. Date of access: November 2016.

Fedorovich, V., Lens, P. and Kalyuzhnyi, S. (2003). Extension of Anaerobic Digestion Model No . 1 with Processes of sulfate reduction. Appied Biochemistry and Biotechnology, 109 (1): 33-45.

Fermoso, F.G., Bartacek, J., Jansen, S. and Lens, P.N.L. (2009). Metal supplementation to UASB bioreactors: from cell-metal interactions to full-scale application. Science of the Total Environmental, 407 12: 3652-3667.

Forgács, G., Niklasson, C., Horváth, I.S. and Taherzadeh, M.J. (2014). Methane production from feather waste pretreated with $Ca(OH)_2$: Process development and economical analysis. Waste and Biomass Valorization, 5 (1): 65-73.

Fuentes, M., Scenna, N.J. and Aguirre, P. A. (2011). A coupling model for EGSB bioreactors: Hydrodynamics and anaerobic digestion processes. Chemical Engineering and Processing: Process Intensification, 50 (3): 316-324.

Fukuzaki, S., Nishio, N. and Nagai, S. (1995). High rate performance and characterization of granular methanogenic sludges in Upflow anaerobic sludge blanket reactor fed with various substrates. Journal of Fermentation and Bioengineering, 79 (4): 354-359.

García, N., Fernández-Torres, M.J. and Caballero, J.A. (2014). Simultaneous environmental and economic process synthesis of isobutane alkylation. Journal of Cleaner Production, 81: 270-280.

Ghangrekar, M.M., Asolekar, S.R. and Joshi, S.G. (2005). Characteristics of sludge developed under different loading conditions during UASB reactor start-up and granulation. Water Research, 39 (6): 1123-1133.

Genc, S., Zadeoglulari, Z., Fuss, S.H. and Genc, K. (2012). The adverse effects of air pollution on the nervous system. Journal of Toxicology, 2012: 23 pages.

Goodwin, J.A.S. and Stuart, J.B. (1994). Anaerobic digestion of malt whisky distillery pot ale using upflow anaerobic sludge blanket reactors. Bioresource Technology, 49 (1): 75-81.

Grady, B. (1997). Energetics of syntrophic cooperation in methanogenic degradation. Microbiology and Molecular Biology Reviews, 61 (2): 262-280.

Grady, C. P. L., Daigger, G. T. and Lim, H. C. (2011). Biological wastewater treatment (3rd edition). *Taylor & Francis*, USA

Granström, T., Lindberg, P., Nummela, J., Jokela, J. and Leisola, M. (2002). Biodegradation of VOCs from printing press air by an on-site pilot plant bioscrubber and laboratory scale continuous yeast cultures. Biodegradation, 13 (2): 155-162.

Grieco, E. and Poggio, A. (2009). Simulation of the influence of flue gas cleaning system on the energetic efficiency of a waste-to-energy plant. Appied Energy, 86 (9): 1517-1523.

Hammervold, R.E., Overcamp, T.J., Grady, C.P.L. and Smets, B.F. (2000). A sorptive slurry bioscrubber for the control of acetone. Journal of the Air & Waste Management Association, 50 (6): 954-960.

Hartley, K. and Lant, P. (2006). Eliminating non-renewable CO_2 emissions from sewage treatment: An anaerobic migrating bed reactor pilot plant study. Biotechnology and Bioengineering, 95 (3): 384-398.

Henry, M.P., Donlon, B.A., Lens, P.N., and Colleran, E.M. (1996). Use of anaerobic hybrid reactor for treatment of synthetic pharmaceutical wastewaters containing organic solvents. Journal of Chemical Technology and Biotechnology, 66 (3): 251-264.

Hayes, T. and Theis, T.L. (1978). The distribution of Heavy Metals in Anaerobic Digestion. Journal Water Pollution Control Federation, 50 (1):61-72

Hulshoff-Pol, L.W., de Castro Lopes, S.I., Lettinga, G. and Lens, P.N.L. (2004). Anaerobic sludge granulation. Water Research, 38 (6): 1376-1389.

Ince, B., Koksel, G.; Cetecioglu, Z., Oz, N.A., Coban, H. and Ince, O. (2011). Inhibition effect of isopropanol on acetyl-CoA synthetase expression level of acetoclastic methanogen, Methanosaeta concilii. Journal of Biotechnology, 165 (2): 95-99.

Intergovernmental Panel on Climate Change (IPCC) (2014). Climate change 2014, synthesis report. Geneva, Switzerland.

Jannelli, E. and Minutillo, M. (2007). Simulation of the flue gas cleaning system of an RDF incineration power plant. Waste Managment, 27 (5): 684-690.

Janssen, A., van den Bosch, P.L.F., van Leerdam, R.C. and de Graaff, M. (2013). Bioprocess for the removal of Volatile sulfur compounds from gas streams. In: C. Kennes and M.C. Veiga (Eds.), Air pollution prevention and control: Bioreactors and Bioenergy. *John Wiley & Sons, Ltd,* United Kingdom.

Kalyuzhnyi, S. V., Fragoso, C.D. and Martinez, J.R. (1997). Biological sulfate reduction in a UASB reactor fed with ethanol as the electron donor. Microbiology, 66 (5): 562-567.

Kawai, F. (2002). Microbial degradation of polyethers. Applied Microbiology and Biotechnology, 58 (1): 30-38.

Kesavan, P. and Law, V.J. (2005). Practical identifiability of parameters in Monod kinetics and statistical analysis of residuals. Biochemical Engineering Journal 24 (2): 95-104.

Kellner, C. and Flauger, M. (1998). Reduction of VOCs exhaust of coating machines with bioscrubber. In: Proceedings 91st Annual Meeting & Exhibition of the Air & Waste manage. Assoc. San Diego, California.

Kennes, C. and Veiga, M.C. (2013). Biotrickling Filters. In: C. Kennes and M.C. Veiga (Eds.), Air pollution prevention and control: Bioreactors and Bioenergy. *John Wiley & Sons, Ltd*, United Kingdom.

Kennes, C., Rene, E,R. and Veiga, M.C. (2009). Bioprocess for air pollution control. Journal of Chemical Technology and Biotechnology, 84 (10): 1419-1436.

Kettunen, R.H. and Rintala, J.A. (1997). The effect of low temperatures (5-29°C) and adaptation on the methanogenic activity of biomass. Applied Microbiology and Biotechnology, 48 (4): 570-576.

Khakharia, P., Huizinga, A., Jurado Lopez, C., Sanchez Sanchez, C., De Miguel Mercader, F., Vlugt, T.J.H. and Goetheer, E. (2014). Acid wash scrubbing as a countermeasure for ammonia emissions from a postcombustion CO2 Capture Plant. Industrial & Engineering Chemistry Research, 53 (33): 13195-13204.

Khan, F.I. and Ghoshal, Kr. A. (2000). Removal of Volatile Organic Compounds from polluted air. Journal of Loss Prevention in the Process Industries, 13 (6): 527-545.

Kleerebezem, R. and van Loosdrecht, M.C.M. (2006). Waste characterization for implementation in ADM1. Water Science and Technology, 54 (4): 167-174.

Kobayashi, H.A., Stenstrom, M.K. and Mah, R.A. (1983). Treatment of low strength domestic wastewater using the anaerobic filter. Water Research, 17 (8): 903-909.

Kolukirik, M. Ince, O. and Ince B.K. (2007). Methanogenic community change in a full-scale UASB reactor operated at a low F/M ratio. Environmental Science and Health, Part A, 42 (7): 903-910.

Lafita, C., Penya-roja, J.M. and Gabaldón, C. (2015). Anaerobic removal of 1-methozy-2-propanol under ambient temperature in an EGSB reactor. Bioprocess and Biosystems Engineering, 38 (11): 2137- 2146.

Le Cloriec, P. and Humeau, P. (2013). Bioscrubbers. In: C. Kennes and M.C. Veiga (Eds.), Air pollution prevention and control: Bioreactors and Bioenergy. *John Wiley & Sons, Ltd,* United Kingdom.

Le Cloriec, P., Humeau, P. and Ramirez-López, E.M. (2001). Biotreatments of Odours control and performance of a biofilter and a bioscrubber. Waster Science and Technology, 44 (9): 219-226.

Ledet, W.P. and Himmelblau, D.M. (1970). Decomposition Procedures for the Solving of Large Scale Systems. Advanced Chemical Engineering, 8: 185-254.

Leitão, R. C. (2004). Robtness of UASB reactor treating sewage under tropical conditions. Ph.D. Thesis. Wageningen University.

Lettinga, G. and Hulshoff Pol, L.W. (1991). UASB-process design for various types of wastewaters. Water Science and Technology, 24 (8): 87-107.

Lettinga, G., Rebac, S., Parshina, S., Nozhevnikova, A., van Lier, J. and Stams, A.J.M. (1999). High-Rate Anaerobic Treatment of Wastewater at low Temperatures. Applied and Environmental Microbiology, 65(4): 1696- 1702.

Lettinga, G., Rebac, S. and Zeeman, G. (2001). Challenge of psychrophilic anaerobic wastewater treatment. Trends in Biotechnology, 19 (9): 363-370.

Lettinga, G., Roersma, R. and Grin, P. (1983). Anaerobic Treatment of Raw Domestic Sewage at Ambient-Temperatures Using a Granular Bed UASB reactor. Biotechnology and Bioengineering, 25 (7): 1701-1723.

Lim, S.J. and Kim, T-H (2014). Applicability and trends or anaerobic granular sludge treatment processes. Biomass and Bioenergy, 60: 189-202.

Lin, C.Y. and Chen, C.C. (1999). Effect of heavy metals on the methanogenic UASB granule. Water Research, 33 (2): 409-416.

Malhautier, L., Lalanne, F. and Fanlo, J.L. (2009). Bioscrubbing as a treatment for a complex mixture of volatile organic compounds: influence of the absorption column characteristics on performance. Canadian Journal of Civil Engineering, 36 (12): 1926-1934.

McCabe, W.L., Smith, J.C., and Harriot, D. (1985). Unit Operations of Chemical Engineering (4th edition). *McGraw-Hill*, EEUU.

Mel, M., Yong, A.S.H.Y., Avicenna, Ihsan, S.I. and Setyobudi, R.H. (2015). Simulation study for economic analysis of biogas production from agricultural biomass. Energy Procedia, 65: 204-214.

McHugh, S., O´Reilly, C., Mahony, T., Colleran, E. and O´Flaherty, V. (2003). Anaerobic granular sludge bioreactor technology. Reviews in Environmental Science and Biotechnology, 2 (2): 225-245.

Mills, N. L., Donaldson, K., Hadoke, P.W., Boon, N.A., MacNee, W., Cassee, F.R., Sandström, T., Blomberg, A. and Newby, D.E (2009). Adverse cardiovascular effects of air pollution. Nature Clinical Practice Cardiovascular Medicine. 6 (1): 36-44.

Nadais, H., Capela, I., Arroja, L. and Duarte, A. (2005). Optimum cycle time for intermittent UASB reactors treating dairy wastewater. Water Research, 39 (8): 1511-1518.

Nadais, H., Capela, I. and Arroja, L. (2006). Intermittent vs continuous operation of upflow anaerobic sludge bed reactors for dairy wastewater and related microbial changes. Water Science and Technology, 54 (2): 103-109.

Nielsen, A. and Richard, K. (1997). Gas purification (5th edition). *Gulf Publishing Company*, USA.

Noyola, A., Capdeville, B. and Roques, H. (1988). Anaerobic treatment of domestic sewage with a rotating-stationary fixed-film reactor. Warter Research, 22 (12): 1585-1592.

Oktem, Y.A., Ince,O., Sallis, P., Donnelly, T. and Ince, B.K. (2007). Anaerobic treatment of chemical synthesis-based pharmaceutical wastewater in a hybrid upflow anaerobic sludge blanket reactor. Bioresource Technology, 99 (5):1089-1096.

O´Flaherty, V., Lens, P.N.L., de Beer, D. and Colleran, E. (1997). Effect of feed composition and upflow velocity on aggregate characteristics in anaerobic upflow reactors. Applied Microbiology and Biotechnology, 47 (2): 102-107.

Organisation for Economic Co-Operation and Development (OECD) (2012). Perspectivas ambientales de la OCDE hacia 2050. Amsterdam, The Netherlands.

Pavlostathis, S.G. and Giraldo-Gomez, E. (1991). Kinetics of anaerobic treatment – a critical review. Critical Reviews in Environmental Control, 21 (5-6): 411-490.

Pho, T.K. and Lapidus, L. (1973). Topics in Computer-aided Design: Part I. An Optimum tearing Algorithm for recycle Systems. AIChE Journal, 19 (6): 1170-1181.

Platen, H. and Schink, B. (1987). Methanogenic degradation of acetone by an enrichment culture. Archives of Microbiology, 149 (2): 136-141.

Quirante, N., Javaloyes, J. and Caballero, J.A., 2015. Rigorous design Distillation Columns Using Surrogate models based on kriging Interpolation. Process Systems Engineering, 61 (7): 2169-2187.

Rajendran, K., Kankanala, H.R., Lundin, M. and Taherzadeh, M.J. (2014). A novel process simulation model (PSM) for anaerobic digestion using Aspen Plus. Bioresource Technology, 168: 7-13.

Rajeshwari, K.V:, Balakrishman, M., Kansal, A., Kusum, L. and Kishore, V.V.N. (2000). State-of-the-art of anaerobic digestion technology for industrial wastewater treatment. Renewable and Sustainable Energy Reviews, 4 (2): 135-156.

Ramirez, I., Volcke, E.I.P., Rajinikanth, R. and Steyer, J.P. (2009). Modeling microbial diversity in anaerobic digestion through an extended ADM1 model. Water Reseacrh, 43 (11): 2787-2800.

Razaviarani, V. and Buchanan, I.D. (2015): Calibration of the anaerobic digestion model No. 1 (ADM1) fro steady-state anaerobic co-digestion of municipal wastewater sludge with restaurant grease trap waste. Chemical Engineering Journal, 266: 91-99.

Rebac, S., Ruskova, J., Gerbens, S., van Lier, J.B., Stams, A.J.M. and Lettinga, G. (1995). High-rate anaerobic treatment of wastewater under psychrophilic conditions. Journal of Fermentation and Bioengineering, 80 (5): 499-506.

Rene, R.E., Veiga, M.C. and Kennes, C. (2013). Biofilters. In: C. Kennes and M.C. Veiga (Eds.), Air pollution prevention and control: Bioreactors and Bioenergy. *John Wiley & Sons, Ltd*, United Kingdom.

Rizvi, H., Ahmad, N., Abbas, F., Bukhari, I.H., Yasar, A., Ali, S., Yasmeen, T. and Riaz, M. (2015). Start-up of UASB reactors treating municipal wastewater and effect of temperature/sludge age and hydraulic retention time (HRT) on its performance. Arabian Journal of Chemistry, 8 (6), 780-786.

Rothenbuhler, M., Heitz, M., Beerli, M. and Marcos, B. (1995). Biofiltration of organic volatile emissions in reference to flexographic printing processes. Water, Air and Soil Pollution, 83 (1): 37-50.

Sánchez, F., Córdoba, P. and Siñeriz, F. (1985). Use of the UASB reactor fo the anaerobic treatment of stillage from sugar Cane Molasses. Biotechnology and Bioengineering, 27 (12): 1710-1716.

Sander, R. (2015). Compilation of Henry's law constant (version 4.0) for water as solvent. Atmospheric Chemistry and Physics, 15: 4399-4981.

San-Valero, P., Penya-Roja, J.M, Álvarez-Hornos, F.J., Marzal, P. And Gabaldón, C. (2015). Dynamic mathematical modelling of the removal of hydrophilic VOCs by biotrickling filters. International Journal of Environmental Research and Public Health, 12 (1): 746-766.

San-Valero, P., Penya-Roja, J.M., Sempere, F. and Gabaldón, C. (2013). Biotrickling filtration of isopropanol under intermittent loading conditions. Bioprocess and Biosystems Engineering, 36 (7): 975-984.

Sargent, R.W.H. and Westerberg, A.W. (1964). Speed up in chemical engineering design. Chemical Engineering Research and Design, 42 (1): 190-197.

Schmidt, J.E. and Ahring, B.K. (1996). Granular sludge formation in upflow anaerobic sludge blanket (UASB) reactors. Biotechnology and Bioengineering, 49 (3): 229-246.

Scully, C., Collins. G. and O´Flaherty, V. (2006). Anaerobic biological treatment of phenol at 9-15°C in an expanded granular sludge bed (EGSB)-based bioreactor. Water Research, 40 (20): 3737- 3744.

Seghezzo, L., Zeeman, G., van Lier J.B., Hamelers, H.V.M. and Lettinga, G. (1998). A review: The anaerobic treatment of sewage in UASB and EGSB reactors. Bioresource Technology, 65 (3): 175-190.

Sempere, F., Gabaldón, C., Martínez-Soria, V., Marzal, P., Penya-roja, J.M. and Álvarez-Hornos, F.J. (2008). Performance evaluation of a biotrickling filter treating a mixture of oxygenated VOCs during intermittent loading. Chemosphere, 73 (9): 1533-1539.

Sempere, F., Martinez-Soria, V., Penya-Roja, J.M., Waalkens, A. and Gabaldón, C. (2012). Control of VOC emissions from a flexographic printing facility using an industrial biotrickling filter. Water Science and Technology, 65 (1):177-182.

Singh, A., Shareefdeen, Z. and Ward, P.O. (2005). Biotechnology for Odor and Air Pollution Control. *Springer.* Germany.

Singh, K.S., Harada, H. and Viraraghavan, T. (1996). Low-strength wastewater treatment by a UASB reactor. Bioresource Technology, 55 (3): 187-194.

Singh, R. P., Kumar, S. and Ojha C.S.P. (1999). Nutrient requirement for UASB process: a review. Biochemical Engineering Journal, 3 (1): 35-54.

Speranza, G., Mueller, B., Orlandi, M., Morelli, C.F., Manitto, P. and Schink, B. (2002). Mechanism of anaerobic ether cleavage: conversion of 2-phenoxyethanol to phenol and acetaldehyde by Acetobacterium sp. Journal of Biological Chemistry, 227 (14): 11684-11690.

Srinivas, S., Field, R.P. and Herzog, H.J. (2013). Modeling tar handling options in biomass gasification. Energy and Fuels, 27 (6): 2859-2873.

Symons, G.E. and Buswell, A.M. (1933). The methane fermentation of carbohydrates. Journal of American Chemical Society, 55 (5): 2028-2036.

Syutsubo, K., Harada, H., Ohashi, A., and Suzuki, H. (1997). An effective start-up of thermophilic reactor UASB reactor by seeding mesophilically-grown granular sludge. Water Science and Technology, 36 (6-7): 391-398.

Tarjan, R. (1971). Depth-first search and linear graph algorithms. 12th Annual Symosium on Switching and Automata Theory, 1 (2): 146-160.

Tartakovsky, B., Mu, S.J., Zeng, Y., lou, S.J., Guiot, S.R., and Wu, P. (2008). Anaerobic digestion model No. 1-based distributed parameter model of an anaerobic reactor: II. Model validation. Bioresource Technology, 99 (9): 3676-3684

Tchobanoglous, G., Burton, F. L. and Stensel, H. D. (2003). Wastewater engineering: treatment and reuse. *McGraw-Hill*.

Thauer, R.K., Jungermann, K. and Decker, K. (1977). Energy conservation in chemotrophic anaerobic bacteria. Bacteriological Reviews, 41 (1): 100-180.

Towler, G. and Sinnott, R.K. (2012). Chemical Engineering Design (5^{th} edition). *Elsevier Limited of The Boulevard*, United Kingdom.

Uemura, S. and Harada, H. (2000). Treatment of sewage by a UASB reactor under moderate to low temperature conditions. Bioresource Technology, 72 (3): 275-282.

Upadhye, R.S. and Grens II, E.A. (1975). Selection of decompositions for chemical process simulation. AIChE Journal, 21 (1): 136-143.

Van Groenestijn, J.W. and Hesselink, P.G.M. (1993). Biotechniques for air pollution control. Biodegradation, 4 (4):283-301.

Van Groenestijn, J.W. and Kraakman, N.J.R. (2005). Recent developments in biological waste gas purification in Europe. Chemical Engineering Journal, 113 (2-3): 85-91.

Van Kempen, E., van Kamp, I., Lebret, E., Lammers, J., Emmen, H. and Stansfeld, S. (2010). Neurobehavioral effects of transportation noise in primary schoolchildren: a cross-sectional study. Environmental Health, 9 (25): 1-13.

Van Lier J.B. (2008) High-Rate anaerobic wastewater treatment: diversifying from end-of-pipe treatment to resource-oriented conversion techniques. Water and Science Technology, 57 (8):1137-1148.

Van Lier, J.B., Mahmoud, N. and Zeeman, G. (2008). Biological wastewater treatment: Principles modelling and design. *IWA Publishing*. United Kingdom.

Van Lier, J.B., van der Zee, F.P., Frijters, C.T.M.J. and Ersahin, M.E. (2015). Celebrating 40 years anaerobic sludge bed reactor for industrial wastewater treatment. Reviews in Environmental Science and Bio/Technology, 14 (4): 681-702.

Wark, K., Warner, C.F. and Warner W.T.D. (1998). Air Pollution. Its origin and control (3rd edition). *Addison Wesley Longman, Inc*., USA.

Weichgrebe, D., Urban, I. and Friedrich, K. (2008). Energy- and CO_2-reduction potentials by anaerobic treatment of wastewater and organic kitchen wastes in consideration of different climatic conditions. Water Science and Technology, 58(2): 379-384.

Widdel, F. (1986). Growth of methanogenic bacteria in pure culture with 2-propanol and other alcohols as hydrogen donors. Applied and Environmental Microbiology, 51 (5): 1056-1062.

Wiegant, W.M., Claassen, J.A. and Lettinga, G (1985). Thermophilic anaerobic digestion of high strength wastewaters. Biotechnology and Bioengineering, 27 (9): 1374-1381.

Wiegel, J. (1990). Temperature spans for growth: hypothesis and discussion. FEMS Microbiology Letters, 75 (2-3): 155-170.

World Health Organization (WHO) (2006). Air quality guidelines for particulate matter, ozone, nitrogen dioxide and sulfur dioxide. Copenhagen, Denmark.

World Health Organization (WHO) (2008). Health risk of ozone from long-range transboundary air pollution. Copenhagen, Denmark.

World Health Organization (WHO) (2013). Review of evidence on health aspects of air pollution. Bonn, Germany.

Xing, W., Zuo, J-e., Dai, N., Cheng, J. and Li, J. (2009). Reactor performance and microbial community of an EGSB reactor operated at 20 and 15°C. Journal of Applied Microbiology, 107 (3): 848-857.

Yanti, H., Wikandari, R., Niklasson, C. and Taherzadeh, M.J. (2014). Effect of ester compounds on biogas production: beneficial or detrimental? Energy Science & Engineering, 2 (1): 22-30.

Yoochatchaval, W, Ohashi, A. Harada, H., Yamaguchi, T. and Syutsubo, K. (2008). Intermittent Effluent Recirculation for the Efficient Treatment of low strength wastewater by an EGSB reactor. International Journal of Environmental Research, 2 (3): 231-238.

Zellner, G. and Winter, J. (1987). Secondary alcohols as hydrogen donors for carbon dioxide reduction by methanogens. FEMS Microbiology Letters, 44 (3): 323-328.

Zoutberg, G.R. and Frankin. R. (1996). Anaerobic treatment of chemical and brewery waste water with a new type of anaerobic reactor; the Biobed® EGSB reactor. Water Science and Technology. 34 (5-6): 375-381.